TOWN OF
FARMINGTON

1000 County Road 8, Farmington, New York 14425-9565

"The Gateway to Ontario County" (Exit 44 NYS Thruway)
The Town of Farmington is an equal opportunity provider
TDD 1-800-662-1220
www.townoffarmingtonny.com

May 15, 2024

Sky Solar, Inc.
1129 Northern Boulevard, Suite 404
Manhasset, New York 11030

Re: PB #0406-24 Sky Solar East Special Use Permit
PB #0407-24 Sky Solar West Special Use Permit
PB #0408-24 Sky Solar East Preliminary Site Plan
PB #0409-24 Sky Solar West Preliminary Site Plan

Materials submitted by **Anne Dunford (6007 Redfield Drive)** and **John Grady (6018 Redfield Drive)**at the Planning Board meeting on May 15, 2024:

#01 Saving Greene: PFAs and other compounds in solar panels, wiring, and coatings

#02 Environmental Research: High exposure to perfluorinated compounds in drinking water and thyroid disease. A cohort study from Ronneby, Sweden

#03 Journal of Hazardous Materials: GenX in water: Interactions and self-assembly

#04 Renewable and Sustainable Energy Reviews: Environmental impacts of utility-scale solar energy

#05 Scientific Reports: The Photovoltaic Heat Island Effect: Larger solar power plants increase local temperatures

#06 Environmental Research: Inflammatory bowel disease and biomarkers of gut inflammation and permeability in a community with high exposure to perfluoralkyl substances through drinking water

#07 Process Safety and Environmental Protection: Environmental pressure effects on thermal runaway and fire behaviors of lithium-ion battery with different cathodes and state of charge

#08 2022 MTOD and MSOD Site Design Guidelines, annotated by Grady

#09 Chapter 165 Zoning, Article VI Special Permit Uses, annotated by Grady

#10 Fires at New York Battery Energy Storage System Facilities Ignite State Response

#11 Planning Board Minutes, April 17, 2024, pp. 22–55, annotated by Grady

#12 An expert talks solar battery farms, how they work and the risks

#13 New York battery storage owners may face new safety rules after fires

#14 Solar farm fire in Upstate New York sends possible toxic smoke billowing into surrounding community

#15 Questions remain after Jefferson Co solar farm battery fire

#16 U.S. solar expansion stalled by rural land-use protests

#17 Citizens for Responsible Solar

#18 The Dangers of Vehicle Exhaust

#19 Do solar farms lower property values? A new study has some answers

#20 Chapter 165 Zoning, Article IV District Regulations

#21 Safety of Grid Scale Lithium-ion Battery Energy Storage Systems

#22 Journal of Hazardous Materials: A comprehensive investigation on the thermal and toxic hazards of large format lithium-ion batteries with $LiFePo_4$ cathode

#23 Journal of Loss Prevention in the Process Industries: Assessment of the explosion risk during lithium-ion battery fires

#24 Health Effects of Diesel Exhaust

SAVING GREENE
CITIZENS FOR SENSIBLE SOLAR

PO Box 369 Coxsackie NY 12051
SavingGreene@gmail.com
SavingGreene.com

PFAS and other compounds in solar panels, wiring, and coatings

Renewable energy should offer more than promises that it is good for the environment. The solar industry promotes photovoltaic (PV) technology in the most wholesome terms: generating clean, free power from the sun. This benevolent assessment potentially omits environmental impacts during the manufacturing, operational lifetime, and disposal of solar panels and battery storage systems. Host towns need proof, not simply promises, when evaluating how solar projects may affect their residents and environment, both now and in the future.

Introduction

In July 2021, the Town of Avon, New York adopted Local Law 3 of 2021. This precedent-setting amendment to the local solar law prohibits using solar panels that "utilize or contain any amount of GenX chemicals or polyfluoroalkyl (PFAS) substances."[1] This position aligns with state and federal laws protecting our water supply. For the long-term safety of Coxsackie residents, Hecate Energy (Hecate) and its successors should agree to a Certificate condition that prior to construction, Hecate will provide documentation verifying that the solar panels and associated electrical equipment used to construct the Greene County Solar Facility (the Facility) do not contain per- and polyfluoroalkyl substances (PFAS), including PFOA, PFOS, and GenX chemicals.

[1] https://www.avon-ny.org/PDFs--Town%20Clerk/ll3-2021.pdf

We would like to believe that Hecate's commitment to our town's public health and safety, as well as their desire to avoid potential future liability, would encourage them to give these comments careful consideration. Hecate must rely on manufacturers' data, which may not be fully transparent for solar panels and lithium-ion batteries, especially when they are manufactured outside of the United States—in this case often in China.

This Certificate condition would help safeguard our soil, surface waters, and groundwater from potential contamination. While such protection would help protect Sleepy Hollow's water supply, it provides important safeguards for all residents living in the vicinity of the Facility. Hecate and the Town of Coxsackie should perform pre- and post-installation soil and water testing, with annual monitoring. In addition, the installer should fund an escrow account for the Town to hire an independent, certified third-party laboratory for soil and water testing.

PFAS and related compounds

According to the National Institute of Environmental Health Sciences, perfluoroalkyl and polyfluoroalkyl substances (PFAS) are toxic, persistent, and bioaccumulative.[2] These synthetic fluorochemicals were first developed in the 1930s and have strong carbon-flourine bonds that make the structure repel both oil and water.[3] The Green Science Policy Institute details that these manmade chemicals are widely used in building materials such as paints, cleaning products, non-stick coatings, sealants, tapes, wire coverings, glass, solar panels, and batteries.[4] PFAS is commonly found in foam used to extinguish electrical fires.[5]

These "forever chemicals" have been linked to cancer and other health issues. Certain PFAS do not break down easily, causing them to remain indefinitely in the soil and water. Their potential hazard and persistence in the environment may pose a cumulative danger to public health. PFAS comprise a group of compounds, including PFOA, PFOS and GenX chemicals. The United States Environmental Protection Agency (EPA) has

[2] https://www.niehs.nih.gov/health/topics/agents/pfc/index.cfm

[3] https://www.nature.com/articles/d41586-019-00441-1

[4] https://greensciencepolicy.org/docs/pfas-building-materials-2021.pdf

[5] https://www.gao.gov/assets/gao-21-421.pdf

identified that the potentially toxic and carcinogenic nature of many of these chemicals demands careful evaluation.[6, 7]

The disposal of PFAS-containing materials is problematic, as evidenced by the recent cleanup and lawsuits filed against Noralite Hazardous Waste Facility in Cohoes, New York.[8] In July 2021, the village of Hoosick Falls reached a $65 million settlement with Saint-Gobain, Honeywell International, 3M, and DuPont for PFOA contamination of their groundwater that affected at least 544 private wells.[9] Unfortunately the water remains contaminated, and the plant that used PFOA chemicals has been declared a Superfund site.

PFAS legislation in New York State

In 2016, the NYS Department of Environmental Conservation (DEC) issued a regulatory impact statement to 6 NYCRR Part 597 adding PFOA and PFOS as hazardous substances. This ruling was adopted by the DEC in March 2017.[10] In July 2020, NYS passed S.8817 and A.4739-C, which ban the use of PFAS in food packaging.[11] And in August 2020, the NYS Department of Public Health (DPH) voted to set the maximum contaminant levels (MCLs) at 10 parts per trillion (10 ppt) for both PFOA and PFOS in our drinking water supply.[12] NYS legislation permits the DPH to require that public water systems are tested for the contaminants and ensure that elevated levels are addressed.[13]

---

[6] https://www.epa.gov/pfas/basic-information-pfas

[7] https://www.epa.gov/assessing-and-managing-chemicals-under-tsca/risk-management-and-polyfluoroalkyl-substances-pfas

[8] https://www.wamc.org/capital-region-news/2020-06-25/cohoes-residents-file-intent-to-sue-norlite-over-burning-firefighting-foam

[9] https://pfasproject.com/hoosick-falls-new-york/

[10] https://www.dec.ny.gov/regulations/104968.html

[11] https://www.nysenate.gov/legislation/bills/2019/s8817

[12] https://www.health.ny.gov/environmental/water/drinking/docs/water_supplier_fact_sheet_new_mcls.pdf

[13] https://news.bloomberglaw.com/environment-and-energy/new-york-moves-on-some-of-strictest-pfas-drinking-water-limits

PFAS legislation in other states

North Carolina is among the top three states for solar development. By February 2018, residents and the state were questioning the presence of PFAS in solar panels.[14] *The North Carolina State Journal* reported that EPA physical scientist Dr. Mark J. Strynar provided 39 records from the SciFinder database used by the EPA to identify applications of PFAS with solar panels.[15] In August 2018, *The Carolina Journal* reported that the EPA confirmed that PFAS are used in solar panel production.[16] While studies may not be conclusive, the lack of definitive conclusions and transparency raises concerns.

In December 2020, Marc Fitch of the Yankee Institute reported that the Connecticut Department for Health was concerned about PFAS in solar panels.[17] "We've asked the question, have received some information, and have also received some push-back when we ask those questions about whether these panels contain PFAS and different PFAS chemicals." It is the lack of answers and documentation that is troubling and raises questions of the long term impact of solar panels and battery storage on our soils and drinking water.

PFAS Federal legislation

Federal regulations surrounding PFAS are being adopted rapidly, and further restrictions at the national level are expected. US Representative Debbie Dingell (D-MI-12) sponsored Bill H.R.2467, PFAS Action Act of 2021, to "establish requirements and incentives to limit the use of perfluoroalkyl and polyfluoroalkyl substances, commonly referred to as PFAS, and remediate PFAS in the environment."[18] The Bill passed the House July 21, 2021 and is awaiting a vote in the Senate.[19] The Executive Office of the President and other advocacy groups such as Consumer Reports support passage of the

---

[14] https://nsjonline.com/article/2018/02/solar-panels-could-be-a-source-of-genx-and-other-perflourinated-contaminants/

[15] https://nsjonline.com/wp-content/uploads/2018/02/perfluoro-and-solar-panels-Reference_02_15_2018_120238-002.pdf

[16] https://www.carolinajournal.com/news-article/epa-confirms-genx-related-compounds-used-in-solar-panels/

[17] https://yankeeinstitute.org/2020/12/03/department-of-public-health-concerned-about-pfas-in-solar-panels-near-drinking-water/

[18] https://debbiedingell.house.gov/news/documentsingle.aspx?DocumentID=2975

[19] https://www.congress.gov/bill/117th-congress/house-bill/2467

Bill. [20, 21] Additionally, the Environmental Protection Agency (EPA) proposes reporting and record-keeping requirements for PFAS under the Toxic Substances Control Act (TSCA).[22]

The August 3, 2021, *National Law Review* included an article by John Gardella of CMBG3 Law in Boston. He concludes that while the US Senate vote has not been determined, that "the pressure is on the EPA to take regulatory action well beyond just drinking water, and companies absolutely must begin preparing now for regulatory actions that will have significant financial impacts down the road."[23]

PFAS in solar panel and battery manufacturing

Despite industry and a few academic assurances to the contrary, broad research consistently indicates that PFAS chemicals are used in solar panel and battery manufacturing and installation. PFAS is found in the coatings on electrical wires, backing panels, tapes, and adhesives.

Of particular concern is the use of PFAS in anti-reflective coatings (ARC) and anti-soil coatings (ASC) that are used to increase solar panel productivity. Material and Data Safety Sheets detail the contents of products manufactured in the United States. However, at this time, China is the major supplier of polysilicon[24] solar panels and batteries.[25] Accountability and transparency for materials and products made outside of the United States is questionable. In June 2021, the Biden administration banned import and use of certain solar energy materials and products from China due to the country's use of forced labor and genocide at polysilicon mines.[26]

Two types of solar panel coatings are commonly used: anti-reflective coatings (ARC) and anti-soil coatings (ASC)

---

[20] https://www.whitehouse.gov/wp-content/uploads/2021/07/HR2467.SAP-Final.docx.pdf?source=email

[21] https://advocacy.consumerreports.org/press_release/house-votes-to-approve-the-pfas-action-act-hr-2467/

[22] https://www.epa.gov/assessing-and-managing-chemicals-under-tsca/risk-management-and-polyfluoroalkyl-substances-pfas

[23] https://www.natlawreview.com/article/congress-presses-forward-pfas-measures

[24] https://www.solarpowerworldonline.com/2021/05/no-avoiding-it-now-soon-the-top-4-polysilicon-manufacturers-will-be-based-in-china/

[25] https://www.forbes.com/sites/rrapier/2019/08/04/why-china-is-dominating-lithium-ion-battery-production/?sh=770793d23786

[26] https://www.ecowatch.com/china-solar-panels-ban-biden-2654961710.html

Anti-Reflective Coating (ARC)

A bare silicon glass surface may have a reflection index of more than 30%.[27] Anti-reflective coatings (ARC) are used to increase solar panel productivity by adding a dielectric coating on the glass surface. This coating textures the glass surface, which results in specific bands of wave lengths to be trapped inside the panel where they can generate additional electricity by coming in contact with the photovoltaic cells.

In their Application Appendix 15-A: Glare Analysis, Hecate Energy states that the panels they expect to use will have an anti-reflective coating, presumably to increase efficiency.

Anti-Soil Coating (ASC)

Dust and dirt can foul the panel surface and hinder the conversion of light to electricity. To maintain steady performance, the panel's surface must be cleaned regularly. Current manual or robotic cleaning methods are expensive and inefficient.

The hydrophobic qualities of ASCs create a non-stick surface that promotes water shedding, resulting in "self-cleaning'" solar panels. This coating is applied to the front facing glass surface at the time of manufacture. The water-repelling surface promotes water cohesions, allowing the water droplets to form fully with minimal surface contact. This enhances water droplet shedding and in the process removes dust and dirt from the surface of the panel. ASCs help decrease maintenance costs while increasing the electricity generated. It can be reapplied in the field with products such as 3M AS Liquid 600.[28]

ASC is typically manufactured with either silicon dioxide (SiO2) or titanium dioxide (TiO2) nanoparticles combined with long chains of fluoropolymers. While SiO2 may be inexpensive it is less durable to environmental elements. TiO2 appears to be more stable and is reported to be more frequently used for solar panel ASC.

There are increasing concerns about the negative impact of TiO2 on the environment and human health. In December 2020, California announced the review of titanium dioxide nanoparticle classification under their Safe Water Act Proposition 65.[29]

Gohar Dar's book *TiO2 Nanoparticles*, published in February 2020, includes a chapter on "Toxicity of TiO2 Nanoparticle". This research indicates that lung tumors are found in

---

[27] https://www.pveducation.org/pvcdrom/design-of-silicon-cells/anti-reflection-coatings

[28] https://www.coatingsworld.com/issues/2012-10/view_paint-amp-coatings-manufacturer-news/3m-rolls-out-pv-anti-soiling-coating/

[29] https://www.paintsquare.com/news/?fuseaction=view&id=23184

mice that have had long term exposure to TiO2.[30] Chapter 2: "Applications in Nanobiotechnology and Nanomedicine" research indicates safety concerns regarding TiO2 nanoparticles on aquatic species.[31]

While the potential for titanium dioxide nanoparticles to contaminate our soils is not conclusive, the possibility warrants further investigation. The evidence appears to be mounting, and the developer should carry the burden of proof.

Research papers call for caution and further study of ARC and ACS on solar panels. Natatajan Shanmugam's May 2020 study "Anti-Reflective Coating Materials: A Holistic Review from PV Perspective,"[32] published in *Energies*, provides a 98-page comprehensive report. On page 67 the author states: "The implementation of ARCs on the solar cell would suppress the reflection, and in turn, enhances the PCE, [power conversion efficiency] but their durability with continuous exposure to the environment and performance degradation characteristics are some novel areas where research is required."

ARC and ASC resist some stresses, but not others:

> [T]he coatings may resist the harsh environmental stresses such as damp heat and humidity freeze, but they are susceptible to damage under UV exposure. XPS analysis revealed a clear reduction in fluorine in the composition of the coating after exposure to UV and outdoor testing. [33]

Kenan Isbilir's 2019 thesis at Loughborough University studies the "performance and durability of anti-reflective and anti-soiling coatings on solar cover glass"[34] His thesis investigated the durability of commercially available two types of single layer (ARC1 and ARC2) and one multilayer anti-reflective (MAR) commercially available coatings, as well as ASCs. After testing several coatings, he concludes that:

> The durability of these coatings against UV light and abrasion resistance would need to be improved if they are to be applied to PV cover glass.

In 2020, Gizelle C. Oehler found that certain ASC break down in as little as two weeks:

---

[30] https://onlinelibrary.wiley.com/doi/abs/10.1002/9783527825431.ch2

[31] https://www.ncbi.nlm.nih.gov/pmc/articles/PMC3720578/

[32] https://www.researchgate.net/publication/341556138_Anti-Reflective_Coating_Materials_A_Holistic_Review_from_PV_Perspective

[33] https://www.researchgate.net/publication/329506058_Testing_of_an_Anti-Soiling_Coating_for_PV_Module_Cover_Glass

[34] https://repository.lboro.ac.uk/articles/thesis/The_performance_and_durability_of_anti-reflective_and_anti-soiling_coatings_on_solar_cover_glass/8132048/1

> Surprisingly, the coatings began to degrade quickly, and the effect was clear after only two weeks of exposure. Degradation resulted in decreasing water contact angle and increasing roll-off angles. As observed by Bhaduri et al., the degradation was much faster than anticipated because the outdoor environment combines the stresses tested in the laboratory [31]. Degradation was caused by a number of mechanisms including solvent release, fluorine loss, thinning of the coating, and increasing surface macro-roughness. [35]

The location or accumulated amounts of the degraded chemicals is not discussed in these studies. It is logical to assume that the chemicals sloughing off with the rainwater are deposited into the underlying soil, groundwater and aquifers. The cumulative effect of tens of thousands of solar panels for 35 or more years would most likely permanently contaminate the site's groundwater, soil, and stormwater runoff. If coatings are reapplied during the projects lifetime then additional concerns are raised. How is the ground protected during reapplication? How often is the coating reapplied to the panels on site? Improper disposal of broken and decommissioned solar panels may permanently contaminate landfills and any nearby aquifers. If regulations continue to become more restrictive, how will the panels be disposed of, and is the decommissioning fund adequate?

Millions upon millions of solar panels will be used and disposed of within New York State during the next two decades. Periodic upgrades and damage or defects will need to be addressed long before the end of the project's life.[36] Developers should carry the burden of proof that their materials and products do not contain PFAS. Towns and taxpayers should trust but verify all materials provided by the developers. The people cannot afford the risk that solar panels and storage batteries may contaminate our drinking water and soil, either upon installation, during use, or during disposal. It seems doubtful that developers' required liability coverage would be sufficient for a large-scale PFAS cleanup project.

In June 2021, Niagara County adopted an Extended Producer Responsibility (EPR) law to protect their landfills from being overburdened by the disposal of solar panel waste. The law requires "producers of solar panels sold in the county to finance and manage their safe reuse and recycling when decommissioned."[37] Phone calls to Greene and Columbia county landfills have not provided confirmation that they will accept large quantities of solar panels, either today or in the future. One company suggested contacting We Recycle Solar, which is located in Arizona. State and federal laws for PFAS are

---

[35] https://repository.lboro.ac.uk/articles/journal_contribution/Testing_the_durability_of_anti-soiling_coatings_for_solar_cover_glass_by_outdoor_exposure_in_Denmark/11558853

[36] https://hbr.org/2021/06/the-dark-side-of-solar-power

[37] https://www.productstewardship.us/news/571089/Niagara-County-Passes-Nations-2nd-Solar-Panel-Producer-Responsibility-Law.htm

likely to become more numerous and stringent. The town and county should consider the possibility of PFAS contamination from solar panels deposited in our local landfills and require developers to prove that their installations will not include products containing PFAS.

Industry Response

Manufacturers of ARC and ASC may understand the environmental concerns and toxicity risks of their products. A few companies are beginning to provide non-toxic coatings. One company's solution is a proprietary nanoparticle coating that is an environmentally friendly.

> WattGlass has addressed and overcome many of the issues typical of other antireflective coatings (ARCs): things such as toxicity, shelf life, and durability. WattGlass is happy to offer a non-toxic, water based, long shelf-life solution to existing ARC technologies that is easily implemented as a drop in replacement.[38]
>
> Solar ARC surpasses the performance of conventional coatings and is resistant to particulate soiling while remaining non-hazardous and 100% water-based. Typically, these coatings result in tradeoffs between performance and functionality and utilize hazardous materials such as solvents, acids, and fluorocarbons. Not with WattGlass.

If Watt Glass feels it is important to stress their environmentally friendly non-fluorocarbon solution again and again, it raises the obvious question: what are the other companies using, and how might their products harm our soil, water, and public health?

What's next

On August 19, 2021, OxyChem announced that it was closing its Niagara Falls plant, the site of America's first major environmental disaster, Love Canal. In 1988, NYS Department of Health Commissioner David Axelrod called the Love Canal incident a "national symbol of failure to exercise a sense of concern for future generations."[39]

Solar energy resources are marketed as an environmentally-friendly way to generate electricity. However, research indicates that solar panels, coatings, wire coverings, tapes, adhesives and batteries contain PFAS that may permanently harm our soils and poison our drinking water.

---

[38] https://www.wattglass.com/technology

[39] https://www.nytimes.com/1988/08/05/nyregion/after-10-years-the-trauma-of-love-canal-continues.html

An October 2020 Bloomberg Law article provides insight into upcoming PFAS regulations in relation to the Development of renewable energy in New York State.

> Overall, along with the CLCPA, the new Siting Law and the expected PFAS regulations fundamentally change long-standing environmental paradigms in New York State. The flurry of regulations expected from Albany in the next few years will usher in a new era of environmental regulation quite different from today. Those well prepared for the transition will be positioned to prosper from it, while those who are not will fall behind or find their business plans or goals outdated or not fully achievable.[40]

Conclusions

Renewable energy developers are responsible to their investors. Not the town. Not the neighbors. And not the environment. Solar projects are held by individual LLCs whose only asset may be an aging infrastructure built on leased ground. At time of decommissioning—or evidence of contaminants—it is unlikely that there will be a deep-pocketed corporation to bring the site into compliance with current or future EPA and DEC standards.

The July 2021 ruling on the Fieldwood Energy, LLC bankruptcy case sets precedent that previous oil well owners, and the insurance companies that issue them bonds, are responsible for the cleanup cost of wells.[41] Insurance company trends with oil and gas may become the standards for the renewable energy sector, making it difficult and costly to insure solar power plants.

Prior to construction, Hecate Energy should be held responsible to neighboring residents and Coxsackie's municipal government by providing documentation that the solar panels, coatings, and electrical infrastructure specified for the project do not contain PFAS or other toxic chemicals. Attempting to remedy a "forever chemical" such as PFAS contamination over more than a thousand acres of solar coverage would likely be impossible.

While there are a few alternative options that may be safer, these products are more expensive and are manufactured in smaller quantities. Utility-scale solar power plants require hundreds of thousands, if not millions, of photovoltaic panels at the time of installation. The ability to manufacture and deliver this quantity is limited to the very largest

---

[40] https://news.bloomberglaw.com/environment-and-energy/impact-of-new-yorks-renewable-energy-permitting-program-pfas-regulation

[41] https://www.bondexchange.com/oil-industry-woes-lead-to-massive-changes-in-the-insurance-industry/

suppliers, most of them based in China, where Material Data and Safety Sheets are limited and if provided the information is questionable.

Reputable solar panel manufacturing companies that freely provide Material Data and Safety Sheets may be limited. Solar developers that provide toxicity guarantees on their panels being free of dangerous chemicals may be even fewer. While the level of toxicity of ARC and ASC may lack clarity, the coatings' exposure to the elements and where the sloughed-off chemicals will be deposited is not. The chemicals are likely to enter the soil and groundwater.

When reviewing this Application, the Siting Board must not rely on good intentions. As has been noted throughout this proceeding, multiple solar projects will be constructed in the watershed of Sleepy Hollow Lake. Measures should be taken to determine that panels, electrical infrastructure, and wiring for these projects is PFAS-free.

What we are discussing here is a matter of public health and safety, we encourage the Board to require developers to provide specification sheets, and to describe preventive measures, testing policies, and Material and Data Safety Sheets in order to protect Coxsackie public health and to protect the town from future liability. Preventative measures—not after-the-fact remediation—are the answer to avoiding PFAS contamination of soil, stormwater runoff, drinking water, and aquifers surrounding the project.

Environmental Research 176 (2019) 108540

Contents lists available at ScienceDirect

Environmental Research

journal homepage: www.elsevier.com/locate/envres

High exposure to perfluorinated compounds in drinking water and thyroid disease. A cohort study from Ronneby, Sweden☆

Eva M. Andersson[a,b,*], Kristin Scott[c], YiYi Xu[a], Ying Li[a], Daniel S. Olsson[d,e], Tony Fletcher[f], Kristina Jakobsson[a,b]

[a] Institute of Medicine, Sahlgrenska Academy, University of Gothenburg, Sweden
[b] Occupational and Environmental Medicine, Sahlgrenska University Hospital, Gothenburg, Sweden
[c] Occupational and Environmental Medicine, Faculty of Medicine, Lund University, Sweden
[d] Department of Internal Medicine and Clinical Nutrition, Institute of Medicine, Sahlgrenska Academy, University of Gothenburg, Sweden
[e] Department of Endocrinology, Sahlgrenska University Hospital, Gothenburg, Sweden
[f] London School of Hygiene and Tropical Medicine, London, United Kingdom

ARTICLE INFO

Keywords:
Per- and polyfluoroalkyl substances (PFAS)
Drinking water
Thyroid disease
Cohort study
Register study

ABSTRACT

Per- and polyfluoroalkyl substances (PFAS) are extremely persistent manmade substances. Apart from exposure through food and indoor air and dust, humans can be exposed through drinking water if the surface or groundwater is contaminated. In 2013 very high levels of PFOS and PFHxS were found in the drinking water from one of the two waterworks supplying the municipality of Ronneby, Sweden.

A cohort was formed, including all individuals who had lived at least one year in Ronneby during the period 1980–2013 (ñ63,000). Each year, addresses that got their drinking water from the contaminated water works were identified. Through the Swedish personal identity number, each individual was linked to registers providing diagnoses and prescriptions for hyper- and hypothyroidism.

In total, 16,150 individuals had ever been exposed. The hazard ratios did not indicate any excess risk of hyperthyroidism among those with contaminated water. For hypothyroidism, the risk of being prescribed medication was significantly increased among women with exposure during the mid part of the study period (but not men). However, the association with period of exposure was non-monotonic, so the significance is considered to be a chance finding. Our research was limited by the relatively simple exposure assessment.

1. Introduction

Per- and polyfluoroalkyl substances (PFAS) are manmade substances, first produced in the 1940s. The widespread use of these substances, which are extremely persistent, resisting both physical and biological degradation, has led to global environmental contamination. The primary sources of PFAS exposure in humans are food and indoor air and dust; but also drinking water may contribute, Boiteux et al. (2012), Ericson et al. (2009), Hu et al. (2019). Contamination from production facilities and firefighter training locations has led to substantial exposure through drinking water in localized general populations, Steenland et al. (2009), Guelfo and Adamson (2018) and Ingelido et al. (2018).

The impact of PFAS on wildlife and humans is inadequately understood. Animal experiments have shown effects on the reproductive, immune and hormone systems, and on blood lipids and liver function. Both acute studies and repeated dose toxicity studies have shown that perfluorooctane sulfonate (PFOS) decreased the serum levels of thyroid hormones triiodothyronine (T3) and thyroxine (T4), Knutsen et al. (2018) and the US National Toxicology Program has concluded that perfluorohexane sulfonic acid (PFHxS) induced decreased thyroid hormone levels, Minnesota Department of Health (2019). Epidemiological studies, mainly with (low) exposure levels that are prevalent in the general population, indicate that there may also be effects in humans. Recently, the European Food Safety Authority published a provisional scientific opinion where the preliminary tolerable weekly intake was set as low as 13 ng/kg body weight per week for PFOS and 6 ng/kg body weight per week for perfluorooctanoate (PFOA), Knutsen et al. (2018).

The associations between PFAS exposure and alterations of mechanisms involved in thyroid homeostasis are complex, and PFAS have

☆ The authors declare they have no actual or potential competing financial interests.

* Corresponding author. Occupational and Environmental Medicine, PO Box 440, SE 405 30 Goteborg, Sweden.
E-mail address: eva.m.andersson@amm.gu.se (E.M. Andersson).

https://doi.org/10.1016/j.envres.2019.108540
Received 12 April 2019; Received in revised form 14 June 2019; Accepted 15 June 2019
Available online 18 June 2019

been indicated to interfere at several levels, but knowledge of the effects and underlying mechanisms is still limited.

Several cross-sectional studies exploring the associations between different per- and polyfluoroalkyl substances and thyroid hormones have been performed in general populations with low exposure levels, but overall, findings on alterations to hormonal levels are not consistent, Knutsen et al. (2018). Regarding actual thyroid disease, only a few studies are available. Analysis of data from the U.S. National Health and Nutrition Examination Survey (NHANES) showed an association between self-reported currently treated thyroid disease and serum perfluorooctanoate (PFOA) in females, and a similar association with serum perfluorooctane sulfonate (PFOS) was reported for males, Melzer et al. (2010). In another NHANES-based study, positive associations between PFOS-levels and subclinical hypothyroidism were observed in men and women; for PFOA (and PFHxS) in women only, Wen et al. (2013). The American C8 population has high exposure to PFOA in drinking water from a chemical production plant: median serum level 28 ng/mL, and for the water district closest to the plant it was 224 ng/mL, Steenland et al. (2009). In contrast, serum levels for PFOS and PFHxS were comparable to those in the general US population, Gallo et al. (2013), Webster et al. (2016). In the main C8 cohort study, including over 32,000 subjects, there was some evidence of increasing hazards with increasing modelled PFOA exposure, both for hyper- and hypothyroidism, strongest among women, Winquist and Steenland (2014).

In summary, knowledge of the effects and underlying mechanisms of PFAS on thyroid function and thyroid disease in human are still limited. Knowledge on causal associations between environmental contaminants and health outcomes is important for public health and for regulatory purposes, but also for risk communication in communities that actually have had high exposure. The C8 studies have provided information regarding thyroid outcomes after high exposure to PFOA, but hitherto no studies have explored the risk after high exposure to PFOS and PFHxS.

The aim of this study is to elucidate the association between historical exposure to PFAS and the incidence of thyroid disease in a general population with long-term high exposure to PFHxS, PFOS and to a lesser extent PFOA through drinking water.

2. Materials and methods

2.1. Study area

In December 2013 high levels of PFAS were detected in one out of two waterworks in Ronneby, Sweden, a municipality with 28,000 inhabitants: PFOS and PFHxS levels in the contaminated water works were 8000 and 1700 ng/L, compared to 27 and 4.6 ng/L in the uncontaminated water works, Li et al. (2018a). The source of contamination was fire fighting foams (Aqueous Film-Forming Foam, AFFF) used since the mid-1980s at a military air field practice site, located approximately 2 km from the waterworks. When the contamination was discovered in December 2013, clean water was promptly provided from the other waterworks. However, the exposed population will have elevated internal body burden of PFAS for decades, due to the long half-lives, Li et al. (2018a). Biomonitoring in the population has revealed very high serum level of PFHxS, PFOS and to a lesser extent PFOA: median levels were 257 ng/mL (PFHxS), 280 ng/mL (PFOS) and 15 ng/mL (PFOA) in the group with late exposure (contaminated water at home at least one year during 2005–2013), Supplemental Material Tables S1 and S2. The contaminated waterworks supplied 1/3 of the households. One area (Kallinge) was supplied from the contaminated waterworks during the entire study period.

2.2. The cohort

The cohort consists of everyone ever registered as living in Ronneby municipality during 1980–2013 (63,074 persons, 33,218 men and 29,856 women). Information on the registered yearly addresses, vital status, and emigration were obtained from Statistics Sweden (www.scb.se). Information on education level, a time-varying variable, was available from Statistics Sweden for almost 80% (49,570) of the cohort members, at least for some years in the study period.

This is an open (dynamic) cohort, defined as people who have lived in Ronneby municipality at any time during the time period 1980–2013. A person's follow-up is censored at the event (diagnosis or prescription), at emigration or at death. Since the date for both diagnosis and prescription is based on the personal identity number and national registries, the study method will collect a person's first event no matter where they reside in Sweden. Thus, every person who once was registered as residing in Ronneby will be followed until censored or end of study follow-up.

2.3. Exposure assessment

The municipal water company provided information on yearly water distribution which was linked to the individual's yearly address data. Thus, for each year (1980–2013) we know which residential addresses were provided with water from the contaminated waterworks. Extensive testing of private wells have not disclosed high PFAS levels; thus, addresses without municipal water supply were assumed to have uncontaminated water, as were residences outside Ronneby municipality. Statistics Sweden also provided address for the work place for subjects gainfully employed, thus providing information about water supply at work. However, in many cases the work place address reflects the administrative address, rather than the individual's actual work place. Since the data quality for residential address was much better than work place address, the main results will be for exposure at residential address.

There is no clear information on start of the drinking water contamination; i.e. when the contaminated ground water plume reached the water wells. At present we have tentatively set 1985 as start of exposure, based on information on the use of AFFFs at the airfield. A dichotomous exposure variable was defined as "not exposed at home" all years when the person lived at unexposed address, and "ever exposed" from first year that the person moved to an exposed address.

We consider that PFAS levels in the drinking water were lowest during the early part of the observation period. The drinking water exposure for the same individual can differ over time since individuals can move, both within Ronneby and in/out of Ronneby. Thus, in addition, a four-category time-based variable was defined. Exposure during different decades was denoted as "not exposed" (1980–1984), "early" (1985–1994), "mid" (1995–2004) and "late" (2005–2013). A person's exposure classification could change over time. "Exposed" during a decade was defined as living at least 1 year at an address with PFAS contaminated water (individuals with private wells excluded). "Not exposed" during a decade was defined as never living at address with PFAS contaminated water (Supplemental Material Table S3).

The PFAS serum levels in 3475 subjects from Ronneby (sampled in 2014–16) were used to compare the categories "not exposed" and "ever exposed, Li et al. (2018a). The participants' self-reported yearly addresses were linked to water distribution data. By exposure group, there were marked differences between subjects in Ronneby who never lived in the contaminated area (median for PFOS and PFHxS was below 60 ng/mL, and median PFOA was ≤5 ng/mL) and subjects in Ronneby living at least a year in the contaminated area (median for PFOS was above 200 ng/mL, median for PFHxS was above 170 ng/mL, and median PFOA around 12 ng/mL), but the inter-individual variation within the exposure groups was high (Supplemental Material Tables S1 and S2).

2.4. Outcome

All information on outcomes was obtained from the National Board of Health and Welfare (www.socialstyrelsen.se), using the personal identity number for linkage to the cohort data. The end of follow-up is 2013-12-31. The cause-of-death register, in function since 1961, includes all people registered in Sweden (both in-country and out of country deaths). Stillborns are not included. Diagnoses are given using ICD (International Classification of Disease) codes, version 8, 9 and 10. The Swedish National Patient Register includes all in-patient care in hospitals from 1987. Since 2001, the register also contains outpatient hospital visits from both private and public care givers. Validation of the inpatient register has shown a high validity for many diagnoses, Ludvigsson et al. (2011). The Swedish Prescribed Drug Register started in mid-2005. It covers all prescribed drugs sold and dispensed at Swedish pharmacies to patients with a personal identity number. Information about the prescription including Anatomic Therapeutic Chemical (ATC) code, date of prescription, the cost, the date of dispensing and the prescriber and their workplace is available. Data from the first year identifies both ongoing and new prescriptions, thus we only used data from 2006 to reflect new prescriptions.

The Prescribed Drug Register also has information on prescriptions from each primary health care (PHC) unit. We obtained aggregated yearly data on the total number of patients with prescription (who also purchased the medication) for hyperthyroidism and hypothyroidism respectively, for the period 2009–2016. Data were from the PHC unit in the hot-spot area (Kallinge), and from the three PHC units in other areas of Ronneby with no or only partial drinking water supply from the contaminated waterworks. Prescription data from three PHC units in Karlshamn, a nearby municipality with non-contaminated water, was also obtained. The number of registered patients at each PHC unit per year was obtained from Region Blekinge.

For *hyperthyroidism* we included diagnoses ICD8/9: 242 and ICD10: E05, Supplemental Material Table S4. When defining a diagnosis event, both primary and secondary diagnoses were taken into account. Correspondingly, both primary and secondary causes of death were used. For prescriptions we included ATC: H03B, Supplemental Material Table S4. All the information available for events indicating hyperthyroidism was scrutinized independently by two physicians (DSO, ass. Professor in Endocrinology, and KJ, specialist on occupational and environmental medicine). Eight cases, due either to thyroiditis during pregnancy or a probable false coding, were disregarded. There were 456 persons with a diagnosis, 171 persons with a prescription and 158 persons with both (Table 1).

We assumed that even if patients may be diagnosed at a PHC unit, they regularly were referred to endocrinologists for treatment. Thus, from 2001, the combination of in-patient- and out-patient data from hospitals likely captures most cases of hyperthyroidism without substantial delay. For the period before 2001, covered only by in-patient data, there may be cases entirely missing, and cases identified through secondary diagnosis are likely to have had an earlier start of disease. Identification of hyperthyroidism based on prescription data alone is not meaningful, since patients treated with radio-active iodine or thyroidectomy will not be identified. Therefore a combination of any event from 2006 is considered to have the best coverage, but the drawback is a too limited number of cases due to the short observation time and the low incidence of the disease. Our predetermined priority order for analysis of hyperthyroidism is 1) first of any event (diagnosis or prescription) and 2) first diagnosis.

For *hypothyroidism* we included diagnoses ICD8/9: 243–244 except 244.00 and ICD10: E01-E03, Supplemental Material Table S4. All diagnoses, not only primary diagnosis, were used for defining a diagnostic event. Correspondingly, both primary and secondary causes of death were used. For prescriptions we include ATC: H03A, Supplemental Material Table S4. If a hyperthyroidism event preceded a diagnosis or prescription indicating hypothyroidism, or if a diagnosis of radioiodine treatment or dysthyroid exophthalmos was present, the hypothyroidism case was assumed to be secondary to hyperthyroidism, and disregarded after careful scrutinization of all available data (74 cases). In the analysis (the period 2006–2013), there were 642 persons with a diagnosis, 1240 persons with a prescription and 283 persons with both (Table 2).

For hypothyroidism, we assumed that patients usually were diagnosed at PHC units, and usually not referred to endocrinologists for treatment. Many cases of hypothyroidism are likely to appear as secondary diagnoses in patients seeking care for other reasons. The combination of in-patient and out-patient data from hospitals from 2001 will capture some, but not all, cases of hypothyroidism. Thus, most cases identified in the patient registries have an earlier start of their disease, and this will be even more so during the period with only in-patient data. This also means that both the duration of exposure and the exposure at the time of diagnosis can be overestimated. Prescription data correctly identifies medical treatment for hypothyroidism from 2005, but only new prescriptions from 2006 can be included for analysis of incidence. Our predetermined priority order for analysis of hypothyroidism is 1) first prescription from 2006, to 2) first of any event (diagnosis or prescription) from 2006.

2.5. Statistical analysis

The association between thyroid disease and exposure to PFAS in drinking water (defined as living at an address with municipality water from the contaminated waterworks) was estimated using a Cox proportional hazards model with calendar year on the time axis, and.

exposure (two or four categories) and age as explanatory variables (and, in one sensitivity analysis, educational level). A test of trend in exposure was performed by including the exposure variable as a linear

Table 1
The Ronneby cohort (individuals ever living in Ronneby, 1980–2013). Number of cases and crude incidence (cases per 100,000 per year) of hyperthyroidism for different calendar years. Primary diagnoses (p) are given in parenthesis.

			Calendar year at event							
			80–84	85–89	90–94	95–99	00–04	05 [a]	06–09	10–13
Diagnosis										
Men	Cases (p)	8 (6)	9 (6)	4 (2)	8 (6)	26 (20)	5 (4)	15 (12)	26 (20)	
	Incidence	10.2	10.7	4.4	8.1	24.3	22.3	16.0	26.4	
Women	Cases (p)	11 (7)	20 (14)	28 (18)	34 (20)	76 (60)	12 (10)	76 (64)	98 (80)	
	Incidence	14.7	24.9	32.2	36.5	76.4	58.0	88.9	109.9	
Prescription										
Men	Cases	–	–	–	–	–	7	10	16	
	Incidence	–	–	–	–	–	31.2	10.7	16.3	
Women	Cases	–	–	–	–	–	23	54	61	
	Incidence	–	–	–	–	–	111.2	63.3	68.7	

[a] Prescription register started in 2005.

Table 2
The Ronneby cohort (individuals ever living in Ronneby, 1980–2013). Number of cases and crude incidence (cases per 100,000) of hypothyroidism for different calendar years. Primary diagnoses (p) are given in parenthesis.

		Calendar year at event							
		80–84	85–89	90–94	95–99	00–04	05 [a]	06–09	10–13
Diagnosis									
Men	Cases (p)	0 (0)	5 (2)	4 (2)	6 (1)	19 (8)	3 (0)	42 (6)	106 (11)
	Incidence	0	6.0	4.4	6.1	17.8	13.4	44.7	107.7
Women	Cases (p)	7 (1)	19 (1)	22 (4)	33 (2)	82 (41)	16 (7)	177 (34)	317 (40)
	Incidence	9.3	23.7	25.3	35.5	82.4	77.4	207.1	355.4
Prescription									
Men	Cases	–	–	–	–	–	235	137	161
	Incidence	–	–	–	–	–	1048.4	147.6	166.2
Women	Cases	–	–	–	–	–	1047	455	487
	Incidence	–	–	–	–	–	5063.8	564.3	587.6

[a] Prescription register started in 2005.

effect. The proportionality assumption was tested by testing if the interaction term, exp*calendar_year, was significant ($p < 0.05$) (PROC PHREG in SAS 9.4 was used).

All analyses were performed separately for men and women. A minimum of 10 cases per stratum was required for any analysis. The following sensitivity analyses were performed.

I. The water supply at the work place address was also considered, i.e. "exposed" was defined as someone who had contaminated municipality water either at their residential address or at their work place address.
II. The highest educational level was included as a covariate in the analyses (cohort restricted to subjects 30 yrs and older).
III. Secondary in- and outpatient-diagnoses and secondary causes of death were excluded, aiming to capture only incident disease, not prevalent diseases with first diagnosis from PHC or private care.
IV. In a set of alternative analyses, age was replaced by calendar year on the time axis and the three decades (1985–1994, 1995–2004, 2005–2013) were allowed to have difference baseline hazards (subcommand STRATA).

An ecological comparison of number of patients with prescriptions (where the patient purchased the medication) for hyperthyroidism (ATC = H03B) or hypothyroidism (ATC = H03A) was made between Kallinge (one PHC unit), the rest of Ronneby municipality (three PHC units) and Karlshamn (three PHC units). A generalized linear model was used to analyze yearly aggregated prescription data (total number of registered patients as an offset variable, Poisson distribution, log link, PROC GENMOD in SAS 9.4).

2.6. Ethics approval

The study has ethical approval from the ethics Committee at Lund University, Sweden (dnr 2014/267 and 2015/902).

3. Results

The Ronneby cohort comprises in total 63,074 subjects (47% women). There were 456 individuals diagnosed with hyperthyroidism and 171 individuals with a prescription. Further there were 858 individuals diagnosed with hypothyroidism and 2522 with a prescription. Characteristics of the cohort before start of the exposure (1980), at approximate start (1985), during the study period (1995 and 2005) and at the end of the study period (2013) are given in Table 3.

Table 3
The Ronneby cohort (individuals ever living in Ronneby, 1980–2013), the entire study period (1980–2013) and at different calendar years.

		All	Men	Women
Entire period	Number of persons	63,074	33,218	29,856
	Ever exposed persons, either at home or at work/school (starting −85)	21,115	11,406	9709
	Ever exposed persons at home (starting −85)	16,150	8327	7823
	Ever exposed persons at work/school (starting −85)	11,884	6860	5024
	Person years from −80	1,303,876	673,859	630,017
	Hyperthyroidism, diagnosis/death	456	101	355
	Hyperthyroidism as primary diagnosis/cause of death	349	76	273
	Hyperthyroidism, prescription	171	33	138
	Hypothyroidism, diagnosis/death	858	185	673
	Hypothyroidism as primary diagnosis/cause of death	160	30	130
	Hypothyroidism, prescription	2522	533	1989
1980	Number of persons	29,478	15,087	14,391
	Age (mean,std)	39.6; 23.3	38.1; 22.8	41.1; 23.8
	Children < 18 yrs (%	22.5%	23.7%	21.3%
	Ever exposed at home	None	None	None
	Ever exposed at home or work	None	None	None
	Ever exposed at work/school	None	None	None
1985	Number of persons	32,042	16,378	15,664
	Age mean std	40.2; 23.2	38.8; 22.6	41.7; 23.8
	Children < 18 yrs (%)	19.8%	20.8%	18.8%
	Ever exposed at home	5100	2582	2518
	Ever exposed at home or work	5613	2967	2646
	Ever exposed at work/school	1690	1068	622
1995	Number of persons	37,254	19,125	18,129
	Age	40.4; 22.5	39.1; 21.7	41.8; 23.2
	Children < 18 yrs (%)	16.7%	17.3%	16.0%
	Ever exposed at home	8658	4419	4239
	Ever exposed at home or work	10,556	5717	4839
	Ever exposed at work/school	4965	3069	1896
2005	Number of persons	43,092	22,416	20,676
	Age	41.6; 21.6	40.5; 20.9	42.9; 22.3
	Children < 18 yrs (%)	14.1%	14.3%	13.9%
	Ever exposed at home	10,837	5543	5294
	Ever exposed at home or work	14,670	7904	6766
	Ever exposed at work/school	8863	5114	3749
2013	Number of persons	47,672	24,949	22,723
	Age	43.1; 21.6	42.3; 20.9	44.0; 22.3
	Children < 18 yrs (%)	13.6%	13.4%	13.9%
	Ever exposed at home	13,267	6809	6458
	Ever exposed at home or work	17,795	9569	8226
	Ever exposed at work/school	10,962	6229	4733

3.1. Hyperthyroidism

The crude incidence of hyperthyroidism is higher among women (Table 1). The marked increase in incidence after year 2000 is explained by inclusion of hospital out-patients. Similarly, the spuriously high "incidence" in prescriptions in 2005 (start year for the register) is

Table 4
The Ronneby cohort (individuals ever living in Ronneby, 1980–2013). Result of Cox proportional hazard regression for any event (first of diagnosis or prescription) and diagnosis (morbidity or mortality) of hyperthyroidism during the period 1980–2013. Exposure (PFAS-contaminated water at home address) was classified into two or four classes.

Outcome		Exposure class [b]	Cases	Person years	HR [c]	95% CI
Primary	Any event [a]					
	Men	Not exposed	87	535,513	1	
		Ever exposed	18	137,364	0.74	0.44–1.23
	Women	Not exposed	286	496,529	1	
		Ever exposed	76	130,657	0.85	0.66–1.09
	Men	Not exposed	87	535,513		
		Early	3	53,054		
		Mid	6	48,637		
		Late	9	35,673		
	Women	Not exposed	286	496,529	1	
		Early	26	50,961	1.12	0.74–1.69
		Mid	24	45,758	0.76	0.50–1.17
		Late	26	33,938	0.74	0.49–1.12
Secondary	Diagnosis					
	Men	Not exposed	83	536,315	1	
		Ever exposed	18	137,544	0.78	0.47–1.31
	Women	Not exposed	280	498,641	1	
		Ever exposed	75	131,376	0.86	0.66–1.11
	Men	Not exposed	83	536,315		
		Early	3	53,155		
		Mid	6	48,657		
		Late	9	35,732		
	Women	Not exposed	280	498,641	1	
		Early	26	51,109	1.14	0.75–1.71
		Mid	24	46,072	0.77	0.50–1.18
		Late	25	34,195	0.74	0.48–1.13

[a] First event of diagnosis (morbidity or mortality) or prescription.
[b] Classification according to Table 1.
[c] Calendar year on time axis and age (0–25, 26–50, 51–75, 76- yrs) included. HR:s not presented for fewer than 10 events.

the result of a combination of new and repeated prescriptions (thus presented separately). The incidence of hyperthyroidism increased with age in both sexes (Supplemental Material Table S5).

There was no increased hazard ratio (HR) for hyperthyroidism, neither in men nor in women, among subjects ever living in the contaminated water district, Table 4. The pattern was similar for the combination of diagnoses and prescription, and diagnoses alone. Similarly, the subgroup with late (and highest) drinking water exposure did not display an increased risk for hyperthyroidism for men, HR = 1.08 (95% CI 0.52-2.23, only 9 cases thus not in the table), or for women, HR = 0.74 (95% CI 0.48-1.13). The results of the tests of the interaction terms were that the assumption of proportionality did hold.

When defining exposure as either at home or at work, the patterns were similar to Table 4, with no increased risk for those who were exposed late in the study period (2005–2013), see Supplemental Material Table S6. In the regression models that included the highest attained education level (cohort members above age 30, Supplemental Material Table S7), the HR pattern was similar to that of Table 4, where education level was not included. In 349 out of 456 diagnoses (77%), hyperthyroidism was the primary diagnosis. The HR patterns were similar when analyzing the primary diagnosis as when analyzing all diagnoses, Supplemental Material Table S8. When the analysis was made with age on the time axis, the results were almost identical to those with calendar year on the time axis, Supplemental Material Table S9.

From the Prescription Register, data were available on the number of patients with medication for hyperthyroidism prescribed at the PHC unit in Kallinge (hotspot area), the rest of Ronneby municipality, or in the neighbouring municipality Karlshamn: during the period 2009–2016 in all 12, 57 and 124 persons, respectively. It should be noted that a single person can contribute to these numbers more than once. Each year, approximately 8000 patients were registered at the PHC unit in Kallinge, 19,500 in the rest of Ronneby and 31,000 in Karlshamn. Regression analysis showed a possibly lower incidence in Kallinge compared to Karlshamn among women (approximately half the incidence, p = 0.06). There were no identified prescriptions among men from Kallinge PHC unit (Fig. 1).

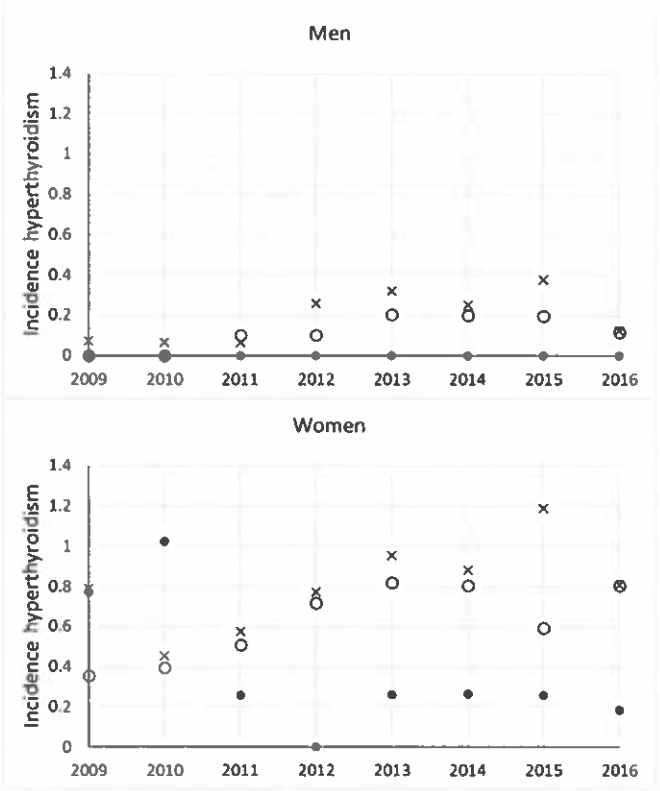

Fig. 1. Prescription data from health care units 2009–2016. The number of patients with a hyperthyroidism prescription (H03B) per 1000 registered patients, among men and women in Kallinge (●, hot spot area in Ronneby), the rest of Ronneby (○) and Karlshamn (×).

3.2. Hypothyroidism

The crude incidence of hypothyroidism is higher among women (Table 2). The marked increase in incidence after year 2000 is explained by inclusion of hospital out-patients. Similarly, the spuriously high "incidence" in prescriptions in 2005 is the result of a combination of new and repeated prescriptions as these numbers catches prevalence rather than incidence. The incidence increased with age in both sexes (Supplemental Material Table S10).

There was no significantly increased HR for hypothyroidism, neither in men nor in women, among subjects ever living in the contaminated water district, for the two most valid outcomes, prescriptions, or a combination of diagnoses and prescriptions during the 2006–2013 (Table 5). Similarly, the subgroup with late (and highest) drinking water exposure did not display an increased risk for hypothyroidism, neither in men nor women (HR for prescriptions were 0.89 (95% CI 0.65-1.22) and 0.96 (95% CI 0.81-1.15)). In contrast, in women with contaminated drinking water at home any time between 1985 and 2004 (combining early and mid), the HR for any event was increased, 1.29 (95% CI 1.05-1.57). However the group with the latest exposure, considered to have the highest exposure, did not show elevated risk in spite of larger numbers and narrower confidence interval, HR = 0.94, (96%

Table 5
The Ronneby cohort (individuals ever living in Ronneby, 1980–2013). Result of Cox proportional hazard regression for prescriptions and any event (first of diagnosis or prescription) of hypothyroidism during the period 2006–2013. Exposure (PFAS-contaminated water at home address) was classified into two or four classes.

Outcome (2006–2013)		Exposure class [a]	Cases	Person years	HR [b]	95% CI
Primary	Prescription					
	Men	Not exposed	229	140,765	1	
		Ever exposed	69	48,901	0.90	0.69–1.18
	Women	Not exposed	679	119,509	1	
		Ever exposed	263	44,013	1.09	0.94–1.25
	Men	Not exposed	229	140,765	1	
		Early	5	7346		
		Mid	18	9483	1.39	0.86–2.26
		Late	46	32,072	0.89	0.65–1.22
	Women	Not exposed	679	119,509	1	
		Early	52	6860	1.26	0.95–1.67
		Mid	61	8137	1.35	1.04–1.76
		Late	150	29,016	0.96	0.81–1.15
Secondary	Any event [c]					
	Men	Not exposed	230	140,761	1	
		Ever exposed	70	48,896	0.91	0.70–1.19
	Women	Not exposed	679	119,451	1	
		Ever exposed	258	43,968	1.06	0.92–1.23
	Men	Not exposed	230	140,761	1	
		Early	5	7346		
		Mid	18	9483	1.40	0.86–2.26
		Late	47	32,067	0.90	0.66–1.23
	Women	Not exposed	679	119,451	1	
		Early	53	6857	1.29	0.97–1.70
		Mid	58	8133	1.28	0.98–1.68
		Late	147	28,978	0.94	0.79–1.13

[a] Classification according to Table 1.
[b] Calendar year on time axis, age (0–25, 26–50, 51–75, 76- yrs) included. HR:s not presented for fewer than 10 events.
[c] First event of diagnosis (morbidity or mortality) or prescription.

CI 0.79-1.13). The results of the tests of the interaction terms was that the assumption of proportionality did hold.

When defining exposure as either at home or at work (water supply at these addresses), which increased the number of any event in ever exposed men from 70 to 109, and in women from 258 to 332, the patterns were similar to Table 5 (see Supplemental Material Table S11). From the regression models that included the highest attained education level (cohort members above age 30, Supplemental Material Table S12), the HR pattern was similar to that of Table 5, where education level was not included. Only 160 of 858 (19%) had hypothyroidism as the primary diagnosis. Thus, there were too few events for a meaningful sensitivity analysis. When the analysis was made with age on the time axis, the results were almost identical to those with calendar year on the time axis, Supplemental Material Table S13.

From the Prescription Register, data were available on the number of patients with medication for hypothyroidism prescribed at the PHC unit in Kallinge, rest of Ronneby municipality, or in Karlshamn; during the period 2009–2016 in all 2,913, 6569 and 10,109 patients, respectively. Regression analysis showed a possibly higher incidence in Kallinge compared to Karlshamn among men (approximately 20% higher; $p = 0.08$), but no significant difference among women (Fig. 2).

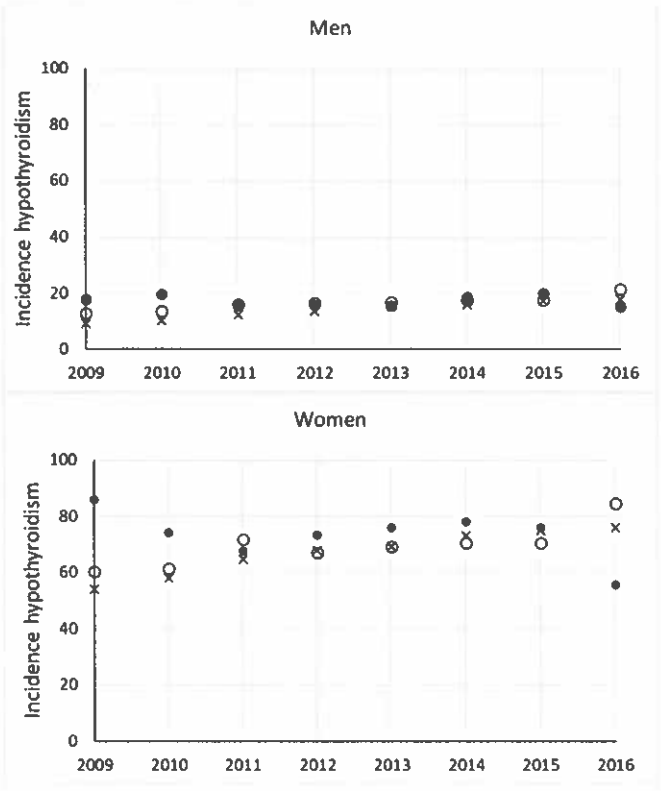

Fig. 2. Prescription data from health care units 2009–2016. The number of patients with a hypothyroidism prescription (H03A) per 1000 registered patients, among men and women in Kallinge (●, hot spot area in Ronneby), the rest of Ronneby (○), and Karlshamn (×).

4. Discussion

In the Ronneby general population cohort, who were exposed to high levels of PFOS, PFHxS and to a lesser extent PFOA, we did not observe an increased risk for clinically detected hyperthyroidism, neither in men nor in women. For hypothyroidism, we did not find any increased risk in the group with ongoing exposure during the last nine years of distribution of contaminated water (2005–2013); this group is indicated to have very high serum levels: above 200 ng/mL for both PFOS and PFHxS. The cohort analyses are based on internal comparisons between groups in Ronneby with different timing of exposure to drinking water. An external comparison, using area-based data on prescriptions, showed no indication of an excess of prescriptions for

hyperthyroidism in the Ronneby municipality; this was indeed more common in the neighbouring municipality (Karlshamn) where exposure to PFAS was no higher than in the general Swedish population. Regarding prescriptions for hypothyroidism, there was a possible slightly higher prescription rate in the hot-spot area in Ronneby (contaminated drinking water during the entire observation period), but only for men.

The study situation can be described as a natural experiment – one third of a population in Ronneby municipality had been exposed to PFAS in municipal drinking water for a long time, without anyone being aware of the contamination. With the personal identity number, we can follow individuals in the registers even when they moved out of Ronneby, as long as they do not emigrate from Sweden. A public health care system, with four primary health care units and two county hospitals, serves the Ronneby municipality. There are no differences between the contaminated and non-contaminated water districts with regard to access to health care, and the Ronneby population is socioeconomically homogenous. We have no reason to believe that cohort members moving out of the municipality, living elsewhere in Sweden, would have differential access to health care related to their previous exposure. Socioeconomic situation was taken into account in the analyses by information on educational level.

One element lacking is the absence of personal exposure information or serum concentrations. Although the registered addresses and water distribution data are very reliable, a person may still live elsewhere, especially so for young people during years of study. The serum PFAS levels in a sample of Ronneby inhabitants, whose homes were supplied from the non-contaminated water works, were higher than in nearby Karlshamn: this finding can be explained by everyday mobility within the municipality and thus access to drinking water from both waterworks. There is, at present, no information on variations on PFAS levels in the distributed water over time and individual water intake can differ markedly. In addition, we have only considered external exposure, whereas true body burden also depends on internal exposure and there is a large inter-individual variation in elimination of PFAS, Li et al. (2018a). This said, our first crude evaluation still gives valuable information on the risk for manifest thyroid disease in the exposed population, especially since there was a marked difference for serum levels of PFAS at a group level between people never having lived in the contaminated area, and those living there between 2005 and 2013. In the future it will be possible to model the exposures in more detail based on ongoing investigations of ground water transportation and environmental samples. The time-varying coverage of the different registries merits careful consideration, and one evident limitation is the short follow-up time for prescribed drugs, as the register was not started until 2005. Another important point is the local health-care seeking pattern, and treatment options for the disease under investigation. For hypothyroidism diagnoses, hospital-based register data are likely not to reflect the real date of incidence, and information from the primary health care, where most of these patients are diagnosed, were not available. A spuriously too late date of diagnosis would tend to move the exposure classification to a later category. However, by using prescription data (without this delay), the possible bias was removed, and in none of the analyses was there a suggestion of an increased risk concentrated in the late exposure period. In contrast, patients with hyperthyroidism are usually referred to the county hospital, and thus registered at a more correct point of time, especially from 2000 and onward.

Previous studies show no consistency regarding the association between thyroid disease and PFAS exposure. Emmett et al (2006) examined a sample of individuals residing in a district with longstanding environmental exposure to PFOA through drinking water, thus all had exposure levels well above those in the general population, and did not find significant increased serum PFOA levels among individuals with a history of self-reported thyroid disease (median serum PFOA was 354 ng/mL). On the other hand, in the C8 study, associations between hypothyroidism and PFOA were indicated, among children (median serum PFOA was 29 ng/mL, Lopez-Espinosa et al. (2012)) and among the male workers at the DuPont plant, producing Teflon (median serum level of PFOA was 113 ng/mL, Steenland et al (2015)). At lower concentrations than in the C8 studies, the NHANES study (general US population) found a higher risk for (self-reported) thyroid disease for serum PFOA levels over 5.7 ng/mL (among women), Melzer et al. (2010). In our study, serum concentrations are not available for all individuals but in a subgroup, the median level of serum PFOA was lower than in the C8 population (17.5 ng/mL) whereas median levels of serum PFOS and PFHxS were very high: 345 and 277 ng/mL, Li et al. (2018a). We have found only a few articles on PFAS and health effects that include thyroid diseases. In a systematic literature review report, Kirk et al (2017), the conclusion was that there is inadequate evidence regarding the association between thyroid disease and PFAS exposure, both among adults, Melzer et al. (2010), Winquist and Steenland (2014) and Steenland et al (2015), but also regarding infants, Kim et al (2016), children, Rappazzo et al (2017), and hypothyroxinemia among pregnant women, Chan et al (2011).

In a sample of the Ronneby cohort (self-selected), serum levels of PFAS were measured along with thyroid hormones. Preliminary results, Li et al. (2018b), suggest that there are no associations between thyroid stimulating hormone (TSH) and any of the substances (PFOA, PFOS and PFHxS). In our study the only suggestion of an excess was for hypothyroidism among women (prescription) who were exposed during the first and second decade only (up to 2005), but the biomarker results for TSH do not support this. One explanation could be that the study groups are slightly different. A meta-analysis on the association between thyroid hormone levels in adults and PFAS showed a positive association between blood PFOS and free T4, and a negative association with total T4, Kim et al (2018), but preliminary results from the Ronneby biomarker study found associations only among pre-pubertal children (between free T3, free T4 and PFAS). Thus, among adults the Ronneby biomarker results are consistent with our register results of no association with PFAS. The number of hyperthyroidism events among children in the register study did not allow a separate analysis.

In conclusion, in the present cohort study using a simple indicator for PFAS exposure through drinking water, i.e. residence address related to water distribution data stratified by date of exposure, we did not observe any consistent pattern of an increased risk of clinically detected thyroid diseases – neither hypothyroidism nor hypothyroidism – in men or in women in Ronneby, where contaminated water was supplied to one-third of the population for decades.

Funding

This research was supported by Formas, Sweden (grant nr 216-2014-1709).

The study has ethical approval from the ethics Committee at Lund University, Sweden (dnr 2014/267 and 2015/902).

CRediT authorship contribution statement

Eva M. Andersson: Methodology, Software, Formal analysis, Writing - original draft, Writing - review & editing. **Kristin Scott:** Project administration, Writing - review & editing. **YiYi Xu:** Writing - review & editing. **Ying Li:** Writing - review & editing. **Daniel S. Olsson:** Validation, Writing - review & editing. **Tony Fletcher:** Methodology, Writing - review & editing. **Kristina Jakobsson:** Conceptualization, Supervision, Writing - original draft, Writing - review & editing, Validation, Funding acquisition.

Acknowledgements

This research was supported by Formas, Sweden (grant nr 216-2014-1709).

Thanks to Kristoffer Martinsson at Occupational and Environmental Medicine, Lund, Sweden who did the work on connecting each address with the correct water work.

Appendix A. Supplementary data

Supplementary data to this article can be found online at https://doi.org/10.1016/j.envres.2019.108540.

References

Boiteux, V., Dauchy, X., Rosin, C., Munoz, J., 2012. National screening study on 10 perfluorinated compounds in raw and treated tap water in France. Arch. Environ. Contam. Toxicol. 63 (1), 1–12.

Chan, E., Burstyn, I., Cherry, N., Bamforth, F., Martin, J., 2011. Perfluorinated acids and hypothyroxinemia in pregnant women. Environ. Res. 111 (4), 559–564.

Emmett, E., Zhang, H., Shofer, F., Freeman, D., Rodway, N., et al., 2006. Community exposure to perfluorooctanoate: relationships between serum levels and certain health parameters. J. Occup. Environ. Med. 48 (8), 771–779.

Ericson, I., Domingo, J., Nadal, M., Bigas, E., Llebaria, X., et al., 2009. Levels of perfluorinated chemicals in municipal drinking water from Catalonia, Spain: public health implications. Arch. Environ. Contam. Toxicol. 57 (4), 631–638.

Gallo, V., Leonardi, G., Brayne, C., Armstrong, B., Fletcher, T., 2013. Serum perfluoroalkyl acids concentrations and memory impariment in a large cross-sectional study. BMJ Open 3, e002414 002410.001136/bmjopen-002012-002414.

Guelfo, J., Adamson, D., 2018. Evaluation of a national data set for insights into sources, composition, and concentrations of per- and polyfluoroalkyl substances (PFASs) in U.S. drinking water. Environ. Pollut. 236, 505–513.

Hu, X., Tokranov, A., Liddie, J., Zhang, X., Grandjean, P., et al., 2019. Tap water contributions to plasma concentrations of poly- and perfluoroalkyl substances (PFAS) in a nationwide prospective cohort of U.S. Women. Environ. Health Perspect. 127 (6) 067006, doi.org/067010.061289/EHP064093.

Ingelido, A., Abballe, A., Gemma, S., Dellatte, E., Iacovella, N., et al., 2018. Biomonitoring of perfluorinated compounds in adults exposed to contaminated drinking water in the Veneto Region, Italy. Environ. Int. 110, 149–159.

Kim, D.-H., Kim, U.-J., Choi, S.-D., Oh, J.-E., 2016. Perfluoroalkyl substances in serum from South Korean infants with congenital hypothyroidism and healthy infants – its relationship with thyroid hormones. Environ. Res. 147, 399–404.

Kim, M., Moon, S., Oh, B., Jung, D., Ji, K., et al., 2018. Association between perfluoroalkyl substances exposure and thyroid function in adults: a meta-analysis. PLoS One 13 (5) e0197244.

Kirk, M., Smurthwaite, M., Bräunig, J., Trevenar, S., D'Este, C., et al., 2017. The Per- and Poly-Fluorinated Alkyl Substances (PFAS) Health Study Systematic Literature Review. Australian National University, Canberra, Australia.

Knutsen, H., Alexander, J., Barregard, L., Bignami, M., Bruschweiler, B., et al., 2018. Risk to human health related to the presence of perfluorooctane sulfonic acid and perfluorooctanoic acid in food. EFSA J. (Eur. Food Saf. Authority) 16 (12), 5194.

Li, Y., Fletcher, T., Mucs, D., Scott, K., Lindh, C., et al., 2018a. Half-lives of PFOS, PFHxS and PFOA after end of exposure to contaminated drinking water. Occup. Environ. Med. 75 (1), 46–51.

Li, Y., Xu, Y., Fletcher, T., Scott, K., Lindh, C., et al., 2018b. Association between Per- and Polyfluoroalkyl Substances (PFASs) and Thyroid Hormones in a High-Exposed Swedish Population. International Society of Exposure Science and the International Society for Environmental Epidemiology, Ottawa, Canada Abstract ISES-ISEE 2018.

Lopez-Espinosa, M.-J., Mondal, D., Armstrong, B., Bloom, M., Fletcher, T., 2012. Thyroid function and perfluoroalkyl acids in children living near a chemical plant. Environ. Health Perspect. 120 (7), 1036–1041.

Ludvigsson, J., Andersson, E., Ekbom, A., Feychting, M., Kim, J.-L., et al., 2011. External review and validation of the Swedish national inpatient register. BMC Public Health 11, 450.

Melzer, D., Rice, N., Depledge, M., Henley, W., Galloway, T., 2010. Association between serum perfluorooctanoic acid (PFOA) and thyroid disease in the U.S. National health and nutrition examination Survey. Environ. Health Perspect. 118 (5), 686–692.

Minnesota Department of Health. www.health.state.mn.us/communities/environment/risk/. **Retrieved May, 2019.**

Rappazzo, K., Coffman, E., Hines, E., 2017. Exposure to perfluorinated alkyl substances and health outcomes in children: a systematic review of the epidemiologic literature. Int. J. Environ. Res. Public Health 14 (7), E691–E712.

Steenland, K., Jin, C., MacNeil, J., Lally, C., Ducatman, A., 2009. Predictors of PFOA levels in a community surrounding a chemical plant. Environ. Health Perspect. 117 (7), 1083–1088.

Steenland, K., Zhao, L., Winquist, A., 2015. A cohort incidence study of workers exposed to perfluorooctanoic acid (PFOA). Occup. Environ. Med. 72, 373–380.

Webster, G., Rauch, S., Ste Marie, N., Mattman, A., Lanphear, B., et al., 2016. Cross-sectional associations of serum perfluoroalkyl acids and thyroid hormones in U.S adults: variation according to TPOAb and iodine status (NHANES 2007-2008). Environ. Health Perspect. 124 (7), 935–942.

Wen, L.-L., Lin, L.-Y., Su, T.-C., Chen, P.-C., Lin, C.-Y., 2013. Association between serum perfluorinated chemicals and thyroid function in U.S. Adults: the national health and nutrition examination Survey 2007–2010. J. Clin. Endocrinol. Metab. 98 (9), E1456–E1464.

Winquist, A., Steenland, K., 2014. Perfluorooctanoic acid exposure and thyroid disease in community and worker cohorts. Epidemiology 25 (2), 255–264.

Journal of Hazardous Materials 428 (2022) 128137

Contents lists available at ScienceDirect

Journal of Hazardous Materials

journal homepage: www.elsevier.com/locate/jhazmat

GenX in water: Interactions and self-assembly

Samhitha Kancharla [a], Aditya Choudhary [b], Ryan T. Davis [b], Dengpan Dong [b], Dmitry Bedrov [b,*], Marina Tsianou [a,*], Paschalis Alexandridis [a,*]

[a] Department of Chemical and Biological Engineering, University at Buffalo, The State University of New York (SUNY), Buffalo, NY 14260-4200, USA
[b] Department of Materials Science and Engineering, University of Utah, 122 South Central Campus Drive, Room 304, Salt Lake City, UT 84112, USA

HIGHLIGHTS

- Complementary molecular simulation and experimental probe of PFAS structure in solution.
- GenX in water above 150 mM associates into small but well-defined micelles.
- Hydration structure and interaction of GenX molecules with water are revealed.
- Capability to predict from first principles GenX micelle formation and structure.
- GenX self-organization informs interactions with various molecules and surfaces.

GRAPHICAL ABSTRACT

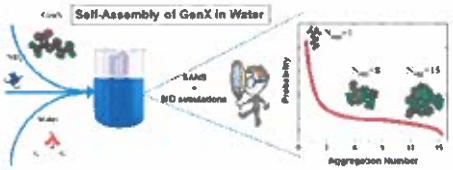

ARTICLE INFO

Editor: Dr. C. LingXin

Keywords:
PFAS
Fluorocarbon
Surfactant
Micelle
Adsorption
Remediation

ABSTRACT

2,3,3,3-tetrafluoro-2-(heptafluoropropoxy) propanoate, a.k.a. "GenX", is a surfactant introduced as a safer alternative to replace perfluorooctanoate (PFOA) in the manufacturing of fluorinated polymers, however, GenX is shown to cause adverse health effects similar to, or even worse than, those of the legacy PFOA. With an overarching goal to understand the behavior of GenX molecules in aqueous media, we report here on GenX micelle formation and structure in aqueous solutions, on the basis of results obtained from a combination of experimental techniques such as surface tension, fluorescence, viscosity, and small-angle neutron scattering (SANS), and molecular dynamics (MD) simulations. To our best knowledge, this is the first report on GenX micelles. The critical micelle concentration (CMC) of GenX ammonium salt in water is 175 mM. GenX forms small micelles with association number 6–8 and 10 Å radius. GenX molecules prefer to align along the micelle surface, and the ether oxygen of GenX has very little interaction with and exposure to water. Information on the surfactant and interfacial properties of GenX is crucial, since such properties are manifestations of interactions between GenX molecules and between GenX and water molecules and, in turn, the amphiphilic character of GenX dictates its fate and transport in the aqueous environment, its interactions with various biomolecules, and its binding to adsorbent materials.

* Corresponding authors.
E-mail addresses: d.bedrov@utah.edu (D. Bedrov), mtsianou@buffalo.edu (M. Tsianou), palexand@buffalo.edu (P. Alexandridis).

https://doi.org/10.1016/j.jhazmat.2021.128137
Received 5 November 2021; Received in revised form 15 December 2021; Accepted 21 December 2021
Available online 3 January 2022

1. Introduction

Per- and polyfluoro alkyl substances (PFAS), also called "Forever Chemicals", are a class of synthetic compounds composed of a carbon chain that is fully or partially fluorinated and can be linear or branched. PFAS comprise fluorinated polymers, surfactants, ethers, esters, alcohols and thiols (Buck et al., 2012; Glüge et al., 2020). A major PFAS subgroup are surfactants that consist of a fluorinated hydrophobic tail and a hydrophilic headgroup. The high electronegativity, low polarizability and small size of fluorine give rise to strong C–F bond, weak $-CF_2-$ intermolecular forces, and strong hydrophobic interactions which, in turn, result in PFAS surfactants exhibiting outstanding properties, including incompatibility with both water and hydrocarbons, high wetting ability, and high chemical and thermal stability (Kissa, 2001; Krafft and Riess, 2015). These properties render PFAS surfactants useful in many applications, including nonstick cookware, food packaging paper, stain repellant and waterproof clothing, paints, cosmetics, and firefighting foams (Buck et al., 2012).

Their widespread use in industrial processes and consumer products has resulted in the release of PFAS into the environment (Alves et al., 2020; Brase et al., 2021; Buck et al., 2011; Prevedouros et al., 2006; Xiao, 2017). PFAS are found in waters around the world (Guelfo and Adamson, 2018; Pan et al., 2018). PFAS concentrations several times higher than the lifetime health advisory (70 ng/L for perfluorooctanoate (PFOA) and perfluorooctane sulfonate (PFOS)) recommended by the U. S. Environmental Protection Agency (EPA) (EPA, 2016) have been detected in drinking water in numerous regions, especially near industrial sites that produce or use PFAS, and near many civilian and military airports that use PFAS-containing aqueous film forming foam (AFFF) (Barzen-Hanson et al., 2017; Dauchy et al., 2017; Sun et al., 2016). The main pathways of human exposure to PFAS are the intake of contaminated water and food, and the migration of PFAS from food packaging (pizza boxes, popcorn bags) or cookware (Domingo and Nadal, 2019; Sunderland et al., 2019). PFAS are distributed predominantly to the liver, blood, and kidney, leading to adverse human health effects such as thyroid dysfunction, immune response suppression, kidney disease, altered cholesterol levels or metabolic diseases, reproductive toxicity, neurodevelopmental problems, and various cancers (Brase et al., 2021; Fenton et al., 2021; Sunderland et al., 2019). Consequently, "legacy" PFAS like PFOA, PFOS, and their related compounds have been banned in many countries, including the U.S., and have been included in the International Stockholm Convention's list of globally restricted Persistent Organic Pollutants (POP) to eliminate their use. In the U.S., EPA is prohibiting companies from manufacturing, processing, or importing products containing certain long-chain PFAS, without prior EPA review and approval (ITRC, 2020).

In response to these restrictions, manufacturers are introducing short chain PFAS and other fluorinated alternatives for commercial applications (Danish-EPA, 2015; Mohamed et al., 2019; Wang et al., 2013). These "emerging" PFAS are categorized into two groups: (i) shorter-chain homologues of long-chain perfluoroalkyl acids and their precursors, e.g., perfluorobutanesulfonic acid, perfluorohexanoic acid, and (ii) functionalized perfluoropolyethers, in particular perfluoroether carboxylic and sulfonic acids (PFECA and PFESA) with acidic functional group attached to a per- or polyfluoroether chain instead of a perfluoroalkyl chain, e.g., GenX from DuPont/Chemours, and ADONA from 3M/Dyneon (Wang et al., 2013).

The tradename "GenX" denotes the PFAS compound ammonium 2,3,3,3-tetrafluoro-2-(heptafluoropropoxy) propanoate (FRD-902) which is the conjugate base ammonium salt of 2,3,3,3-tetrafluoro-2-(heptafluoropropoxy) propanoic acid (FRD-903), introduced by DuPont in 2009 as a safer replacement of PFOA in the manufacturing of fluoropolymers such as Teflon (Beekman et al., 2016; DuPont, 2010). GenX has received significant attention recently owing to it being detected in the environment (Brandsma et al., 2018; Gebbink et al., 2017; Heydebreck et al., 2015; Hopkins et al., 2018; Sun et al., 2016), and thus raising concern over possible adverse health effects. GenX causes health effects similar to those from legacy PFOA and PFOS (Beekman et al., 2016; Gomis et al., 2018), which include changes in cholesterol levels, reproductive problems, cancer, liver and kidney damage (Beekman et al., 2016; Blake et al., 2020; Brase et al., 2021; Chappell et al., 2020; Conley et al., 2021; Coperchini et al., 2020; Shea, 2018; Sun et al., 2019; Wen et al., 2020). EPA's toxicity assessment for GenX just concluded that there is suggestive evidence of carcinogenic potential of oral exposure to GenX in humans, and GenX is more toxic than the PFOA surfactant it was intended to replace (EPA, 2021). EPA set a safe daily dose of GenX as 3 ng/kg of body weight, and plans to develop drinking water health advisories for GenX in spring 2022 (EPA, 2021).

The studies published so far on GenX address analytical techniques (Mullin et al., 2019; Munoz et al., 2019), distribution in rivers and drinking water near fluoropolymer manufacturing plants (Brandsma et al., 2018; Gebbink et al., 2017; Hopkins et al., 2018; Sun et al., 2016), in global surface waters (Heydebreck et al., 2015; Pan et al., 2018) and in human serum and urine (Kato et al., 2018). Also, toxicology studies (Beekman et al., 2016; Brase et al., 2021; Caverly Rae et al., 2015; Conley et al., 2021; Shea, 2018; Sun et al., 2019), mechanisms of toxicity (Chappell et al., 2020; Wen et al., 2020); development of an oral reference dose (Thompson et al., 2019), binding affinity for proteins (Allendorf et al., 2019; Cheng and Ng, 2018), toxicity and bioconcentration in aquatic organisms (Hoke et al., 2016), toxicity comparison to long-chain PFAS (Blake et al., 2020; Gomis et al., 2018), absorption, distribution, metabolism and elimination profiles in mammals (Gannon et al., 2016), effects on cell-viability, proliferation, DNA-damage (Coperchini et al., 2020). Also, adsorption on activated carbons (AC) (Sun et al., 2016; Wang et al., 2019a), anion-exchange resins (Dixit et al., 2020; Wang et al., 2019a, 2019b), functionalized hydrogels (Ateia et al., 2019; Huang et al., 2018), covalent organic frameworks (Ji et al., 2018), and cyclodextrins (CDs) (Weiss-Errico and O'Shea, 2019), and chemical degradation (Bao et al., 2018; Bentel et al., 2020). The adsorption of GenX is inferred to involve anion exchange, electrostatic and hydrophobic interactions, however, no direct evidence has been reported (Wang et al., 2019a). Competitive adsorption experiments on AC and anion-exchange resins (IRA67 and IRA400) showed that the adsorbed GenX can be replaced by the relatively more hydrophobic PFOA (Wang et al., 2019a, 2019b), which was ascribed to "the ether bond in the GenX molecule may cause the instability of the negatively charged head adsorbed on adsorbent surface, leading to the replacement of the adsorbed GenX by PFOA" (Wang et al., 2019b). The charge density of perfluorinated ether acids (PFEAS) reportedly governs their removal via ion exchange (Dixit et al., 2020). The efficiency of an ion exchange resin (Purolite® A860) to remove from water GenX, perfluoromethoxy butanoic acid (PFMOBA, $CF_3O(CF_2)_3COOH$), and perfluoromethoxy propanoic acid (PFMOPrA, $CF_3OCF(COOH)CF_3$) followed the order of their respective charge densities GenX < PFMOBA < PFMOPrA. Among the investigated short-chain PFAS, GenX has the lowest charge density (13.8 meq/g C) (Dixit et al., 2020).

The physicochemical properties of GenX have attracted rather limited attention. The available literature reports the standard enthalpy of formation, sublimation vapor pressure, and the adsorption of GenX at the air–water and solid–water interfaces (where the solids tested are natural quartz sand, Eustis soil, Vinton soil, and Qingdao soil; GenX concentration range: 3×10^{-5}–30 mM) (Gomis et al., 2015; Lukyanova and Papina, 2013; Wang and Niven, 2021; Yan et al., 2020; Zhang et al., 2020). GenX is a surfactant, however, its surfactant properties, such as self-assembly into micelles, remain unknown. Information on these is crucial, since such properties are manifestations of molecular interactions between GenX molecules and between GenX and water molecules and, in turn, the amphiphilic character of GenX dictates its fate and transport in the aqueous environment, its interactions with various biomolecules, and its binding to adsorbent materials (Lin et al., 2002).

With an overarching goal to understand the behavior of GenX

molecules in aqueous media, we report here the GenX critical micelle concentration (CMC) and micelle structure and interactions in aqueous solutions, on the basis of results obtained from experimental techniques such as surface tension, fluorescence, viscosity, and small-angle neutron scattering (SANS), and from molecular dynamics (MD) simulations. To our best knowledge, this is the first report on GenX micelles.

2. Materials and methods

2.1. Materials

Ammonium 2,3,3,3-tetrafluoro-2-(heptafluoropropoxy) propionate (GenX ammonium salt) ($C_6H_4F_{11}NO_3$, CAS number: 62037-80-3, MW = 347.08 g/mol, 97% purity), also known as ammonium perfluoro(2-methyl-3-oxahexanoate) or ammonium 2-(heptafluoropropoxy) tetrafluoro- propionate, was obtained from SynQuest Laboratories (Alachua, FL, USA) and used as received. Undecafluoro-2-methyl-3-oxahexanoic acid (GenX acid) ($C_6HF_{11}O_3$, CAS number: 13252-13-6, MW = 330.05 g/mol, 97% purity), also known as perfluoro(2-methyl-3-oxahexanoic) acid or 2,3,3,3-tetrafluoro-2-(heptafluoropropoxy)propanoic acid, was obtained from SynQuest Laboratories (Alachua, FL, USA) and used as received. Deuterium oxide (D, 99.9%), (D_2O, MW = 20.03 g/mol, 99.5% purity), also known as deuterated water, was obtained from Cambridge Isotope Laboratories, Inc. (Tewksbury, MA, USA) and used as received. Samples studied by SANS were prepared using D_2O. Samples for surface tension, pyrene fluorescence, and viscosity experiments were prepared using Milli-Q purified water (0.055 μS/cm). All samples were allowed sufficient time to equilibrate following the mixing of ingredients. The GenX ammonium salt concentrations selected for the SANS experiments (500 and 800 mM) are well above the CMC so that GenX micelles are well-defined. These may be high concentrations for GenX present in the environment, but they are relevant to the capture of GenX via adsorption or membranes, where the local concentration can be even higher. Furthermore, the assembly of GenX into micelles is expected (Bodratti et al., 2017) to occur at much lower concentrations in the vicinity of surfaces such as adsorbent materials, mineral particles, or natural organic matter.

2.2. Methods

2.2.1. Surface tension

The surface tension of aqueous surfactant solutions was measured at 21 °C by the Wilhelmy plate method using a Kruss model K100 tensiometer. When the surface tension is plotted as a function of surfactant concentration, the surfactant concentration where the surface tension approaches a plateau like region is considered as CMC. The slope of the surface tension vs logarithm of surfactant concentration plot ($d\gamma/d\log C$) determined close to the CMC can be used to estimate surface properties like the maximum surface excess concentration Γ_{max} and the minimum area occupied by a surfactant molecule (A_{min}) at air/liquid interface (Ito et al., 1996; Jin et al., 2005; Prosser and Franses, 2001):

$$\Gamma_{max} = -\frac{1}{2.303nRT}\left(\frac{d\gamma}{d\log C}\right)_{T,P} \quad (1)$$

$$A_{min} = \frac{1}{N\Gamma_{max}} \quad (2)$$

where γ is the surface tension, R is the universal gas constant (8.314 J mol^{-1} K^{-1}), T is absolute temperature, C is surfactant concentration in mM, and N is the Avogadro number (Ito et al., 1996; Jin et al., 2005). The constant n is taken as 2 for surfactants in which the surfactant ion and counterion are monovalent (Jin et al., 2005).

The tendency of surfactants to self-assemble into structures of specific shape (e.g., sphere, cylinder) can be informed by the critical packing parameter (CPP) which is defined as:

$$CPP = \frac{V_0}{A_{min}l_c} \quad (3)$$

where V_0 is the volume and l_c is the extended length of the surfactant hydrophobic chain (Kronberg et al., 2014; Nagarajan, 2002).

2.2.2. Micropolarity

Pyrene fluorescence was used to study the micropolarity of aqueous surfactant solutions. 2 μL of 1 mM pyrene (Fluka, Buchs, Switzerland) in ethanol was added to 3 g sample solutions. The resulting overall pyrene and ethanol concentrations were about 0.7 μM and 6.7×10^{-4} vol%, respectively. Pyrene fluorescence spectra of GenX aqueous solutions were recorded at 22 °C using a Hitachi F-2500 (Stoughton, MA, USA) fluorescence spectrophotometer for 350–450 nm emission wavelength. The excitation wavelength of pyrene was λ = 335 nm. The pyrene monomer emission spectrum exhibits a vibronic fine structure, and the ratio of the intensities of first and third vibronic peaks (I_1/I_3) strongly depends on the polarity of its microenvironment (Nivaggioli et al., 1995; Xing et al., 2013; Yang and Alexandridis, 2000). Pyrene is hydrophobic and it tends to move from the aqueous phase to a hydrophobic environment above the CMC, which is reflected in a decrease in I_1/I_3 values. The concentration value obtained from the intersection of straight lines fitted to the first plateau region of the I_1/I_3 vs surfactant concentration curve and to the linear part of I_1/I_3 decrease region (near the inflection point) provided CMC values that are consistent with those obtained from surface tension (Kancharla et al., 2019).

2.2.3. Viscosity

The viscosity of aqueous surfactant solutions was measured using Cannon-Fenske capillary viscometer of size 50 (Cannon Instrument Co, State College, PA). The kinematic viscosity (η) is calculated by multiplying the efflux time with the viscometer calibration constant (provided by the manufacturer). The ratio of the kinematic viscosity of the solution (η) and the kinematic viscosity of pure solvent (η_o) gives the relative viscosity ($\eta_r = \eta/\eta_o$) of the solution. η_r can be expressed in terms of the volume fraction of micelles (φ) (Kancharla et al., 2019; Nagarajan, 1982; Zoeller and Blankschtein, 1998):

$$\eta_r = 1 + \nu\phi + k_1(\nu\phi)^2 + O(\phi)^3 \quad (4)$$

where ν is a shape factor representing the micelle shape and k_1 a coefficient corresponding to pair-wise hydrodynamic interactions between micelles (Zoeller and Blankschtein, 1998). The term $k_1(\nu\phi)^2$ accounts for hydrodynamic interactions, and the term $O(\phi)^3$ arises due to direct micelle-to-micelle interactions and can be neglected for dilute solutions (Nagarajan, 1982; Zoeller and Blankschtein, 1998). The volume fraction of micelles which includes the water of hydration associated with micelles is given by $\phi = V_s^{hyd}(c_s - c_1)$, where V_s^{hyd} is the hydrated volume of a surfactant molecule, c_s total surfactant concentration, and c_1 concentration of unassociated surfactant (taken to be the CMC) (Zoeller and Blankschtein, 1998). For spherical micelles, the shape factor ν is considered to be 2.5 (Nagarajan, 1982; Zoeller and Blankschtein, 1998). We used this value since the GenX micelles are approximately spherical.

2.2.4. Small-angle neutron scattering (SANS)

SANS has been widely used to determine the size and structure of surfactant micelles (Berr and Jones, 1989; Burkitt et al., 1987; Fajalia and Tsianou, 2014; Iijima et al., 1998; Kancharla et al., 2022). SANS measurements of aqueous GenX ammonium salt solutions were performed on the NG-7 30 m SANS instruments at the Center for Neutron Research (NCNR), National Institute of Standards and Technology (NIST), Gaithersburg, MD. Neutrons with 6 Å wavelength were focused on samples kept in quartz cells of 2 mm thickness. Sample-to-detector distances (SDD) of 2, 6.5 or 10 m were used for each sample in order to cover the wave vector (q) range 0.01 $Å^{-1}$ < q < 0.35 $Å^{-1}$. The

measurement time was in the range 180–7200 s. Procedures for the treatment of raw SANS intensity data are described elsewhere (Dong et al., 2021; Kancharla et al., 2021a).

SANS data from GenX micelles in D_2O have been fitted with the monodisperse core-shell ellipsoid form factor and the Hayter–Penfold structure factor with rescaled mean spherical approximation (RMSA) (Fajalia and Tsianou, 2014). The ellipsoid shape is consistent with the findings from MD reported in this study, and encountered in typical PFAS surfactants (Dong et al., 2021; Kancharla et al., 2021a, 2021b). The overall scattering intensity I(q) is given by:

$$I_{micelle}(q) = A.\phi.P(q).S(q) + B_{inc} \quad (5)$$

P(q) is the form factor representing the shape and structure of a micelle, while S(q) is the structure factor representing the intermicelle interactions in the solution. φ is the volume fraction of the micelles which in turn depends on the overall surfactant concentration. The parameters A and B_{inc} account for additional contributions due to the absolute scaling and incoherent noise, respectively. The form factor and structure factor models employed here are presented in detail in SI. The major fitting parameters to describe scattering from GenX micelles in D_2O are the surfactant association number (N_{agg}), micelle volume fraction (φ), and charge on a micelle (Z).

The micelle core minor radius (b) was taken to be the extended length of $CF_3(CF_2)_2OCF$: $l_{f,c}$ = 8.0 Å (calculated from atom-atom distances in GenX molecule provided by MD). The volume of the micelle core V_{core} (in Å^3) was calculated given the surfactant association number N_{agg} using:

$$V_{core} = N_{agg}(V_{t,GenX} + N_{H,O}V_{D_2O}) \quad (6)$$

where $V_{t,GenX}$ = 200.66 Å^3 is the volume of a $CF_3(CF_2)_2OCF$ chain, $N_{H,O}$ is the number of water molecules hydrating the $CF_3(CF_2)_2OCF$ chain in the micelle core, and V_{D_2O} is the volume of a D_2O molecule (Kancharla et al., 2019).

The volume of the micelle shell, considering its contents: hydrophilic headgroups of the surfactant, CF_3 branch, counterions, and associated water molecules, can be written as:

$$V_{shell} = N_{agg}\left(V_{COO^-} + V_{CF_3} + (1-\alpha)V_{NH_4^+} + N_H V_{D_2O}\right) \quad (7)$$

where V_{COO^-} is the volume of the GenX hydrophilic headgroup, V_{CF_3} volume of the CF_3 group, $V_{NH_4^+}$ volume of the counterion NH_4^+, and N_H hydration number, i.e., number of water molecules associated per surfactant molecule. $\alpha = Z/N_{agg}$ is the fractional charge on a micelle.

The scattering length density of the micelle core is calculated by Eq. (8).

$$\rho_{core} = \frac{N_{agg}(b_{CF_3(CF_2)_2OCF} + N_{H,O}b_{D_2O})}{V_{core}} \quad (8)$$

where b_i is the coherent scattering length of molecule i. b_i values are reported in Table S1.

The scattering length density of the micelle shell is calculated using Eq. (9), which includes the individual contributions to the scattering from surfactant headgroups, CF_3 groups, counterions, and associated water molecules:

$$\rho_{shell} = \frac{N_{agg}\left[b_{COO^-} + b_{CF_3} + (1-\alpha)b_{NH_4^+} + N_H b_{D_2O}\right]}{V_{shell}} \quad (9)$$

The scattering length density of the solvent $\rho_{solvent}$ was calculated using the scattering lengths and concentrations of surfactant and heavy water. The concentration of the GenX ammonium salt present in the bulk solution was considered as its CMC (obtained from pyrene fluorescence). The dielectric constant of water was obtained from literature (Malmberg, 1958).

SANS data originating from GenX micelles in D_2O have also been fitted with other form factor models, including the monodisperse sphere form factor, monodisperse or polydisperse core-shell sphere form factor, and the Hayter–Penfold structure factor with RMSA. The expressions describing these form factor models and micelle structure/composition, SANS fits and important parameters are presented in the SI document. Here we discuss results from what we consider to be the better representation of micelles among all those we tested.

2.2.5. Molecular dynamics (MD) simulations

MD simulations were preformed using an in-house simulation package that utilizes a non-polarizable version of the Atomistic Polarizable Potentials for Liquids, Electrolytes and Polymers (APPLE&P) force field (Bedrov et al., 2019; Borodin, 2009). The parameters for the APPLE&P force field were derived based on fitting an extensive database of ab initio calculations of binding and conformational energies for a variety of small molecule clusters and representative oligomers, as well as systematic empirical adjustments to reproduce a variety of experimentally measured thermodynamic, dynamics, and structural characteristics in various systems. A periodic cubic simulation cell contained 32 GenX and ammonium pairs dissolved in 4032 water molecules (Fig. 1), which corresponds to a surfactant concentration of about 395 mM (which is well above the experimentally determined CMC of GenX in water). In the initial configuration, all molecules were distributed homogeneously in a large simulation cell of size 800 Å in each direction, which was subsequently shrunk over 30 ps to achieve a reasonable density. Then the system was equilibrated in the NPT ensemble for 20 ns, followed by production runs of up to 100 ns.

During the simulation, a temperature of 300 K was maintained by employing the Nosé–Hoover thermostat (Hoover, 1985) (coupling frequency 0.01 fs^{-1}) and barostat (coupling frequency 0.0005 fs^{-1}). A cut-off distance of 15.0 Å was set for computing van der Waals interactions and electrostatic interactions in the real space. The Ewald summation method was utilized for the calculation of the reciprocal space contribution to electrostatic interactions. All bonds were constrained using the SHAKE algorithm (Palmer, 1993). A multiple time-step integration scheme (Martyna et al., 1996) was used with the small step (0.5 fs) for calculating bonds and bends, a medium step (1.5 fs) for calculating torsions and short range non-bonded interactions, and a large step (3 fs) for calculating long-range non-bonded interactions and the reciprocal part of Ewald summation. This protocol and force field have been successfully used in our previous simulations of perfluorinated surfactants in aqueous solutions, and have shown good consistency with experimental data characterizing their self-assembly and micellar structure (Dong et al., 2021; Kancharla et al., 2021a).

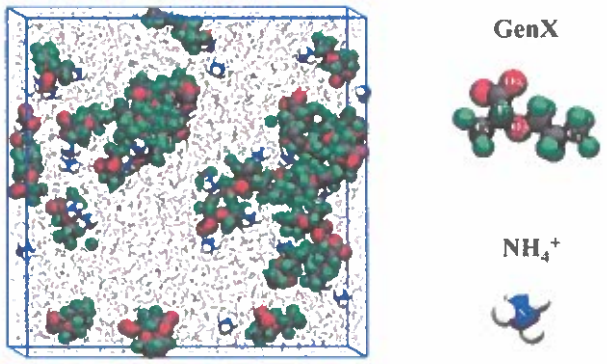

Fig. 1. A typical snapshot of the equilibrated system containing GenX and ammonium ions, and water as a solvent. (Carbon-gray; Oxygen-red; Fluorine-green; Nitrogen-blue; Hydrogen-white).

3. Results and discussion

The association behavior of GenX in aqueous solution is revealed here from combined experimental measurements and atomistic MD simulations. The critical micelle concentration (CMC), surface area per GenX headgroup, and micelle hydration are determined from analysis of surface tension, pyrene fluorescence spectroscopy and viscosity data. Structural information such as the GenX micelle shape, size, and composition is obtained from complementary analysis of MD and SANS data. MD simulations provided additional molecular-level insights into the GenX self-assembly and intermolecular interactions. There is no information available in the literature on GenX surfactant properties, such as self-assembly into micelles or micelle structure.

3.1. Premicellar region and onset of micelle formation

Surface tension data of GenX acid or GenX ammonium salt in aqueous solution are plotted in Fig. 2 as a function of surfactant concentration. For GenX acid aqueous solution, the slope ($d\gamma/d\log C$) determined close to the CMC is −30.12 mN/m, Γ_{max} calculated from Eq. (1) is 2.67×10^{-10} mol cm^{-2}, and A_{min} is 62.1 Å^2. For GenX ammonium salt aqueous solution, $(d\gamma/d\log C) = -23.01$ mN/m, $\Gamma_{max} = 2.04 \times 10^{-10}$ mol cm^{-2}, and $A_{min} = 81.3$ Å^2. Interfacial tension parameters are important in the atmospheric transport of PFAS, and in PFAS retention and transport in natural porous media (Brusseau, 2019); also in PFAS treatment and remediation processes (Lee et al., 2017; Meng et al., 2014).

It is appropriate to compare the properties of GenX to properties of PFAS surfactants that have (i) the same number of carbons with GenX, sodium perfluorohexanoate (NaPFHx, $C_5F_{11}COONa$), and (ii) the same counterion, ammonium perfluorooctanoate (APFO, $C_7F_{15}COONH_4$) (Kancharla et al., 2019). The surface area per headgroup of the GenX acid is close to that of NaPFHx (A_{min} = 63.4 Å^2) (Kancharla et al., 2021b) and APFO (64.0 Å^2) (Kancharla et al., 2019), whereas the surface area per headgroup of the GenX ammonium salt is 30% greater than that of NaPFHx and APFO.

CPP values are calculated for GenX acid and GenX ammonium salt considering the volume of surfactant hydrophobic chain (V_0) equal to the volume of a $CF_3(CF_2)_2OCF$ chain = 200.7 Å^3 (leaving out the CF_3 side-group of GenX molecule, as intimated by MD results presented below), and the extended length of a $CF_3(CF_2)_2OCF$ chain l_c = 8.0 Å (obtained by MD), are 0.40 and 0.31, respectively. The CPP value 0.31 suggests spherical micelles (CPP < 0.33) for GenX ammonium salt. CPP = 0.40 suggests that GenX acid forms cylindrical micelles (0.33 < CPP < 0.5).

The CMC value obtained from surface tension for GenX acid and GenX ammonium salt in aqueous solution is 150 ± 10 mM and 150 ± 50 mM, respectively. The surface tension of GenX acid remained constant above the CMC, however, for GenX ammonium salt, a dip and subsequent slight increase in the surface tension is observed. The concentration of GenX ammonium salt at the dip where the surface tension is lowest is considered to be the CMC. The origin of the increase in the surface tension above the CMC has not been established here, but it does not affect the analysis of the surface tension data to obtain Γ_{max} and A_{min}.

Pyrene fluorescence is used to also obtain CMC and, further, assess the polarity of the GenX micelle microenvironment. The I_1/I_3 ratio of GenX acid or GenX ammonium salt aqueous solutions decreased above the CMC due to the partition of pyrene from the polar aqueous solution to the GenX micellar environment (Fig. 3). Similar behavior has been previously observed with pyrene for other fluorinated surfactants including PFOA (Dong et al., 2021; Kalyanasundaram, 1988; Muto et al., 1987), which was ascribed to the pyrene molecules residing in the outer palisade layer of the surfactant micelles due to the immiscibility between pyrene and the fluorocarbon core (Xing et al., 2013). The CMC of GenX acid and GenX ammonium salt in aqueous solution obtained from pyrene fluorescence are 140 ± 5 mM and 175 ± 5 mM, respectively.

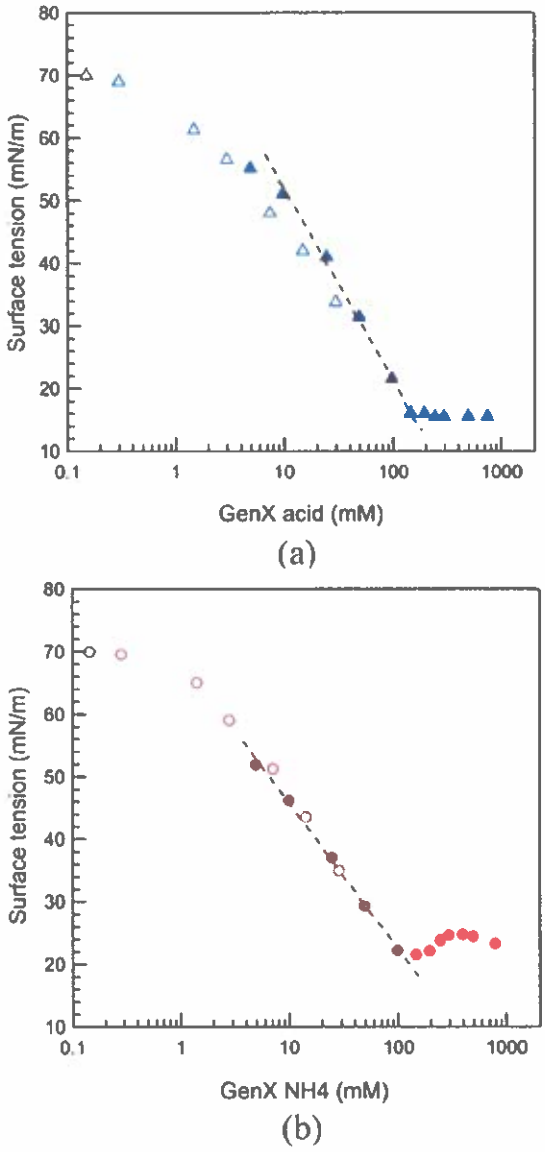

Fig. 2. Surface tension of (a) GenX acid (20.5 °C) and (b) GenX ammonium salt (23.5 °C) aqueous solutions, plotted as a function of surfactant concentration. The surface tension data at low surfactant concentrations (open symbols) were taken from reference (Yan et al., 2020). Linear fits have been applied to the data points where the surface tension decreases prior to reaching the CMC.

Above CMC, the I_1/I_3 ratio of GenX ammonium salt aqueous solutions at a particular concentration is lower than the I_1/I_3 ratio of NaPFHx solutions (Fig. S1). This indicates that GenX micelles offer a more hydrophobic environment for pyrene, presumably allowing more contact between pyrene and fluorocarbon chains. The CMC reported in the literature for the 6-carbon fluorinated surfactants perfluorohexane sulfonic acid (PFHxS, $C_6F_{13}SO_3H$) is 12 mM, perfluorohexanoic acid (PFHxA, $C_5F_{11}COOH$) is 82 mM, and sodium perfluorohexanoate (NaPFHx, $C_5F_{11}COONa$) is 200 mM (Alves et al., 2020; Kancharla et al., 2021b). The CMC of GenX ammonium salt is close to the CMC of NaPFHx. The low CMC of PFHxS compared to PFHxA is due to the presence of 6 carbon atoms in fluorocarbon chain of PFHxS (more hydrophobic), while PFHxA has 5 carbon atoms. The CMC of GenX acid is greater than the CMC of PFHxA, whereas the CMC of GenX ammonium salt is slightly lower than the NaPFHx CMC. GenX acid and PFHxA have

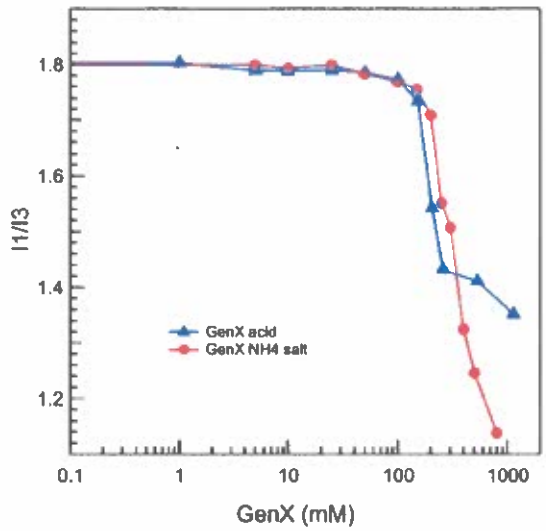

Fig. 3. Pyrene fluorescence intensity I_1/I_3 ratio of GenX acid and GenX ammonium salt aqueous solutions (22 °C).

the same headgroup and counterion. Therefore, the difference in the CMC of GenX acid and PFHxA is due to the difference between the perfluoroalkyl chain in PFHxA and the perfluoroether chain in GenX acid. When the counterion is changed, the CMC trend became the opposite. The contribution of micellization of the GenX fluorocarbon chain is assessed next.

The Gibbs free energy of micellization (ΔG_{mic}) is the net free-energy gain for transferring a free surfactant molecule and its counterion from the bulk aqueous solution into a micelle. ΔG_{mic} includes various contributions, the most important of which account for formation of the hydrophobic micelle core, and electrostatic interactions in the micelle shell (Kancharla et al., 2021b). For ionic surfactants, ΔG_{mic} is related to CMC according to $\Delta G_{mic} = (2-\alpha)RT\ln X_{CMC}$, where X_{CMC} is the surfactant mole fraction at the CMC, and α the degree of counterion dissociation (Kancharla et al., 2021b). For GenX ammonium salt, $\Delta G_{mic} \approx -18.0$ kJ/mol considering $\alpha = 0.72$ (obtained from SANS fits presented later). $\Delta G_{mic} = -17.9$ kJ/mol for NaPFHx, while the free energy contribution due to the formation of the micelle hydrophobic core is −17.5 kJ/mol (Kancharla et al., 2021b). For APFO (CMC = 26.5 mM, $\alpha = 0.47$) (Kancharla et al., 2019) the electrostatic free energy is −8.1 kJ/mol (Kancharla et al., 2021b). Since GenX ammonium salt and APFO have the same counterion, we assumed the electrostatic free energy of GenX ammonium salt equal to that of APFO, and calculated (following the procedure described in Kancharla et al., 2021b) at −4.3 kJ/mol the free energy contributions related to the formation of the GenX ammonium salt micelle hydrated shell and entropy lost by the counterions upon binding onto the micelle charged surface. Subtracting this value from ΔG_{mic} of GenX ammonium salt gives −13.7 kJ/mol for the free energy associated with the formation of the GenX micelle hydrophobic core. Whereas the ΔG_{mic} values of GenX ammonium salt and NaPFHx are almost the same, the free energy associated with the formation of the micelle hydrophobic core is 30% less negative for the ether-containing GenX compared to NaPFHx with linear fluorocarbon chain.

3.2. Micelle structure

In order to understand the structure of GenX micelles in water, we combine in this section discussion of results from atomistic MD simulations and SANS analysis. First we discuss the micelle shape and size, and then present information on molecular arrangements inside the micelle.

3.2.1. MD simulations analysis

A broad range of micelle association numbers (i.e., number of surfactant molecules in a micelle) has been observed in MD simulations. A GenX molecule is considered here to be a part of a micelle/cluster only when any of its atoms lie within a cutoff distance of 5.0 Å from any atom of another GenX molecule belonging to the same micelle. We set up two systems with different initial distributions of GenX molecules. In one, the GenX molecules were randomly distributed through the system without forming clusters; in another, they were biased to belong to one large micelle. After 20 ns equilibration, both systems show similar micelle size distributions, with about 30–33% of GenX molecules present as unimers or dimers, and the remaining GenX molecules distributed between micelles of association number $N_{agg} = 3$–25. Unfortunately, the relatively small size of investigated system (i.e., 32 surfactant molecules) and the slow kinetics of micelle formation/breaking (particularly for larger micelles) do not lead to a converged micelle size distribution even from a 100 ns long trajectory. The micellar size distribution and kinetics of micelle formation and dissociation will be addressed in future work. Nevertheless, the population of unimers shows steady fluctuation around 24% (see Supplemetary Information). Given the 395 mM surfactant concentration in MD simulations, the fraction of unimers observed in MD is in good aggreement with the experimentally determined value of the GenX CMC (150 mM).

While we cannot conclude on equilibrium size distribution of micelles from MD simulation, we have sufficient statistics to analyze the micellar structure and shape for different size micelles observed in our simulations. First, we characterized the shape and dimensions of the formed micelles by calculating the micellar gyration tensor using the following equation:

$$S^2_{xy} = \frac{1}{M} < \sum_{i=1}^{N} m_i x_i y_i > \qquad (10)$$

where N is the number of atoms in a micelle, M total mass of the micelle, x_i, y_i coordinates of atom i relative to the micelle center-of-mass, m_i corresponding mass of atom i, and $< >$ denotes averaging over the entire trajectory. Diagonalization of the gyration tensor matrix yields the principal moments, i.e., S_{xx}, S_{yy}, S_{zz} that can be related to the radius of gyration (R_g) as: $R_g^2 = S^2_{xx} + S^2_{yy} + S^2_{zz}$. The calculated R_g^2 and the corresponding components of the gyration tensor are plotted in Fig. 4a as the function of micelle association number. As expected, the R_g^2 and the principal moments monotonically increase with increasing micelle size. Furthermore, Fig. 4b clearly shows that the GenX micelles are not spherical, as one of the principal moments of gyration tensor is substantially larger than the other two ($S_{zz}/S_{xx} > 2.1$ and $S_{zz}/S_{yy} > 1.6$), corresponding to a prolate shape of the micelle. The ellipsoidal micellar shape observed in MD allowed us to select the core-shell ellipsoid form factor for fitting SANS data (see discussion below).

To understand the structure of individual micelles, we have examined the interaction with water of different parts of the GenX molecule, and their distribution inside the micelle. Fig. 5 shows several radial distribution functions ($g(r)$) which reflect the probability of finding a specific atom (e.g., oxygen of water molecule) at a certain distance r from the selected atom (e.g., oxygen of GenX), and the corresponding coordination numbers (CN) for the selected atom types identified in Fig. 5a: O_W is water oxygen atom, O= oxygen atom of GenX headgroup, O_E ether oxygen atom of GenX fluorinated tail, C_T CF_3 carbon at the end of the fluorinated tail, and C_S CF_3 carbon on the side group connected to the GenX headgroup. The first coordination shell is typically defined by the first minimum in $g(r)$ (e.g., $r = 3.65$ Å for O= of GenX with O_W correlation shown in Fig. 5b), and the number of different atoms in that shell (i.e., CN) provides a good description of the local environment. As expected, a sharp peak for O= -O_W pair and CN = 3.2 for the first coordination shell (defined as a sphere with r = 3.65 Å) in Fig. 5b confirms

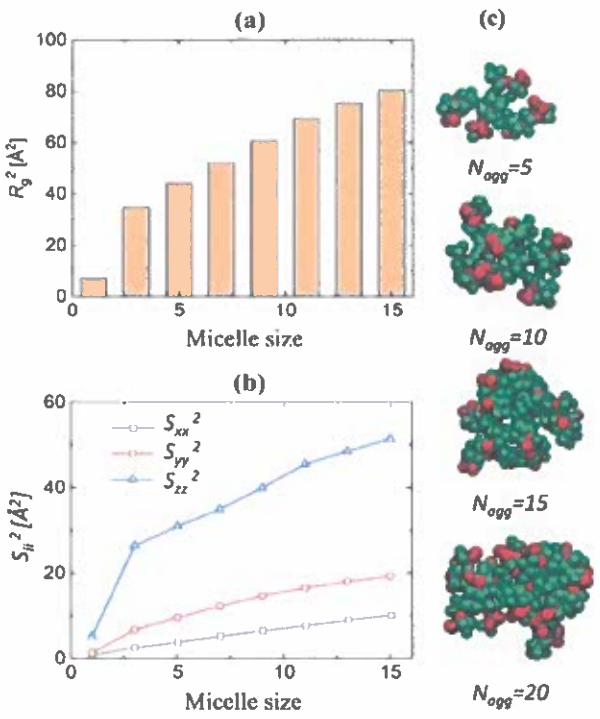

Fig. 4. (a) Average R_g^2 of a GenX micelle as a function of micelle association number, (b) principal moments of the gyration tensor as a function of micelle association number, and (c) representative snapshots of several GenX micelles of different association numbers observed in MD simulations.

a strong interaction of water molecules with the GenX anionic headgroup. On the other hand, the ether oxygen has very little interaction with water (note the absence of a strong peak at short distances and CN = 0.1 within the first coordination shell r = 3.65 Å), indicating that it is sterically hindered from water by fluorinated groups and the headgroup. Fig. 5c shows that the g(r) and CN of O_W around the CF_3 carbon atoms of fluoroalkyl tail (C_T) and the side group (C_S) are very similar in behavior for both carbons in the first coordination shell within r < 5.5 Å, indicating that both groups have similar hydration structure and exposure to water. Within a sphere of 5.5 Å, these groups have on average 14 water molecules. The snapshots in Fig. 4c, as well as F-O_W correlations shown in Fig. 5d, indicate that a significant number of F atoms of GenX molecules are interacting with water molecules. On average, within a 4.2 Å sphere each F atom interacts with about 5 water molecules despite the fact that the majority of GenX molecules are in micelles.

It is interesting to examine the extent of hydration of GenX molecules. This information is important for the environmental applications of GenX, and also useful in the fitting of SANS data. Using MD simulation trajectories, we have calculated how many water molecules are in contact with each GenX micelle. To consider a water molecule to be in contact with a micelle, the O_w should be within R_c distance from any GenX atom in the micelle. We have considered three values of R_c = 3.0, 3.5 and 4.0 Å, which fall between the values defining the boundaries of O and F atoms first coordination shells. Fig. 6a shows the dependence of the number of water molecules hydrating the GenX micelle as a function of micelle association number, normalized by the number of GenX molecules in the micelle (i.e., per one GenX molecule). Fig. 6b shows distributions of these hydration numbers for each R_c and averaged for all micelle sizes. Note that in these calculations, if a water molecule was in contact with two different GenX molecules or atoms, then it was counted only once. As expected, for smaller size micelles, the number of hydrating waters per GenX molecule is higher but, as the size of the micelle increases, the average hydration number also increases. For the tighter definition of hydrating water (R_c = 3.0 Å) the number of hydrating water molecules saturates around 4 whereas, for the looser definition of interfacial water (R_c = 4.0 Å), it is around 12 waters per GenX molecule. These values of hydration can be considered as the lower and upper bounds for the average water hydration number.

Another interesting structural feature to examine is how GenX molecules are oriented in the micelle. We have investigated the molecular orientation of each GenX molecule in micelles of different sizes by computing the angle (θ) between two vectors $\vec{v_1}$ and $\vec{v_2}$, where $\vec{v_1}$ is a vector between the center-of-mass of the micelle and the C_T group of the GenX molecule belonging to the micelle, while $\vec{v_2}$ is a vector from C_T to the junction carbon atom of the headgroup (Fig. 7a). θ = 0° indicates that the GenX molecule tail is oriented toward the micelle center and the headgroup is radially outwards. θ = 90° corresponds to GenX molecules oriented tangentially to the surface of the micelle, while the 180° angle denotes that the GenX headgroup points inside the micelle core. The probability distribution of finding GenX molecule with θ orientation (normalized by sin(θ) to reflect the different phase space available for realization of each angle value) is shown in Fig. 7b. A broad peak around 90° indicates that GenX molecules prefer to align along the micelle surface.

3.2.2. Viscosity

The hydration of GenX micelles can be experimentally assessed from viscosity measurements. Fig. 8 shows the relative viscosity of aqueous solutions of GenX ammonium salt, plotted as a function of the micellized surfactant concentration (C-CMC) which accounts for the contribution to viscosity of only the micelles. A linear equation (Eq. (4) neglecting the $k_1(\nu\phi)^2$ and $O(\phi)^3$ terms) was fitted to the viscosity measurement data set in Fig. 8 and, from the x-coefficient value obtained, the hydrated volume of a GenX molecule V_s^{hyd} is calculated to 569.7 Å^3. After subtracting from this value the "dry" molecular volume of GenX (332.1 Å^3), the volume of the water hydrating a GenX molecule is estimated to 237.6 Å^3 which corresponds to ~8 water molecules. This number falls right in the middle between the upper and lower bounds of hydration numbers obtained from MD simulations, as discussed above in the context of Fig. 6. The hydration number of NaPFHx or ammonium perfluorooctanoate (PFOA) reported in the literature is ~11 water molecules, 40% higher than the GenX hydration number (Kancharla et al., 2019, 2021b).

3.2.3. SANS analysis

When fitting SANS intensity data for GenX micelles in D_2O, we considered the micelle core to consist of $CF_3(CF_2)_2OCF$ chains and 0, 1, or 2 water molecules hydrating a $CF_3(CF_2)_2OCF$ chain (to account for GenX hydrophobic chain contact with water), and the shell to consist of carboxylate headgroups, CF_3 branch, counterions, and associated water molecules. We assigned the CF_3 branch in the micelle shell following information from MD. Further, we fixed the total number of water molecules hydrating a GenX molecule in the micelle ($N_H + N_{H,O}$). Two cases have been considered, (i) $N_H + N_{H,O}$ = 8, based on the GenX hydration number obtained from viscosity, and (ii) $N_H + N_{H,O}$ = 12, based on upper bound of the GenX hydration number obtained from MD results. For instance, case (i) if $N_{H,O}$ = 0, N_H = 8; $N_{H,O}$ = 1, N_H = 7; $N_{H,O}$ = 2, N_H = 6, and case (ii) if $N_{H,O}$ = 0, N_H = 12; $N_{H,O}$ = 1, N_H = 11; $N_{H,O}$ = 2, N_H = 10.

Fig. 9 shows the SANS absolute intensity profiles of GenX ammonium salt in D_2O at 22 °C and the corresponding fits using the monodisperse core-shell ellipsoid form factor with Hayter rescaled MSA structure factor considering 8 water molecules hydrating each GenX molecule in the micelle. The correlation peak reflects repulsive interactions between the micelles. The intermicelle distance d can be estimated from the q value at the peak maximum $d = 2\pi/q_{max}$. Table 1 summarizes important

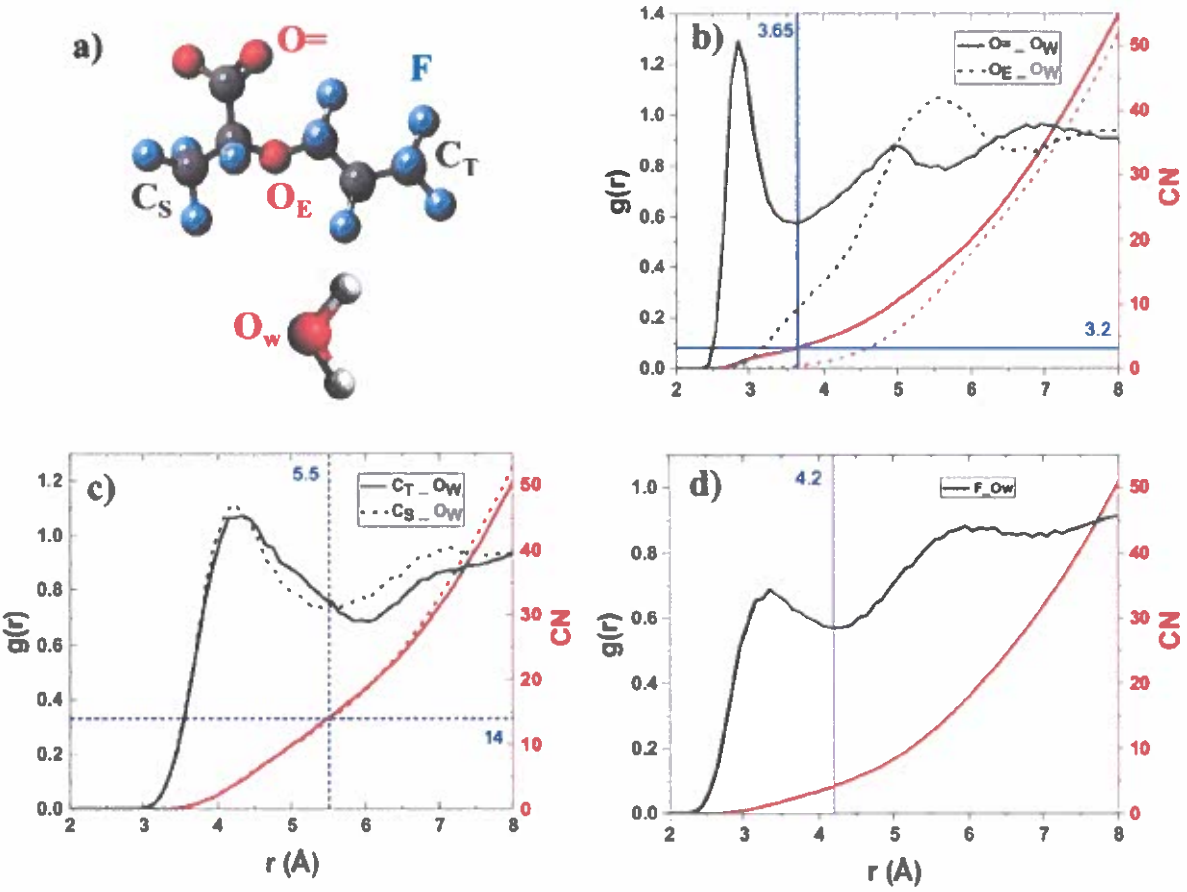

Fig. 5. (a) Definition of atom types considered for radial distribution functions g(r) and coordination number CN, (b) comparison of O= -O_W and O_E-O_W g(r) and CN, (c) comparison of C_T-O_W and C_S-O_w g(r) and CN, and (d) F-O_W g(r) and CN obtained from MD simulations. Vertical lines indicate the distance defining the first coordination shell for each pair correlation, while horizontal lines show a corresponding CN in the first coordination shell.

parameters obtained by fitting GenX SANS data.

The average association number of GenX ammonium salt micelles in aqueous solution obtained from SANS is 5.9 at 500 mM GenX and 8.3 at 800 mM GenX, a 40% increase upon surfactant concentration increase from 500 to 800 mM. The GenX micelle size (R_{eq}) increased by 12%, the fractional charge on a micelle (α) (degree of counterion dissociation) increased by 28%, and the intermicelle distance decreased by 11% with the increase in GenX concentration from 500 to 800 mM. Our SANS results show that the ratio of the micelle core major to minor radius (ε) is smaller than 1, which means that the micelle core major radius is smaller than the extended length of surfactant (set to equal the micelle core minor radius). This is in good agreement with the tendency of GenX molecules to tilt along the micelle surface, established by MD (Fig. 7). The average area per surfactant headgroup at the core-shell interface obtained from SANS parameters for the case of dry core ($N_{H,O}$ = 0) is 96.3 Å^2 for 500 mM GenX and 82.9 Å^2 for 800 mM GenX. These values are in excellent agreement with the A_{min} value obtained from the surface tension data.

SANS parameters obtained using the monodisperse core-shell ellipsoid form factor with Hayter rescaled MSA structure factor considering 12 water molecules (the upper bound hydration value obtained from MD) hydrating each GenX molecule in the micelle are presented in SI (refer to Table S5) together with the corresponding fits. A comparison of GenX micelle parameters obtained considering 8 or 12 water molecules of hydration shows that the micelle association number, fractional charge, and axial ratio do not change, only the shell thickness (where water resides) increases by 20–30%. Considering water in the micelle core ($V_{h,c}$ = 13% or 23%) resulted in no big difference in the micelle parameters.

We have also fitted SANS intensity data of GenX micelles using the monodisperse and polydisperse core-shell sphere form factor and Hayter rescaled MSA structure factor (results are presented in SI). The results obtained show that there is no difference in the GenX micelle association number, fractional charge, and size, whether we consider monodisperse core-shell sphere form factor or monodisperse core-shell ellipsoid form factor. Applying polydispersity to the radius of the micelle core, using the Schulz distribution, gave PD = 0.066 for 500 mM GenX and PD = 0.007 for 800 mM GenX, and there is no difference in the micelle parameters obtained when compared to monodisperse core-shell sphere fits. PD = σ/R_A is the ratio of the standard deviation of the core radius size distribution (σ) and the average micelle core radius (R_A) obtained from the fit. The low value of the polydispersity indicates that the system was essentially monodisperse. Small clusters contribute very little to the scattering intensity (refer to Fig. S9).

Comparing the structure (obtained from SANS) of GenX micelles to that of NaPFHx micelles, both surfactants have 6 carbon atoms, however, NaPFHx forms larger micelles with N_{agg} = 14.7, ε = 1.41 and R_{eq} = 13 Å (Kancharla et al., 2021b). This could be ascribed to the chemical structure of GenX. GenX has a CF_3 branch, whereas NaPFHx has a linear $CF_3(CF_2)_4$ chain. Comparing 6 carbon fluorinated surfactant micelles to 8 carbon fluorinated surfactant micelles, APFO forms ellipsoidal micelles with N_{agg} = 30, ε = 1.73, and R_{eq} = 17.6 Å (Dong et al., 2021;

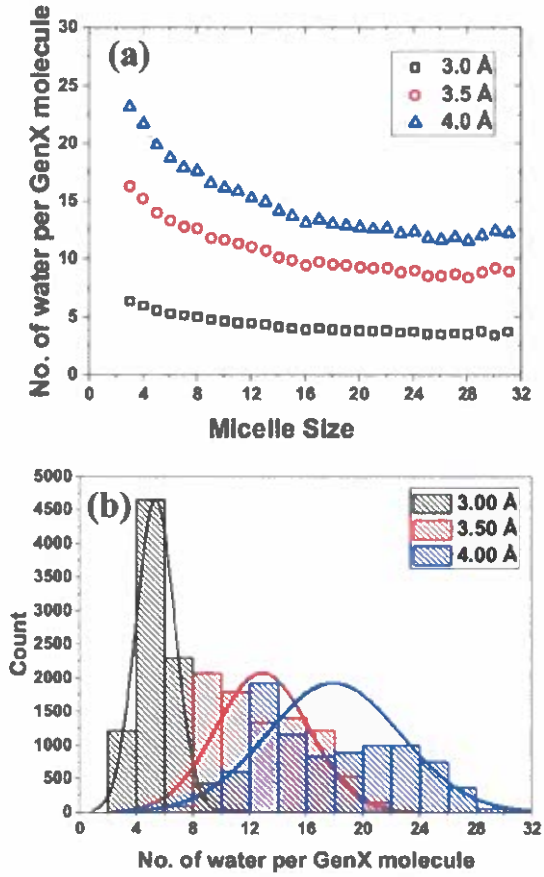

Fig. 6. (a) Average number of water molecules in the first coordination shell of the micelle (defined using three cutoff radii: R_c = 3.0, 3.5 and 4.0 Å from any GenX atom) plotted as function of the micelle association number. (b) Distribution of hydrating waters per GenX molecule for three different cut off radii.

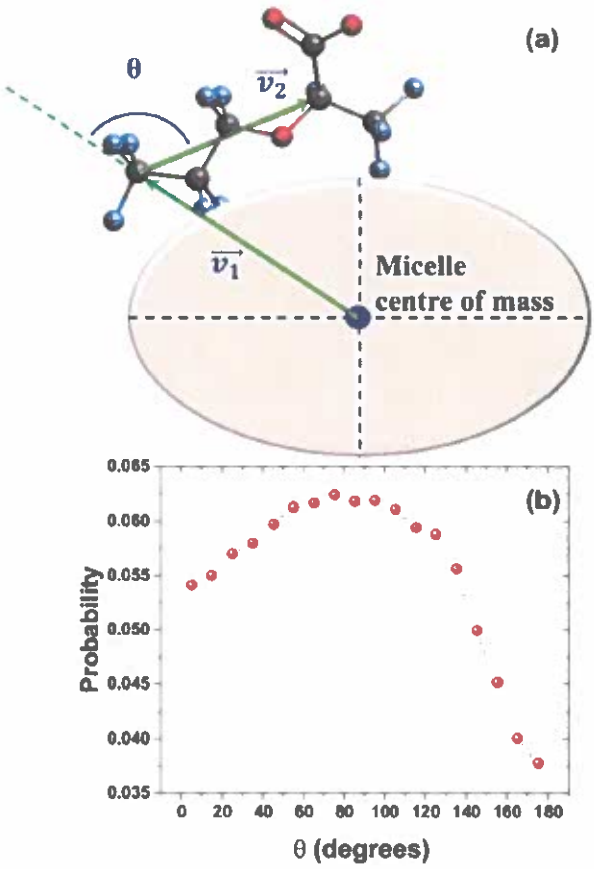

Fig. 7. (a) Schematic representation of the method employed to compute the relative molecular orientation. The angle θ is between vector $\vec{v_1}$, which is from the center-of-mass of micelle to C_T, and the vector $\vec{v_2}$, which is from C_T to the carbon at the junction of headgroup and side-group. (b) Normalized distribution of computed molecular orientation (θ).

Kancharla et al., 2021a). APFO micelles have association number 5 times that of GenX micelles and 2 times that of NaPFHx micelles. The size of APFO micelles is 88% greater than that of GenX micelles, and 35% greater than NaPFHx micelles. For sodium perfluoroalkyl carboxylates, upon an increase in the hydrophobic part of the surfactant by 2 $-CF_2-$ groups, the micelle association number increases by 70% and the size increases by 30% (Kancharla et al., 2021b).

The SANS results of GenX forming small micelles with association number in the range 6–8 are in a very good agreement with the findings from MD. The ratio of micelle core major to minor radius (ε) < 1 indicates elongated micelles which agrees with the MD results. MD simulations have shown that, for association number = 7, radius of gyration (R_g) = 7.2 Å (Fig. 6a), which is not far from the GenX micelle size (R_{eq}) obtained from SANS fits.

In the micelle composition that we considered while fitting the SANS data, the CF_3 side group of GenX is assigned to the micelle shell and is exposed to water, which is consistent with the MD results. MD simulations have shown that GenX molecules prefer to align along the micelle surface, and the CF_3 carbon atoms of the GenX tail are exposed to water. The SANS models that we used do not explicitly account for these. Having said this, the different models and micelle composition scenario considered while fitting SANS data, including monodisperse sphere, monodisperse or polydisperse core-shell sphere with and without water in the micelle core, and monodisperse core-shell ellipsoid with and without water in the micelle core, all resulted in the same micelle parameters, lending confidence that these parameters describe well the

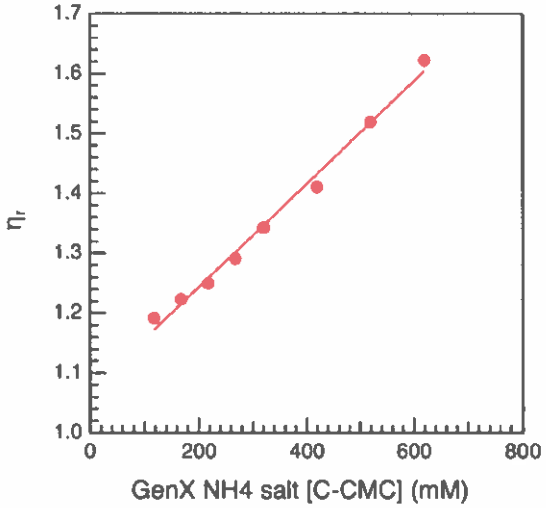

Fig. 8. Relative viscosity of GenX ammonium salt aqueous solutions (21 °C) plotted as a function of micellized surfactant concentration. The line through the viscosity data points is fit to Eq. (4).

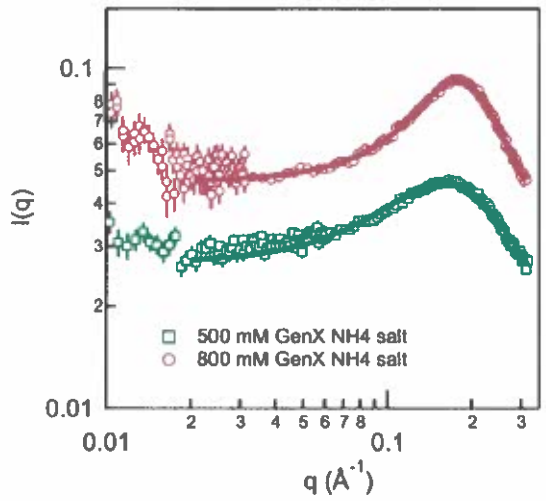

Fig. 9. SANS intensity profiles of GenX ammonium salt in D_2O corrected for solvent (D_2O) scattering. Markers represent the experiment data and solid lines represent the fits using monodisperse core-shell ellipsoid model form factor with Hayter RMSA structure factor described in the text, considering 8 water molecules hydrating each GenX molecule in the micelle.

GenX micelles.

We note that the surfactants properties reported here are for GenX in plain water. The presence in natural water of electrolytes or organic matter will modulate the surfactant association. For example, added NaCl decreased the CMC and increased the micelle size of PFOA, as we have recently shown (Kancharla et al., 2021b). We expect a similar trend in the case of GenX.

4. Conclusions

Emerging PFAS surfactants such as GenX have been introduced as less harmful alternatives to legacy PFAS (PFOA, PFOS) which are banned because they cause serious health issues. However, GenX is now present in waters and is generating concern as it has been found to adversely affect health. GenX is a surface-active molecule for which we know very little about its surfactant properties. The present study aims to fill this gap in knowledge.

Consistent and quantitative information on the formation and structure of GenX micelles emerges from analysis of experiments and MD simulations. Due to its short fluorocarbon chain, GenX has relatively high CMC (175 mM) and forms small micelles: association number of 6–8 and radius 10 Å. GenX molecules participating in micelles are hydrated by an average eight water molecules; the GenX anionic headgroup interacts strongly with water, whereas the ether oxygen is sterically hindered from water. The branched fluoroether chain of GenX is found 30% less hydrophobic than a linear fluorocarbon chain with the same number of carbon atoms. Having a linear $CF_3(CF_2)_4$ chain, NaPFHx forms larger micelles with association number = 15 and radius = 13 Å.

Self-assembly into micelles is a key feature of surfactants in aqueous solution. Analysis of CMC reveals specific contributions of hydrophobic tail and hydrophilic headgroup, while the micelle structure and composition provide information on how surfactants interact with themselves and with solvent (water) and other molecules present in solution. In a way, the micelles "amplify" subtle interactions that are always present, even if difficult to discern. Furthermore, the capability established in this study to predict from first principles micelle formation and structure confirms that such multiple and often competing interactions have been properly accounted for. This knowledge can be deployed to probe computationally other PFAS pollutants for which experimental results are lacking. A "simple" system as that examined here provides easier access to the fundamentals, and this helps the understanding of more complex systems encountered in environmental applications. Micelles are also relevant to environment and health in that PFAS surfactants, while typically found in very low bulk solution concentrations, they tend to concentrate a lot (partition) in the vicinity of surfaces in the context of separations (AC, ion exchange resins) and in the context of biointerfaces (proteins, lipid membranes).

This is the very first study of GenX micelles; further, this is the first MD study of surfactants with ether oxygen along the chain. The high-resolution structure and interactions knowledge presented here informs the GenX fate and transport in the aqueous environment, its interactions with various natural substances (e.g., minerals, humic acid) and biomolecules, and its binding to adsorbent materials. In a very recent study, photo-reductive destruction of GenX was significantly promoted when GenX was in the form of mixed micelles with hydroxyphenylacetic acids (hydrated electron precursors) and cetyl trimethyl ammonium bromide (Chen et al., 2021).

CRediT authorship contribution statement

Samhitha Kancharla: Methodology, Investigation, Formal analysis, Writing – original draft, Writing – review & editing. **Aditya Choudhary:** Methodology, Software, Investigation, Formal analysis, Visualization, Writing – original draft. **Ryan T. Davis:** Investigation, Formal analysis. **Dengpan Dong:** Methodology, Software, Investigation, Formal analysis, Visualization, Validation. **Dmitry Bedrov:** Funding acquisition, Conceptualization, Methodology, Project administration, Supervision, Writing – review & editing. **Marina Tsianou:** Funding acquisition, Conceptualization, Supervision, Writing – review & editing. **Paschalis Alexandridis:** Funding acquisition, Conceptualization, Methodology, Project administration, Supervision, Writing – review & editing.

Declaration of Competing Interest

The authors declare that they have no known competing financial interests or personal relationships that could have appeared to influence

Table 1
Parameters obtained by fitting SANS intensity data of GenX ammonium salt in D_2O, corrected for solvent (D_2O) scattering, using the monodisperse core-shell ellipsoid form factor and the Hayter rescaled MSA structure factor, and considering the number of water molecules hydrating each GenX molecule in the micelle 8 (obtained from viscosity measurements). $N_{H,O}$ number of water molecules hydrating an oxygen atom in the core, N_{agg} association number (number of surfactant molecules per micelle); α fractional charge or charge per surfactant molecule in a micelle; b micelle core minor radius; ε ratio of micelle core major to minor radius; δ shell thickness; R_{eq} equivalent spherical micelle radius; $V_{h,c}$ volume percentage of water in the micelle core; φ volume fraction of the micelles; d inter-micelle distance; and I_{peak} intensity at the correlation peak maximum. χ^2_R is a statistical parameter that quantifies the differences between the calculated and experimental SANS data sets.

GenX (mM)	$N_{H,O}$	N_{agg}	α	b (Å)	ε	δ (Å)	R_{eq} (Å)	$V_{h,c}$ (%)	Φ	d (Å)	I_{peak}	χ^2_R
500	0	5.9 (± 0.1)	0.72 (± 0.03)	8.0	0.55 (± 0.006)	2.7	9.35 (± 0.02)	0	0.0519 (± 0.002)	39.3	0.046	2.20
500	1	5.9 (± 0.1)	0.75 (± 0.03)	8.0	0.64 (± 0.006)	2.4	9.34 (± 0.02)	13	0.0519 (± 0.001)	39.3	0.046	1.85
500	2	5.9 (± 0.1)	0.78 (± 0.03)	8.0	0.72 (± 0.006)	2.1	9.33 (± 0.02)	23	0.0522 (± 0.001)	39.3	0.046	1.53
800	0	8.3 (± 0.1)	0.93 (± 0.03)	8.0	0.78 (± 0.005)	3.1	10.45 (± 0.02)	0	0.0883 (± 0.001)	34.9	0.093	0.99
800	1	8.3 (± 0.1)	0.96 (± 0.03)	8.0	0.89 (± 0.005)	2.7	10.44 (± 0.02)	13	0.0909 (± 0.001)	34.9	0.093	0.95
800	2	8.3 (± 0.1)	0.99 (± 0.03)	8.0	1.01 (± 0.005)	2.4	10.45 (± 0.02)	23	0.0939 (± 0.001)	34.9	0.093	1.17

the work reported in this paper.

Acknowledgments

This research was funded by the U.S. National Science Foundation (NSF), grant numbers CBET-1930959 and CBET-1930935. We acknowledge the support of the National Institute of Standards and Technology (NIST), U.S. Department of Commerce, in providing the neutron research facilities used in this work. Access to the CHRNS 30m Small-angle neutron scattering instrument was provided by the Center for High Resolution Neutron Scattering (CHRNS), a partnership between NIST and NSF under Agreement No. DMR-1508249. We thank Dr. Yimin Mao at NIST for valuable assistance with the SANS data acquisition. We thank Honeywell Buffalo Research Labs (Greg Smith and Roy Robinson) for providing access to a surface tension instrument.

Appendix A. Supporting information

Supplementary data associated with this article can be found in the online version at doi:10.1016/j.jhazmat.2021.128137.

References

Allendorf, F., Berger, U., Goss, K.-U., Ulrich, N., 2019. Partition coefficients of four perfluoroalkyl acid alternatives between bovine serum albumin (BSA) and water in comparison to ten classical perfluoroalkyl acids. Environ. Sci. – Process. Impacts 21, 1852–1863.

Alves, A.V., Tsianou, M., Alexandridis, P., 2020. Fluorinated surfactant adsorption on mineral surfaces: implications for PFAS Fate and Transport in the Environment. Surfaces 3, 516–566.

Ateia, M., Arifuzzaman, M., Pellizzeri, S., Attia, M.F., Tharayil, N., Anker, J.N., Karanfil, T., 2019. Cationic polymer for selective removal of GenX and short-chain PFAS from surface waters and wastewaters at ng/L levels. Water Res. 163, 114874–114885.

Bao, Y., Deng, S., Jiang, X., Qu, Y., He, Y., Liu, L., Chai, Q., Mumtaz, M., Huang, J., Cagnetta, G., Yu, G., 2018. Degradation of PFOA Substitute – GenX (HFPO-DA ammonium salt) : oxidation with UV/Persulfate or Reduction with UV/Sulfite? Environ. Sci. Technol. 52, 11728.

Barzen-Hanson, K.A., Roberts, S.C., Choyke, S., Oetjen, K., McAlees, A., Riddell, N., McCrindle, R., Ferguson, P.L., Higgins, C.P., Field, J.A., 2017. Discovery of 40 classes of per- and polyfluoroalkyl substances in historical aqueous film-forming foams (AFFFs) and AFFF-impacted groundwater. Environ. Sci. Technol. 51, 2047–2057.

Bedrov, D., Piquemal, J.-P., Borodin, O., MacKerell, A.D., Roux, B., Schröder, C., 2019. Molecular dynamics simulations of ionic liquids and electrolytes using polarizable force fields. Chem. Rev. 119, 7940–7995.

Beekman, M., Zweers, P., Muller, A., DeVries, W., Janssen, P., Zeilmaker, M., 2016. Evaluation of substances used in the GenX technology by Chemours, Dordrecht. in, Rijksinstituut voor Volksgezondheid en Milieu (RIVM) Letter report, Vol. 0174, pp. 1–92.

Bentel, M.J., Yu, Y., Xu, L., Kwon, H., Li, Z., Wong, B.M., Men, Y., Liu, J., 2020. Degradation of perfluoroalkyl ether carboxylic acids with hydrated electrons: structure-reactivity relationships and environmental implications. Environ. Sci. Technol. 54, 2480–2499.

Berr, S.S., Jones, R.R.M., 1989. Small-angle neutron scattering from aqueous solutions of sodium perfluorooctanoate above the critical micelle concentration. J. Phys. Chem. 93, 2555–2558.

Blake, B.E., Cope, H.A., Hall, S.M., Keys, R.D., Mahler, B.W., McCord, J., Scott, B., Stapleton, H.M., Strynar, M.J., Elmore, S.A., Fenton, S.E., 2020. Evaluation of maternal, embryo, and placental effects in CD-1 mice following gestational exposure to perfluorooctanoic acid (PFOA) or hexafluoropropylene oxide dimer acid (HFPO-DA or GenX). Environ. Health Perspect. 128, 27006.

Bodratti, A.M., Sarkar, B., Alexandridis, P., 2017. Adsorption of poly(ethylene oxide) containing amphiphilic polymers on solid-liquid interfaces: fundamentals and applications. Adv. Colloid Interface Sci. 244, 132–163.

Borodin, O., 2009. Polarizable force field development and molecular dynamics simulations of ionic liquids. J. Phys. Chem. B 113, 11463–11478.

Brandsma, S.H., Koekkoek, J.C., van Velzen, M.J.M., de Boer, J., 2018. The PFOA substitute GenX detected in the environment near a fluoropolymer manufacturing plant in the Netherlands. Chemosphere 220, 493.

Brase, R.A., Mullin, E.J., Spink, D.C., 2021. Legacy and emerging per- and polyfluoroalkyl substances: analytical techniques, environmental fate, and health effects. Int. J. Mol. Sci. 22, 995.

Brusseau, M.L., 2019. The influence of molecular structure on the adsorption of PFAS to fluid-fluid interfaces: Using QSPR to predict interfacial adsorption coefficients. Water Res. 152, 148–158.

Buck, R.C., Franklin, J., Berger, U., Conder, J.M., Cousins, I.T., de Voogt, P., Jensen, A.A., Kannan, K., Mabury, S.A., van Leeuwen, S.P.J., 2011. Perfluoroalkyl and polyfluoroalkyl substances in the environment: Terminology, classification, and origins. Integr. Environ. Assess. Manag. 7, 513–541.

Buck, R.C., Murphy, P.M., Pabon, M., 2012. Chemistry, properties, and uses of commercial fluorinated surfactants. In: Knepper, T.P., Lange, F.T. (Eds.), Polyfluorinated Chemicals and Transformation Products. Springer, Berlin, Heidelberg, pp. 1–24.

Burkitt, S.J., Ottewill, R.H., Hayter, J.B., Ingram, B.T., 1987. Small angle neutron scattering studies on micellar systems part 1. Ammonium octanoate, ammonium decanoate and ammonium perfluorooctanoate. Colloid Polym. Sci. 265, 619–627.

Caverly Rae, J.M., Craig, L., Slone, T.W., Frame, S.R., Buxton, L.W., Kennedy, G.L., 2015. Evaluation of chronic toxicity and carcinogenicity of ammonium 2,3,3,3-tetrafluoro-2-(heptafluoropropoxy) propanoate in Sprague-Dawley rats. Toxicol. Rep. 2, 939–949.

Chappell, G.A., Thompson, C.M., Wolf, J.C., Cullen, J.M., Klaunig, J.E., Haws, L.C., 2020. Assessment of the mode of action underlying the effects of GenX in mouse liver and implications for assessing human health risks. Toxicol. Pathol. 48, 494–508.

Cheng, W., Ng, C.A., 2018. Predicting relative protein affinity of novel per- and polyfluoroalkyl substances (PFASs) by an efficient molecular dynamics approach. Environ. Sci. Technol. 52, 7972–7980.

Chen, Z., Teng, Y., Huang, L., Mi, N., Li, C., Ling, J., Gu, C., Jin, X., 2021. Rapid photo reductive destruction of hexafluoropropylene oxide trimer acid (HFPO-TA) by a stable self-assembled micelle system of producing hydrated electrons. Chem. Eng. J. 420, 130436.

Conley, J.M., Lambright, C.S., Evans, N., McCord, J., Strynar, M.J., Hill, D., Medlock-Kakaley, E., Wilson, V.S., Gray, L.E., 2021. Hexafluoropropylene oxide dimer acid (HFPO-DA or GenX) alters maternal and fetal glucose and lipid metabolism and produces neonatal mortality, low birthweight, and hepatomegaly in the Sprague-Dawley rat. Environ. Int. 146, 106204.

Coperchini, F., Croce, L., Denegri, M., Pignatti, P., Agozzino, M., Netti, G.S., Imbriani, M., Rotondi, M., Chiovato, L., 2020. Adverse effects of in vitro GenX exposure on rat thyroid cell viability, DNA integrity and thyroid-related genes expression. Environ. Pollut. 264, 114778.

Danish EPA, 2015. Short chain Polyfluoroalkyl Substances (PFAS). (https://cswab.org/wp-content/uploads/2018/05/Short-chain-PFAS-literature-review-Danish-EPA-2015.pdf) (Accessed October 2021).

Dauchy, X., Boiteux, V., Bach, C., Rosin, C., Munoz, J.-F., 2017. Per- and polyfluoroalkyl substances in firefighting foam concentrates and water samples collected near sites impacted by the use of these foams. Chemosphere 183, 53–61.

Dixit, F., Barbeau, B., Mostafavi, S.G., Mohseni, M., 2020. Efficient removal of GenX (HFPO-DA) and other perfluorinated ether acids from drinking and recycled waters using anion exchange resins. J. Hazard. Mater. 384, 121261.

Domingo, J.L., Nadal, M., 2019. Human exposure to per- and polyfluoroalkyl substances (PFAS) through drinking water: a review of the recent scientific literature. Environ. Res. 177, 108648.

Dong, D., Kancharla, S., Hooper, J., Tsianou, M., Bedrov, D., Alexandridis, P., 2021. Controlling the self-assembly of perfluorinated surfactants in aqueous environments. Phys. Chem. Chem. Phys. 23, 10029–10039.

DuPont, 2010. DuPont™ GenX Processing Aid for Making Fluoropolymer Resins. (https://bladenonline.com/wp-content/uploads/2017/06/Chemours_GenX_Brochure_Final_07July2010.pdf) (accessed October 2021).

EPA, 2016. Drinking Water Health Advisories for PFOA and PFOS. (https://www.epa.gov/ground-water-and-drinking-water/drinking-water-health-advisories-pfoa-and-pfos).

EPA, 2021. Human Health Toxicity Assessments for GenX Chemicals. (https://www.epa.gov/chemical-research/human-health-toxicity-assessments-genx-chemicals) (accessed October 2021).

Fajalia, A.I., Tsianou, M., 2014. Charging and uncharging a neutral polymer in solution: a small-angle neutron scattering investigation. J. Phys. Chem. B 118, 10725–10739.

Fenton, S.E., Ducatman, A., Boobis, A., DeWitt, J.C., Lau, C., Ng, C., Smith, J.S., Roberts, S.M., 2021. Per- and polyfluoroalkyl substance toxicity and human health review: current state of knowledge and strategies for informing future research. Environ. Toxicol. Chem. 40, 606–630.

Gannon, S.A., Fasano, W.J., Mawn, M.P., Nabb, D.L., Buck, R.C., Buxton, L.W., Jepson, G.W., Frame, S.R., 2016. Absorption, distribution, metabolism, excretion, and kinetics of 2,3,3,3-tetrafluoro-2-(heptafluoropropoxy)propanoic acid ammonium salt following a single dose in rat, mouse, and cynomolgus monkey. Toxicology 340, 1–9.

Gebbink, W.A., van Asseldonk, L., van Leeuwen, S.P.J., 2017. Presence of emerging per- and polyfluoroalkyl substances (PFASs) in river and drinking water near a fluorochemical production plant in the Netherlands. Environ. Sci. Technol. 51, 11057–11065.

Glüge, J., Scheringer, M., Cousins, I.T., DeWitt, J.C., Goldenman, G., Herzke, D., Lohmann, R., Ng, C.A., Trier, X., Wang, Z., 2020. An overview of the uses of per- and polyfluoroalkyl substances (PFAS). Environ. Sci.: Process. Impacts 22, 2345–2373.

Gomis, M.I., Vestergren, R., Borg, D., Cousins, I.T., 2018. Comparing the toxic potency in vivo of long-chain perfluoroalkyl acids and fluorinated alternatives. Environ. Int. 113, 1–9.

Gomis, M.I., Wang, Z., Scheringer, M., Cousins, I.T., 2015. A modeling assessment of the physicochemical properties and environmental fate of emerging and novel per- and polyfluoroalkyl substances. Sci. Total Environ. 505, 981–991.

Guelfo, J.L., Adamson, D.T., 2018. Evaluation of a national data set for insights into sources, composition, and concentrations of per- and polyfluoroalkyl substances (PFASs) in U.S. drinking water. Environ. Pollut. 236, 505–513.

Heydebreck, F., Tang, J., Xie, Z., Ebinghaus, R., 2015. Alternative and legacy perfluoroalkyl substances: differences between European and Chinese river/estuary systems. Environ. Sci. Technol. 49, 8386–8395.

Hoke, R.A., Ferrell, B.D., Sloman, T.L., Buck, R.C., Buxton, L.W., 2016. Aquatic hazard, bioaccumulation and screening risk assessment for ammonium 2,3,3,3-tetrafluoro-2-(heptafluoropropoxy) propanoate. Chemosphere 149, 336–342.

Hoover, W.G., 1985. Canonical dynamics: equilibrium phase-space distributions. Phys. Rev. A 31, 1695–1697.
Hopkins, Z.R., Sun, M., DeWitt, J.C., Knappe, D.R.U., 2018. Recently detected drinking water contaminants: GenX and other per- and polyfluoroalkyl ether acids. J. - Am. Water Works Assoc. 110, 13–28.
Huang, P. J., Hwangbo, M., Chen, Z., Liu, Y., Kameoka, J., Chu, K. H., 2018. Reusable functionalized hydrogel sorbents for removing long- and short-chain perfluoroalkyl acids (PFAAs) and GenX from aqueous solution. ACS Omega 3, 17447–17455.
Iijima, H., Kato, T., Yoshida, H., Imai, M., 1998. Small-angle X-ray and neutron scattering from dilute solutions of cesium perfluorooctanoate. Micellar growth along two dimensions. J. Phys. Chem. B 102, 990–995.
Ito, A., Sakai, H., Kondo, Y., Yoshino, N., Abe, M., 1996. Micellar solution properties of fluorocarbon-hydrocarbon hybrid surfactants. Langmuir 12, 5768–5772.
ITRC, 2020. Interstate Technology & Regulatory Council (ITRC). 2020. PFAS Technical and Regulatory Guidance Document and Fact Sheets. (https://pfas-1.itrcweb.org/8-basis-of-regulations/) (accessed October 2021).
Jin, C., Yan, P., Wang, C., Xiao, J.-X., 2005. Effect of counterions on fluorinated surfactants I. Surface activity and micellization. Acta Chim. Sin. 63, 279–282.
Ji, W., Xiao, L., Ling, Y., Ching, C., Matsumoto, M., Bisbey, R.P., Helbling, D.E., Dichtel, W.R., 2018. Removal of GenX and perfluorinated alkyl substances from water by amine-functionalized covalent organic frameworks. J. Am. Chem. Soc. 140, 12677–12681.
Kalyanasundaram, K., 1988. Pyrene fluorescence as a probe of fluorocarbon micelles and their mixed micelles with hydrocarbon surfactants. Langmuir 4, 942–945.
Kancharla, S., Bedrov, D., Tsianou, M., Alexandridis, P., 2022. Structure and composition of mixed micelles formed by nonionic block copolymers and ionic surfactants in water determined by small-angle neutron scattering with contrast variation. J. Colloid Interface Sci. 609, 456–468. https://doi.org/10.1016/j.jcis.2021.10.176.
Kancharla, S., Canales, E., Alexandridis, P., 2019. Perfluorooctanoate in aqueous urea solutions: micelle formation, structure, and microenvironment. Int. J. Mol. Sci. 20, 5761.
Kancharla, S., Dong, D., Bedrov, D., Tsianou, M., Alexandridis, P., 2021a. Structure and interactions in perfluorooctanoate micellar solutions revealed by small-angle neutron scattering and molecular dynamics simulations studies: effect of urea. Langmuir 37, 5339–5347.
Kancharla, S., Jahan, R., Bedrov, D., Tsianou, M., Alexandridis, P., 2021b. Role of chain length and electrolyte on the micellization of anionic fluorinated surfactants in water. Colloids Surf. A: Physicochem. Eng. Asp. 628, 127313.
Kato, K., Kalathil, A.A., Patel, A.M., Ye, X., Calafat, A.M., 2018. Per- and polyfluoroalkyl substances and fluorinated alternatives in urine and serum by on-line solid phase extraction–liquid chromatography–tandem mass spectrometry. Chemosphere 209, 338–345.
Kissa, E., 2001. Fluorinated Surfactants and Repellents, second ed. Marcel Dekker, Incorporated, New York.
Krafft, M.P., Riess, J.G., 2015. Selected physicochemical aspects of poly- and perfluoroalkylated substances relevant to performance, environment and sustainability part one. Chemosphere 129, 4–19.
Kronberg, B., Holmberg, K., Lindman, B., 2014. Surface Chemistry of Surfactants and Polymers. John Wiley & Sons, Incorporated, Somerset.
Lee, Y. C., Wang, P.-Y., Lo, S.-L., Huang, C.P., 2017. Recovery of perfluorooctane sulfonate (PFOS) and perfluorooctanoate (PFOA) from dilute water solution by foam flotation. Sep. Purif. Technol. 173, 280–285.
Liu, Y., Smith, T.W., Alexandridis, P., 2002. Adsorption of a polymeric siloxane surfactant on carbon black particles dispersed in mixtures of water with polar organic solvents. J. Colloid Interface Sci. 255, 1–9.
Lukyanova, V.A., Papina, T.S., 2013. Standard enthalpies of formation of perfluoro(2-methyl-3-oxa)hexanoic and perfluoro(2,5-dimethyl-3,6-dioxa)nonanoic acids. Russ. J. Phys. Chem. A 87, 340–341.
Malmberg, C.G., 1958. Dielectric constant of deuterium oxide. J. Res. Natl. Bur. Stand. 60, 609–612.
Martyna, G.J., Tuckerman, M.E., Tobias, D.J., Klein, M.L., 1996. Explicit reversible integrators for extended systems dynamics. Mol. Phys. 87, 1117–1157.
Meng, P., Deng, S., Lu, X., Du, Z., Wang, B., Huang, J., Wang, Y., Yu, G., Xing, B., 2014. Role of air bubbles overlooked in the adsorption of perfluorooctanesulfonate on hydrophobic carbonaceous adsorbents. Environ. Sci. Technol. 48, 13785–13792.
Mohamed, A., Amith, M., Nishanth, T., Tanju, K., 2019. The overlooked short- and ultrashort chain poly- and perfluorinated substances: a review. Chemosphere 220, 866–882.
Mullin, L., Katz, D.R., Riddell, N., Plumb, R., Burgess, J.A., Yeung, L.W.Y., Jogsten, I.E., 2019. Analysis of hexafluoropropylene oxide-dimer acid (HFPO-DA) by liquid chromatography-mass spectrometry (LC-MS): review of current approaches and environmental levels. TrAC Trends Anal. Chem. 118, 828–839.
Munoz, G., Liu, J., Vo Duy, S., Sauvé, S., 2019. Analysis of F-53B, Gen-X, ADONA, and emerging fluoroalkylether substances in environmental and biomonitoring samples: a review. Trends Environ. Anal. Chem. 23, e00066.
Muto, Y., Esumi, K., Meguro, K., Zana, R., 1987. Aggregation behavior of mixed fluorocarbon and hydrocarbon surfactants in aqueous solutions. J. Colloid Interface Sci. 120, 162–171.
Nagarajan, R., 1982. Are large micelles rigid or flexible? A reinterpretation of viscosity data for micellar solutions. J. Colloid Interface Sci. 90, 477–486.
Nagarajan, R., 2002. Molecular packing parameter and surfactant self-assembly: the neglected role of the surfactant tail. Langmuir 18, 31–38.
Niwaggioli, T., Alexandridis, P., Hatton, T.A., Yekta, A., Winnik, M.A., 1995. Fluorescence probe studies of pluronic copolymer solutions as a function of temperature. Langmuir 11, 730–737.
Palmer, B.J., 1993. Direct application of shake to the Velocity Verlet Algorithm. J. Comput. Phys. 104, 470–472.
Pan, Y., Zhang, H., Cui, Q., Sheng, N., Yeung, L.W.Y., Sun, Y., Guo, Y., Dai, J., 2018. Worldwide distribution of novel perfluoroether carboxylic and sulfonic acids in surface water. Environ. Sci. Technol. 52, 7621–7629.
Prevedouros, K., Cousins, I.T., Buck, R.C., Korzeniowski, S.H., 2006. Sources, fate and transport of perfluorocarboxylates. Environ. Sci. Technol. 40, 32–44.
Prosser, A.J., Franses, E.I., 2001. Adsorption and surface tension of ionic surfactants at the air–water interface: review and evaluation of equilibrium models. Colloids Surf. A: Physicochem. Eng. Asp. 178, 1–40.
Shea, D., 2018. Proposed Drinking Water Health Advisory Value for GenX: 2, 3, 3, 3-tetrafluoro-2-(heptafluoropropoxy)-propanoic acid. (https://www.chemours.com/en/-/media/files/corporate/shea-toxicology-analysis-2018-04.pdf) (accessed October 2021).
Sunderland, E.M., Hu, X.C., Dassuncao, C., Tokranov, A.K., Wagner, C.C., Allen, J.G., 2019. A review of the pathways of human exposure to poly- and perfluoroalkyl substances (PFASs) and present understanding of health effects. J. Expo. Sci. Environ. Epidemiol. 29, 131–147.
Sun, M., Arevalo, E., Strynar, M., Lindstrom, A., Richardson, M., Kearns, B., Pickett, A., Smith, C., Knappe, D.R.U., 2016. Legacy and emerging perfluoroalkyl substances are important drinking water contaminants in the Cape Fear River Watershed of North Carolina. Environ. Sci. Technol. Lett. 3, 415–419.
Sun, S., Guo, H., Wang, J., Dai, J., 2019. Hepatotoxicity of perfluorooctanoic acid and two emerging alternatives based on a 3D spheroid model. Environ. Pollut. 246, 955–962.
Thompson, C.M., Fitch, S.E., Ring, C., Rish, W., Cullen, J.M., Haws, L.C., 2019. Development of an oral reference dose for the perfluorinated compound GenX. J. Appl. Toxicol. 39, 1267–1282.
Wang, Z., Cousins, I.T., Scheringer, M., Hungerbühler, K., 2013. Fluorinated alternatives to long-chain perfluoroalkyl carboxylic acids (PFCAs), perfluoroalkane sulfonic acids (PFSAs) and their potential precursors. Environ. Int. 60, 242–248.
Wang, W., Mi, X., Zhou, Z., Zhou, S., Li, C., Hu, X., Qi, D., Deng, S., 2019b. Novel insights into the competitive adsorption behavior and mechanism of per- and polyfluoroalkyl substances on the anion exchange resin. J. Colloid Interface Sci. 557, 655–663.
Wang, J., Niven, R.K., 2021. Unification of surface tension isotherms of PFOA or GenX salts in electrolyte solutions by mean ionic activity. Chemosphere 280, 130715.
Wang, R., Wang, W., Maimaiti, A., Shi, H., Wu, R., Li, Z., Qi, D., Yu, G., Deng, S., 2019a. Adsorption behavior and mechanism of emerging perfluoro-2-propoxypropanoic acid (GenX) on activated carbons and resins. Chem. Eng. J. 364, 132–138.
Weiss-Errico, M.J., O'Shea, K.E., 2019. Enhanced host–guest complexation of short chain perfluoroalkyl substances with positively charged β-cyclodextrin derivatives. J. Incl. Phenom. Macrocycl. Chem. 95, 111–117.
Wen, Y., Mirji, N., Irudayaraj, J., 2020. Epigenetic toxicity of PFOA and GenX in HepG2 cells and their role in lipid metabolism. Toxicol. Vitr. 65, 104797.
Xiao, F., 2017. Emerging poly- and perfluoroalkyl substances in the aquatic environment: a review of current literature. Water Res. 124, 482–495.
Xing, H., Yan, P., Xiao, J.-X., 2013. Unusual location of the pyrene probe solubilized in the micellar solutions of tetraalkylammonium perfluorooctanoates. Soft Matter 9, 1164–1171.
Yang, L., Alexandridis, P., 2000. Polyoxyalkylene block copolymers in formamide–water mixed solvents: micelle formation and structure studied by small-angle neutron scattering. Langmuir 16, 4819–4829.
Yan, N., Ji, Y., Zhang, B., Zheng, X., Brusseau, M.L., 2020. Transport of GenX in saturated and unsaturated porous media. Environ. Sci. Technol. 54, 11876–11885.
Zhang, M., Yamada, K., Bourguet, S., Guelfo, J., Suuberg, E.M., 2020. Vapor pressure of nine perfluoroalkyl substances (PFASs) determined using the Knudsen Effusion Method. J. Chem. Eng. Data 65, 2332–2342.
Zoeller, N., Blankschtein, D., 1998. Experimental determination of micelle shape and size in aqueous solutions of dodecyl ethoxy sulfates. Langmuir 14, 7155–7165.

Renewable and Sustainable Energy Reviews 29 (2014) 766–779

Contents lists available at ScienceDirect

Renewable and Sustainable Energy Reviews

journal homepage: www.elsevier.com/locate/rser

Environmental impacts of utility-scale solar energy

R.R. Hernandez [a,b,*], S.B. Easter [b,c], M.L. Murphy-Mariscal [d], F.T. Maestre [e], M. Tavassoli [b], E.B. Allen [d,f], C.W. Barrows [d], J. Belnap [g], R. Ochoa-Hueso [h], S. Ravi [a], M.F. Allen [d,i,j]

[a] Department of Environmental Earth System Science, Stanford University, Stanford, CA, USA
[b] Department of Global Ecology, Carnegie Institution for Science, Stanford, CA, USA
[c] Ecofactor, Redwood City, CA, USA
[d] Center for Conservation Biology, University of California, Riverside, CA, USA
[e] Departamento de Biología y Geología, Universidad Rey Juan Carlos, Móstoles, Spain
[f] Department of Botany and Plant Science, University of California, Riverside, CA, USA
[g] U.S. Geological Survey, Southwest Biological Science Center, Moab, UT, USA
[h] Hawkesbury Institute for the Environment, University of Western Sydney, Penrith, 2751, New South Wales, Australia
[i] Department of Biology, University of California, Riverside, CA, USA
[j] Department of Plant Pathology, University of California, Riverside, CA, USA

ARTICLE INFO

Article history:
Received 22 February 2013
Received in revised form
29 July 2013
Accepted 11 August 2013
Available online 28 September 2013

Keywords:
Biodiversity
Conservation
Desert
Greenhouse gas emissions
Land use and land cover change
Photovoltaic
Renewable energy

ABSTRACT

Renewable energy is a promising alternative to fossil fuel-based energy, but its development can require a complex set of environmental tradeoffs. A recent increase in solar energy systems, especially large, centralized installations, underscores the urgency of understanding their environmental interactions. Synthesizing literature across numerous disciplines, we review direct and indirect environmental impacts – both beneficial and adverse – of utility-scale solar energy (USSE) development, including impacts on biodiversity, land-use and land-cover change, soils, water resources, and human health. Additionally, we review feedbacks between USSE infrastructure and land-atmosphere interactions and the potential for USSE systems to mitigate climate change. Several characteristics and development strategies of USSE systems have low environmental impacts relative to other energy systems, including other renewables. We show opportunities to increase USSE environmental co-benefits, the permitting and regulatory constraints and opportunities of USSE, and highlight future research directions to better understand the nexus between USSE and the environment. Increasing the environmental compatibility of USSE systems will maximize the efficacy of this key renewable energy source in mitigating climatic and global environmental change.

Contents

* Corresponding author. Department of Environmental Earth System Science, 51 Dudley Lane, Apt 125, 260 Panama Street, Stanford, CA 94305, USA. Tel.: +1 650 681 7457.
E-mail address: rebecca.hernandez@stanford.edu (R.R. Hernandez).

1364-0321/$ - see front matter © 2013 Elsevier Ltd. All rights reserved.
http://dx.doi.org/10.1016/j.rser.2013.08.041

1. Introduction

Renewable energy is on the rise, largely to reduce dependency on limited reserves of fossil fuels and to mitigate impacts of climate change ([58, 110, 150]). The generation of electricity from sunlight directly (photovoltaic) and indirectly (concentrating solar power) over the last decade has been growing exponentially worldwide [150]. This is not surprising as the sun can provide more than 2500 terawatts (TW) of technically accessible energy over large areas of Earth's surface [82,125] and solar energy technologies are no longer cost prohibitive [9]. In fact, solar power technology dwarfs the potential of other renewable energy technologies such as wind- and biomass-derived energy by several orders of magnitude [150]. Moreover, solar energy has several positive aspects – reduction of greenhouse gases, stabilization of degraded land, increased energy independence, job opportunities, acceleration of rural electrification, and improved quality of life in developing countries [17,126] – that make it attractive in diverse regions worldwide.

In general, solar energy technologies fall into two broad categories: photovoltaic (PV) and concentrating solar power (CSP). Photovoltaic cells convert sunlight into electric current, whereas CSP uses reflective surfaces to focus sunlight into a beam to heat a working fluid in a receiver. Such mirrored surfaces include heliostat power towers (flat mirrors), parabolic troughs (parabolic mirrors), and dish Stirling (bowl-shaped mirrors). The size and location of a solar energy installation determines whether

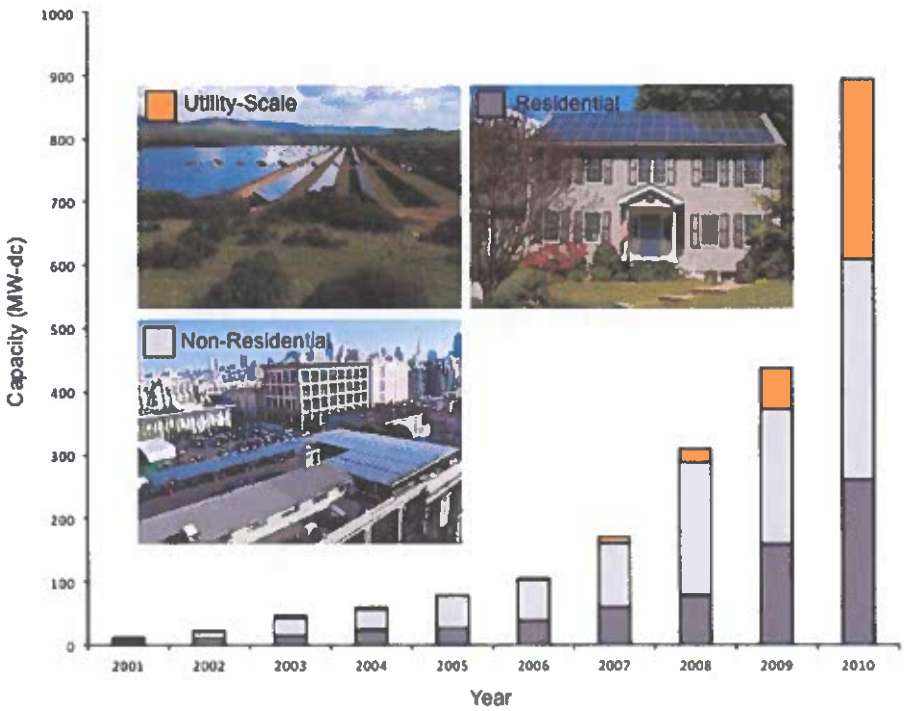

Fig. 1. Annual installed grid-connected photovoltaic (PV) capacity for utility-scale (>20 MW) solar energy schemes and distributed solar energy schemes (i.e., non-residential and residential) in the United States. Total PV capacity was 900 MW in 2010, approximately double the capacity of 2009. Data reprinted from Sherwood [114]. Photo credits: RR Hernandez, Jeff Qvale, National Green Power.

it is distributed or utility-scale. Distributed solar energy systems are relatively small in capacity (e.g., < 1 megawatt [MW]). They can function autonomously from the grid and are often integrated into the built environment (e.g., on rooftops of residences, commercial or government buildings; solar water heating systems; portable battlefield and tent shield devices; [25,102]). Distributed solar contrasts strikingly with utility-scale solar energy (USSE) enterprises, as the latter have relatively larger economies of scale, high capacity (typically > 1 MW), and are geographically centralized —sometimes at great distances from where the energy will be consumed and away from population centers. In the United States (US), solar energy has grown steadily over the past decade and rapidly in recent years (Fig. 1). The USSE capacity in this country quadrupled in 2010 from 2009, while both residential and nonresidential capacity increased over 60% during that same period. Similar increases in USSE have also been observed in Australia, China, Germany, India, Italy, and Spain [90,111,113,128,139].

As a paradigm of clean and sustainable energy for human use, reviews on the environmental impacts of solar energy date back to the 1970s [49,71]. For example, Lovins [71] provided a conceptual framework by which an energy scheme's position along a gradient from soft (benign) to hard (harmful) is determined by the energetic resiliency (or waste) and environmental conservation (or disruption) for its complete conversion from source to final end-use form. More recent reviews of the environmental impacts of solar energy systems have emphasized fundamental life-cycle elements (upstream and downstream environmental impacts associated with development; [126]) or were focused on specific regions (e.g., Serbia; [90]) or fauna of interest (Lovich and Ennen, 2012). The observed increase in USSE and studies elucidating their environmental properties underscores the importance of understanding environmental interactions associated with solar energy development, especially at regional and global scales and how these impacts may reduce, augment, or interact with drivers of global environmental change.

Here, we provide a review of current literature spanning several disciplines on the environmental impacts of USSE systems, including impacts on biodiversity, water use and consumption, soils, human health, and land-use and land-cover change, and land-atmosphere interactions, including the potential for USSE systems to mitigate climate change. Drawing from this review, we show (1) mechanisms to integrate USSE environmental co-benefit opportunities, (2) permitting and regulatory issues related to USSE, and (3) highlight key research needs to better understand the nexus between USSE and the environment.

2. Environmental impacts of utility-scale solar energy systems

Environmental impacts (see Fig. 2 for complete list) of USSE systems may occur at differential rates and magnitudes throughout the lifespan (i.e., construction, operation, and decommission) of a USSE power plant, which varies between 25 and 40 years. Drawing from experiments evaluating direct and indirect impacts of USSE systems and studies evaluating processes that are comparable in likeness to USSE activities, we discuss impacts related to biodiversity, water use and consumption, soils and dust, human health and air quality, transmission corridors, and land-use and land-cover change.

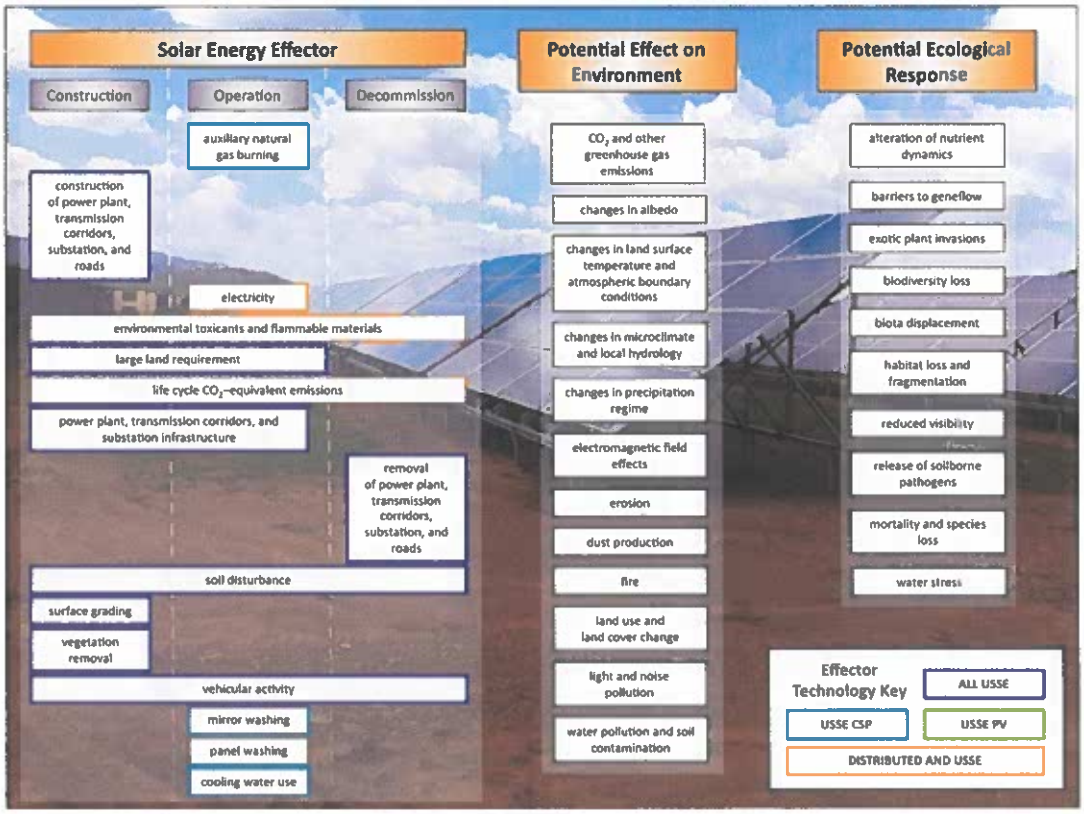

Fig. 2. Solar energy effectors for utility-scale solar energy technologies (ALL USSE), including concentrating solar power (USSE CSP) and photovoltaics (USSE PV), and for both utility-scale and distributed schemes (distributed and USSE). Effectors have one or more potential effects on the environment with one or more potential ecological responses. Photo credit: RR Hernandez.

2.1. Biodiversity

In general, distributed and USSE installations integrated into the existing built environment (e.g., roof-top PVs) will likely have negligible direct effects that adversely impact biodiversity [25]. Studies quantifying the direct impact of USSE on biodiversity in otherwise undisturbed habitats are few ([75,107]; Lovich and Ennen [70]; Cameron et al. [142]; [81]); however, these combined with other disturbance-related studies provide insight into how USSE power plants may impact biodiversity losses locally within the USSE footprint (i.e., all areas directly transformed or impacted by an installation during its life cycle), where the aboveground vegetation is cleared and soils typically graded, and regionally by landscape fragmentation that create barriers to the movement of species and their genes [101].

2.1.1. Proximate impacts on biodiversity

As USSE sites typically remove vegetation and soils are graded, locating USSE on land where biodiversity impacts are relatively small has been shown to be a feasible strategy for meeting both renewable energy and conservation goals ([39]; Cameron et al., 2012). For example, Fluri [39] showed that the strategic siting of USSE infrastructure in South Africa could create a nominal capacity of 548 gigawatts (GW) of CSP while avoiding all habitats supporting endangered or vulnerable vegetation. After a site has been chosen, solar energy projects may employ repatriation and translocation programs—when individuals of key native species are collected from impacted habitat, moved, and released into reserve areas previously inhabited and not previously inhabited by the species, respectively. The low success rates of repatriation and translocation programs (e.g., < 20%; [29,38]) have rendered them an expedient when all other mitigation options are unavailable [19]. These and other 'post-siting' compliance measures to minimize biodiversity impacts (e.g., land acquisition, road fencing) are expensive, usually target a single species, and do not guarantee benefits to the organisms they are designed to support [70]. The repatriation and translocation of organisms is complicated by climate change, which requires taking into account the dynamic character of species' distributions for both assessing biodiversity impacts of single and collective USSE projects and for determining suitable habitat for repatriation or translocation. Additionally, some species, such as birds, cannot be moved and may be attracted to certain USSE infrastructural elements. McCrary [75] found mortality rates, compared to other anthropogenic impacts on birds, low for USSE systems, and Hernandez (unpublished data) observed nests on the backside of PV module infrastructure (Fig. 3). Soil disturbances and roads can further increase mortality rates of organisms or serve as conduits for exotic invasions, which can competitively extirpate native species [42,140].

2.1.2. Indirect and regional effects on biodiversity

Less proximate impacts on biodiversity may also occur indirectly within the USSE footprint (i.e., all areas directly transformed or impacted by an installation during its life cycle), beyond the footprint, and regionally by landscape fragmentation that create barriers to the movement of species and their genes [101]. In the southwest US, anthropogenic sources of oxidized and reduced nitrogen may be elevated due to emissions from increased vehicle activity or the use of CSP auxiliary natural gas burners, promoting invasions by exotic annual grasses that increase fire frequencies [5,94]. Additionally, environmental toxicants required for USSE operation (e.g., dust suppressants, rust inhibitors, antifreeze agents) and herbicides may have insalubrious, and potentially

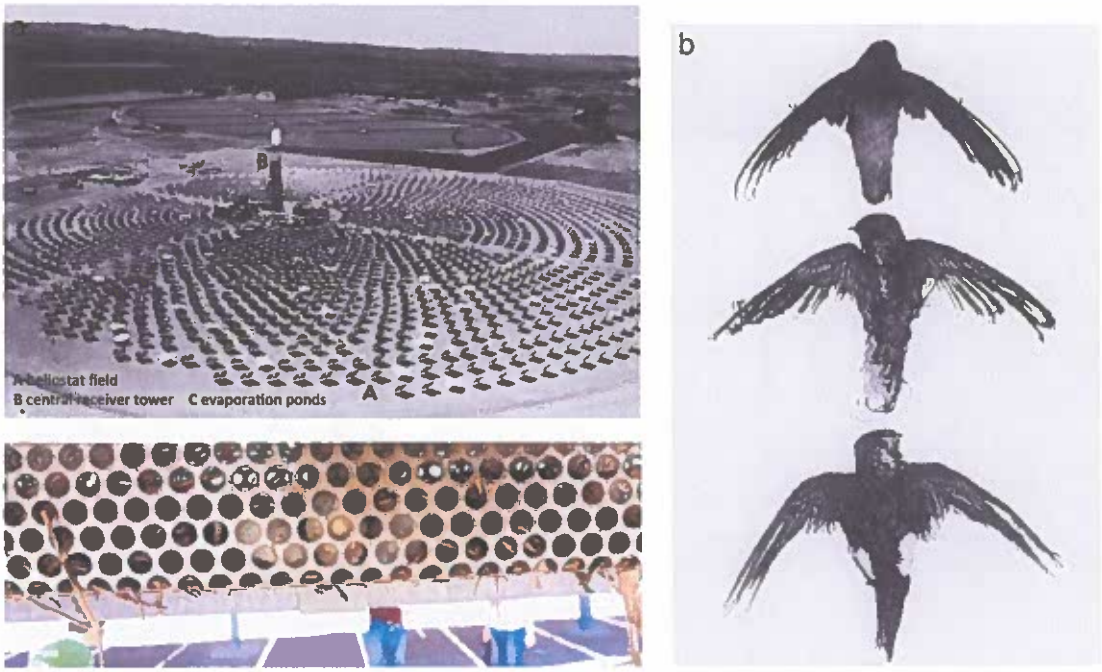

Fig. 3. ((a) and (b)) McCrary et al. [76] documented the death of 70 birds (26 species) over 40 weeks, including effects of scavenger bias, resulting from the operation of a 10 MW concentrating solar thermal power plant (Solar One, Mojave Desert, CA; 1). This equates to a mortality rate of 1.9–2.2 individual birds per week. Two causes of death were identified: most prevalent was collision with site infrastructure (81%), particularly with heliostats, and to a lesser degree, burning when heliostats were oriented towards standby points (19%), especially for aerial foraging species. Additionally, they found that the large, man-made evaporation pools increased the number of species five-fold in the local area. Impacts on bird mortality may increase non-linearly with increasing USSE capacity. (c) Hernandez (unpublished data) observed several bird nests on the backside of PV module infrastructure at a USSE power plant in the Central Valley of California (San Joaquin Irrigation District PV Plant, Valley Home, CA, USA). Photo credit: Madison Hoffacker.

long-term, consequences on both local and regional biodiversity [1,70].

Habitat loss and fragmentation are recognized as the leading threats to biological diversity [35,136]. The land-use efficiency, footprint, and infrastructural design of individual USSE installations vary significantly [51] and therefore individual power plants affect landscapes in unique ways. Utility-scale solar energy infrastructure may fragment habitat and serve as linear barriers to the movement patterns of certain wildlife species. Whereas highly mobile or wide-ranging species may be able to circumvent USSE infrastructure, some features may be insurmountable to less mobile species, increasing the risk of gene flow disruption between populations. Decisions regarding the placement of USSE infrastructure likely take into account current species distributions, but climate change may alter future distributions and wildlife dispersal corridors [52]. Determining species' responses to novel climate shifts is inherently uncertain and scale dependent, but nevertheless tools exist to model such distributional shifts (e.g., [11]).

2.2. Water use and consumption

Energy and water are interdependent [129]. USSE technologies vary in their water withdrawal (total volume removed from a water source) and consumption (volume of withdrawn water not returned to the source) rates, creating unique tradeoffs. Photovoltaic energy systems have low rates (0.02 m^3/megawatt hours [MW h]), consuming water only for panel washing and dust suppression in places where dust deposition is problematic [41]. Currently, washing panels or mirrors with water is the most common strategy for dust removal in large solar installations [73]. A recent analysis of water use by USSE installations in the southwestern US indicates that water for dust control is a major component (60–99%) of total water consumption in both dry cooled CSP and PV installations (Ravi et al., in review), whereas no information is available for other regions where USSE installations are expected to increase in the near future. Even though other cleaning technologies (e.g., electrostatic) exist, most are not yet commercially available, and the impacts of conventional technologies (e.g., cleaning using chemical sprays) on the environment are not completely understood [50,65].

In the case of CSP, the water consumption depends on the cooling system adopted—wet cooling, dry cooling, or a combination of the two (hybrid cooling) [108]. Concentrating solar power consumes vast quantities of water in wet cooling (i.e., 3.07 m^3/MW h), which is greater than coal and natural gas consumption combined [18,108]. The use of dry cooling, which reduces water consumption by 90% to 95%, is a viable option in water-limited ecosystems. Historically, reduced efficiency and higher startup costs have been an economic deterrent to dry cooling [108]. However, Holbert and Haverkamp [53] found that dry cooling startup costs are offset by 87–227% over a 20-year time interval, owing to cost savings in water use and consumption. Global regions already water stressed, such as many arid and semiarid habitats, may be vulnerable to changes in local hydrology [133], such as those incurred by USSE activities. In water-constrained areas, the deployment of USSE projects may also conflict with the use of water by other human activities (e.g., domestic use, agriculture), at least at the local scale [18,108]. Ultimately, the choice of dry or wet cooling in a CSP plant can lead to highly divergent hydrological impacts for USSE facilities.

2.3. Soil erosion, aeolian sediment transport, and feedbacks to energetic efficiency

Aridlands, where USSE facilities are often concentrated [51], are also areas where high winds result in aeolian transport of sand and dust. Some of that sediment transport is controlled by desert vegetation, but the installation of USSE infrastructure requires extensive landscape modification. Such modifications include vegetation removal, land grading, soil compaction, and the construction of access roads; activities that increase soil loss by wind and water [14,37].

The major agents of natural degradation are soil particulates (silt and clay), as well other particulate pollutants such as industrial carbon (C) [98,99]. Given its variable composition, dust emissions have a broad spectrum of impacts ranging from human health, global biogeochemical cycle, hydrologic cycle, climate, and desertification (e.g., [46,87,88,95]). In one semiarid ecosystem, Li et al. [68] recorded a 25% loss of total organic C and total nitrogen in the top 5 cm of soil following devegetation. Studies conducted in southeast Spain have found that 15 years after the removal of vegetation in a semiarid site, the total organic C remained ~30% lower compared to undisturbed areas, which also showed greater microbial biomass and activity levels [12]. Decreases in the availability of resources resulting from soil erosion can result in biodiversity losses and impede the recovery of vegetation [4,47,104]. Moreover, reduction in vegetative cover are strongly linked to increased dust production and even modest reductions in grass or shrub cover have been shown to dramatically increase dust flux [68,80].

Dust deposition can incur a negative feedback to solar energetic performance by decreasing the amount of solar radiation absorbed by PV cells [45]. Even suspended dust in the near surface atmosphere decreases the amount of solar radiation reaching the panel surface [45]. Deposition on solar panels or mirrors is site-specific and modulated by several factors, including soil parent material, microclimate, and frequency and intensity of dust events, but several studies have demonstrated energy production losses exceeding 20% [33,34,45,85]. Nonetheless, long-term field studies to quantify dust impacts on solar energy production are limited. For example, Ibrahim [55] experimentally demonstrated that solar modules installed in the Egyptian desert that have been exposed to dust for a period of one year showed an energy reduction of about 35%. Kimber et al. [61] investigated the effects of deposition on energy production for large grid-connected systems in the US and developed a modeling framework for predicting soiling losses. These authors found that for North American deserts, PV system efficiency declines by an average of 0.3% per day during periods without rain [61]. The National Renewable Energy Laboratory analyzed 24 PV systems throughout the US and calculated a typical derate factor (percentage decrease in power output) due to dust deposition of 0.95% [74]. In many desert ecosystems dust deposition rates are sufficiently high as to adversely impact solar power generation [67,98].

Challenges to manage dust loads may be amplified by increases in dust production related to land-use change, climate change (e.g., increases in aridity) or disturbance to biological soil crusts (e.g., fires, grazing, agriculture, energy exploration/development; [13]; Field et al.[37]; [95]). Even if USSE-related dust production is kept at bay, climate models predict an increase in aridity and recurrent droughts in dryland regions of the world (e.g., [109]), which may enhance soil erosion by wind and subsequent dust emissions. As these emissions can compromise the success of a USSE installation itself when they reduce its potential to generate electricity, effective dust management is advantageous to ensure efficient power generation while minimizing deleterious environmental and health impacts.

2.4. Human health and air quality

As with the development of any large-scale industrial facility, the construction of USSE power plants can pose hazards to air quality, the health of plant employees, and the public [122]. Such hazards include the release of soil-borne pathogens [91], increases

in air particulate matter (including $PM_{2.5}$, [46,100]), decreases in visibility for drivers on nearby roads, and the contamination of water reservoirs [70]. For example, disturbance of soils in drylands of North and South America, which are places targeted for USSE, aids transmission of *Coccidioides immitis*, a fungus causing Valley Fever in humans [10]. In areas where surface soil contains traces of chemical and radioactive contaminants (e.g., radionucleotides, agrochemical residues), increased aeolian transport resulting from soil disturbances increases contaminant concentrations in airborne dust [95].

During the decommissioning phase, PV cells can be recycled to prevent environmental contamination due to toxic materials contained within the cell, including cadmium, arsenic, and silica dust [144,145]. In the case of inappropriate handling or damaged cells, these industrial wastes can become exposed, which can be hazardous to the public and environment [144]. For example, inhalation of silica dust over long periods of time can lead to silicosis, a disease that causes scar tissue in the lungs and respiratory decline. In severe cases, it can be fatal [148]. In addition, chemical spills of materials such as dust suppressants, coolant liquids, heat transfer fluids, and herbicides can pollute surface ground water and deep water reservoirs [70,126].

On rooftops, solar PV panels have also been shown to reduce roof heat flux, conferring energy savings and increases in human comfort from cooling [31]. In that vein, the insulating properties of rooftop solar PV may serve co-beneficially to mitigate heat wave-related illness and mortality [131]. The fire hazard potential of both rooftop and ground-mounted USSE infrastructural materials (e.g., phosphine, diborane, cadmium), and their proper disposal, presents an additional challenge to minimizing the environmental impacts of USSE facilities [43]. This is particularly true in light of the dramatic increases in the frequency and intensity of wildland fires in arid and semiarid regions of the world as a result of climate change ([134], [15]).

2.5. Ecological impacts of transmission lines and corridors

Centralized USSE operations require transmission of generated electricity to population centers where consumption occurs. This necessitates the development of expanded transmission infrastructure, the availability of which has not kept up with demand [21,30]. As of 2007, over 333 kilometers (km; 207,000 miles) of high-voltage transmission lines (> 230 kV) were constructed in the US electricity transmission system [78] and this number is expected to rise as transmission infrastructure expands to growing population centers and connects with new renewable energy sources. As the potential for solar resources in other countries are being discovered so too are the plans to harness that energy and transmit it across international borders [27]; such plans are being actively developed to transmit energy from Middle Eastern and North African regions to European countries (requiring over 78,000 km of transmission lines by project completion in 2050; [124]). Although essential for transporting energy, the construction of such extensive transmission line networks has both long- and short-term ecological effects, including displacement of wildlife, removal of vegetative cover, and degradation of habitat quality [8], the degree of which may depend on land-use history, topography, and physical features of the sites, as well as productivity and vegetation types. For example, Lathrop and Archbold [66] estimated that biomass recovery at Mojave Desert sites disturbed for transmission line tower construction might take 100 years whereas recovery of disturbed transects directly beneath the transmission lines might take 20 years.

Fragmentation created by transmission corridors in forested habitats may displace permanent resident species and disrupt regular dispersal patterns [7,97,107]. While wide transmission corridors may facilitate new habitat types resulting in higher diversity or the introduction of new communities [7,58,81], they also experience greater edge effects. Sites at different stages of vegetative recovery have exhibited distinct recolonization patterns, with lower native and higher introduced species diversity at primary successional stages and an increase in native diversity at mid- and late-successional stages [20]. The ecological effects of transmission lines and corridors have proven to be varied and depend on a multitude factors, making appropriate siting crucial.

2.6. Land-use and land-cover change

2.6.1. Land-use dynamics of energy systems

Land and energy are inextricably linked [25]. When energy systems are developed, biophysical characteristics of the land may change (land-cover change, m^2), the human use or intent applied to the land may change (land-use change, m^2), and the land may be used for a specific duration of time (land occupation, m^2 x yr; [40,64]). Terrestrial ecosystems vary in their net primary productivity (rate of accumulation of organic C in plants), from tropical evergreen forests (1 to 3.2 $kg/m^2/yr^1$) to deserts (up to 0.6 $kg/m^2/yr^1$), and in their ability to sequester C in soil [105]. When land-use and land-cover change occurs – for example, when vegetation or biological soil crust is cleared or when soils are disturbed – above- and below-ground pools may release C back into the atmosphere as carbon dioxide (CO_2; [26]). Hence, developing energy-related infrastructure on previously disturbed or contaminated land may result in lower net C losses than infrastructure erected on undisturbed lands [26,62,89].

Other key land-use characteristics of energy include land-use efficiency and reversibility. Land-use efficiency (e.g., watts per square meter, $/m^2$) defines the installation's power relative to its footprint; the "footprint" being the land area transformed or impacted by the installation throughout the energy system's complete conversion chain [40,51]. As energy systems may impact land through materials exploration, materials extraction and acquisition, processing, manufacture, construction, production, operation and maintenance, refinement, distribution, decommissioning, and disposal, energy footprints can become incrementally high [40]. Some of this land may be utilized for energy in such a way that returning to a pre-disturbed state necessitates energy input or time, or both, whereas other uses are so dramatic that incurred changes are irreversible [79]. Irreversibility cost assessments can be employed to monetize restoration and irreversibility; a function of the original land cover type and properties of the land-use and land-cover change incurred [138,141].

2.6.2. Land-use of utility-scale solar energy

Likely due to its nascent expansion [9], studies evaluating land-use characteristics of USSE systems are relatively recent, few, and focused geographically. Hsu et al. [54] described the complete energy conversion chain of PV USSE systems, which necessitates materials acquisition, infrastructure and module manufacture, construction, operation and maintenance, material disposal, and decommissioning. The complete energy conversion chain of CSP is similar, but complicated by auxiliary natural gas and electricity consumption [16]. Fthenakis and Kim [40] stated that indirect land impacts related to materials (e.g., modules and balance-of-system) and energy for PV is negligible – between 22.5 and 25.9 m^2/GWh^1 – compared to direct land use. Data on land occupation are rare; however, the lifetime of USSE infrastructure, including modules, is typically assumed to be between 30 and 60 years [40].

Studies targeting the direct impact of USSE on land-cover change are few [51,143,149]. Furthermore, factors controlling sequestration of C in soils, particularly in aridlands, are not well understood [72,106], complicating the ability to quantify C losses

from USSE-related land-cover changes in the ecosystems where they are most likely to occur [51]. In western US, 97,000 ha (ha) of federal lands were approved or have pending leases for the development of USSE while over 18 million ha of land in this region were identified as suitable for USSE development [135]. In the same region, Pocewicz et al. [92] found that USSE development may impact shrublands greater than any other ecosystem type, with estimates of conversion ranging from 0.60 to 19.9 million ha, and especially for North American shrubland ecosystems. Smaller leases on grasslands and wetland ecosystems were approved, and therefore may also be impacted but to a lesser extent. Hernandez et al. [51] found that USSE (> 20 MW; planned, under construction, and operating) in California may impact approximately 86,000 ha; concentrated in the agricultural center of the state (the Central Valley) and the arid, interior of southern California. In the Mojave Desert, over 220,000 ha of Bureau of Land Management land has pending applications for USSE development. If constructed, creosote-white bursage desert scrub, the Mojave mid-elevation mixed desert scrub, and over 10,000 ha of desert tortoise habitat would be converted (Cameron et al., 2012).

Land-use efficiency of USSE is determined by the architectural and infrastructural design and capacity of the power plant but indirectly influenced by a project's geography, capacity factor, technology type, and developer priorities. Hernandez et al. [51] found the nominal LUE efficiency of USSE in California to be 35 W/m^2 where a capacity factor of 13% and 33% would generate a realized LUE of approximately 4.6 and 11.2 W m^{-2} for PV and CSP, respectively. Fthenakis and Kim [40] used a nominal packing factor (based on a single footprint specification) to determine the land use efficiency of PV and their results, ranging between 229 and 552 m^2/GWh^1, were comparable to [51].

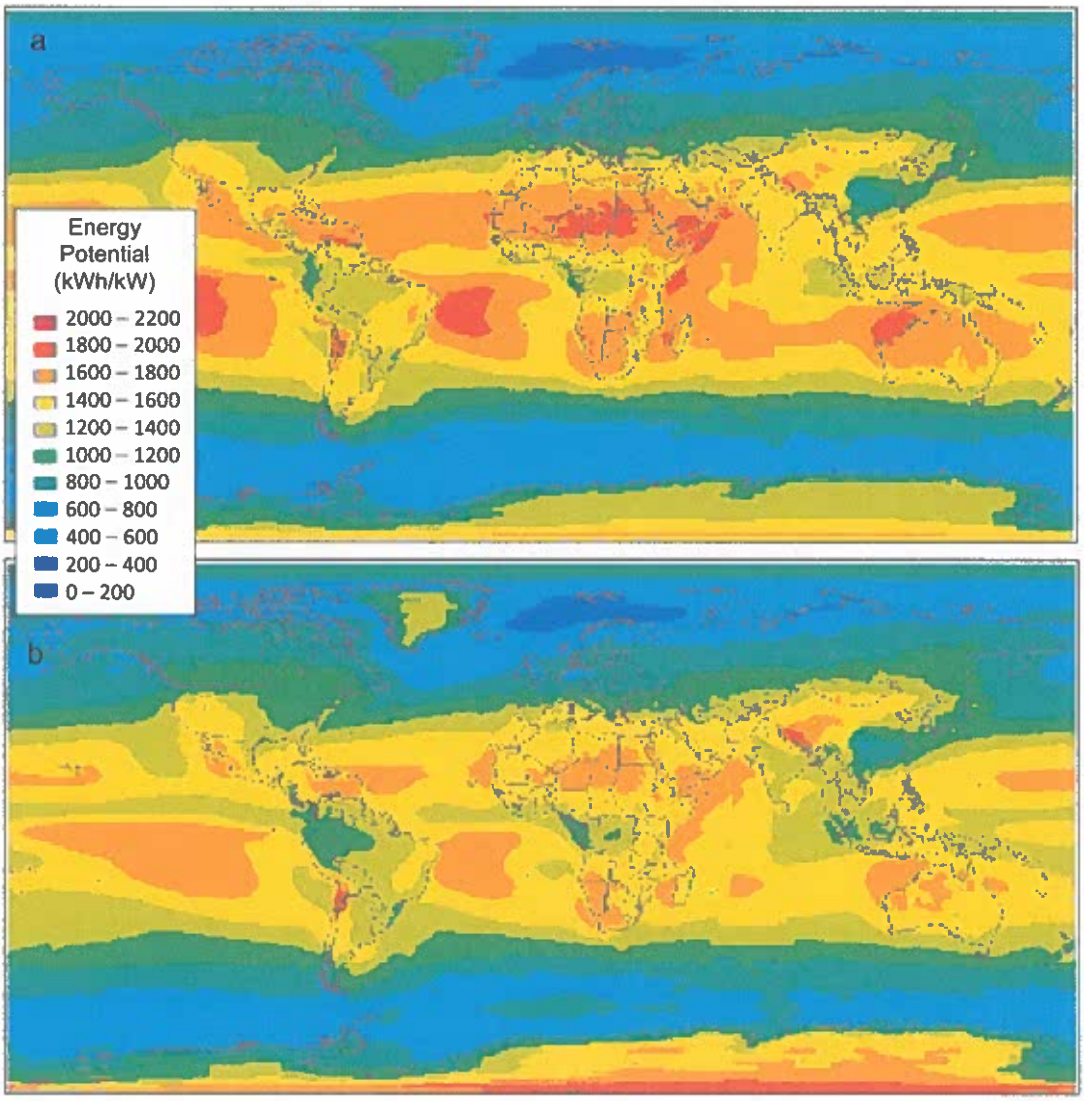

Fig. 4. Impact of temperature on global photovoltaic solar energy potential. In general, photovoltaic (PV) solar energy output increases with increasing irradiance but decreases with increasing ambient temperatures. These maps show (a) the global potential of PV energy (kWh/kW PV) for a crystalline silicon (c-Si) module, the most widely employed in the current market, without considering temperature effect, and (b) the global potential of PV energy (kWh/kW pV) for a crystalline silicon (c-Si) module including temperature effect. High irradiance coupled with low temperatures render the Himalayas, the Southern Andes, and Antarctica high in potential, > 1800 kWh/kW. High temperatures reduce PV solar energy potential in places including southwest United States deserts, northern Africa, and northern Australia. Both (a) and (b) include impacts from cloud cover (maps reprinted from Kawajiri et al. [59]). Not well understood is how changes in land surface temperatures from climate change, especially heat waves, will impact future global PV energy output.

To date, no study has evaluated how USSE land use efficiency (W/m^2) and layout – the infrastructural and architectural design of a USSE power plant – may impact ecosystem recovery or reversibility. However, the natural recovery of aridlands and other ecosystems after disturbance can be exceptionally slow. For example, leases for USSE development on public land in southern California deserts are typically at the decadal-scale, while complete ecosystem recovery from USSE activities there may require over 3000 years [69].

2.6.3. Comparing land-use across all energy systems

Land-use and land-cover change impacts from USSE are relatively small when compared to other energy systems [146]. In five ecosystems in western United States, Copeland et al. [21] found that *actively producing* oil and gas leases impact 20.7 million ha of land (4.5% of each terrestrial ecosystem evaluated) but the total potential for lands to be disturbed exceeded 50 million ha (11.1%). In contrast, potential land-cover change impacts from USSE development was < 1% of all ecosystems combined. In terms of land-use efficiency, PV energy systems generate the greatest amount of power per area among renewables, including wind, hydroelectric, and biomass [40,51]. Notably, ground-mounted PV installations have a higher land use efficiency (when incorporating both direct and indirect effects [e.g., resource extraction]) than surface coal mining, which is how 70% of all coal in the United States is extracted [40]. These results underscore the environmental potential solar energy development may have on land-cover and land-use change impacts, relative to carbon-intensive energy and other renewable energy sources.

3. Utility-scale solar energy, land-atmosphere interactions, and climate change

Assessments of USSE impacts on land-atmosphere interactions, especially those with climate feedbacks, are increasing in number. While there are two principal types of solar technologies (i.e., PV and CSP) recent research on land-atmosphere attributes of USSE have focused largely on PV [31,76,121], given their relatively larger deployment globally (65 GW of PV versus 1.5 GW of CSP; International Energy Agency, 2013).

3.1. Utility-scale solar energy and albedo

The radiative balance at the land-atmosphere interface can shift when the albedo of a PV solar installation differs from the former background albedo. Given their absorptivity, PV panels have an *effective albedo* (averaging 0.18–0.23), a function of its inherent reflectivity *and* solar conversion efficiency [83]. Using a fully coupled regional climate model, Millstein and Menon [76] showed that a 1 TW PV USSE installation (at 11% efficiency) in the Mojave Desert would decrease desert surface albedo, thereby increasing temperatures up to 0.4 °C. In cities, albedos average 0.15 to 0.22 and consequently installed PV arrays can potentially increase albedo for a cooling effect. Taha [121] modeled a high-density deployment of roof-mounted PV panels (i.e., a distributed scheme) in the Los Angeles Basin and found no adverse impacts on air temperature or the urban heat island and predicted up to 0.2 °C decrease in air temperatures under higher efficiency panels.

Although local- and regional-scale land-atmosphere impacts are important to consider, particularly in environmentally sensitive ecosystems, the global-scale substitution of carbon-intensive energy for solar energy cannot be understated. Nemet [84] found that when PV is substituted for fossil fuels at the global scale, the reduced radiative forcing is 30 times larger than the increase in radiative forcing from reduced albedo. Further underscoring their potential, as PV technologies increase in efficiency over time so too will their effective albedo.

3.2. Utility-scale solar energy and surface roughness

Changes in radiative balance can also occur due to changes in surface roughness. In the built environment, changes in roughness length (mean horizontal wind speed near the ground) is likely to be negligible given that PV panels are typically roof-embedded or resting slightly above the roof. In natural environments, specifically deserts, roughness length typically increases given the tall infrastructure of USSE plants. Indeed, Millstein and Menon [76] found that the solar arrays influenced local and regional wind dynamics up to 300 km away.

3.3. Utility-scale solar energy and climate change

Complicating our understanding of land-atmosphere interactions with USSE is climate change. Arguably one of the biggest challenges to the deployment of these facilities will be anticipating reductions in water resources in areas that are already water-stressed [80]. In 2009, all operating CSP facilities in the US were wet cooled [18]. Reductions in water availability will have consequences for both USSE facility operation and dust deposition on mirrors or panels (utility-scale and distributed). In places where more frequent, intense storms may occur, managing operational and ecological impacts of erosion will be an exigent concern [93].

Another part of the challenge lies in the shifting of climate envelopes and incidence of extreme weather. Photovoltaic technologies use both direct and diffuse light to convert energy from the sun into electricity, but high ambient temperatures reduce panel efficiency almost linearly (Fig. 4). Consequently, cool places with high irradiance are the best locations for capturing solar with PV [59]. Currently, combined uncertainty (i.e., standard deviation) of PV yield is roughly 8% during the PV system lifetime [123]. Uncertainty may increase if climate change projections are taken into consideration. Concentrating solar power efficiency increases linearly with increasing ambient temperature and proportionally to direct light and therefore changes in climate also impact CSP output. Indeed, site-specific favorability for PV and CSP are projected to vary over time under different climate change scenarios; for example, CSP may increase up to 10% in Europe under the Intergovernmental Panel on Climate Change A1B scenario [22].

The substitution of carbon-intensive energy sources for solar energy has enormous potential to mitigate climate change by directly reducing greenhouse gas emissions [150]. In the US, Zhai et al. [137] modeled a reduction of CO_2 emissions from 6.5% and up to 18.8%, if PV were to comprise 10% of the grid. Recently, a suite of studies harmonized (i.e., standardized and performed a meta-analysis of data from a large number of studies) current life cycle analysis literature to evaluate life cycle greenhouse gas emissions from various solar energy technologies, including upstream (e.g., resource and raw material acquisition, product manufacturing), operational, and downstream (e.g., selling and distribution of product, decommissioning and disposal) processes (Table 1). Photovoltaic solar technologies ranged from 14 to 45 g CO_2-eq kWh^{-1} [54,60], where CO_2-eq is the carbon dioxide equivalent, a measure for quantifying the climate-forcing strength of greenhouse gases by normalizing for the amount equivalent to CO_2. Concentrating solar power ranged from 26 to 38 g CO_2-eq kWh^{-1}, for parabolic trough and power tower, respectively [16]. These emission values were a magnitude of order less than greenhouse gas emissions from coal, gas, or oil Varun and Prakash [132].

4. Utility-scale solar energy co-benefit opportunities

Solar energy is one of the most promising alternatives to fossil fuels, especially as an attractive climate change mitigation option [150]. Clear-cut advantages of solar energy such as utilizing the sun as a renewable source of electrons and heat, and the reduction of air and water pollution by fossil fuels, can be complemented by additional environmental co-benefit opportunities [118,127]. Opportunities include, but are not limited to the (1) utilization of degraded lands, (2) co-location of solar panels with agriculture, (3) hybrid power systems, (4) floatovoltaics, and (5) novel panel architecture and design that serves to concomitantly conserve water and land resources (Fig. 5).

Table 1
Comparison of life cycle emissions for solar (grams of carbon dioxide equivalent per kWh) and conventional, carbon-intensive (grams of carbon dioxide per kWh) energy generation.

Conventional systems		Renewable systems[a]	
System	g-CO_2/kWh	System	g-CO_2-eq/kWh
Coal[c]	975	*Concentrating solar power*[b]	
Gas[c]	608	Parabolic trough[d]	26
Oil[c]	742	Power tower[d]	38
Nuclear[c]	24	*Photovoltaics*	
		Crystalline-silicon[e]	45
		Thin-film amorphous silicon[f]	21
		Thin-film cadmium telluride[f]	14
		Copper indium gallium Diselenide[f]	27

[a] Median values, assuming life span of 30 years.
[b] Excludes auxiliary natural gas combustion and electricity consumption.
[c] Varun and Prakash [132].
[d] [16].
[e] [155].
[f] [61].

4.1. Utilization of degraded lands

Degraded lands comprise approximately one-fourth of all land on Earth [63]. The development of "brightfields" on degraded lands [153]—including brownfields, landfills, mine sites, and other types of contaminated lands—confer several environmental co-benefits, including obviating additional land-use or land-cover change. For example, 12,000 ha of salt-contaminated agricultural land in the San Joaquin Valley (California, USA; Fig. 5a) are planned for conversion into a 2.4 GW solar power plant (www.westlandssolarpark.com). Employing water-efficient PV solar technology, the park's location stands to divert large amounts of water to active, water-stressed agricultural sites nearby; hence garnering broad support from various interest groups.

Utilizing degraded land can offer additional environmental benefits when reclamation of these lands is prioritized. On-site landscaping using native plants and soil amendments can add to ecosystem service provisioning (e.g., soil stability, C sequestration) without the use of additional water and fertilizer inputs. A 550 MW PV power plant spread over 1400 ha of private, non-prime agricultural land in San Luis Obispo (California, USA) will use economical, thin-film PV cells that operate efficiently in the relatively low light conditions characterizing this area (Fig. 5b). This mesic site reduces water consumption for panel cleaning and is also the location of an effort to re-establish the native grasslands that once dominated [6]. Under and around the panels, sheep will graze the taller grasses every two months to prevent obstruction of panels.

Fig. 5. Environmental co-benefit opportunities of utility-scale photovoltaic solar energy: ((a) and (b)) Utilization of degraded lands, (c) Co-locating solar energy and agriculture, and (d) Photo credits: Westlands Solar Park, Optisolar, Bert Bostelmann/Getty Images, [111].

4.2. Co-location with agriculture

Environmental co-benefits can occur when existing agricultural land is co-located with solar. With potential minimal risks to food security, co-location schemes can reduce land deficits for energy, food, and fiber production [25]. A preliminary study by Dahlin et al. [24] found that US electricity production could be met by utilizing approximately 11% of of US cropped land. The co-existence of grazing habitat for livestock, such as sheep and goats, may curtail the need for vegetation removal and maintenance, or both, and limit erosion, while supporting both energy and food/fiber production (Fig. 5c). Yet such sites need not be agricultural land *sensu stricto*. For example, Japan announced a co-location plan to diversify their grid by integrating 30 MW of PV in the unoccupied spaces adjacent to and on top of livestock barns, agricultural distribution centers, and parking lots [84]. Where land for agriculture is limited in aridlands, coupled USSE infrastructure and biofuel cultivation has been suggested as a strategy to minimize the socioeconomic and environmental issues resulting from biofuel cultivation in agricultural lands [96].

4.3. Hybrid power systems

The United States Department of Energy [130] estimates that more than one million ha of land would be required in the US to achieve the USSE 2030 SunShot scenario of 642 TW h. In the US and other countries where land is limited, co-location with other energy systems (e.g., wind, biomass, conventional thermal or natural gas power plants) may prove advantageous [115,120]. Hybridization and optimization methodologies for co-locating solar and wind power are currently being implemented in diverse geographic regions [115,120]: Charanka village in India provides an example of a wind-solar colocation region with 0.5 GW of combined wind and solar energy capacity [113]; a conventional fossil fuel 44 MW coal plant in Cameo, Colorado has been co-located with a 4 MW USSE trough for preheating feed water (IEA, [56]); and, Ordos City, Mongolia is co-locating the largest USSE facility in the world at a capacity of 2 GW PV alongside nearby wind and coal facilities [28]. Uncovering novel synergies between solar and other energy sources will continue to require diverse project implementations and industry-relevant field experiments, along with modeling studies on the energetic advantages and trade-offs of co-locating USSE with other facilities.

4.4. Floatovoltaics

A unique water-based design element is the use of "floatovoltaics". Innovative designs for reservoir-based PV modules – such as polyethylene floating arrays that utilize elastic fasteners to adapt to varying water levels – are beginning to proliferate globally [36]. Such water-borne PV systems are also being deployed in diverse water features including the muddy waters of a wastewater treatment site (Richmond, CA; NRG [86]), a pond where electricity is generated for the adjacent vineyard located in the Napa Valley, California [116,117], and an irrigation canal in Gujarat, India (Fig. 5d; [112]). This 750-m stretch of irrigation canal in India has been covered by 1 MW of PV panels, thereby reducing the need for land transformation and conserving roughly 9-million liters of water per year owing to reduced evaporation.

4.5. Photovoltaics in design and architecture

Integrating PVs into infrastructure and architectural elements can create numerous co-benefits, first by obviating the need for additional land-use or land-cover change. One study [103] found PV noise barriers to be economically profitable when ecological benefits were included in the cost benefit analysis. Photovoltaic noise barriers originated in Switzerland in 1989, and today over 9 MW of PV noise barriers have been erected alongside rail and highway systems in Europe, Australia, and China.

In addition to ground-mounted panels, PV installation on rooftops has enhanced solar energy production as well [118]. Government incentives known as feed-in-tariffs used in 48 countries encourage the use and growth of renewable energy in both commercial and residential sectors, including PV deployment on rooftops as it has the potential to contribute energy on a utility scale. For example, the Canadian province of Ontario has begun a large-scale PV integration into infrastructure since 2009 and it is estimated that its total area of viable rooftops can produce up to 30 GW of solar energy as compared to 90 GW from ground-mounted panels in utility-scale solar plants [118]. Similar to Ontario, USSE companies in Amsterdam are capitalizing on PV integration into the built-environment through rooftop installations on residential homes [155].

While land and rooftop-based PV installations are typically connected to a grid system, PV panels can also be used to generate power for off-grid domestic and non-domestic environments [156]. This setup offers a reliable source of energy for communities and villages in remote locations that lack access to a central utility power-line. Off-grid PV systems are vital to rural communities by providing electricity for basic needs and have a particularly large impact in developing countries such as India, Indonesia, Sri Lanka, and Kenya, where only a small percent of rural communities are grid-connected [147,154].

5. Minimizing adverse impacts of solar energy: Permitting and regulatory implications

Permitting and regulatory constraints for USSE vary with land ownership (e.g., public versus private land), ecological characteristics (e.g., undisturbed versus previously degraded, critical habitat for rare species) and cultural significance [152]. From the perspective of the public, the benefits of renewable energy development ought to be weighed against the loss of ecological function, loss of public access, and the loss of irreplaceable cultural resources [126,151]. From a perspective of energy development alone, possible delays from permitting requirements and regulatory reviews may be seen as having negative effects on financial returns.

Like other forms of renewable energy, each USSE project will ineluctably have its own unique set of social, cultural, environmental, technical, and political characteristics [152]. Project implementation may be further complicated by wavering market prices for land acquisition and materials in addition to environmental regulations and legislation that may vary across county, state, and national boundaries. Collectively, the wide variation in requirements to develop USSE marks a discrepancy in solar energy implementation amongst different regions.

In general, policies underlying the development of energy systems in all countries have yet to address all key impacts and externalities. Consequently, all the actors and entities involved in a single enterprise may be working independently to minimize adverse impacts in ways not regulated or incentivized by policy. Ways to minimize impacts include: (1) understanding the environmental implications of siting decisions using adequate inventories of species and processes Tsoutsos et al. [126], (2) monetizing the actual value of natural capital and ecosystem services attributed to a parcel of land, (3) siting USSE systems on land that maximizes energetic output and minimizes economic and environmental costs Tsoutsos et al. [126] [19]), (4) having individuals and entities involved with long-term commitments to the project, and (5) requiring developers to internalize costs.

In addition, standardizing the rigidity and quality of regulations for all USSE projects may serve to streamline USSE development.

6. Solar energy and the environment: Future research

Below, we suggest a list of research questions to springboard future studies aimed at expanding our understanding of the interaction between USSE and the environment. We have developed these questions to bridge empirical gaps that were identified as a result of this review. Where applicable, we have provided citations for studies that have addressed each question, in part, or existing studies that prompted our proposed research questions. Gaps in the literature where empirical research is lacking are indicated by the absence of citations.

6.1. Research questions addressing environmental impacts of utility-scale solar energy systems

Direct, indirect, and regional effects on biodiversity

- How do infrastructural design, module configuration, and shape of a USSE power plant affect biodiversity?
- To what degree are native species impacted by USSE power plants? ([75]; Lovich and Ennen, [70]) Are there certain taxa, life histories, or functional types that are more compatible with USSE than others?
- To what degree does USSE infrastructure serve as a corridor or impasse for the movement of species and their genes?

Water use and consumption

- How much water is displaced from agricultural and domestic use for USSE construction and operation? [44]

Soil erosion, aeolian sediment transport, and feedbacks to energetic efficiency

- What is the relationship among USSE electrical generation, location, and dust?
- Does vegetation beneath panels reduce dust deposition on modules?

Human health and air quality

- What are best practices for use of dust suppressants, coolant liquids, heat transfer fluids, and herbicides at USSE facilities? (Lovich and Ennen,)[70].

Ecological impacts of transmission lines and corridors

- How can existing transmission infrastructure and corridors be maximized for USSE development? [39]

Land-use and land-cover change

- What are the land-use and land-cover impacts of USSE globally and compared to other energy systems? [40,51,92]
- What is the relationship between land use efficiency and reversibility? For example, is it better to arrange modules as close together as possible or spread them out? [51]

6.2. Research questions addressing utility-scale solar energy, land-atmosphere interactions, and climate change

Utility-scale solar energy and albedo

- To what extent can the spatial arrangement and materials of USSE infrastructure be used to enhance cooling (e.g., in urban heat islands)? ([31]; Taha, *In press*)

Utility-scale solar energy and surface roughness

- How does USSE impact local and regional wind dynamics [76]

Utility-scale solar energy and climate change

- How will climate change impact utility-scale solar energy? [22]
- What is the potential of USSE to mitigate climate change in various regions worldwide and globally [137]

6.3. Research questions addressing utility-scale solar energy co-benefit opportunities

Utilization of degraded lands

- To what extent are USSE power plants erected on degraded lands?
- Does USSE infrastructure (e.g., shading) and maintenance requirements (e.g., panel washing) increase soil C sequestration in degraded lands?

Co-location with agriculture

- What are the environmental tradeoffs between allocating lands to USSE development versus agriculture?
- What are the socioeconomic consequences of USSE development in agricultural areas? How does USSE development impact local food security and employment opportunities?
- Can transpiration from vegetation/agriculture reduce solar panel temperature thereby increasing efficiency?
- When combining USSE systems and agriculture, what are the effects on crop yield? [24]

Hybrid power systems

- What environmental and economic advantages and disadvantages lie in the co-location of solar energy with other energy technologies?
- How can solar hybrid energy systems be optimized? [115,120]

Photovoltaics in design and architecture

- What is the technical potential of USSE as deployed in the built environment?
- What is the cost-benefit of roof-embedded and roof-top solar, including savings derived from reduced cooling needs? [31]
- What are the economic and environmental impacts of distributed/built environment solar schemes versus USSE in undeveloped lands? Is there an ideal portfolio ratio?

6.4. Research questions addressing permitting and regulatory implications

- How do environmental regulations and legislation impacting USSE development vary across county, state, and national boundaries?
- How effective are renewable energy policy measures in facilitating USSE growth? [118]

7. Conclusion

Utility-scale solar energy systems are on the rise worldwide, an expansion fueled by technological advances, policy changes, and the urgent need to reduce both our dependence on carbon-intensive sources of energy and the emission of greenhouse gases to the atmosphere. Recently, a growing interest among scientists, solar energy developers, land managers, and policy makers to understand the environmental impacts – both beneficial and adverse – of USSE, from local to global scales, has engendered novel research and findings. This review synthesizes this body of knowledge, which conceptually spans numerous disciplines and crosses multiple interdisciplinary boundaries.

The disadvantageous environmental impacts of USSE have not heretofore been carefully evaluated nor weighted against the numerous environmental benefits – particularly in mitigating climate change – and co-benefits that solar energy systems offer. Indeed, several characteristics and development strategies of USSE systems have low environmental impacts relative to other energy systems, including other renewable energy technologies. Major challenges to the widespread deployment of USSE installations remain in

technology, research, and policy. Overcoming such challenges, highlighted in the previous sections, will require multidisciplinary approaches, perspectives, and collaborations. This review serves to induce communication across relatively disparate disciplines but intentional and structured coordination will be required to further advance the state of knowledge and maximize the environmental benefits of solar energy systems at the utility-scale.

Acknowledgements

RRH acknowledges funding by the McGee Research Grant of the School of Earth Sciences of Stanford University, the Wiliam W. Orcutt Memorial Fellowship of the School of Earth Sciences of Stanford University, and the Department of Global Ecology at the Carnegie Institution for Science (Stanford, California). FTM acknowledges support from the European Research Council under the European Community's Seventh Framework Programme (FP7/2007–2013)/ERC Grant agreement 242658 (BIOCOM). SR acknowledges TomKat Center for Sustainable Energy at Stanford University. JB acknowledges support by the USGS Ecosystems and Climate and Land Use program. The use of trade, product, or firm names in this publication is for descriptive purposes only and does not imply endorsement by the U.S. Government.

References

[1] Abbasi SA, Abbasi N. The likely adverse environmental impacts of renewable energy sources. Applied Energy 2000;65(1):121–44.
[4] Alados CL, Pueyo Y, Barrantes O, Escós J, Giner L, Robles AB. Variations in landscape patterns and vegetation cover between 1957 and 1994 in a semiarid Mediterranean ecosystem. Landscape Ecology 2004;19(5):543–59.
[5] Allen EB, Rao LE, Steers RJ, Bytnerowicz A, Fenn ME. Impacts of atmospheric nitrogen deposition on vegetation and soils at Joshua Tree National Park. The Mojave desert ecosystem processes and sustainability. In: Webb RH, Fenstermaker LF, Heaton JS, Hughson DL, McDonald EV, Miller DM, editors. The Mojave Desert: ecosystem processes and sustainability. Las Vegas: University of Nevada Press; 2009. p. 78–100.
[6] Althouse, Meade,LLC. 2011. Habitat restoration and revegetation plan: Topaz Solar Farm (Draft). Available: (http://www.sloplanning.org/EIRs/topaz/FEIR/V2Apps/RTC_3/03_HabitatRestorationRevegPlan.pdf) (accessed 07.10.13).
[7] Anderson SH, Mann K, Shugart Jr. HH. The effect of transmission-line corridors on bird populations. American Midland Naturalist 1977;97(1):216–21.
[8] Andrews A. Fragmentation of habitat by roads and utility corridors: a review. Australian Zoologist 1990;26(3):130–41.
[9] Bazilian M, Onyeji I, Liebreich M, MacGill I, Chase J, Shah J, et al. Re-considering the economics of photovoltaic power. Renewable Energy 2013;53(2013):329–38.
[10] Baptista-Rosas RC, Hinojosa A, Riquelme M. Ecological niche modeling of *Coccidioides* spp. in western North American deserts. Annals of the New York Academy of Sciences 2007;1111(1):35–46.
[11] Barrows CW, Murphy-Mariscal ML. Modeling impacts of climate change on Joshua trees at their southern boundary: how scale impacts predictions. Biological Conservation 2012;152(2012):29–36.
[12] Bastida F, Moreno L, Hernández T, García C. Microbiological activity in a soil 15 years after its devegetation. Soil Biology & Biochemistry 2006;38(8):2503–7.
[13] Belnap J. Biological soil crusts and wind erosion. In: Belnap J, Lange OL, editors. Biological soil crusts: structure, function, and management. Berlin: Springer-Verlag; 2003. p. 339–47.
[14] Belnap J, Munson SM, Field JP. Aeolian and fluvial processes in dryland regions: the need for integrated studies. Ecohydrology 2011;4(5):615–22.
[15] Bowman DM, et al. Fire in the Earth system. Science 2009;324(5926):481–4.
[16] Burkhardt JJ, Heath G, Cohen E. Life cycle greenhouse gas emissions of trough and tower concentrating solar power electricity generation. Journal of Industrial Ecology 2012;16(s1):S93–109.
[17] Burney J, Woltering L, Burke M, Naylor R, Pasternak D. Solar-powered drip irrigation enhances food security in the Sudano-Sahel. Proceedings of the National Academy of Sciences of the United States of America 2010;107(5):1848–53.
[18] Carter, NT, Campbell, RJ. 2009. Water issues of concentrating solar power (CSP) electricity in the U.S. Southwest. Congressional Research Service, Washington DC.
[19] CBI (Conservation Biology Institute). 2010. Recommendations of independent science advisors for the California Desert Renewable Energy Conservation Plan (DRECP). CBI. Available at (http://www.energy.ca.gov/2010publications/DRECP-1000-2010-008/DRECP-1000-2010-008-F.PDF) (accessed 06.30.13).
[20] Clarke DJ, White JG. Recolonisation of powerline corridor vegetation by small mammals: timing and the influence of vegetative management. Landcsape and Urban Planning 2008;87(2):108–16.
[21] Copeland HE, Pocewicz A, Kiesecker J. Geography of energy development in Western North America: potential impacts to terrestrial ecosystems. In: Naugle DE, editor. Energy development and wildlife conservation in Western North America. Island Press; 2011. p. 7–22.
[22] Crook JA, Jones LA, Forster PM, Crook R. Climate change impacts on future photovoltaic and concentrated solar power energy output. Energy and Environmental Science 2011;4:3101–9.
[24] Dahlin, K, Anderegg W, Hernandez, RR, Hiza, N, Johnson, J, Maltais-landry, G, et al. 2011. Prospects for integrating utility-scale solar photovoltaics and industrial agriculture in the U.S. American Geophysical Union fall meeting, San Francisco, CA. Abstract #B23B-0419.
[25] Dale VH, Efroymson RA, Kline KL. The land use-climate change-energy nexus. Landscape Ecology 2011;26(6):755–73.
[26] DeFries R, Field C, Fung I, Collatz G. Combining satellite data and biogeochemical models to estimate global effects of human-induced land cover change on carbon emissions and primary productivity. Global Biogeochemical Cycles 1999;13(3):803–15.
[27] Delucchi MA, Jacobson MZ. Providing all global energy with wind, water, and solar power, Part II: Reliability, system and transmission costs, and policies. Energy Policy 2011;39:1170–90.
[28] Devabhaktuni V, Alam M, Depuru SSSR, Green RC, Nims D, Near C. Solar energy: trends and enabling technologies. Renewable and Sustainable Energy Reviews 2013;19(1):555–64.
[29] Dodd CK, Seigel RA. Relocation, repatriation, and translocation of amphibians and reptiles: are they conservation strategies that work? Herpetologica 2012;47:336–50.
[30] DOE (Department of Energy). 2002. National transmission grid study. U.S. Department of Energy, Washington, DC. Available at (http://www.ferc.gov/industries/electric/gen-info/transmission-grid.pdf) (accessed 08.09.13).
[31] Dominguez A, Kleissl J, Luvall JC. Effects of solar photovoltaic panels on roof heat transfer. Solar Energy 2011;85(9):2244–55.
[33] El-Shobokshy MS, Hussein F. Effect of the dust with different physical properties on the performance of photovoltaic cells. Solar Energy 1993;51(6):505–11.
[34] Elminir H, Ghitas A, Hamid R, Elhussainy F, Beheary M, Abdelmoneim K. Effect of dust on the transparent cover of solar collectors. Energy Conversion and Management 2006;47(18-19):3192–203.
[35] Fahrig L. Effects of habitat fragmentation on biodiversity. Annual Review of Ecology, Evolution, and Systematics 2003;34(2003):487–515.
[36] Ferrer-Gisbert C, Ferrán-Gozálvez JJ, Redón-Santafé M, Ferrer-Gisbert P, Sánchez-Romero FJ, Torregrosa-Soler JB. A new photovoltaic floating cover system for water reservoirs. Renewable Energy 2013;60:63–70.
[37] Field JP, et al. The ecology of dust. Frontiers in Ecology and the Environment 2010;8(8):423–30.
[38] Fischer J, Lindenmayer DB. An assessment of the published results of animal relocations. Biological Conservation 2000;96(1):1–11.
[39] Fluri TP. The potential of concentrating solar power in South Africa. Energy Policy 2009;37(12):5075–80.
[40] Fthenakis V, Kim HC. Land use and electricity generation: a life-cycle analysis. Renewable and Sustainable Energy Reviews 2009;13(6):1465–74.
[41] Fthenakis V, Kim HC. Life-cycle uses of water in U.S. electricity generation. Renewable and Sustainable Energy Reviews 2010;14(7):2039–48.
[42] Gelbard JL, Belnap J. Roads as conduits for exotic plant invasions in a semiarid landscape. Conservation Biology 2003;17(2):420–32.
[43] Gevorkian P. Large-scale solar power system design: an engineering guide for grid-connected solar power. The McGraw-Hill Companies, Inc; 704.
[44] Glassman, D, Wucker, M, Isaacman, T, Champilou, C. 2011. The water-energy nexus. Adding water to the energy agenda, a world policy paper. EGB Capital, Environmental Investments, New York. Available at (http://www.nationalfoodhub.com/images/THE_WATER-ENERGY_NEXUS_REPORT.pdf) (accessed 07.14.13).
[45] Goossens D, Van Kerschaever E. Aeolian dust deposition on photovoltaic solar cells: the effects of wind velocity and airborne dust concentration on cell performance. Solar Energy 1999;66(4):277–89.
[46] Griffin DW, Kellogg CA, Shinn EA. Dust in the wind: long range transport of dust in the atmosphere and its implications for global public and ecosystem health. Global Change and Human Health 2001;2(1):20–33.
[47] Guerrero-Campo J, Montserrat-Martí G. Comparison of floristic changes on vegetation affected by different levels of soil erosion in Miocene clays and Eocene marls from Northeast Spain. Plant Ecology 2004;173(1):83–93.
[49] Harte J, Jassby A. Energy technologies and natural environments: the search for compatability. Annual Review of Energy 1978;3(1):101–46.
[50] He G, Zhou C, Li Z. Review of self-cleaning method for solar cell array. Procedia Engineering 2011;16(2011):640–5.
[51] Hernandez, RR, Hoffacker, M, Field, CB. in review. The land-use efficiency of big solar.
[52] Hobbs RJ, Hopkins AJM. The role of conservation corridors in a changing climate. In: Saunders DA, Hobbs RJ, editors. Nature conservation 2: The role

of corridors. Chipping Norton, Australia: Surrey Beatty & Sons; 1991. p. 281–90.
[53] Holbert, KE, Haverkamp, CJ. 2009. Impact of solar thermal power plants on water resources and electricity costs in the Southwest. In: North American Power symposium (NAPS), Starkville, Mississippi, pp. 1–6.
[54] Hsu DD, et al. Life cycle greenhouse gas emissions of crystalline silicon photovoltaic electricity generation. Journal of Industrial Ecology 2012;16(s1): S122–S135.
[55] Ibrahim A. Effect of shadow and dust on the performance of silicon solar cell. Journal of Applied Sciences Research 2011;1:222–30.
[56] International Energy Agency. Solar (PV and CSP). Available at: (http://www.iea.org/topics/solarpvandcsp/), accessed 02.04.13.
[58] Johnson WC, Shreiber RK, Burgess RL. Diversity of small mammals in a powerline right-of-way and adjacent forest in east Tennessee. American Midland Naturalist 1979;101(1):231–5.
[59] Kawajiri K, Oozeki T, Genchi Y. Effect of temperature on PV potential in the world. Environmental Science & Technology 2011;45(20):9030–5.
[60] Kim HC, Fthenakis V, Choi JK, Turney DE. Life cycle greenhouse gas emissions of thin-film photovoltaic electricity generation. Journal of Industrial Ecology 2012;16(s1):S110–21.
[61] Kimber, A, et al. 2006. The effect of soiling on large grid-connected photovoltaic systems in California and the Southwest Region of the United States. In: Conference record of the 2006 IEEE fourth world conference on photovoltaic energy conversion 2, 2391–2395.
[62] Lal R. Soil carbon sequestration impacts on global climate change and food security. Science 2004;304(5677):1623–7.
[63] Lambin EF, Meyfroidt P. Global land use change, economic globalization, and the looming land scarcity. Proceedings of the National Academy of Sciences 2011;108:3465–72.
[64] Lambin EF, Turner BL, Geist HJ, Agbola SB, Angelsen A, Bruce JW, et al. The causes of land-use and land-cover change: moving beyond the myths. Global Environmental Change 2001;11(2001):261–9.
[65] Lamont L, El Charr L. Enhancement of a stand-alone photovoltaic system's performance: reduction of soft and hard shading. Renewable Energy 2011;36 (4):1306–10.
[66] Lathrop EW, Archbold E. Plant response to utility right of way construction in the Mojave Desert. Environmental Management 1980;4(3):215–26.
[67] Lawrence CR, Neff JC. The contemporary physical and chemical flux of aeolian dust: a synthesis of direct measurements of dust deposition. Chemical Geology 2009;267(1):46–63.
[68] Li J, Okin GS, Alvarez L, Epstein H. Quantitative effects of vegetation cover on wind erosion and soil nutrient loss in a desert grassland of southern New Mexico, USA. Biogeochemistry 2007;85(3):317–32.
[69] Lovich JE, Bainbridge D. Anthropogenic degradation of the Southern California Desert ecosystem and prospects for natural recovery and restoration. Environmental Management 1999;24(3):309–26.
[70] Lovich JE, Ennen JR. Wildlife conservation and solar energy development in the desert southwest, United States. BioScience 2011;61(2):982–92.
[71] Lovins BAB. Energy strategy: the road not taken? Foreign Affairs 1976;55: 65–96.
[72] Maestre FT, Salguero-Gómez R, Quero JL. It is getting hotter in here: determining and projecting the impacts of global environmental change on drylands. Philosophical Transactions of the Royal Society Biological Sciences 2012;367:3062–75.
[73] Mani M, Pillai R. Impact of dust on solar photovoltaic (PV) performance: research status, challenges and recommendations. Renewable and Sustainable Energy Reviews 2010;14(9):3124–31.
[74] Marion, B, et al. 2005. Performance parameters for grid-connected PV systems. In: The 31st institute of electrical and electronics engineers (IEEE) photovoltaic specialists conference, Lake Buena Vista, FL. Available at (http://www.nrel.gov/docs/fy05osti/37358.pdf) (accessed 10.03.12).
[75] McCrary MD, McKernan RL, Schreiber RL, Wagner WD, Sciarrotta TC. Avian mortality at a solar energy power plant. Journal of Field Ornithology 1986;57 (2):135–41.
[76] Millstein D, Menon S. Regional climate consequences of large-scale cool roof and photovoltaic array deployment. Environmental Research Letters 2011;6 (3):034001.
[78] Molburg, JC, Kavicky, JA, Picel, KC. 2007. The design, construction, and operation of long-distance high-voltage electricity transmission technologies. Environmental Science Division, Argonne National Laboratories, Technical Memorandum ANL/EVS/TM/08-4. Available at (http://solareis.anl.gov/documents/docs/APT_61117_EVS_TM_08_4.pdf) (accessed 08.09.13).
[79] Morton RA, Bernier JC, Barras JA. Evidence of a regional subsidence and associated interior wetland loss induced by hydrocarbon production, Gulf Coast region, USA. Environmental Geology 2006;50(2):261–74.
[80] Munson SM, Belnap J, Okin GS. Responses of wind erosion to climate-induced vegetation changes on the Colorado Plateau. Proceedings of the National Academy of Sciences of the United States of America 2011;108 (10):3854–9.
[81] Nekola JC. The impact of a utility corridor on terrestrial gastropod biodiversity. Biodiversity and Conservation 2012;21(3):781–95.
[82] Nelson J. The physics of solar cells. London: Imperial College; 2003.
[83] Nemet GF. Net radiative forcing from widespread deployment of photovoltaics. Environmental Science & Technology 2009;43(6):2173–8.
[84] Nesheiwat J, Cross JS. Japan's post-Fukushima reconstruction: a case for implementation of sustainable energy technologies. Energy Policy 2013 (doi: http://dx.doi.org/10.1016/j.enpol.2013.04.065).
[85] Norton B, et al. Enhancing the performance of building integrated photovoltaics. Solar Energy 2011;85(8):1629–64.
[86] NRG Solar. 2012. West County Wastewater District. Available at: (http://www.nrgsolar.com/docs/factsheet_wcwd2013.pdf), Accessed on 10 July 2013, 6 pp.
[87] Painter TH, et al. Impact of disturbed desert soils on duration of mountain snow cover. Geophysical Research Letters 2007;34(12):1–6.
[88] Painter TH, Deems JS, Belnap J, Hamlet AF, Landry CC, Udall B. Response of Colorado River runoff to dust radiative forcing in snow. Proceedings of the National Academy of Sciences of the United States of America 2010;107 (40):17125–30.
[89] Pan Y, et al. A large and persistent carbon sink in the world's forests. Science 2011;333(6045):988–93.
[90] Pavlović TM, Radonjić IS, Milosavljević DD, Pantić LS. A review of concentrating solar power plants in the world and their potential in Serbia. Renewable and Sustainable Energy Reviews 2012;16(6):3891–902.
[91] Pepper IL, Gerba CP, Newby DT, Rice CW. Soil: a public health threat or savior? Critical Reviews in Environmental Science and Technology 2009;39 (5):416–32.
[92] Pocewicz A, Copel HE, Kiesecker JM. Potential impacts of energy development on shrublands in western North America. In: Monaco TA, et al., editors. Proceedings—threats to shrubland ecosystem integrity. Logan, UT: SJ and Jessie E Quinney Natural Resources Research Library; 2011.
[93] Ralph, M, et al. 2012. Water supply and flooding. In: Pierce, DW, editor, California climate extremes workshop report, Scripps Institution of Oceanography, pp. 8–9.
[94] Rao LE, Allen EB, Meixner T. Risk-based determination of critical nitrogen deposition loads for fire spread in southern California deserts. Ecological Applications 2010;20(5):1320–35.
[95] Ravi S, et al. Aeolian processes and the biosphere. Review of Geophysics 2011;49(3):1–45.
[96] Ravi S, Lobell DB, Field CB, Tradeoffs and synergies between biofuel production and large-scale solar infrastructure in deserts. Energy and Environmental Science, under review.
[97] Reed F. A regional landscape approach to maintain diversity. BioScience 1983;33(11):700–6.
[98] Reheis MC. Dust deposition downwind of Owens (Dry) Lake, 1991–1994—Preliminary findings. Journal of Geophysical Research: Atmospheres 1997;102(D22):25999–6008.
[99] Reheis MC, et al. Quaternary soils and dust deposition in southern Nevada and California. Geological Society of America Bulletin 1995;107(9): 1003–22.
[100] Russell AG, Brunekreef B. A focus on particulate matter and health. Environmental Science & Technology 2009;43(13):4620–5.
[101] Saunders DA, Hobbs RJ, Margules CR. Biological consequences of ecosystem fragmentation: a review. Conservation Biology 1991;5(1):18–32.
[102] SEIA, Solar Energy Industries Association. 2012. Utility-scale solar projects in the United States: Operating, under construction, or under development. Available at: (http://www.seia.org/sites/default/files/resources/Major%20Solar%20Projects%20List%2012.13.12.pdf), accessed on 15 January 2013, 7 pp.
[103] Schepper ED, Passel SV, Manca J, Thewys T. Combining photovoltaics and sound barriers—a feasibility study. Renewable Energy 2012;46(2012): 297–303.
[104] Schlesinger WH, et al. Biological feedbacks in global desertification. Science 1990;247(4946):1043–8.
[105] Schlesinger WH. Biogeochemistry: an analysis of global change. New York: Academic Press; 432.
[106] Schleshinger WH, Belnap J, Marion G. On carbon sequestration in desert ecosystems. Global Change Biology 2009;15(6):1488–90.
[107] Schreiber RK, Graves JH. Powerline corridors as possible barriers to the movement of small mammals. American Midland Naturalist 1977;97(2):504–8.
[108] Schwartz C. Concentrated thermal solar power and the value of water for electricity. In: Kennedy DS, Wilkinson R, editors. The water-energy nexus in the American West. Massachusetts, USA: Edward Elgar Publishing; 2011. p. 71–83.
[109] Seager R, et al. Model projections of an imminent transition to a more arid climate in southwestern North America. Science 2007;316(5828):1181–4.
[110] Shafiee S, Topal E. When will fossil fuel reserves be diminished? Energy Policy 2009;37(1):181–9.
[111] Sharma A. A comprehensive study of solar power in India and World. Renewable and Sustainable Energy Reviews 2011;15(4):1767–76.
[112] Sharma DC. India launches solar power project. Frontiers in Ecology and the Environment 2012;10(5):228–32.
[113] Sharma NK, Tiwari PK, Sood YR. Solar energy in India: strategies, policies perspectives, and future potential. Renewable and Sustainable Energy Reviews 2012;16(1):933–41.
[114] Sherwood, L, 2012. U.S. Solar Market Trends 2011. Interstate Renewable Energy Council, Inc. Available at (http://www.irecusa.org/wp-content/uploads/IRECSolarMarketTrends-2012-Web-8-28-12.pdf) (accessed 12.13.12).
[115] Sioshansi R, Denholm P. Transmission benefits of co-locating concentrating solar power and wind. National Renewable Energy Laboratory; 2012.

[116] Smyth M. Solar photovoltaic installations in American and European wine-making facilities. Journal of Cleaner Production 2012;31:22–9.
[117] Smyth M, Russell J. From graft to bottle—analysis of energy use in viticulture and wine production and the potential for solar renewable technologies. Renewable and Sustainable Energy Reviews 2009;13(8):1985–93.
[118] Solangi KH, Islam MR, Saidur R, Rahim NA, Fayaz H. A review on global solar energy policy. Renewable and Sustainable Energy Reviews 2011;15(4):2149–63.
[120] Sreeraj ES, Chatterjee K, Bandyopadhyay S. Design of isolated renewable hybrid power systems. Solar Energy 2010;84(7):1124–36.
[121] Taha H. The potential for air-temperature impact from large-scale deployment of solar photovoltaic arrays in urban areas. Solar Energy 2013;91(2013):358–67.
[122] TEEIC (Tribal Energy and Environmental Information Clearinghouse). Solar energy construction impacts. Environmental resources for tribal energy development, Office of Indian Energy and Economic Development. Available at (http://teeic.anl.gov/er/solar/impact/construct/index.cfm) (accessed 07.01.13).
[123] Thevenard D, Pelland S. Estimating the uncertainty in long-term photovoltaic yield predictions. Solar Energy 2013;91:432–45.
[124] Trieb F, Schillings C, Pregger T, O'Sullivan M. Solar electricity imports from the Middle East and North Africa to Europe. Energy Policy 2012;42(2012):341–53.
[125] Tsao, J, Science, BE, Lewis, N, Crabtree, G. 2006. Solar FAQs. Sandia National Labs, 1–24.
[126] Tsoutsos T, Frantzeskaki N, Gekas V. Environmental impacts from the solar energy technologies. Energy Policy 2005;33(3):289–96.
[127] Turney D, Fthenakis V. Environmental impacts from the installation and operation of large-scale solar power plants. Renewable and Sustainable Energy Reviews 2011;15(6):3261–70.
[128] Ummadisingu, A, Soni, MS. 2011. Concentrating solar power—technology, potential and policy in India 15 (9), 5169-5175.
[129] US DOE. 2006. Energy demands on water resources: report to congress on the interdependency of energy and water. U.S. Department of Energy. Washington, DC. Available at (http://www.sandia.gov/energy-water/docs/121-RptToCongress-EWwEIAcomments-FINAL.pdf) (accessed 07.10.12).
[130] US DOE, 2012. SunShot Initiative: SunShot Vision Study. Available at (http://www1.eere.energy.gov/solar/sunshot/vision_study.html) (accessed 07.10.12).
[131] Vandentorren S, Bretin P, Zeghnoun A, Mandereau-Bruno L, Croisier A, Cochet C, et al. August 2003 heat wave in France: risk factors for death of elderly people living at home. European Journal of Public Health 2006;16(6):583–91.
[132] Varun Bhat, Prakash, R. IK. LCA of renewable energy for electricity generation systems—a review. Renewable and Sustainable Energy Reviews 2009;13(5):1067–73.
[133] Vörösmarty CJ, Green P, Salisbury J, Lammers RB. Global water resources: vulnerability from climate change and population growth. Science 2000;289(5477):284–8.
[134] Westerling AL, Hidalgo HG, Cayan DR, Swetnam TW. Warming and earlier spring increase western U.S. forest wildfire activity. Science 2006;313(5789):940–3.
[135] Western Governors' Association. 2009. Western renewable energy zones, phase 1 report: mapping concentrated, high quality resources to meet demand in the Western Interconnection's distant markets. National Renewable Energy Laboratory, Golden, Colorado. Available at www.nrel.gov/docs/fy10osti/46877.pdf (accessed 09.19.12).
[136] Wilcove DS, Rothstein D, Dubow J, Losos E. Quantifying threats to imperiled species in the United States. BioScience 1998;48(8):607–15.
[137] Zhai P, Larsen P, Millstein D, Menon S, Masanet E. The potential for avoided emissions from photovoltaic electricity in the United States. Energy 2012;47(1):443–50.
[138] Zhao J, Zilberman D. Irreversibility and restoration in natural resource development. Oxford Economic 1999;Papers 51(1999):559–73.
[139] Zhang D, Chai Q, Zhang X, He J, Yue L, Dong X, et al. Economical assessment of large-scale photovoltaic power development in China. Energy 2012;40(1):370–5.
[140] Zink TA, Allen MF, Heindl-Tenhunen B, Allen EB. The effect of a disturbance corridor on an ecological reserve. Restoration Ecology 1995;3(4):304–10.
[141] Zipper CE, Burger JA, Skousen JG, Angel PN, Barton CD, Davis V, et al. Restoring forests and associated ecosystem services on Appalachian coal surface mines. Environmental Management 2011;47(5):751–65.
[142] Cameron DR, Cohen BS, Morrison SA. An Approach to Enhance the Conservation-Compatibility of Solar Energy Development. PloS one 2012;7(6):e38437.
[143] Denholm P, Margolis RM. 2008. Impacts of array configuration on land-use requirements for large-scale photovoltaic deployment in the United States. National Renewable Energy Laboratory. Available at: http://www.nrel.gov/docs/fy08osti/42971.pdf (accessed 09.06.13).
[144] Fthenakis VM, Moskowitz PD, Lee JC. Manufacture of amorphous silicon and GaAs thin film solar cells: an identification of potential health and safety hazards. Solar Cells 1984;13:43–58.
[145] VM Fthenakis. End-of-life management and recycling of PV modules. Energy Policy 2000;28:1051–8.
[146] McDonald, Robert I., Joseph Fargione, Joe Kiesecker, William M. Miller, and Jimmie Powell. "Energy sprawl or energy efficiency: climate policy impacts on natural habitat for the United States of America." PLoS One 4.8 (2009): e6802.
[147] Miller D, Hope C. Learning to lend for off-grid solar power: policy lessons from World Bank loans to India, Indonesia, and Sri Lanka. Energy Policy 2000;28(2):87–105.
[148] Hnizdo E, Vallathan V. Chronic obstructive pulmonary disease due to occupational exposure to silica dust: a review of epidemiological and pathological evidence. Occup Environ Med 2003;60(4):237–43.
[149] Ong S, Campbell C, Denholm P, Margolis RM, Heath G. Land-use requirements for solar power plants in the United States. 2013. National Renewable Energy Laboratory. Available at: http://www.nrel.gov/docs/fy13osti/56290.pdf (accessed 09.06.13).
[150] IPCC, 2011: IPCC Special Report on Renewable Energy Sources and Climate Change Mitigation. Prepared by Working Group III of the Intergovernmental Panel on Climate Change [O. Edenhofer, R. Pichs-Madruga, Y. Sokona, K. Seyboth, P. Matschoss, S. Kadner, T. Zwickel, P. Eickemeier, G. Hansen, S. Schlömer, C. von Stechow (eds)] Cambridge University Press, Cambridge, United Kingdom and New York, NY, USA, 1075 pp.
[151] Jacobsson S, Johnson A. The diffusion of renewable energy technology: an analytical framework and key issues for research. Energy policy 2000;28(9):625–40.
[152] Painuly JP. Barriers to renewable energy penetration; a framework for analysis. Renewable Energy 2001;24(1):73–89.
[153] Ribeiro L. 2007. Waste to watts: A "brightfield" installation has the potential to bring reviewed life to a brownfield site. Refocus 8: 46–49.
[154] Maher, P., Smith, N. P. A., Williams, A. A., 2003. Assessment of pico hydro as an option for off-grid electrification in Kenya. Renewable Energy 28 (9), 1357-1369.
[155] Spaargaren, G., 2003. Sustainable consumption: a theoretical and environmental policy perspective. Society & Natural Resources 16 (8), 687–701.
[156] Zahedi, A., 2006. Solar photovoltaic (PV) energy; latest developments in the building integrated and hybrid PV systems. Renewable Energy 31 (5), 711–718.

SCIENTIFIC REPORTS

OPEN

The Photovoltaic Heat Island Effect: Larger solar power plants increase local temperatures

Received: 26 May 2016
Accepted: 23 September 2016
Published: 13 October 2016

Greg A. Barron-Gafford[1,2], Rebecca L. Minor[1,2], Nathan A. Allen[3], Alex D. Cronin[4], Adria E. Brooks[5] & Mitchell A. Pavao-Zuckerman[6]

While photovoltaic (PV) renewable energy production has surged, concerns remain about whether or not PV power plants induce a "heat island" (PVHI) effect, much like the increase in ambient temperatures relative to wildlands generates an Urban Heat Island effect in cities. Transitions to PV plants alter the way that incoming energy is reflected back to the atmosphere or absorbed, stored, and reradiated because PV plants change the albedo, vegetation, and structure of the terrain. Prior work on the PVHI has been mostly theoretical or based upon simulated models. Furthermore, past empirical work has been limited in scope to a single biome. Because there are still large uncertainties surrounding the potential for a PHVI effect, we examined the PVHI empirically with experiments that spanned three biomes. We found temperatures over a PV plant were regularly 3–4 °C warmer than wildlands at night, which is in direct contrast to other studies based on models that suggested that PV systems should decrease ambient temperatures. Deducing the underlying cause and scale of the PVHI effect and identifying mitigation strategies are key in supporting decision-making regarding PV development, particularly in semiarid landscapes, which are among the most likely for large-scale PV installations.

Electricity production from large-scale photovoltaic (PV) installations has increased exponentially in recent decades[1–3]. This proliferation in renewable energy portfolios and PV powerplants demonstrate an increase in the acceptance and cost-effectiveness of this technology[4,5]. Corresponding with this upsurge in installation has been an increase in the assessment of the impacts of utility-scale PV[4,6–8], including those on the efficacy of PV to offset energy needs[9,10]. A growing concern that remains understudied is whether or not PV installations cause a "heat island" (PVHI) effect that warms surrounding areas, thereby potentially influencing wildlife habitat, ecosystem function in wildlands, and human health and even home values in residential areas[11]. As with the Urban Heat Island (UHI) effect, large PV power plants induce a landscape change that reduces albedo so that the modified landscape is darker and, therefore, less reflective. Lowering the terrestrial albedo from ~20% in natural deserts[12] to ~5% over PV panels[13] alters the energy balance of absorption, storage, and release of short- and longwave radiation[14,15]. However, several differences between the UHI and potential PVHI effects confound a simple comparison and produce competing hypotheses about whether or not large-scale PV installations will create a heat island effect. These include: (*i*) PV installations shade a portion of the ground and therefore could reduce heat absorption in surface soils[16], (*ii*) PV panels are thin and have little heat capacity per unit area but PV modules emit thermal radiation both up and down, and this is particularly significant during the day when PV modules are often 20 °C warmer than ambient temperatures, (*iii*) vegetation is usually removed from PV power plants, reducing the amount of cooling due to transpiration[14], (*iv*) electric power removes energy from PV power plants, and (*v*) PV panels reflect and absorb upwelling longwave radiation, and thus can prevent the soil from cooling as much as it might under a dark sky at night.

Public concerns over a PVHI effect have, in some cases, led to resistance to large-scale solar development. By some estimates, nearly half of recently proposed energy projects have been delayed or abandoned due to local opposition[11]. Yet, there is a remarkable lack of data as to whether or not the PVHI effect is real or simply an issue

[1]School of Geography & Development, University of Arizona, Tucson, AZ, USA. [2]Office of Research & Development, College of Science, Biosphere 2, University of Arizona, Tucson, AZ, USA. [3]Nevada Center of Excellence, Desert Research Institute, Las Vegas, NV, USA. [4]Department of Physics, University of Arizona, Tucson, AZ, USA. [5]Department of Electrical and Computer Engineering, University of Wisconsin-Madison, Madison, WI, USA. [6]Department of Environmental Science & Technology, University of Maryland, College Park, MD, USA. Correspondence and requests for materials should be addressed to G.A.B.-G. (email: gregbg@email.arizona.edu)

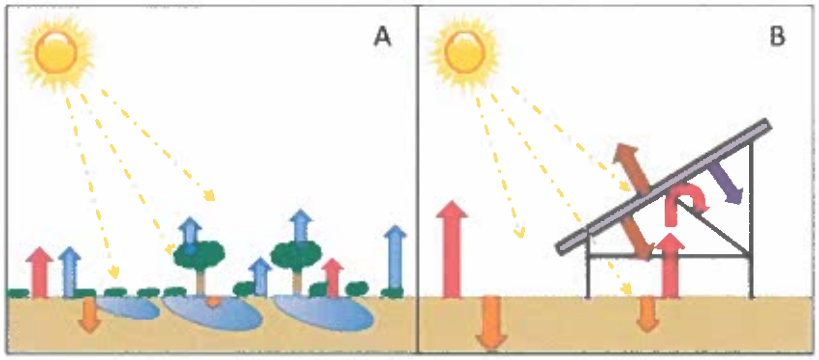

Figure 1. Illustration of midday energy exchange. Assuming equal rates of incoming energy from the sun, a transition from (**A**) a vegetated ecosystem to (**B**) a photovoltaic (PV) power plant installation will significantly alter the energy flux dynamics of the area. Within natural ecosystems, vegetation reduces heat capture and storage in soils (orange arrows), and infiltrated water and vegetation release heat-dissipating latent energy fluxes in the transition of water-to-water vapor to the atmosphere through evapotranspiration (blue arrows). These latent heat fluxes are dramatically reduced in typical PV installations, leading to greater sensible heat fluxes (red arrows). Energy re-radiation from PV panels (brown arrow) and energy transferred to electricity (purple arrow) are also shown.

associated with perceptions of environmental change caused by the installations that lead to "not in my backyard" (NIMBY) thinking. Some models have suggested that PV systems can actually cause a cooling effect on the local environment, depending on the efficiency and placement of the PV panels[17,18]. But these studies are limited in their applicability when evaluating large-scale PV installations because they consider changes in albedo and energy exchange within an urban environment (rather than a natural ecosystem) or in European locations that are not representative of semiarid energy dynamics where large-scale PV installations are concentrated[10,19]. Most previous research, then, is based on untested theory and numerical modeling. Therefore, the potential for a PHVI effect must be examined with empirical data obtained through rigorous experimental terms.

The significance of a PVHI effect depends on energy balance. Incoming solar energy typically is either reflected back to the atmosphere or absorbed, stored, and later re-radiated in the form of latent or sensible heat (Fig. 1)[20,21]. Within natural ecosystems, vegetation reduces heat gain and storage in soils by creating surface shading, though the degree of shading varies among plant types[22]. Energy absorbed by vegetation and surface soils can be released as latent heat in the transition of liquid water to water vapor to the atmosphere through evapotranspiration – the combined water loss from soils (evaporation) and vegetation (transpiration). This heat-dissipating latent energy exchange is dramatically reduced in a typical PV installation (Fig. 1 transition from A-to-B), potentially leading to greater heat absorption by soils in PV installations. This increased absorption, in turn, could increase soil temperatures and lead to greater sensible heat efflux from the soil in the form of radiation and convection. Additionally, PV panel surfaces absorb more solar insolation due to a decreased albedo[13,23,24]. PV panels will re-radiate most of this energy as longwave sensible heat and convert a lesser amount (~20%) of this energy into usable electricity. PV panels also allow some light energy to pass, which, again, in unvegetated soils will lead to greater heat absorption. This increased absorption could lead to greater sensible heat efflux from the soil that may be trapped under the PV panels. A PVHI effect would be the result of a detectable increase in sensible heat flux (atmospheric warming) resulting from an alteration in the balance of incoming and outgoing energy fluxes due to landscape transformation. Developing a full thermal model is challenging[17,18,25], and there are large uncertainties surrounding multiple terms including variations in albedo, cloud cover, seasonality in advection, and panel efficiency, which itself is dynamic and impacted by the local environment. These uncertainties are compounded by the lack of empirical data.

We addressed the paucity of direct quantification of a PVHI effect by simultaneously monitoring three sites that represent a natural desert ecosystem, the traditional built environment (parking lot surrounded by commercial buildings), and a PV power plant. We define a PVHI effect as the difference in ambient air temperature between the PV power plant and the desert landscape. Similarly, UHI is defined as the difference in temperature between the built environment and the desert. We reduced confounding effects of variability in local incoming energy, temperature, and precipitation by utilizing sites contained within a 1 km area.

At each site, we monitored air temperature continuously for over one year using aspirated temperature probes 2.5 m above the soil surface. Average annual temperature was 22.7 + 0.5 °C in the PV installation, while the nearby desert ecosystem was only 20.3 + 0.5 °C, indicating a PVHI effect. Temperature differences between areas varied significantly depending on time of day and month of the year (Fig. 2), but the PV installation was always greater than or equal in temperature to other sites. As is the case with the UHI effect in dryland regions, the PVHI effect delayed the cooling of ambient temperatures in the evening, yielding the most significant difference in overnight temperatures across all seasons. Annual average midnight temperatures were 19.3 + 0.6 °C in the PV installation, while the nearby desert ecosystem was only 15.8 + 0.6 °C. This PVHI effect was more significant in terms of actual degrees of warming (+3.5 °C) in warm months (Spring and Summer; Fig. 3, right).

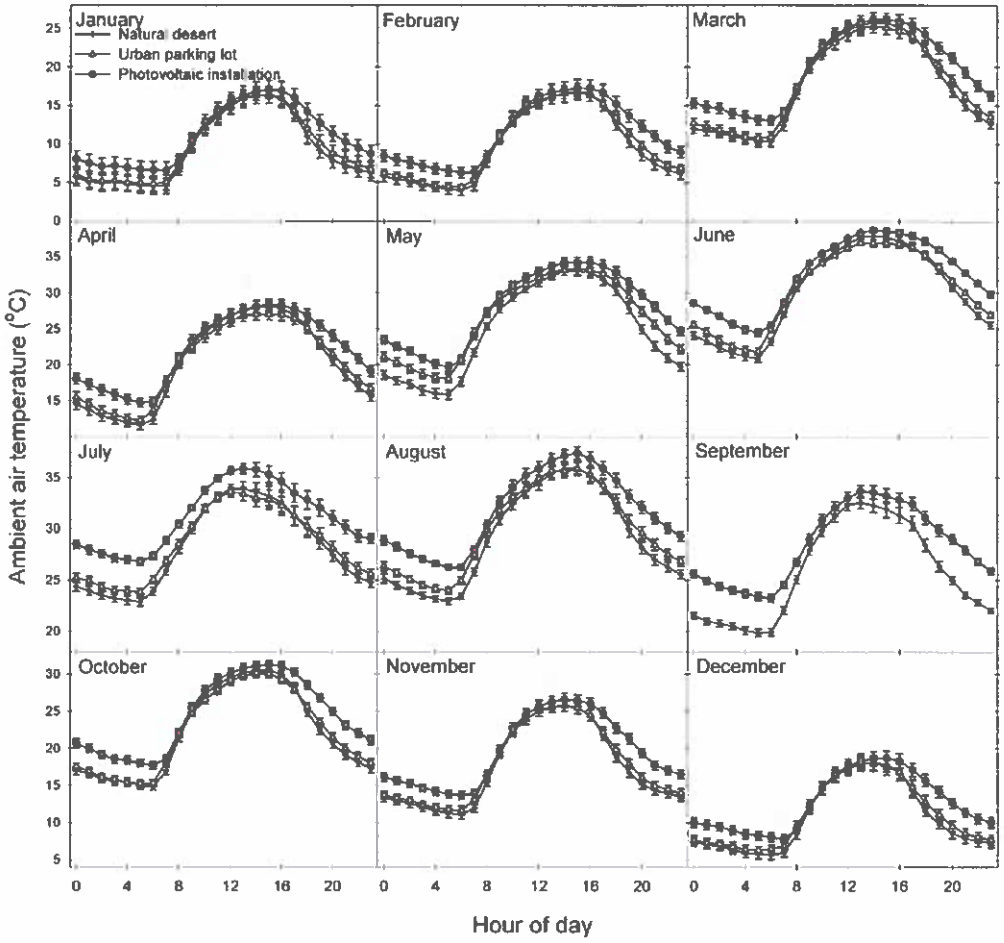

Figure 2. Average monthly ambient temperatures throughout a 24-hour period provide evidence of a photovoltaic heat island (PVHI) effect.

In both PVHI and UHI scenarios, the greater amount of exposed ground surfaces compared to natural systems absorbs a larger proportion of high-energy, shortwave solar radiation during the day. Combined with minimal rates of heat-dissipating transpiration from vegetation, a proportionally higher amount of stored energy is reradiated as longwave radiation during the night in the form of sensible heat (Fig. 1)[15]. Because PV installations introduce shading with a material that, itself, should not store much incoming radiation, one might hypothesize that the effect of a PVHI effect would be lesser than that of a UHI. Here, we found that the difference in evening ambient air temperature was consistently greater between the PV installation and the desert site than between the parking lot (UHI) and the desert site (Fig. 3). The PVHI effect caused ambient temperature to regularly approach or be in excess of 4 °C warmer than the natural desert in the evenings, essentially doubling the temperature increase due to UHI measured here. This more significant warming under the PVHI than the UHI may be due to heat trapping of re-radiated sensible heat flux under PV arrays at night. Daytime differences from the natural ecosystem were similar between the PV installation and urban parking lot areas, with the exception of the Spring and Summer months, when the PVHI effect was significantly greater than UHI in the day. During these warm seasons, average midnight temperatures were 25.5 + 0.5 °C in the PV installation and 23.2 + 0.5 °C in the parking lot, while the nearby desert ecosystem was only 21.4 + 0.5 °C.

The results presented here demonstrate that the PVHI effect is real and can significantly increase temperatures over PV power plant installations relative to nearby wildlands. More detailed measurements of the underlying causes of the PVHI effect, potential mitigation strategies, and the relative influence of PVHI in the context of the intrinsic carbon offsets from the use of this renewable energy are needed. Thus, we raise several new questions and highlight critical unknowns requiring future research.

What is the physical basis of land transformations that might cause a PVHI?

We hypothesize that the PVHI effect results from the effective transition in how energy moves in and out of a PV installation versus a natural ecosystem. However, measuring the individual components of an energy flux model remains a necessary task. These measurements are difficult and expensive but, nevertheless, are indispensable in identifying the relative influence of multiple potential drivers of the PVHI effect found here. Environmental

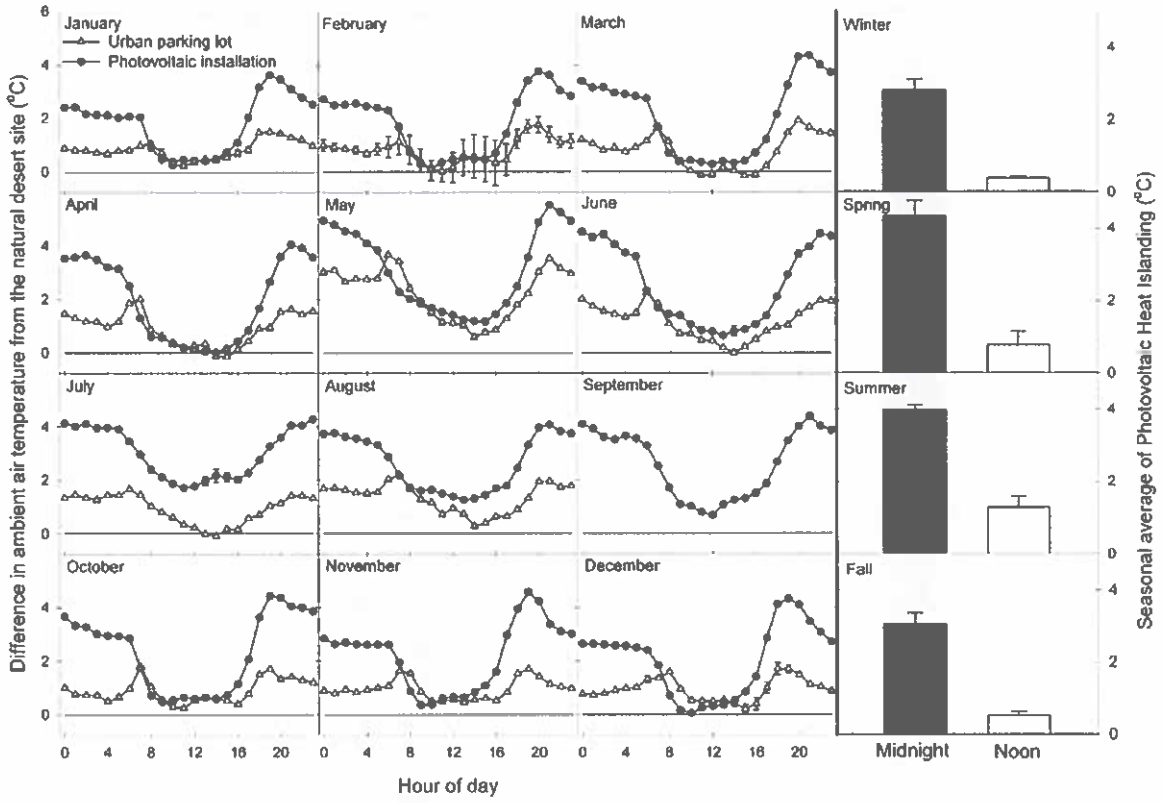

Figure 3. (Left) Average monthly levels of Photovoltaic Heat Islanding (ambient temperature difference between PV installation and desert) and Urban Heat Islanding (ambient temperature difference between the urban parking lot and the desert). (Right) Average night and day temperatures for four seasonal periods, illustrating a significant PVHI effect across all seasons, with the greatest influence on ambient temperatures at night.

conditions that determine patterns of ecosystem carbon, energy, and water dynamics are driven by the means through which incoming energy is reflected or absorbed. Because we lack fundamental knowledge of the changes in surface energy fluxes and microclimates of ecosystems undergoing this land use change, we have little ability to predict the implications in terms of carbon or water cycling[4,8].

What are the physical implications of a PVHI, and how do they vary by region?

The size of an UHI is determined by properties of the city, including total population[26–28], spatial extent, and the geographic location of that city[29–31]. We should, similarly, consider the spatial scale and geographic position of a PV installation when considering the presence and importance of the PVHI effect. Remote sensing could be coupled with ground-based measurements to determine the lateral and vertical extent of the PVHI effect. We could then determine if the size of the PVHI effect scales with some measure of the power plant (for example, panel density or spatial footprint) and whether or not a PVHI effect reaches surrounding areas like wildlands and neighborhoods. Given that different regions around the globe each have distinct background levels of vegetative ground cover and thermodynamic patterns of latent and sensible heat exchange, it is possible that a transition from a natural wildland to a typical PV power plant will have different outcomes than demonstrated here. The paucity in data on the physical effects of this important and growing land use and land cover change warrants more studies from representative ecosystems.

What are the human implications of a PVHI, and how might we mitigate these effects?

With the growing popularity of renewable energy production, the boundaries between residential areas and larger-scale PV installations are decreasing. In fact, closer proximity with residential areas is leading to increased calls for zoning and city planning codes for larger PV installations[32,33], and PVHI-based concerns over potential reductions in real estate value or health issues tied to Human Thermal Comfort (HTC)[34]. Mitigation of a PVHI effect through targeted revegetation could have synergistic effects in easing ecosystem degradation associated with development of a utility scale PV site and increasing the collective ecosystem services associated with an area[4]. But what are the best mitigation measures? What tradeoffs exist in terms of various means of revegetating degraded PV installations? Can other albedo modifications be used to moderate the severity of the PVHI?

Figure 4. Experimental sites. Monitoring a (1) natural semiarid desert ecosystem, (2) solar (PV) photovoltaic installation, and (3) an "urban" parking lot – the typical source of urban heat islanding – within a 1 km² area enabled relative control for the incoming solar energy, allowing us to quantify variation in the localized temperature of these three environments over a year-long time period. The Google Earth image shows the University of Arizona's Science and Technology Park's Solar Zone.

To fully contextualize these findings in terms of global warming, one needs to consider the relative significance of the (globally averaged) decrease in albedo due to PV power plants and their associated warming from the PVHI against the carbon dioxide emission reductions associated with PV power plants. The data presented here represents the first experimental and empirical examination of the presence of a heat island effect associated with PV power plants. An integrated approach to the physical and social dimensions of the PVHI is key in supporting decision-making regarding PV development.

Methods

Site Description. We simultaneously monitored a suite of sites that represent the traditional built urban environment (a parking lot) and the transformation from a natural system (undeveloped desert) to a 1 MW PV power plant (Fig. 4; Map data: Google). To minimize confounding effects of variability in local incoming energy, temperature, and precipitation, we identified sites within a 1 km area. All sites were within the boundaries of the University of Arizona Science and Technology Park Solar Zone (32.092150°N, 110.808764°W; elevation: 888 m ASL). Within a 200 m diameter of the semiarid desert site's environmental monitoring station, the area is composed of a sparse mix of semiarid grasses (*Sporobolus wrightii*, *Eragrostis lehmanniana*, and *Muhlenbergia porteri*), cacti (*Opuntia* spp. and *Ferocactus* spp.), and occasional woody shrubs including creosote bush (*Larrea tridentata*), whitethorn acacia (*Acacia constricta*), and velvet mesquite (*Prosopis velutina*). The remaining area is bare soil. These species commonly co-occur on low elevation desert bajadas, creosote bush flats, and semiarid grasslands. The photovoltaic installation was put in place in early 2011, three full years prior when we initiated monitoring at the site. We maintained the measurement installations for one full year to capture seasonal variation due to sun angle and extremes associated with hot and cold periods. Panels rest on a single-axis tracker system that pivot east-to-west throughout the day. A parking lot with associated building served as our "urban" site and is of comparable spatial scale as our PV site.

Monitoring Equipment & Variables Monitored. Ambient air temperature (°C) was measured with a shaded, aspirated temperature probe 2.5 m above the soil surface (Vaisala HMP60, Vaisala, Helsinki, Finland in the desert and Microdaq U23, Onset, Bourne, MA in the parking lot). Temperature probes were cross-validated for precision (closeness of temperature readings across all probes) at the onset of the experiment. Measurements of temperature were recorded at 30-minute intervals throughout a 24-hour day. Data were recorded on a data-logger (CR1000, Campbell Scientific, Logan, Utah or Microstation, Onset, Bourne, MA). Data from this

instrument array is shown for a yearlong period from April 2014 through March 2015. Data from the parking lot was lost for September 2014 because of power supply issues with the datalogger.

Statistical analysis. Monthly averages of hourly (on-the-hour) data were used to compare across the natural semiarid desert, urban, and PV sites. A Photovoltaic Heat Island (PVHI) effect was calculated as differences in these hourly averages between the PV site and the natural desert site, and estimates of Urban Heat Island (UHI) effect was calculated as differences in hourly averages between the urban parking lot site and the natural desert site. We used midnight and noon values to examine maximum and minimum, respectively, differences in temperatures among the three measurement sites and to test for significance of heat islanding at these times. Comparisons among the sites were made using Tukey's honestly significant difference (HSD) test[35]. Standard errors to calculate HSD were made using pooled midnight and noon values across seasonal periods of winter (January-March), spring (April-June), summer (July-September), and fall (October-December). Seasonal analyses allowed us to identify variation throughout a yearlong period and relate patterns of PVHI or UHI effects with seasons of high or low average temperature to examine correlations between background environmental parameters and localized heat islanding.

References

1. IPCC. IPCC Special Report on Renewable Energy Sources and Climate Change Mitigation. *Prepared by Working Group III of the Intergovernmental Panel on Climate Change* (Cambridge University Press, Cambridge, United Kingdom and New York, NY, USA, 2011).
2. REN21. Renewables 2014 Global Status Report (Paris: REN21 Secretariat; ISBN 978-3-9815934-2-6, 2014).
3. U.S. Energy Information Administration. June 2016 Monthly Energy Review. U.S. Department of Energy: Office of Energy Statistics. Washington, DC (2016).
4. Hernandez, R. R. *et al.* Environmental impacts of utility-scale solar energy. *Renewable & Sustainable Energy Reviews* **29**, 766–779, doi: 10.1016/j.rser.2013.08.041 (2014).
5. Bazilian, M. *et al.* Re-considering the economics of photovoltaic power. *Renewable Energy* **53**, 329–338, doi: http://dx.doi.org/10.1016/j.renene.2012.11.029 (2013).
6. Dale, V. H., Efroymson, R. A. & Kline, K. L. The land use-climate change-energy nexus. *Landsc. Ecol.* **26**, 755–773, doi: 10.1007/s10980-011-9606-2 (2011).
7. Copeland, H. E., Pocewicz, A. & Kiesecker, J. M. In *Energy Development and Wildlife Conservation in Western North America* (ed Naugle, David E.) 7–22 (Springer, 2011).
8. Armstrong, A., Waldron, S., Whitaker, J. & Ostle, N. J. Wind farm and solar park effects on plant-soil carbon cycling: uncertain impacts of changes in ground-level microclimate. *Global Change Biology* **20**, 1699–1706, doi: 10.1111/gcb.12437 (2014).
9. Hernandez, R. R., Hoffacker, M. K. & Field, C. B. Efficient use of land to meet sustainable energy needs. *Nature Climate Change* **5**, 353–358, doi: 10.1038/nclimate2556 (2015).
10. Hernandez, R. R., Hoffacker, M. K. & Field, C. B. Land-Use efficiency of big solar. *Environmental Science & Technology* **48**, 1315–1323, doi: 10.1021/es4043726 (2014).
11. Pociask, S. & Fuhr, J. P. Jr. Progress Denied: A study on the potential economic impact of permitting challenges facing proposed energy projects (U.S. Chamber of Commerce, 2011).
12. Michalek, J. L. *et al.* Satellite measurements of albedo and radiant temperature from semi-desert grassland along the Arizona/Sonora border. *Climatic Change* **48**, 417–425, doi: 10.1023/a:1010769416826 (2001).
13. Burg, B. R., Ruch, P., Paredes, S. & Michel, B. Placement and efficiency effects on radiative forcing of solar installations. *11th International Conference on Concentrator Photovoltaic Systems* **1679**, doi: 10.1063/1.4931546 (2015).
14. Solecki, W. D. *et al.* Mitigation of the heat island effect in urban New Jersey. *Environmental Hazards* **6**, 39–49, doi: 10.1016/j.hazards.2004.12.002 (2005).
15. Oke, T. R. The energetic basis of the urban heat island (Symons Memorial Lecture, 20 May 1980). *Quarterly Journal, Royal Meteorological Society* **108**, 1–24 (1982).
16. Smith, S. D., Patten, D. T. & Monson, R. K. Effects of artificially imposed shade on a Sonoran Desert ecosystem: microclimate and vegetation. *Journal of Arid Environments* **13**, 65–82 (1987).
17. Taha, H. The potential for air-temperature impact from large-scale deployment of solar photovoltaic arrays in urban areas. *Solar Energy* **91**, 358–367, doi: 10.1016/j.solener.2012.09.014 (2013).
18. Masson, V., Bonhomme, M., Salagnac, J.-L., Briottet, X. & Lemonsu, A. Solar panels reduce both global warming and Urban Heat Island. *Frontiers in Environmental Science* **2**, 14, doi: 10.3389/fenvs.2014.00014 (2014).
19. Roberts, B. J. Solar production potential across the United States. *Department of Energy, National Renewable Energy Laboratory*. http://www.climatecentral.org/news/eastern-us-solar-development-18714. *19 September* (2012).
20. Monteith, J. L. & Unsworth, M. H. *Principles of Environmental Physics Third Edition* (Elsevier, San Diego, CA, USA, 1990).
21. Campbell, G. S. & Norman, J. M. *An Introduction to Environmental Biophysics Second Edition* (Springer, New York, USA, 1998).
22. Breshears, D. D. The grassland-forest continuum: trends in ecosystem properties for woody plant mosaics? *Frontiers in Ecology and the Environment* **4**, 96–104, doi: 10.1890/1540-9295(2006)004[0096:tgctie]2.0.co;2 (2006).
23. Oke, T. R. *Boundary Layer Climates. Second Edition* (Routledge New York, 1992).
24. Ahrens, C. D. *Meteorology Today. An Introduction to Weather, Climate, and the Environment Eighth Edition* (Thompson, Brooks/Cole USA 2006).
25. Fthenakis, V. & Yu, Y. Analysis of the potential for a heatisland effect in large solar farms. *Analysis of the potential for a heatisland effect in large solar farms; 2013 IEEE 39th Photovoltaic Specialists Conference* 3362–3366 (2013).
26. Santamouris, M. Analyzing the heat island magnitude and characteristics in one hundred Asian and Australian cities and regions. *Science of The Total Environment* **512–513**, 582–598, doi: http://dx.doi.org/10.1016/j.scitotenv.2015.01.060 (2015).
27. Oke, T. R. City size and the urban heat island. *Atmospheric Environment* **7**, 769–779, doi: 10.1016/0004-6981(73)90140-6 (1973).
28. Wang, W.-C., Zeng, Z. & Karl, T. R. Urban heat islands in China. *Geophysical Research Letters* **17**, 2377–2380, doi: 10.1029/GL017i013p02377 (1990).
29. Nasrallah, H. A., Brazel, A. J. & Balling, R. C. Jr Analysis of the Kuwait City urban heat island. *International Journal of Climatology* **10**, 401–405 (1990).
30. Montávez, J. P., Rodríguez, A. & Jiménez, J. I. A study of the Urban Heat Island of Granada. *International Journal of Climatology* **20**, 899–911, doi: 10.1002/1097-0088(20000630)20:8<899::aid-joc433>3.0.co;2-i (2000).
31. Buyantuyev, A. & Wu, J. Urban heat islands and landscape heterogeneity: Linking spatiotemporal variations in surface temperatures to land-cover and socioeconomic patterns. *Landsc. Ecol.* **25**, 17–33, doi: 10.1007/s10980-009-9402-4 (2010).
32. White, J. G. A Model Ordinance for Energy Projects; Oregon Department of Energy. http://www.oregon.gov/ENERGY/SITING/docs/ModelEnergyOrdinance.pdf (2005).

33. Lovelady, A. Planning and Zoning for Solar in North Carolina. *University of North Carolina at Chapel Hill, School of Government* (2014).
34. Coutts, A. M., Tapper, N. J., Beringer, J., Loughnan, M. & Demuzere, M. Watering our cities: The capacity for Water Sensitive Urban Design to support urban cooling and improve human thermal comfort in the Australian context. *Progress in Physical Geography* **37**, 2–28, doi: 10.1177/0309133312461032 (2013).
35. Zar, J. H. *Biostatistical analysis, Prentice-Hall, Englewood Cliffs, p 215* (1974).

Acknowledgements

The authors thank Ken Marcus for access to the University of Arizona Solar Zone and the Science and Technology Park and to Tucson Electric Power for access to their PV installation. This research was supported by the University of Arizona Institute of the Environment and the Office of Research & Development through the TRIF-funded Water, Environmental and Energy Solutions initiative.

Author Contributions

G.A.B.-G., R.L.M. and N.A.A. established research sites and installed monitoring equipment. G.A.B.-G. directed research and R.L.M. conducted most site maintenance. G.A.B.-G., N.A.A., A.D.C. and M.A.P.-Z. led efforts to secure funding for the research. All authors discussed the results and contributed to the manuscript.

Additional Information

Competing financial interests: The authors declare no competing financial interests.

How to cite this article: Barron-Gafford, G. A. *et al.* The Photovoltaic Heat Island Effect: Larger solar power plants increase local temperatures. *Sci. Rep.* **6**, 35070; doi: 10.1038/srep35070 (2016).

Environmental Research 181 (2020) 108923

Contents lists available at ScienceDirect

Environmental Research

journal homepage: www.elsevier.com/locate/envres

Inflammatory bowel disease and biomarkers of gut inflammation and permeability in a community with high exposure to perfluoroalkyl substances through drinking water☆

Yiyi Xu[a,*], Ying Li[a], Kristin Scott[b], Christian H. Lindh[b], Kristina Jakobsson[a,c], Tony Fletcher[d], Bodil Ohlsson[e], Eva M. Andersson[a,c]

[a] School of Public Health and Community Medicine, Institute of Medicine, Sahlgrenska Academy, University of Gothenburg, Gothenburg, Sweden
[b] Division of Occupational and Environmental Medicine, Department of Laboratory Medicine, Lund University, Lund, Sweden
[c] Department of Occupational and Environmental Medicine, Sahlgrenska University Hospital, Gothenburg, Sweden
[d] London School of Hygiene and Tropical Medicine, London, UK
[e] Department of Internal Medicine, Skåne University Hospital, Lund University, Malmö, Sweden

ARTICLE INFO

Keywords:
PFOA
PFOS
PFHxS
Drinking water
Inflammatory bowel diseases

ABSTRACT

Perfluoroalkyl substances (PFAS) can act as surfactants and have been suggested to be capable of affecting gut mucosa integrity, a possible factor in the pathogenesis of inflammatory bowel disease (IBD). So far, only PFOA has been shown to have a positive association with ulcerative colitis. The present study aimed to investigate the association of PFAS and clinically diagnosed IBD in the Ronneby cohort, a population with high PFAS exposure (especially high PFOS and PFHxS) from Aqueous Film-Forming Foam through drinking water, using registry data. Additionally, to explore associations of PFAS with fecal zonulin and calprotectin, subclinical biomarkers of gut inflammation and permeability, in a sub-set of participants from Ronneby and Karlshamn (a nearby control municipality). The registry study included all people that ever resided in Ronneby municipality at least one year between 1980 and 2013. Yearly exposure to contaminated drinking water was assessed based on residential addresses and waterworks supply data, and the population classified by early, mid and late periods in ascending level of contamination. Diagnosed IBD cases were retrieved from the Swedish National Patient register and cause-of-death register. The Cox proportional hazards model was used to derive the hazard ratios (HRs) for diagnosed IBD. The biomarker study included 189 individuals who provided fecal samples. Serum PFAS were measured using LC-MS/MS. Fecal zonulin and calprotectin were measured using ELISA. Linear regression was used to assess the associations between measured PFAS and biomarker levels. In the registry study, no raised HRs for diagnosed IBD were found for cohort subjects with mid (1995–2004) or late period (2005–2013) exposure compared to never exposure. Early period exposure only (1985–1994) showed raised HRs for Crohn's disease (HR = 1.58, p = 0.048) and other non-specified IBD (HR = 1.38, p = 0.037). In the biomarker study, Karlshamn showed higher fecal calprotectin levels (median = 99.6 mg/kg in Karlshamn vs. 66.8 mg/kg in Ronneby, p = 0.04). A trend of decreased calprotectin with increased serum PFAS indicated higher PFAS was associated with lower degree of gut inflammation (p = 0.002). No association between serum PFAS and fecal zonulin was found. In conclusion, the present study found no consistent evidence to support PFAS exposure as a risk factor for IBD.

1. Introduction

The incidence and prevalence of non-infectious inflammatory bowel diseases (IBD) is increasing in the western world, and the annual incidence is around 1 per 1000 inhabitants (Molodecky et al., 2012). IBD is divided into Crohn's disease, ulcerative colitis, microscopic colitis and non-specified colitis. The etiology and pathophysiology are mainly unknown, but environmental factors, imbalance in the gut microbiota and genetic factors are suggested to contribute to the development of IBD (Dolan and Chang, 2017; Uniken Venema et al., 2017). The

☆ The authors declare they have no actual or potential competing financial interests.

* Corresponding author. Box 414, 40530, Göteborg, Sweden.
E-mail address: yiyi.xu@amm.gu.se (Y. Xu).

https://doi.org/10.1016/j.envres.2019.108923
Received 12 April 2019; Received in revised form 10 November 2019; Accepted 11 November 2019
Available online 14 November 2019

intestinal barrier is an important protection of the internal milieu from hazardous external factors, including pathogens. Paracellular intestinal permeability is carefully controlled by different types of intercellular junctions that regulate the space between epithelial cells and are regularized by several proteins (Chiba et al., 2008).

Perfluoroalkyl substances (PFAS) are manmade substances that are persistent and ubiquitously distributed in the environment, and have grown into a global contamination problem. The widespread presence of PFAS in drinking water of localized general populations has been reported from different parts of the world (Eriksson et al., 2013; Guelfo and Adamson, 2018; Hu et al., 2016), and also in Sweden. In December 2013, one-third of the households in Ronneby, a municipality with 29 000 inhabitants in southern Sweden, were found to have been supplied by PFAS-contaminated municipal drinking water. The contamination had developed over decades. The source of PFAS was Aqueous Film-Forming Foam (AFFFs), which had been used at a nearby military airfield since the mid-1980s. Biomonitoring in more than 3500 Ronneby participants approximately 6 months after cessation of the contamination showed very high serum levels of PFAS, especially perfluorohexane sulfonic acid (PFHxS) and perfluorooctane sulfonic acid (PFOS), while perfluorooctanoic acid (PFOA) levels were markedly low. Serum PFHxS, PFOS and PFOA concentrations showed very high correlations in the Ronneby population (spearman's $r > 0.8$) (Li et al., 2018).

A large and increasing number of studies have reported that PFAS are associated with adverse effects (Domingo, 2012; European Food Safety Authority, 2018) . The association between PFAS exposure and IBD is, however, little studied and limited to PFOA. In the C8 community cohort with 32 000 individuals, Steenland et al. (2013) found a significant association between retrospectively estimated serum PFOA and ulcerative colitis, but not with Crohn's disease. An increased risk of ulcerative colitis was also found in a cohort with more than 3000 workers (Steenland et al., 2015). Additionally, in a case-control study, ulcerative colitis was inversely associated with serum PFHxS and PFOS, and positively but more weakly for PFOA, in a population with generally low PFAS levels (i.e. median in controls PFOA 1.3 ng/mL, median PFHxS < 1.6 ng/ml, median PFOS < 4.2 ng/ml) (Steenland et al., 2018). However, in this design, serum measurements were made after diagnosis so the PFAS prior to diagnosis is uncertain.

Although a potential association between PFOA and ulcerative colitis was found in the C8 study, the underlying mechanism is unclear. A tentative mechanism could be that as PFAS act as surfactants they might negatively affect gut mucosa integrity (Csáki, 2011). Biochemical analysis for selected biomarkers can provide an opportunity to investigate early effects of PFAS on the gastrointestinal tract. Calprotectin, a neutrophil cytosolic protein mainly expressed in cells of the myeloid lineage (Ehrchen et al., 2009; Odink et al., 1987; Zwadlo et al., 1988), is a mediator of chronic inflammation via its role in monocyte recruitment to the inflammatory site (Eue et al., 2000). The measurement of calprotectin concentrations in feces thus serves to screen efficiently for the presence of any kind of inflammation throughout the gastrointestinal tract with high sensitivity, and is frequently used as a diagnostic tool to follow the course of IBD in clinical practice (Erbayrak et al., 2009; Walsham and Sherwood, 2016). An increase level of fecal calprotectin indicates a relapse of IBD (Walsham and Sherwood, 2016). Another biomarker, zonulin, has been reported to be associated with increased intestinal permeability in the *in vitro* studies (Fasano, 2012; Sapone et al., 2006), and has been suggested to play a plausible role in IBD (Vanuytsel et al., 2013). However, since zonulin is secreted not only by the gut epithelium but also by several extra-intestinal tissues such as adipose tissue, brain, heart and immune cells (Vanuytsel et al., 2013; Żak-Gołąb et al., 2013), the levels of zonulin in serum do not only reflect only intestinal secretion. Fecal zonulin, therefore, has been suggested as a marker of intestinal permeability (Malíčková et al., 2017). Fecal calprotectin and zonulin are relatively new biomarkers, and this is the first study investigating their associations with PFAS exposure.

In the present study, we aimed to: 1) investigate the relative risk of clinically relevant IBD in relation to PFAS exposure using a registry-linkage study design, by assessing the associations between degree of historical PFAS exposure and diagnosed IBD in the Ronneby cohort; and 2) investigate subclinical indicators of risk for IBD and understanding potential mechanisms of PFAS activity using selected biomarkers in a cross-sectional study design, by assessing the associations between measured serum PFAS and biomarkers in feces reflecting intestinal inflammation and permeability (i.e. fecal calprotectin and zonulin) among subjects from Ronneby and a nearby municipality with clean drinking water (Karlshamn). We hypothesized that PFAS exposure through drinking water could increase intestinal permeability and induce inflammatory changes, reflected as elevated levels of the biomarkers, and further lead to increased incidence of IBD, reflected as higher hazard ratio in the region.

2. Methods

2.1. Registry study

2.1.1. Ronneby cohort

The cohort consists of all people that ever resided in Ronneby municipality at least one year between 1980 and 2013 (n = 63 074, 33 218 men and 29 856 women). From Statistics Sweden (www.scb.se), we obtained information about registered yearly addresses, vital status and emigration. A person was censored at the event, at emigration, at death or at the end of the study period. Using the personal identity number and national diagnosis registries, a person's outcome is available no matter where they reside in Sweden.

2.1.2. Exposure assessment

The exposure assessment was based on a person's yearly residence addresses and the archive indicating the area of waterworks supply over time. After connecting the addresses to the waterworks supply data, we could determine if a residential address was provided with clean or contaminated municipal water for each year during 1980–2013. Extensive measurements in private wells in the municipality had not revealed any substantial PFAS levels; thus, residents with private wells were considered unexposed. All addresses outside Ronneby municipality were assumed to have uncontaminated water. Although no clear information was available about when the drinking water contamination started, we tentatively set 1985 as the start of exposure since it is known that the use of AFFFs at the airfield started in the mid-1980s. Moreover, due to the fact that PFAS are not degrade and very persistent in the environment, we assume that PFAS levels in the contaminated water was accumulated over years after 1985.

First, a very crude exposure assessment was performed using a dichotomous exposure variable (never/ever living at address with contaminated municipal drinking water supply).

Next, a four-category time-based variable was created. PFAS levels in the contaminated water were likely increased over time as emissions accumulated and due to its persistence in the environment. A person can move, both within Ronneby and in/out of the municipality over the whole study period, but given the long half-life of PFAS in serum their exposure classification each was the highest exposure group they had reached up to then. A residential address in the contaminated water district was denoted as "not exposed" (1980–1984; assumed no water contamination before 1985), "early" (at least one year during 1985–1994, the lowest PFAS exposure category), "mid" (at least one year during 1995–2004) and "late" (at least one year during 2005–2013, the highest PFAS exposure category). The cut-off of each exposure period was set reflecting the half-lives of PFAS (3–7 years, Li et al., 2018). The early, mid and late exposure periods last at least one half-life of PFHxS and about 2–3 half-lives of PFOA and PFOS. In another Ronneby study with the same exposure assessment, it has been

confirmed that PFAS exposure at late period was higher than the other two periods (Andersson et al., 2019).

Using the four-category time-based variable, the exposure classification (Exp) for a person could change over time. A person was exposed in a given exposure period, and remained at that level unless exposure occurred in a later time period. For instance, if one person continuously lived in the contaminated area from 1985 to 2013, Exp was "early" 1985–1994, "mid" 1995–2004 and "late" 2005–2013. For details see Supplementary Tables S1. The exposure assessment has been previously used to analyze the associations to thyroid disease in the Ronneby cohort (Andersson et al., 2019).

In the cohort, 6.5% of the persons were exposed at residential address during all three periods (i.e. their Exp changed from early to mid to late), and 2% were exposed during early and mid but not during late period. 74% were never exposed at residential address during the whole study period. The percentage of persons in each exposure scenario are given in Supplementary Tables S1.

2.1.3. Outcome assessment

Health outcomes were collected from two national registers. 1) The Swedish National Patient Register, which includes hospital in-patient care since 1987. From 2001, also hospital out-patient visits from both public and private healthcare systems are included. 2) The cause-of-death register, which includes the death information of all persons registered in Sweden since 1961.

We obtained diagnoses of Crohn's disease, ulcerative colitis and other IBD (other or non-specified diagnoses) according to the ICD codes in Table 1. When defining an event, both primary and secondary diagnoses, as well as primary and secondary causes of death, were considered. 26 (2%) out of 1284 IBD events were retrieved only from cause-of-death register (i.e. no prior IBD diagnosis in the National Patient Register). Microscopic colitis was included in the "other or non-specified IBD" group because of low prevalence. The outcome assessment was scrutinized by a senior specialist in gastroenterology (B Ohlsson). There were some patients who had different IBD diagnoses at different times (e.g. Crohn's disease at some visits and ulcerative colitis at other visits). These patients were included in the "other or non-specified IBD" group. The date of the first registered event in those cases was used for analysis.

2.1.4. Statistical analysis

A Cox proportional hazards model, with calendar year on the time axis, was used to estimate the associations between the PFAS exposure variable (dichotomous or four categories, based on residence address with/without contaminated water supply, see section 2.1.2) and each IBD outcome. Gender and age (categorical variable: 0–25, 26–50, 51–75, 76 and older) were included in the model. A test of trend in exposure was performed by including the four-category time-based indicator variable as a linear effect. The proportionality assumption was tested by testing if the interaction term, exposure*calendar year, was significant ($p < 0.05$) (PROC PHREG in SAS 9.4 was used).

True IBD is very rare in pre-teenagers (Ludvigsson et al., 2017), thus, the analyses were made for ages 11 years and older. A minimum of 10 cases per exposure classification (i.e. never/ever, or never/early/mid/late) was required for each analysis.

Several sensitivity analyses were performed using the same Cox model. First, we performed separate analyses for men and women, since a recent published paper reported a gender-based difference in the incidence of IBD (Shah et al., 2018). Then, we performed analyses including only the in-patient registry (1980–2013) since the out-patient registry started after 2001, and analyses for post 2001 included both in-patient and out-patient registry. Third, we performed separate analyses for subjects below and above 45 years-old, since studies showed that people aged above 45 years had higher incidence and prevalence of IBD (Hou et al., 2013; Dahlhamer et al., 2016). Forth, we performed analyses with additional adjustment for highest educational level as an indicator for socioeconomic status in subjects over 30 years-old (highest educational level was only available for adults), since socioeconomic status may be a potential confounder.

2.2. Biomarker study

2.2.1. Study participants

There were in total 189 subjects from Ronneby and Karlshamn (the control municipality) who provided fecal samples for biomarker analysis. The subjects came from three subgroups in the larger Ronneby study:

1. Subgroup 1 (n = 57) was a pilot study, which included subjects from a panel study established in 2014 (Li et al., 2018). These subjects were repeatedly sampled 10 times from June 2014 to May 2018. At the 6th blood sampling in March 2016, they provided fecal samples. The fecal biomarkers were analyzed in March 2016.
2. Subgroup 2 (n = 113) included subjects participating both in open blood sampling in the municipality 2014–2015 and a resampling in May 2016, which also included fecal samples. The fecal biomarkers were analyzed in January 2017.
3. Subgroup 3 (n = 19) included subjects from Karlshamn (a nearby municipality with clean drinking water) who provided parallel blood and fecal samples in May 2016. The fecal biomarkers were analyzed in January 2017.

2.2.2. Exposure biomarker measurement

PFAS measurements in serum were carried out at the Division of Occupational and Environmental Medicine, Lund University, using liquid chromatography coupled to tandem mass spectrometry (LC-MS/MS) and determined as the total, non-isomer specific compounds (Li et al., 2018). Briefly, aliquots of serum were added with isotopically labeled internal standards and proteins precipitated before analyzes on a LC (UFLCXR, SHIMADZU Corporation, Kyoto, Japan) connected to the MS/MS (QTRAP 5500, AB Sciex, Foster City, CA, USA). The analyses of PFOS and PFOA are part of a quality control program between analytical laboratories (Erlangen-Nuremberg, Germany). We also calculated and presented the sum of three PFAS (Σ3PFAS, unit: nmol/ml), which refer to the sum of the molar concentration of PFHxS, PFOS and PFOA.

Table 1
ICD codes used to identify diagnoses of various inflammatory bowel disease.

Disease	ICD 8	ICD 9	ICD 10
Crohn's disease	563.00	555	K50
Ulcerative colitis	561.02, 563.10, 569.02	556	K51
Other or non-specified inflammatory bowel disease	561.03[a], 561.04[a], 563.99[a]	558[a]	K52.1, K52.2, K52.3[a], K52.8, K52.9[a]

Note: ICD, International Statistical Classification of Diseases and Related Health Problems.
[a] Non-specified diagnosis. If a non-specified diagnosis is followed by a specified one, the early date of the first non-specified diagnosis is used as the start date of the specified diagnosis.

2.2.3. Effect biomarker measurement

Fecal samples were stored at −80 °C until analyzed within a few months after collection. All tests were carried out in duplicate in a blinded manner. 15 mg fecal samples were used for each biomarker.

The calprotectin concentration was determined by an enzyme-linked immunosorbent assay (ELISA) kit (Immundiagnostik AG, Bensheim, Germany, Batch number K6927-161 124) based on the two-site sandwich technique in which the intensity of the color was directly related to the calprotectin concentration in the sample. Samples were read at 450 nm, and the 4-parameter-algorithm was used to form the standard curve and to calculate data. The concentration is presented as mg/kg. Mean concentration in fresh feces from healthy volunteers is 25 mg/kg, and > 50 mg/kg is considered a positive value. Inter-assay and intra-assay coefficients of variance (CVs) for controls are 4.4%–8.9% and 4.4%–5.6%, respectively, according to the manufacturer.

The zonulin concentration was determined by an ELISA kit (Immundiagnostik AG, Batch number K5600-160 519) using the competitive binding technique. Biotinylated zonulin tracer was added to the samples, standards, and positive and negative controls as a competitor to the sample's own zonulin. The intensity of the color was inversely proportional to the zonulin concentration in the sample. Samples were read at 450 nm, and the 4-parameter-algorithm was used to form the standard curve and to calculate data. The concentration is presented in ng/ml. Based on the manufacturer's studies of apparently healthy persons (n = 40), a mean value of 61 ± 46 ng/ml was estimated in feces. Inter-assay and intra-assay CVs for controls are 12.7%–13.9% and 3.2%–5.9%, respectively, according to the manufacturer.

The fecal calprotectin and zonulin measurements were performed with the same reagent batches but on different date, i.e. in March 2016 for subgroup 1 (pilot) and in January 2017 for subgroup 2 and 3.

2.2.4. Statistical analysis

In the present study, serum PFAS levels for 2 samplings for subgroup 1 and 2 (i.e. PFAS 2014 and PFAS 2016) together with PFAS in 2016 for subgroup 3 were reported and used for association analysis. Zonulin and calprotectin were natural logarithm-transformed to improve the model fit. The correlation between zonulin and calprotectin were tested using Spearman's correlation. The associations between serum PFAS and fecal biomarkers were assessed using linear regression model adjusted for age, gender and BMI. First, all analyses were performed separately in each subgroup, since subgroup 1 had biomarker measurements a half-year earlier than the other two subgroups, and levels of biomarkers were different between two times of lab measurements (see Table 6). For subgroup 2 and subgroup 3, where the fecal biomarkers were analyzed at the same time, the adjusted mean differences of biomarkers were tested. In the next step, an additional analysis was performed with merged subgroup 2 and 3 together. We calculated Σ3PFAS and then divided subjects into four PFAS groups: the first group consisted everyone in subgroup 3 (as the reference since they were subjects from control region Karlshamn); the second to fourth groups were divided based on the tertiles of Σ3PFAS in subgroup 2. Linear regression was used to test if there was a trend between increased PFAS levels and increased biomarker levels by including the indicator for the 4 PFAS groups as a linear effect.

Several sensitivity analyses were carried out. In subgroup 2, there were six subjects treated with proton pump inhibitors, a class of drugs that inhibit gastric acid secretion in the treatment of ulcers and gastroesophageal reflux disease, which may influence fecal calprotectin and zonulin levels (Katzka et al., 2014; Poullis et al., 2003). Therefore, a sensitivity analysis was performed by excluding these six subjects in subgroup 2. Additionally, 79% of the subjects in subgroup 1 had smoking data. A sensitivity analysis was performed in subgroup 1 using the same linear regression model with smoking habits (never/ever smoker) as an additional adjustment, since smoking has been reported to be associated with IBD (Mahid et al., 2006). Statistical analyses were performed using R version 3.3.2.

Table 2
The characteristics of the Ronneby cohort (all persons ever living in Ronneby municipality) during the entire study period (1980–2013) and at different calendar years.

	All	Men	Women
Entire period			
Counts of persons	63 074	33 218	29 856
Counts of persons ever exposed at home address (start from 1985)	16 150	8327	7823
Person years (start from 1980)	1 303 876	673 859	630 017
Crohn's disease diagnosis and/or death	194	102	92
Ulcerative colitis diagnosis and/or death	298	165	133
Other or non-specified IBD diagnosis and/or death	792	351	441
All IBD diagnosis and/or death	1284	618	666
1980 (before start of the exposure)			
Counts of persons	29 478	15 087	14 391
Age (mean ± std)	39.6 ± 23.4	38.1 ± 22.8	41.1 ± 23.8
Children < 18 yrs (%)	22%	24%	21%
Ever exposed at home	None	None	None
1985 (at start of the exposure)			
Counts of persons	32 042	16 378	15 664
Age (mean ± std)	40.2 ± 23.2	38.8 ± 22.6	41.7 ± 23.8
Children < 18 yrs (%)	20%	21%	19%
Ever exposed at home	5100	2582	2518
1995 (during the study period)			
Counts of persons	37 254	19 125	18 129
Age (mean ± std)	40.4 ± 22.5	39.1 ± 21.7	41.8 ± 23.2
Children < 18 yrs (%)	17%	17%	16%
Ever exposed at home	8658	4419	4239
2005 (during the study period)			
Counts of persons	43 092	22 416	20 676
Age (mean ± std)	41.6 ± 21.6	40.5 ± 20.9	42.9 ± 22.3
Children < 18 yrs (%)	14%	14%	14%
Ever exposed at home	10 837	5543	5294
2013 (at the end of the study period)			
Counts of persons	47 672	24 949	22 723
Age (mean ± std)	43.1 ± 21.6	42.3 ± 20.9	44.0 ± 22.3
Children < 18 yrs (%)	13%	13%	13%
Ever exposed at home	13 267	6809	6458

Note: IBD, inflammatory bowel diseases.

Table 3
Number of cases and crude incidence (cases per 100 000) of inflammatory bowel diseases (IBD) for different calendar years in the Ronneby cohort (individuals ever living in Ronneby, 1980–2013).

	Calendar year						
	80–85	86–90	91–95	96–00	01–05	06–10	11–13
Crohn's disease							
Cases [a]	15	22	20	22	36	48	31
Incidence [a]	8.1	13.2	11.1	11.3	17.2	21.3	22.0
Ulcerative colitis							
Cases [a]	29	19	27	19	105	58	41
Incidence [a]	15.6	11.4	15.0	9.8	50.4	25.8	29.2
Other or non-specified IBD							
Cases [a]	4	45	92	86	217	218	130
Incidence [a]	2.2	27.0	51.0	44.3	104.4	97.6	93.3
All IBD							
Cases [a]	48	86	139	127	358	324	202
Incidence [a]	25.9	51.7	77.3	65.7	173.2	146.2	146.2

[a] All ages are included.

Table 4
Number of cases and crude incidence (cases per 100 000) of inflammatory bowel diseases (IBD) in different age groups in the Ronneby cohort during the period 1980–2013.

	Age at event							
	0–10	11–15	16–20	21–30	31–45	46–65	66–85	86-
Crohn's disease								
Cases	2	11	16	50	60	32	21	2
Incidence	1.7	17	21.6	24.5	19.4	10.2	10.9	8.1
Ulcerative colitis								
Cases	2	2	15	65	77	91	44	2
Incidence	1.7	3.1	20.3	31.8	24.9	29.2	22.8	8.1
Other or non-specified IBD								
Cases	226	31	25	78	98	127	173	34
Incidence	193.5	48.2	34.0	38.2	31.7	40.7	89.9	138.1
All IBD								
Cases	230	44	56	193	235	250	238	38
Incidence	197.0	68.5	76.2	95.0	76.4	80.6	124.2	154.6

Table 5
Result of Cox proportional hazard regression for diagnosis (morbidity or mortality) of inflammatory bowel diseases (IBD) during 1980–2013 in the Ronneby cohort (children aged 0–10 years excluded).

Exposure classification [a]	Cases	Person-year	HR (95%CI) [b]	p
Crohn's disease				
Never	146	939 638	1	
Ever	46	243 798	1.07 (0.76, 1.50)	0.70
Never	146	939 638	1	
Early	23	96 550	1.58 (1.00, 2.49)	0.048
Mid	11	85 201	0.73 (0.39, 1.37)	0.33
Late	12	62 047	0.87 (0.47, 1.62)	0.66
Ulcerative colitis				
Never	238	938 745	1	
Ever	58	243 629	0.83 (0.62, 1.11)	0.20
Never	238	938 745	1	
Early	20	96 576	0.88 (0.55, 1.40)	0.58
Mid	24	85 093	0.86 (0.56, 1.32)	0.48
Late	14	61 960	0.73 (0.42, 1.28)	0.28
Other or non-specified IBD				
Never	418	937 311	1	
Ever	148	242 970	1.13 (0.94, 1.36)	0.20
Never	418	937 311	1	
Early	51	96 413	1.38 (1.02, 1.86)	0.037
Mid	52	84 972	0.99 (0.74, 1.33)	0.94
Late	45	61 585	1.08 (0.78, 1.50)	0.63
All IBD				
Never	802	933 129	1	
Ever	252	241 447	1.03 (0.90, 1.19)	0.65
Never	802	933 129	1	
Early	94	95 963	1.26 (1.01, 1.57)	0.038
Mid	87	84 415	0.91 (0.72, 1.14)	0.42
Late	71	61 069	0.96 (0.74, 1.23)	0.72

[a] Exposure (PFAS-contaminated water supply at **residential address**) was classified into two or four classes, according to section 2.1.2.
[b] Calendar year on time axis, gender and age (11–25, 26–50, 51–75, 76 and older) were included.

3. Results

3.1. Registry study

Table 2 describes the characteristics of the Ronneby cohort subjects and IBD diagnoses for the entire study period and at specific calendar years, i.e. before start (1980), at start (1985), during (1995 and 2005), and at the end of the study period (2013).

Table 3 shows the crude incidence for IBD diagnosis categories over time. Before 2000, there were only in-patients registered in the Swedish National Patient Register. The marked apparent increase in incidence after year 2000 is an artefact due to the inclusion of hospital out-patient visits, which started in 2001. The high incidence of other or non-specified IBD is largely explained by patients with multiple different registered diagnoses at different hospital visits (e.g. a diagnosis of Crohn's disease at one visit and ulcerative colitis at another visit). Separate incidence for men and women are given in Supplementary Table S2.

Table 4 shows the crude incidence by IBD diagnosis category in different age groups. As expected, Crohn's disease and ulcerative colitis were very rare diagnoses among children. However, a spuriously high incidence of other IBD among children at 0–10 years old was observed. This is probably due to misdiagnosis of non-specific abdominal pain or infectious gastroenteritis. Separate incidence for men and women are given in Supplementary Table S3.

There was no increased hazard ratio (HR) for any kind of diagnosed IBD when comparing subjects ever exposed to subjects never exposed. Higher HRs for Crohn's disease (HR = 1.58, 95% CI: 1.00, 2.49), other or non-specified IBD (HR = 1.38, 95% CI: 1.02, 1.86) and all IBD (HR = 1.26, 95% CI: 1.01, 1.57) were found in the cohort subjects with early exposure (1985–1994) compared to subjects never exposed. However, the increased HRs were not found for the subjects with mid exposure (1995–2004) (50% of them also had early exposure) or the subjects with late exposure (67% of them also had early and/or mid exposure). For ulcerative colitis, no signs of increased HRs were found for any exposure period (Table 5).

When analyses were performed in men and women separately, no significantly higher HRs were found for any kind of IBD in either men or women (Supplementary Table S4). The sensitivity analyses with only

Table 6
The characteristics, concentrations of serum PFAS and fecal biomarkers for study subjects in each subgroup.

	min	25%	Median	Mean	75%	max
Subgroup 1 (Ronneby Panel study, n = 57)						
Age	4	35	49	48	66	83
BMI	14	22	24	24	27	36
PFHxS (2014) (ng/ml)	52	182	363	403	574	1304
PFOA (2014) (ng/ml)	4	11	20	23	29	74
PFOS (2014) (ng/ml)	34	118	216	224	300	604
Σ3PFAS (2014) (nmol/ml) [a]	0.3	0.7	1.4	1.5	2.1	4.3
PFHxS (2016) (ng/ml)	20	127	274	314	443	1011
PFOA (2016) (ng/ml)	2	8	12	15	20	52
PFOS (2016) (ng/ml)	22	68	142	149	202	542
Σ3PFAS (2016) (nmol/ml)	0.1	0.4	1.0	1.1	1.5	3.7
Zonulin (2016) (ng/ml)	9.7	66.3	105.7	132.7	168.4	482.1
Calprotectin (2016) (mg/kg)	0.9	12.9	19.7	42.1	47.0	403.7
Subgroup 2 (Ronneby,Re-sampling, n = 113)						
Age	15	36	46	44	52	69
BMI (2016)	18	24	26	27	30	40
PFHxS (2014) (ng/ml)	1	124	231	285	408	1097
PFOA (2014) (ng/ml)	1	9	16	17	23	62
PFOS (2014) (ng/ml)	1	147	271	314	449	1063
Σ3PFAS (2014) (nmol/ml)	0.01	0.6	1.2	1.4	2.0	4.8
PFHxS (2016) (ng/ml)	1	99	205	239	341	1016
PFOA (2016) (ng/ml)	1	5	9	10	14	40
PFOS (2016) (ng/ml)	1	105	188	223	314	916
Σ3PFAS (2016) (nmol/ml)	0.01	0.5	0.9	1.1	1.5	4.5
Zonulin (2016) (ng/ml)	22.7	78.4	111.4	135.8	155.3	937.6
Calprotectin (2016) (mg/kg)	3.2	27.9	66.8	92.7	126.9	529.4
Subgroup 3 (Karlshamn, n = 19)						
Age	26	34	52	49	58	68
BMI (2016)	21	23	25	27	29	39
PFHxS (2016) (ng/ml)	1	1	1	1	2	2
PFOA (2016) (ng/ml)	1	1	2	2	2	3
PFOS (2016) (ng/ml)	1	4	5	6	7	19
Σ3PFAS (2016) (nmol/ml)	0.01	0.01	0.02	0.02	0.02	0.05
Zonulin (2016) (ng/ml)	27.1	63.1	79.7	99.7	131.7	228.7
Calprotectin (2016) (mg/kg)	34.0	60.1	99.6	119.9	161.4	296.4

[a] Sum of the molar concentration of PFOS, PFHxS and PFOA.

hospital in-patient visits (1980–2013), as well as with in-patient and out-patient visit for post 2001, did not shown any statistically significant HRs (Supplementary Table S5 and S6). The age-specific sensitivity analyses showed a very high HR for Crohn's disease (HR = 3.06, 95% CI: 1.51–6.19) for cohort subjects above 45 years-old with early exposure (Supplementary Table S7, part II), but not for those with younger age (Supplementary Table S7, part I). However, it should be noted that there were only a few cases for the age-specific analysis, and due to the few cases for mid and late exposure, we could not get HR for those exposure periods. The sensitivity analyses with additional adjusted for highest education level showed similar HRs in the models with and without education level (Supplementary Table S8), indicating that socioeconomic status is not a serious confounder in this study.

3.2. Biomarker study

There were 60%, 66% and 79% females in subgroup 1, 2 and 3, respectively. The median age and BMI were comparable across the three subgroups (Table 6). PFAS were measured at two time points for subgroup 1 and 2 (from Ronneby population), and, as expected, a clear decrease was observed for each PFAS from 2014 to 2016. PFAS from subgroup 3 (Karlshamn) were only measured once in 2016 and showed low levels (Table 6).

There was very little correlation between fecal zonulin and calprotectin in subgroup 1 (spearman's $r = -0.18$, $p = 0.18$) and subgroup 3 (spearman's $r = 0.079$, $p = 0.75$), but a positive correlation in subgroup 2 (spearman's $r = 0.41$, $p < 0.001$). Subgroup 2 showed slightly higher zonulin levels ($p = 0.10$), but significantly lower calprotectin levels ($p = 0.04$), than the unexposed subjects in subgroup 3 after adjusting for age, BMI and gender.

No significant association was found between Σ3PFAS and fecal zonulin in each subgroup, neither measured concurrently nor using serum PFAS, measured approximately two years earlier. Similarly, no association was found for calprotectin (Table 7). The separate associations with PFOS, PFHxS and PFOA are listed in Supplementary Table S9. Only one negative significant association was found, and it was between concurrent PFOA and fecal zonulin in subgroup 2 (out of 30 comparisons).

The analyses with merged subgroup 2 and 3 (i.e. biomarkers analyzed at the same time) showed a significant trend of decreased calprotectin levels across increased Σ3PFAS (p for trend = 0.002), and a significant lower calprotectin level in group 4 (with highest Σ3PFAS level), together with a close to significant lower calprotectin in group 3 compared to group 1 (Table 8). No such trend was evident for zonulin.

The sensitivity analysis without subjects with treatment of proton pump inhibitors showed similar results to the original analyses (Supplementary Table S10). Moreover, the sensitivity analysis in subgroup 1 with additional adjustment for smoking habits did not change the significance of the effects (Supplementary Table S11).

Table 7
Associations between Σ3PFAS and fecal zonulin and calprotectin.

	Zonulin [a]		Calprotectin [a]	
	β (95%CI) [b]	p	β (95%CI) [b]	p
Subgroup 1 (Ronneby Panel study, n = 57)				
Σ3PFAS (2014)	0.01 (-0.25, 0.28)	0.92	-0.10 (-0.47, 0.26)	0.57
Σ3PFAS (2016)	0.04 (-0.29, 0.38)	0.80	-0.02 (-0.49, 0.44)	0.92
Subgroup 2 (Ronneby, Re-sampling, n = 115)				
Σ3PFAS (2014)	-0.03 (-0.17, 0.11)	0.68	-0.13 (-0.37, 0.11)	0.27
Σ3PFAS (2016)	-0.10 (-0.26, 0.07)	0.26	-0.14 (-0.42, 0.14)	0.31
Subgroup 3 (Karlshamn controls, n = 19)				
Σ3PFAS (2016)	-6.51 (-37.0, 24.0)	0.65	-9.27 (-45.6, 27.0)	0.59

[a] Zonulin and calprotectin were natural logarithm transformed.
[b] Linear models adjusted for age, BMI and gender.

4. Discussion

In this study, we hypothesized that PFAS exposure through drinking water could be a risk factor for IBD, evidenced by positive associations to fecal biomarkers (indicators for intestinal inflammation and permeability) and subsequently higher incidence of diagnosed IBD. However, a lack of a dose response across estimated retrospective time-based exposure (indicating increasing exposure levels during the study period) in the registry study, together with a lack of positive association between measured serum PFAS and fecal biomarkers (i.e. calprotectin and zonulin) in the biomarker study does not support an association between PFAS exposure and risk of IBD.

Our findings contrasted the evidence found in the C8 study, where increased risk of ulcerative colitis in adults exposed to PFOA through contaminated drinking water near a chemical plant was reported (Steenland et al., 2013). In the C8 study, PFOA exposure derived from emissions from a Du Pont factory. PFOA was the dominant PFAS component serum on average. They investigated six autoimmune diseases (i.e. ulcerative colitis, Crohn's disease, rheumatoid arthritis, type 1 diabetes, lupus and multiple sclerosis) in the PFOA-exposed population, and the only positive finding was an increased risk of ulcerative colitis in relation to degree of PFOA exposure. This finding along with the absence of associations with other autoimmune diseases, especially with Crohn's disease, prompted us to seek confirmation in another PFAS exposed population, though with a different PFAS exposure profile. The exposure in Ronneby was unique, almost a natural experiment: one third of the households in the municipality had been exposed to high levels of PFAS in drinking water for a long time and with a sudden cessation. The AFFF-induced PFAS contamination caused high exposure to PFOS and PFHxS, but to a lesser extent to PFOA. Notably, PFOS and PFHxS levels were highly correlated.

In the registry study, using persons never living at an address with contaminated drinking water as reference category, we found significantly higher HRs for Crohn's disease and other or non-specified IBD for cohort subjects with only early period exposure, in contrast, subjects with mid and late period exposure had lower HRs (although not significant). In the Ronneby cohort, it has been confirmed that PFAS serum levels for those exposed in the late period were high (Andersson et al., 2019). In addition, after checking the historical exposure of the cases, it was found that cases with early exposure had on average 2.5 years of early period exposure prior to diagnosis, whereas cases with late exposure had had on average 4.8 years of early period exposure. Therefore, the higher HRs for the cases with early period exposure are not explained by higher PFAS exposure level nor longer exposure time during the early period. If not a chance finding, or due to unmeasured confounders (e.g. smoking or alcohol intake), it could be speculated that higher HRs for the early period followed by lower HRs for the mid and later period for the certain IBD could stem from susceptibility in segments of the population: Under this hypothesis, subjects who were more predisposed to develop these diseases, and therefore more susceptible to PFAS would be more likely to get disease in the early period and became censored in the analysis, while those who did not get a diagnosis during the early period exposure were subsequently less susceptible to getting the disease.

However, it should be noticed that the incidence rate of Crohn's disease and ulcerative colitis were slightly higher in the Ronneby cohort than other populations in Sweden. Lapidus (2006) reported an incidence rate of Crohn's disease of 8.3 per 100 000 person-years in Stockholm county during 1990–2001, compared to 10.5 in the Ronneby cohort from 1990 to 2000. For ulcerative colitis, Rönnblom et al. (2010) reported an incidence of ulcerative colitis of 17.5 per 100 000 person-years in Uppsala during 2005–2007, compared to 23.9 from 2005 to 2009 in the Ronneby cohort. The difference in incidence rate may be due to regional difference. We speculate that some other unmeasured environmental exposure or people's individual behavior in Blekinge province (Ronneby, Karlshamn and Karlskrona) could affect gut mucosa

Table 8
Association between Σ3PFAS exposure and fecal zonulin and calprotectin in the subjects from Ronneby and Karlshamn controls.

PFAS group [a]	Median				Zonulin [b]			Calprotectin [b]		
	Σ3PFAS (nmol/ml)	PFHxS (ng/ml)	PFOA (ng/ml)	PFOS (ng/ml)	β (95%CI) [c]	p	P for trend	β (95%CI) [c]	p	P for trend
Reference (subgroup 3)	0.02	1.1	1.7	5.5	–	–	0.56	–	–	0.002
Tertiles 1	0.3	61	3	65	0.31 (-0.03, 0.66)	0.074		-0.17 (-0.73, 0.39)	0.56	
Tertiles 2	0.9	196	9	184	0.27 (-0.06, 0.61)	0.11		-0.51 (-1.05, 0.04)	0.068	
Tertiles 3	1.8	397	16	364	0.17 (-0.16.0.50)	0.32		-0.73 (-1.27, -0.20)	0.008	

[a] PFAS tertiles was defined based on Σ3PFAS in subgroup 2 in 2016.
[b] Zonulin and calprotectin were natural logarithm transformed.
[c] Linear models adjusted for age, BMI and gender.

and be responsible for the slightly increased incidence rate, evidenced by higher calprotectin in the Karlshamn subjects (without PFAS exposure) compared to the Ronneby subjects in the biomarker study.

The biomarker study with cross-sectional serum PFAS and fecal calprotectin and zonulin provided no evidence of a positive association between PFAS exposure and the subclinical risk of IBD. Instead, a trend of decreased calprotectin across increased exposure was found, indicating that lower gut inflammation was associated with higher exposure, and the drop of calprotectin was about 48% in the highest PFAS tertile (e.g. median PFHxS = 397 ng/ml) compared to the lowest reference (median PFHxS = 1.1 ng/ml). The strong negative trend was opposite to what we expected and the causality is not clear. It could be that PFAS causes a reduction in calprotectin. On the other hand, it is also possible that people with lower calprotectin have better gut integrity and better enterohepatic circulation with higher reabsorption of PFAS, which in turn, leads to higher serum PFAS level. Moreover, the significantly lower calprotectin in the highest compared to the lowest PFAS tertiles may rather be due to ecologic differences other than PFAS exposure. The reference group in the analysis was set as subjects from the nearby municipality, who had significantly higher calprotectin levels compared to Ronneby subjects. Taken together with the absence of an association between measured PFAS and calprotectin within subgroup 2 and subgroup 1 (subjects from Ronneby), there may be some other unmeasured factors which are responsible for the higher calprotectin levels in Karlshamn. Zonulin levels were not different between Karlshamn and Ronneby subjects, and it was not associated with PFAS levels in any subgroup. No trend was found for zonulin across PFAS groups, either. All these results suggested that there was no association between PFAS exposure and fecal zonulin.

The biomarker study is novel in assessing fecal calprotectin and zonulin associated to PFAS exposure. These two relatively new biomarkers of gut inflammation and permeability represent a new approach to explore the underlying mechanism of PFAS exposure on gastrointestinal health, as well as a possible tool to explore PFAS elimination through gastrointestinal tract in future studies. Calprotectin is a recent and sensitive biomarker for measuring mucosal inflammation, and is found at increased levels in response to all kinds of ulcer, inflammation or malignancy. The reference range is < 50 mg/kg feces for fresh samples and the clinically important level is recommended as < 100–150 mg/kg feces (Erbayrak et al., 2009; Walsham and Sherwood, 2016). However, unexpectedly high levels were noticed in some subjects from subgroup 2 and 3. We measured biomarkers in frozen samples, thus preanalytical variation cannot be ruled out. Zonulin is described as a biomarker reflecting intestinal permeability (Fasano, 2012). The ELISA kit commercially available has recently been shown to identify properdin, in addition to zonulin or pre-haptoglobin2 (Scheffler et al., 2018). Studies performed so far have described how zonulin is associated with metabolic syndrome and higher levels of weight, glucose and insulin (Ohlsson et al., 2017), factors associated with increased intestinal permeability, but no study has hitherto examined a potential association with PFAS exposure. Our finding of the negative association with calprotectin warrants further studies with larger sample size or longitudinal design to address the direction of causality.

The strength of the registry study is the complete follow-up through national registration on yearly residency, hospital-based diagnoses and information on the waterworks' distribution networks in the municipality. The limitation is the crude exposure assessment since information about PFAS drinking water levels only exists from 2013. While are confident that PFAS exposure and serum levels in this population have increased over time, the relative extent of exposure between the time-based exposure variables is uncertain, and some exposure misclassification may have occurred. Additionally, lack of information of the possible intake of PFAS contaminated water from outside the home address, other exposures and covariates than age and gender may conceivably have contributed to the significant higher HRs for the subjects with only early drinking water exposure.

In the biomarker study with cross-sectional design, the causality between PFAS exposure and subclinical risk of IBD could not be inferred. It is possible that intestinal permeability or inflammation would affect PFAS reabsorption or excretion and in turn affect PFAS serum levels. The smaller sample size in the biomarker study, especially in the stratified analysis, limits the statistical power to identify true associations. Moreover, although smoking has been reported to be associated with IBD (Mahid et al., 2006), we could not adjust for smoking for all analyses due to the large proportion of missing data. However, in the pilot study (subgroup 1) we had good quality smoking data and results with adjustment for smoking habits remained the same: no associations between serum PFAS and fecal biomarkers were found. Biomarkers for subgroup 1 were measured at different time point than the two other subgroups. The laboratory used the same batch of ELISA kits for biomarker measurements at the two different time points, but the notable difference in the levels, especially for calprotectin, may be due to pre-analytical variation in sample preparation. Such a large difference made it inappropriate to pool the data from all subgroups, since the associations could be affected by the inter-laboratory differences in measurements. The high correlation between PFOS, PFHxS and PFOA in the Ronneby population limited the possibility to distinguish individual PFAS, instead, our study investigated the associations between a total mixture of PFAS exposure from AFFFs and risk of IBD. Additionally, we could not link the registry study to the biomarker study due to sensitive personal data protection. Therefore, it is not possible to exclude subjects who already had IBD in the biomarker study, and it is not possible to test if there is an association between IBD incidence and fecal biomarkers in our cohort. However, due to the fact that IBD is not a common disease, the proportion and number of subjects with IBD would be very small.

5. Conclusion

We did not observe consistent increased HRs for IBD incidence based on estimated PFAS exposure in the registry study, or any positive association between measured serum PFAS and fecal biomarkers in the cross-sectional study. Therefore, our findings provide no evidence of an association between PFAS exposure from AFFFs and risk of IBD.

Funding sources

This research was supported by Formas (grant number: 216-2014-1709) and FORTE (grant number: 2015-732).

Ethics approval

All participants gave informed written consent to take part in the study. The study was approved by the Regional Ethical Review Board in Lund, Sweden.

Acknowledgments

We gratefully thanks to Ronneby and Karlshamn residents who took part in the study and the field staffs for their assistance with sample collection. Thanks to Kristoffer Mattisson at Occupational and Environmental Medicine, Lund University, who did the work on connecting each residence address with the correct waterwork supply data. This research was supported by Formas (grant number: 216-2014-1709) and FORTE (grant number: 2015-732).

Appendix A. Supplementary data

Supplementary data to this article can be found online at https://doi.org/10.1016/j.envres.2019.108923.

References

Andersson, E.M., Scott, K., Xu, Y., Li, Y., Olsson, D.S., Fletcher, T., Jakobsson, K., 2019. High exposure to perfluorinated compounds in drinking water and thyroid disease. A cohot study from Ronneby, Sweden. Environ. Res. 176, 108540.

Chiba, H., Osanai, M., Murata, M., Kojima, T., Sawada, N., 2008. Transmembrane proteins of tight junctions. Biochim. Biophys. Acta Biomembr. 1778, 588–600.

Csáki, K.F., 2011. Synthetic surfactant food additives can cause intestinal barrier dysfunction. Med. Hypotheses 76, 676–681.

Dahlhamer, J.M., Zammitti, E.P., Ward, B.W., Wheaton, A.G., Croft, J.B., 2016. Prevalence of inflammatory bowel disease among adults aged ≥ 18 years-United States. 2015. MMWR Morb. Mortal. Wkly. Rep. 65 (42), 1166–1169.

Dolan, K.T., Chang, E.B., 2017. Diet, gut microbes, and the pathogenesis of inflammatory bowel diseases. Mol. Nutr. Food Res. 61, 1600129.

Domingo, J.L., 2012. Health risks of dietary exposure to perfluorinated compounds. Environ. Int. 40, 187–195.

Ehrchen, J.M., Sunderkötter, C., Foell, D., Vogl, T., Roth, J., 2009. The endogenous toll-like receptor 4 agonist s100a8/s100a9 (calprotectin) as innate amplifier of infection, autoimmunity, and cancer. J. Leukoc. Biol. 86, 557–566.

Erbayrak, M., Turkay, C., Eraslan, E., Cetinkaya, H., Kasapoglu, B., Bektas, M., 2009. The role of fecal calprotectin in investigating inflammatory bowel diseases. Clinics 64, 421–425.

Eriksson, U., Kärrman, A., Rotander, A., Mikkelsen, B., Dam, M., 2013. Perfluoroalkyl substances (pfass) in food and water from Faroe Islands. Environ. Sci. Pollut. Res. Int. 20, 7940–7948.

Eue, I., Pietz, B., Storck, J., Klempt, M., Sorg, C., 2000. Transendothelial migration of 27e10+ human monocytes. Int. Immunol. 12, 1593–1604.

European Food Safety Authority, 2018. Risk to Human Health Related to the Presence of Perfluorooctane Sulfonic Acid and Perfluorooctanoic Acid in Food. EFSA Journal. vol. 16, e05194.

Fasano, A., 2012. Intestinal permeability and its regulation by zonulin: diagnostic and therapeutic implications. Clin. Gastroenterol. Hepatol. 10, 1096–1100.

Guelfo, J.L., Adamson, D.T., 2018. Evaluation of a national data set for insights into sources, composition, and concentrations of per-and polyfluoroalkyl substances (pfass) in us drinking water. Environ. Pollut. 236, 505–513.

Hou, J.K., Kramer, J.R., Richardson, P., Mei, M., El-Serag, H.B., 2013. The incidence and prevalence of inflammatory bowel disease among U.S. veterans: a national cohort study. Inflamm. Bowel Dis. 19 (5), 1059–1064.

Hu, X.C., Andrews, D.Q., Lindstrom, A.B., Bruton, T.A., Schaider, L.A., Grandjean, P., et al., 2016. Detection of poly-and perfluoroalkyl substances (pfass) in us drinking water linked to industrial sites, military fire training areas, and wastewater treatment plants. Environ. Sci. Technol. Lett. 3, 344–350.

Katzka, D.A., Tadi, R., Smyrk, T.C., Katarya, E., Sharma, A., Geno, D.M., et al., 2014. Effects of topical steroids on tight junction proteins and spongiosis in esophageal epithelia of patients with eosinophilic esophagitis. Clin. Gastroenterol. Hepatol. 12, 1824–1829 e1821.

Lapidus, A., 2006. Crohn's disease in stockholm county during 1990-2001: an epidemiological update. World J. Gastroenterol. 12, 75–81.

Li, Y., Fletcher, T., Mucs, D., Scott, K., Lindh, C.H., Tallving, P., et al., 2018. Half-lives of pfos, pfhxs and pfoa after end of exposure to contaminated drinking water. Occup. Environ. Med. 75, 46–51.

Ludvigsson, J.F., Büsch, K., Olén, O., Askling, J., Smedby, K., Ekbom, A., et al., 2017. Prevalence of paediatric inflammatory bowel disease in Sweden: a nationwide population-based register study. BMC Gastroenterol. 17, 23.

Mahid, S.S., Minor, K.S., Soto, R.E., Hornung, C.A., Galandiuk, S., 2006. Smoking and inflammatory bowel disease: a meta-analysis. Mayo Clin. Proc. 81, 1462–1471.

Malíčková, K., Francová, I., Lukáš, M., Kolář, M., Králíková, E., Bortlík, M., et al., 2017. Fecal zonulin is elevated in crohn's disease and in cigarette smokers. Pract Lab Med 9, 39–44.

Molodecky, N.A., Soon, S., Rabi, D.M., Ghali, W.A., Ferris, M., Chernoff, G., et al., 2012. Increasing incidence and prevalence of the inflammatory bowel diseases with time, based on systematic review. Gastroenterology 142, 46–54 e42.

Odink, K., Cerletti, N., Brüggen, J., Clerc, R.G., Tarcsay, L., Zwadlo, G., et al., 1987. Two calcium-binding proteins in infiltrate macrophages of rheumatoid arthritis. Nature 330, 80.

Ohlsson, B., Roth, B., Larsson, E., Höglund, P., 2017. Calprotectin in serum and zonulin in serum and feces are elevated after introduction of a diet with lower carbohydrate content and higher fiber, fat and protein contents. Biomed Rep 6, 411–422.

Poullis, A., Foster, R., Mendall, M.A., 2003. Proton pump inhibitors are associated with elevation of faecal calprotectin and may affect specificity. Eur. J. Gastroenterol. Hepatol. 15, 573–574.

Rönnblom, A., Samuelsson, S.-M., Ekbom, A., 2010. Ulcerative colitis in the county of uppsala 1945–2007: incidence and clinical characteristics. J Crohns Colitis 4, 532–536.

Sapone, A., De Magistris, L., Pietzak, M., Clemente, M.G., Tripathi, A., Cucca, F., et al., 2006. Zonulin upregulation is associated with increased gut permeability in subjects with type 1 diabetes and their relatives. Diabetes 55, 1443–1449.

Scheffler, L., Crane, A., Heyne, H., Tönjes, A., Schleinitz, D., Ihling, C.H., et al., 2018. Widely used commercial elisa does not detect precursor of haptoglobin2, but recognizes properdin as a potential second member of the zonulin family. Front Endocrinol 9–22.

Shah, S.C., Khalili, H., Gower-Rousseau, C., et al., 2018. Sex-Based Differences in Incidence of Inflammatory Bowel Diseases-Pooled Analysis of Population-Based Studies From Western Countries. Gastroenterology 155 (4), 1079–1089. https://doi.org/10.1053/j.gastro.2018.06.043.

Steenland, K., Zhao, L., Winquist, A., Parks, C., 2013. Ulcerative colitis and perfluorooctanoic acid (pfoa) in a highly exposed population of community residents and workers in the mid-Ohio valley. Environ. Health Perspect. 121, 900.

Steenland, K., Zhao, L., Winquist, A., 2015. A cohort incidence study of workers exposed to perfluorooctanoic acid (pfoa). Occup. Environ. Med. 72, 373–380.

Steenland, K., Kugathasan, S., Barr, D.B., 2018. Pfoa and ulcerative colitis. Environ. Res. 165, 317–321.

Uniken Venema, W.T., Voskuil, M.D., Dijkstra, G., Weersma, R.K., Festen, E.A., 2017. The genetic background of inflammatory bowel disease: from correlation to causality. J. Pathol. 241, 146–158.

Vanuytsel, T., Vermeire, S., Cleynen, I., 2013. The role of haptoglobin and its related protein, zonulin, in inflammatory bowel disease. Tissue Barriers 1, e27321.

Walsham, N.E., Sherwood, R.A., 2016. Fecal calprotectin in inflammatory bowel disease. Clin. Exp. Gastroenterol. 9, 21–29.

Żak-Gołąb, A., Kocełak, P., Aptekorz, M., Zientara, M., Juszczyk Ł, Martirosian G., et al., 2013. Gut microbiota, microinflammation, metabolic profile, and zonulin concentration in obese and normal weight subjects. Internet J. Endocrinol. 2013, 674106.

Zwadlo, G., Brüggen, J., Gerhards, G., Schlegel, R., Sorg, C., 1988. Two calcium-binding proteins associated with specific stages of myeloid cell differentiation are expressed by subsets of macrophages in inflammatory tissues. Clin. Exp. Immunol. 72, 510–515.

Process Safety and Environmental Protection 130 (2019) 250–256

Contents lists available at ScienceDirect

Process Safety and Environmental Protection

journal homepage: www.elsevier.com/locate/psep

Environmental pressure effects on thermal runaway and fire behaviors of lithium-ion battery with different cathodes and state of charge

Mingyi Chen [a,*], Dongxu Ouyang [b], Jingwen Weng [b], Jiahao Liu [c], Jian Wang [b]

[a] School of the Environment and Safety Engineering, Jiangsu University, Zhenjiang, 212013, Jiangsu, China
[b] State Key Laboratory of Fire Science, University of Science and Technology of China, Hefei, 230026, Anhui, China
[c] College of Ocean Science and Engineering, Shanghai Maritime University, Shanghai, 201306, China

ARTICLE INFO

Article history:
Received 11 July 2019
Received in revised form 18 August 2019
Accepted 21 August 2019
Available online 23 August 2019

Keywords:
Lithium-ion battery
Environmental pressure
Thermal runaway
Fire
Combustion heat

ABSTRACT

The environmental pressure effect on thermal runaway and fire behaviors in the 18650 lithium-ion battery (LIB) with various cathodes and states of charge (SOC) are experimentally investigated in this work. The fire hazards were characterized by the combustion process, total mass loss (TML) and total heat release (THR). The TML and THR increase with the ascending of the SOC at two pressures. The amount of materials ejected by both $LiFePO_4$ and $LiCoO_2$ batteries during the combustion is slightly affected by the environmental pressure. Meanwhile, the environmental pressure has a significant influence on the combustion heat that the THR value at high pressure is relatively bigger than that at low pressure. The unit growth rate in combustion heat between the two pressures also increases with the SOC.

1. Introduction

Lithium-ion battery (LIB) is widely used in the field of energy storage and conversion because of its greatly improved energy density, no memory effect, long cycle life and low environmental pollution. At present, LIBs have the potential and prospects of becoming the mainstream technology for power devices, but the bottleneck is the safety (Lisbona and Snee, 2011). In recent years, the fire accidents of electric vehicles and large-scale energy storage power stations appearing worldwide are on the rise, and the thermal runaway of LIBs has become the most serious safety accident in the usage (Wang et al., 2012; Ouyang et al., 2018a). Thermal runaway is often caused by separator broken due to extrusion deformation, puncture or high temperature baking, causing a short circuit between the positive and negative electrodes, or due to external short circuit of the battery (Wang et al., 2018). The LIB internally accumulates a large amount of heat in a short time (Wang et al., 2019a). The decomposition of the positive and negative materials and the electrolyte happens causing the LIB to ignite and explode, which seriously threatens the safety of the user's life and property. With the demand for high capacity, the thermal stability of the battery will be worse, and the safety risk will be greater in the future (Liu et al., 2016a; Larsson et al., 2018). Therefore, it is necessary to take measures to prevent safety problems.

Fire is one of the most serious accidents in various industries, may lead to serious property damage and casualties (Scarponi et al., 2018). So the researchers conducted in-depth studies on the fire such as the flame characters (Li et al., 2019a), detection approach (Wu et al., 2019), and fire-fighting methods (Lv et al., 2019; Tang et al., 2019). In recent years, the problem of LIB fire has received extensive attention and achieved many research results. The researchers conducted a detailed analysis of the thermal runaway principle of LIB, and discussed the differences in their combustion behavior (Said et al., 2019a; Ouyang et al., 2019; Mao et al., 2018; Wang et al., 2017). Lithium batteries undergo complex thermal runaway reactions before the ignition releasing a large amount of heat and gases (Feng et al., 2018; Shah et al., 2016; Larsson et al., 2014). Wang et al. found that the probability of LIB thermal runaway occurrence increases with the charging current in the charging process and decrease with the discharging resistance during discharging (Wang et al., 2019b). At the same time, the fires of LIBs are manifested in various forms, which are mainly affected by the battery cathode materials, state of charge (SOC), and pack structure (Fu et al., 2015; Huang et al., 2015; Chen et al., 2017a; Chen et al., 2019; Ouyang et al., 2018b). The increase in SOC results in a decrease in the thermal runaway initial temperature and maximum

* Corresponding author.
E-mail address: chenmy@ujs.edu.cn (M. Chen).

https://doi.org/10.1016/j.psep.2019.08.023
0957-5820/

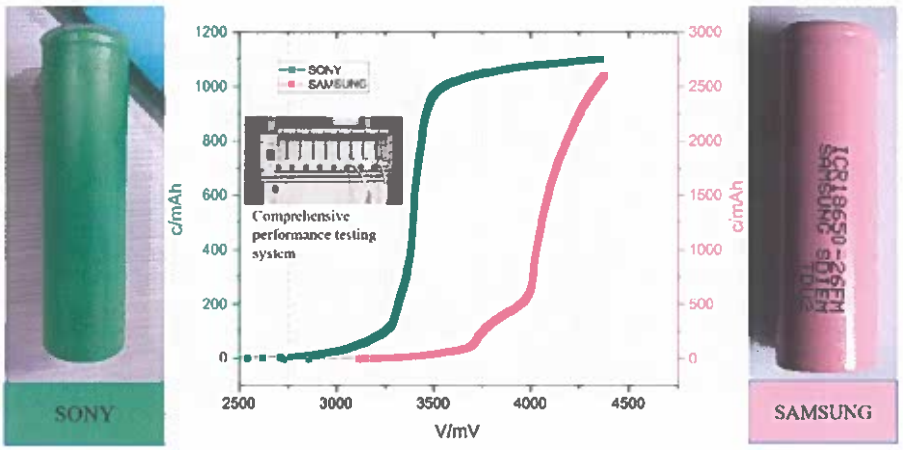

Fig. 1. Appearance and charge process of two LIBs.

temperature (Jiang et al., 2018). The surrounding environment of LIB has a significant impact on its thermal runaway behavior such as that the critical current causing thermal runaway declines with the increase of environmental temperature (Guo et al., 2017). Lithium battery fires can also release toxic gases such as hydrogen fluoride and sulfur dioxide, which have a great impact on personnel safety (Larsson et al., 2017; Lecocq et al., 2016). In the case of toxic gas leaks, especially for large lithium battery powered buses, it is important to accurately identify hazardous areas and take effective measures to quickly evacuate people from hazardous areas and minimize accidental losses (Li et al., 2011). In the meanwhile, the research on fire propagation model and fire extinguishing technology of LIB pack is developed (Li et al., 2019b; Ping et al., 2018; Huang et al., 2016). Said et al. found that the thermal runaway propagation speed of LIBs in air was much higher than that in nitrogen (Said et al., 2019b). Changing the SOC of LIBs is also an effective way to slow down the thermal runaway propagation speed in the battery pack (Lee et al., 2019). Thermal management of the LIB pack by phase change material (PCM), air cooling, liquid cooling, etc., can significantly suppress the overheating and thermal runaway, and reduce the probability of fire (Yuan et al., 2019; Ye et al., 2018; Zhao et al., 2018). On the other hand, in some low-pressure situations such as at high altitudes, aircraft or spacecraft, the occurrence and development of LIB fires differs from the standard atmospheric conditions. The environmental pressure has a significant impact on the ignition and combustion characteristics of combustible materials (Fu et al., 2018; Chen et al., 2017b; Bjerre et al., 2017). Previous studies have found that the environmental pressure changes the burning rate and combustion heat through the experiments on common materials (Liu et al., 2016b; Zhou et al., 2014; Panchal et al., 2016; Tao et al., 2013; Giurcan et al., 2017). However, little research has been done on the thermal runaway and combustion characteristics of lithium batteries at low pressures. In this paper, the effects of environmental pressure on the thermal runaway and combustion performance of lithium batteries were tested. LIBs with two kinds of cathode materials and three SOCs were tested under two environmental pressures. The research on fire safety of LIBs under different environmental pressures has high practical significance and scientific value, which is conducive to the safety of air cargo.

2. Experimental setup

The batteries used in recent studies are SONY SE US18650FT LIBs which use $LiFePO_4$ as a cathode material and SAMSUNG $LiCoO_2$ IRC18650-26FM LIBs as shown in Fig. 1. The detailed specifications of these batteries are shown in Table 1. Both kinds of batteries were tested for charge and discharge before thermal runaway and fire experiments, and the charging mode was constant current charging. The comprehensive performance testing system manufactured by NEWARE China with 8 channels and separate constant current and voltage source was used to charge and discharge the LIBs. It can be seen from the Fig. 1 that the electrical performance of them meets the standard requirements. The battery that satisfied the electrical performance was charged and discharged to the specified SOC (0%, 50%, and 100%), and it was performed in the thermal runaway and fire test after standing for 24 h.

Table 1
Specifications of 18650 cylindrical LIBs.

Brand	SONY	SAMSUNG
Cell type	Cylindrical type 18650	Cylindrical type 18650
Cathode material	$LiFePO_4$	$LiCoO_2$
Anode material	Graphite	Graphite
Electrolyte	Carbonate based	Carbonate based
Nominal capacity	1100 mAh	2600 mAh
Size	Diameter 18 mm, height 65mm	Diameter 18 mm, height 65mm
Standard voltage	3.2 V	3.7 V
State of charge	0%, 50, 100%	0%, 50, 100%
Weight	40 g	44 g

The test platforms which were set to test the thermal runaway and combustion characteristics of LIBs as shown in Fig. 2 in current study were the in-situ calorimeters constructed both in Hefei, China (sea-level, 100.8 kPa, 24 m) and Lhasa, China (64.3 kPa, 3650 m), respectively. The structure and test method of the in-situ calorimeters were identical at two locations. The experiments were operated both under over-ventilated conditions. In this experiment, an electric heating device which was a square coiled electrical resistance with a power of 2 kW was used to simulate the thermal runaway of the battery. An electronic scale is placed under the heater to support the entire experimental setup while measuring changes in battery quality. The balance has a measurement range of 9 kg and an error resolution of 0.01 g. The oxygen consumption method is used to measure and calculate the heat release rate (HRR) (Chow and Han, 2011). There exists some variation in LIB fire experiments. Based on this consideration, the fire test of each configuration was repeated three times under the same condition.

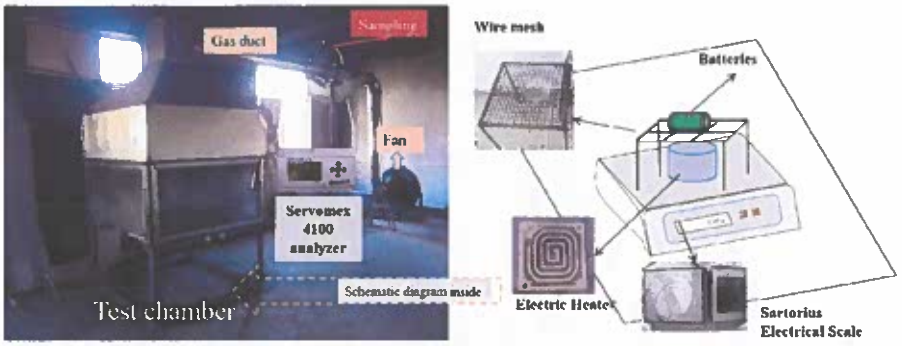

Fig. 2. Schematic diagram of the experimental platforms.

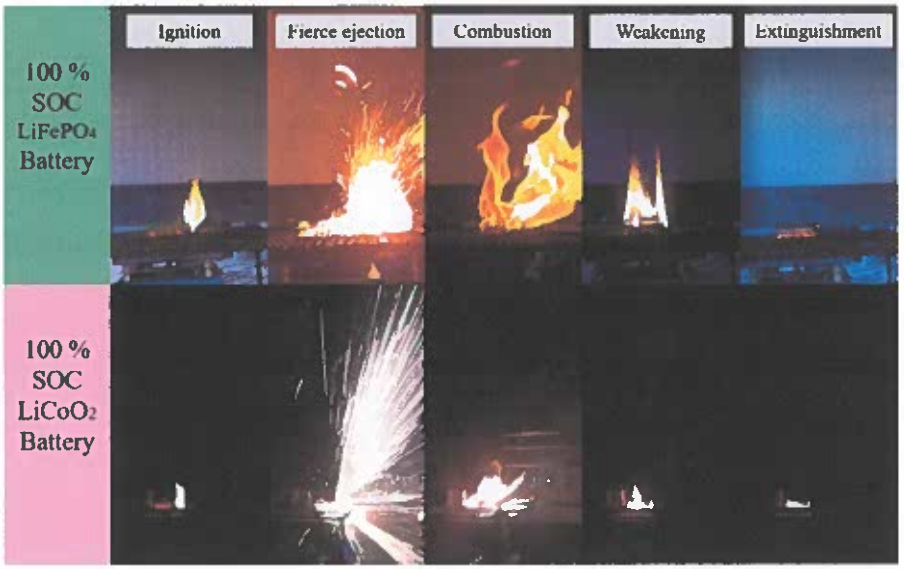

Fig. 3. Combustion processes of $LiFePO_4$ and $LiCoO_2$ battery.

3. Results and discussion

The combustion processes of 100% SOC $LiFePO_4$ and $LiCoO_2$ batteries are shown in Fig. 3. In general, the combustion characters of LIBs can be summarized into the four stages: ignition, fierce ejection, combustion, weakening and extinguishment. After continuous heating, the LIB undergoes thermal runaway, and generates a large amount of heat and gas. The leaked combustibles are ignited at high temperature, and then there is a fierce ejection with molten metal. After intense ejection, a large flame is formed and then gradually weakened until it is extinguished. It can be seen from the pictures taken at typical moments that the burning behavior of the two batteries is different. In the fierce ejection stage, the $LiCoO_2$ battery which forms a bundle of sparks in multiple directions has a significantly higher ejection power than the $LiFePO_4$ battery. The ejection of $LiFePO_4$ battery is relatively weak, and there are more combustion flames in the spray. In the subsequent combustion stage, the $LiFePO_4$ battery has a bigger combustion flame height and width than the $LiCoO_2$ battery. These phenomena preliminarily indicate that there are some differences in ejection combustion behavior between the two kinds of batteries. Its mechanism needs to be analyzed, and it is also necessary to discuss how the environmental pressure affects this difference.

Thermal runaway and fire process of LIBs are shown in Fig. 4. LIBs consist of positive and negative electrode, separator and electrolyte. When the heat generation rate of LIB is significantly higher than the heat dissipation rate, thermal runaway is easily triggered. A series of self-accelerating exothermic reactions including solid electrolyte interphase (SEI) decomposition, electrolyte oxidative decomposition, cathode and anode decomposition, and their interaction reactions occur inside the LIBs. During the thermal runaway process, the heat content of the battery continues to accumulate and the temperature is getting high quickly. Thereby, a large amount of decomposed combustibles and gas products are generated inside the battery. These chemical reactions cause the internal temperature of the battery to be very high and the internal pressure to gradually increase. When the internal pressure builds up too much, it exceeds the pressure relief valve structural stress and external pressure, causing the pressure relief valve to crack. A large amount of gas and combustibles are ejected out of the battery, leading to fire and explosion.

When a cylindrical 18650 LIB is fabricated, it can be thought of as a closed container containing electrolyte, electrodes, and so on. There is an initial pressure inside the battery as a closed container. Fig. 5 depicts a simplified diagram of the pressures during the relief valve crack, which is determined by the competition between the internal pressure and environmental pressure. So, the crack pressure is defined as:

$$P_{Crack} = P_{In} - P_{out} \quad (1)$$

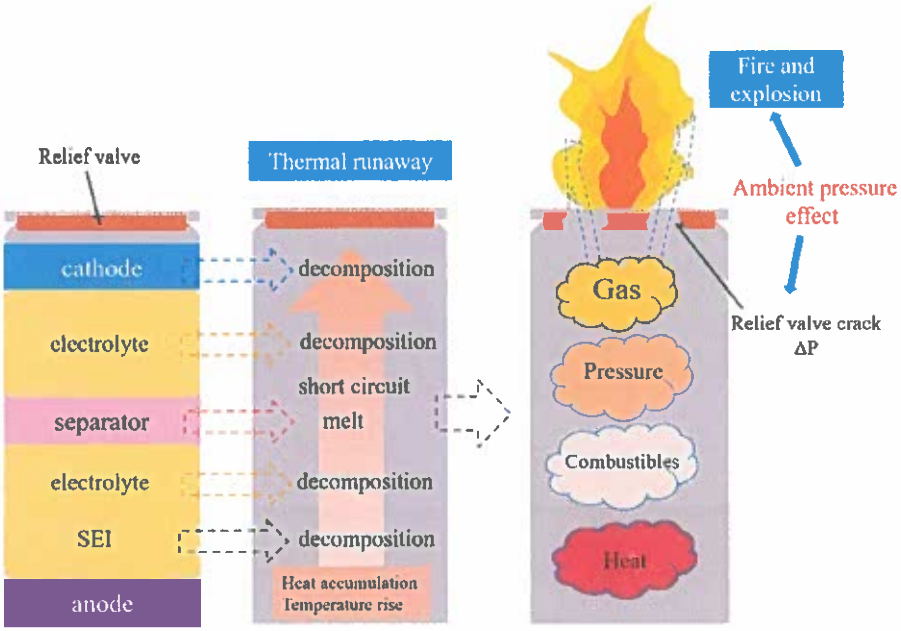

Fig. 4. Thermal runaway and fire process of LIBs.

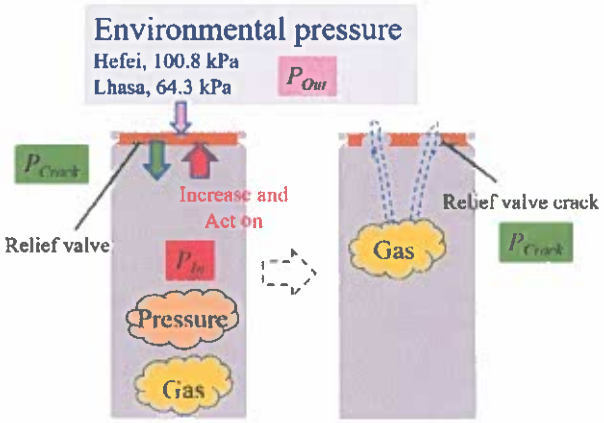

Fig. 5. Simplified diagram of the pressures.

where P_{Crack} is the relief valve crack pressure, P_{In} refers to the pressure inside the battery, which is a changing parameter during the thermal runway. The accumulation of the gases, combustibles and heat of thermal runaway reactions causes the internal pressure (P_{In}) to rise. P_{Out} refers to outside pressure, here is the environmental pressure. This value is a constant parameter at the same altitude, which is 100.8 kpa in Hefei and 64.3 kPa in Lhasa. The force of the internal generated gas to the relief valve is equal to the sum of the force of the external environment and the force that the relief valve can withstand. From the perspective of pressure, the crack of the LIB is due to the continuous accumulation of internal pressure (P_{In}) which exceeds the sum of the environmental pressure (P_{Out}) and the pressure relief valve cracks (P_{Crack}). In other words, the internal pressure overcomes the environmental pressure and relief valve structure.

On the other hand, P_{In} varies with the thermal runaway reaction rate and the temperature rise.

$$P_{In} \sim dTv \quad (2)$$

where T is the battery temperature, and v is the thermal runaway reaction rate. P_{Out} is the corresponding environmental pressure, and P_{Out} is 100.8 kPa in Hefei, and 64.3 kPa in Lhasa. The differential pressure is defined as the different relief valve crack pressure between the LIBs at two environmental pressures.

$$dP_{Crack} = P_{Crack\text{-}Hefei} - P_{Crack\text{-}Lhhasa} = (P_{In} - P_{out})_{Hefei} - (P_{In} - P_{out})_{Lhasa}$$
$$= P_{Out-Lhasa} - P_{Out-Hefei} = 64.3\,kPa - 100.8\,kPa = -36.5kPa \quad (3)$$

The difference in relief valve crack pressure has the effect on the combustion behavior of LIB. As can be seen from the difference in relief valve crack pressure, the pressure required for the LIB to crack in Lhasa is 36.5 kPa less than that in Hefei. It can be concluded that LIB will crack more easily and faster under low environmental pressures. The early occurrence of the crack leads to the advancement of the combustion behavior. Meanwhile, LIB requires a low thermal runaway crack temperature at low environmental pressures under the same heating conditions because of faster crack. It is necessary to pay more attention to the problem of LIB thermal runaway and cracking under the low environmental pressure, because it is easier to achieve.

On the other hand, the influence of environmental pressure on the combustion behavior of LIBs includes two aspects, one is the impact on the battery crack pressure, time and temperature, and the other is the effect on the combustion of ejected materials after crack. The combustions of gases and most ejected combustibles are significantly affected by the environmental pressure. Previous studies clearly confirmed that the fire developed more slowly as the environmental pressure decreases. Specifically, an empirical formula of burning rates ($\dot{m}''$) on environmental pressure (P) was summarized for common fuels, such as n-heptane, propane and cardboards, under low pressure.

$$\dot{m}'' \sim P^{\alpha} (\alpha \approx 1.3) \quad (4)$$

where α is an experimentally derived exponential power coefficient and has no physical meaning. The burning rate is proportional to the 1.3 power of the environmental pressure, which means that as the environmental pressure decreases, the burning rate slows.

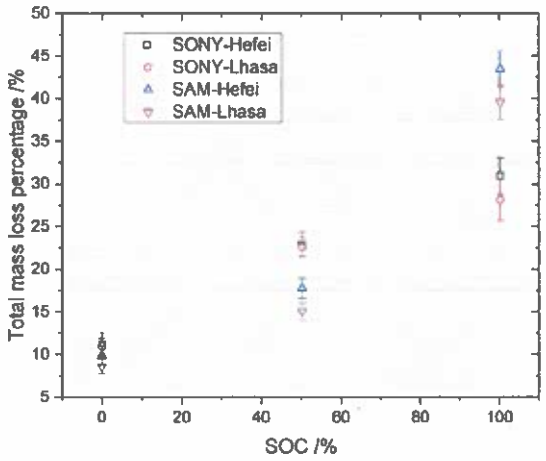

Fig. 6. Total mass loss data of $LiFePO_4$ and $LiCoO_2$ battery.

For the lithium battery fire, a reduction in environmental pressure means that the burning rate of the ejected gas and combustibles is reduced.

The total mass loss (TML) data is shown in Fig. 6. The experimental results are average values of three experiments, and the error bars are the upper and lower limits of fluctuation. It can be seen that the TML is obviously affected by the battery SOC. The battery with higher SOC has a larger TML. The difference in lithium ion distribution and content leads to such experimental results. The $LiFePO_4$ 18650 battery has the electrochemical reaction during charging and discharging (Wang et al., 2012):

$$LiFePO_4 + 6C \leftrightarrow Li_{1-x}FeO_4 + Li_xC_6 \quad (5)$$

Simlarly, the overall charging and discharging reaction equation of $LiCoO_2$ battery can be expressed as:

$$LiCoO_2 + 6C \leftrightarrow Li_{1-x}CoO_2 + Li_xC_6 \quad (6)$$

When a LIB is charged, lithium ions move from its cathode to its anode. x in Eqs. (5 and 6) represents the degree of charge and discharge, that is, the amount of lithium ions in the cathode and anode. Therefore, under normal use of LIBs, lithium ions are in an active and constantly migrating state. However, thermal runaway results in the formation of $LiCoO_2$ (stable species) and Co_3O_4 (another stable compound) with the subsequent release of oxygen. This process is the decomposition reactions of the cathode and visualized by the Eq. (7). Subsequently Co_3O_4 would decompose to CoO and release more oxygen at specific high temperatures (MacNeil and Dahn, 2001).

$$Li_xCoO_2 \rightarrow xLiCoO_2 + \frac{1-x}{3}Co_3O_4 + \frac{1-x}{3}O_2 \quad (7)$$

$$Co_3O_4 \rightarrow 3CoO + \frac{1}{2}O_2 \quad (8)$$

where x is the parameter related to SOC. The SOC directly affects the number of x in Eq. (7), which results in a difference in the amount of $LiCoO_2$, Co_3O_4 and oxygen formed. In the case where the SOC is high, the value of x decreases, and the amount of oxygen generated increases. In conclusion, during the process of thermal runaway, the decomposition reactions of the cathode occur, and the reaction degree is related to the SOC. For $LiFePO_4$ battery, the thermal decomposition reaction of cathode materials is (Feng et al., 2018):

$$2Li_0FePO_4 \rightarrow Fe_2P_2O_7 + \frac{1}{2}O_2 \quad (9)$$

Table 2
Initial mass and mass loss data of 100% SOC LIBs.

Brand	SOC	Combustible	Cathode	Location	Mass loss
SONY	100%	20%	26%	Hefei (100.8 kPa)	30.9%
				Lhasa (64.3 kPa)	28.1%
SAMSUNG	100%	14.8%	40.8%	Hefei (100.8 kPa)	43.5%
				Lhasa (64.3 kPa)	39.6%

It is noted that oxygen is generated from the decomposition reactions of the cathode. The electrolyte which is mainly consisted of carbonate organic solvents such as ethylene carbonate (EC), propylene carbonate (PC), dimethyl carbonate (DMC), diethyl carbonate (DEC), methy-ethyl carbonated (EMC), etc is more dangerous with the presence of oxygen (Feng et al., 2018).

$$Electrolyte + O_2 \rightarrow CO_2 + H_2O + Heat \quad (10)$$

As shown in these equations, the LIB with higher SOC can accumulate more energy inside the battery and the higher energy value converted into combustion. The LIBs with higher SOCs are more dangerous than the others. It can be seen from the mass loss percentage of the batteries in Fig. 6 that the mass loss of the larger SOC battery is significantly higher. In the thermal runaway and combustion process of LIBs, the mass loss mainly comes from two aspects, one is from the combustion of combustibles, and the other is the gas releasing caused by the decomposition of cathode materials. Table 2 shows the quantity of the cathode and combustibles and the mass loss percentage. The data for the combustible and cathode mass percentages is primarily obtained by measuring and calculating from the battery samples. Combustible materials mainly include electrolyte, separator and polymer packaging. The mass loss results in Table 2 do not distinguish well which part of the mass loss is due to the combustion of combustibles and which part is due to the decomposition of the cathode materials. However, some conclusions can be drawn from the comparison of the percentage of combustible and cathode mass and the mass loss percentages. $LiCoO_2$ battery has a lower percentage of combustibles than $LiFePO_4$ battery, while its cathode materials account for a higher percentage. The total mass loss percentages of $LiFePO_4$ battery are more than $LiCoO_2$ battery for 0% SOC and 50% SOC as shown in Fig. 6, because $LiFePO_4$ battery has more combustibles than $LiCoO_2$ battery. LIBs are mainly burned with combustibles under low SOCs. With the increase of SOC, the internal thermal runaway reaction of the battery is more intense. It produces more combustible gas and oxygen, and results in violent ejection or even explosion. For $LiFeO_4$ battery, the total mass loss percentage slightly increase with the SOC. However, a very sharp growth is obtained for 100% SOC $LiCoO_2$ battery. This results indicate that the 100% SOC $LiCoO_2$ battery have much higher ejection power than the low SOC ones and the $LiFeO_4$ battery. The mass loss caused by the decomposition of the cathode materials of 100% SOC $LiCoO_2$ battery is greater than that of $LiFePO_4$ battery. It can also be seen in Fig. 3 that the ejection strength of 100% SOC $LiCoO_2$ battery is much greater than 100% SOC $LiFePO_4$ battery. It is accompanied by non-combustible substances and molten metal during violent ejection for 100% SOC $LiCoO_2$ battery. It leads to the results that the total mass loss percentage of $LiFeO_4$ battery are less than $LiCoO_2$ battery at 100% SOC. This result is important for us to better understanding the process of gas generating and relief valve cracking of LIBs with different cathodes.

Assume an extreme case, that is, lithium ions are all transferred from its cathode to its anode. In this case, the amount of oxygen that can be released is the highest. All CoO_2 is converted into CoO and oxygen, and $FePO_4$ is all converted into $Fe_2P_2O_7$ and oxygen, which can be found from Eqs. (7–9). According to Tables 1 and 2, it can be estimated that the cathode quantity of the SONY battery is

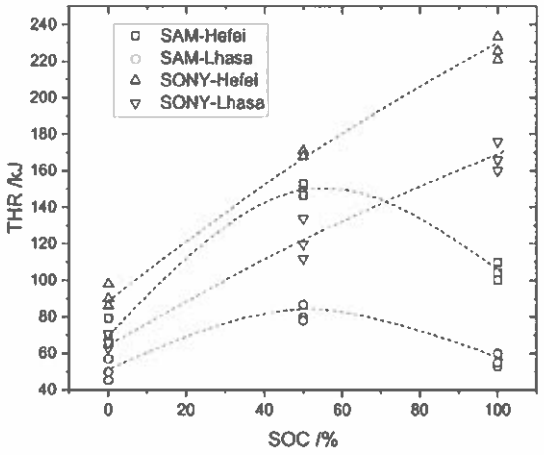

Fig. 7. Total heat release data of LIBs.

about 10.4 g, and the SAMSUNG battery is about 18.0 g. The mass of $FePO_4$ and CoO_2 is approximately 9.9 g and 16.7 g. In the extreme case where all of the $FePO_4$ and CoO_2 generate oxygen, the amount of oxygen generated is 0.52 g and 2.94 g for $LiFePO_4$ and $LiCoO_2$ battery, respectively. On the other hand, this calculation result is only a rough estimation process, and the actual amount of oxygen generated during the thermal runaway of the lithium battery needs further research. It can be concluded that the $LiFePO_4$ battery releases less oxygen than the $LiCoO_2$ battery. This means that the gas and internal pressure generated by the thermal runaway of the $LiFePO_4$ battery is smaller than that of the $LiCoO_2$ battery.

At the same time, there are little difference between TMLs of $LiFePO_4$ and $LiCoO_2$ batteries in Hefei (100.8 kPa) and Lhasa (64.3 kPa). Especially for 0% SOC and 50% SOC $LiFePO_4$ batteries, the TMLs are almost the same. The TML of 100% SOC $LiFePO_4$ battery in Hefei is slightly higher than that in Lhasa, with an average difference quantity of 1.1 g. That is to say, for lithium iron phosphate batteries under different environmental pressures, the amount of materials ejected by the battery during the combustion is not greatly affected by the pressure. The effect of environmental pressure on the mass loss of lithium cobalt oxide battery is slightly larger. The average difference in mass loss of 100% SOC battery between the two pressures is about 1.7 g.

The total heat release (THR) data of all test repetitions which is calculated by integrating the HRR curve in the battery fire is shown in Fig. 7. HRR is an important parameter in the combustion tests, but the LIB fire do have errors. Although all batteries were heated as evenly as possible, the thermal runaway and combustion process of them which involves a lot of reactions maybe a little different. Indeed, even with the same type, make and bundle configuration, variabilities have been observed in the flammability characteristics. There are also some errors in the experiment results because of the potential of battery explosion. These subtle differences are extremely complicated and this randomness determined the error leading to the uncertainty in the reported HRR integrals. So, the THR results in this paper were presented and discussed by average ones. The calculated average THR values are the average of three repeated experiments. Meanwhile, it can be seen that SOC has a significant effect on THR, which is similar with the TML data. The average THR values of $LiFePO_4$ batteries in Hefei (100.8 kPa) are 90 kJ, 171 kJ, and 225 kJ for 0%, 50%, and 100% SOC, and those in Lhasa (64.3 kPa) were 70 kJ, 133 kJ, and 168 kJ, respectively. The environmental pressure has a very significant effect on the THR of lithium iron phosphate battery. The battery with larger SOC is more obviously affected by the environmental pressure. This conclusion is also consistent with the results of TML. The THR results for $LiCoO_2$ batteries differ from $LiFePO_4$ batteries. The difference is that the THR of the 100% SOC $LiCoO_2$ battery is less than that of 50% SOC battery. The main reason for this result is that the ejection behavior of the $LiCoO_2$ battery at 100% SOC is more intense, and a large amount of combustibles are not effectively combusted, thus causing a decrease in the heat release rate. On the other hand, the effect of environmental pressure on the $LiCoO_2$ battery is the same as that of the $LiFePO_4$ battery, and the THR value of the battery at low pressure is smaller.

From the previous analysis, it can be concluded that the cathode materials, SOC and environmental pressure have great effects on the thermal failure and combustion behaviors of the LIBs. The most affected data is the heat of combustion. It can be analyzed from the unit growth rate which factor (environmental pressure or SOC) has a greater impact on the burning heat of LIBs. It can be seen from the heat of combustion data that the combustion heat of the $LiFePO_4$ battery in Hefei (100.8 kPa) increases by 135.1 kJ on average from 0% to 100% SOC, and it is 100.7 kJ in Lhasa (64.3 kPa). That is, for every 1% increase in SOC, the $LiFePO_4$ battery increases the heat by 1.35 kJ in Hefei and 1.01 kJ in Lhasa. The reduced pressure from Hefei to Lhasa is 36.5 kPa, so reduced unit combustion heats at low environmental pressure are 0.68, 1.32, and 1.63 kJ/kPa for 0%, 50%, and 100% SOC, respectively. The batteries at high environmental pressure have a greater unit growth rate of combustion heat for every 1% increase in SOC. At the same time, the burn heat of batteries with higher SOC increase or decrease quicker when the environmental pressure changes. For $LiCoO_2$ batteries, the effect of SOC on combustion heat is discussed without considering 100% SOC, and the average unit heat increase is calculated from 0% to 50% SOC. For every 1% increase in SOC, the $LiCoO_2$ battery increases the heat by 1.57 kJ in Hefei and 0.62 kJ in Lhasa. Then, the reduced combustion heats of unit pressure are 0.58, 1.89, and 1.34 kJ/kPa for 0%, 50%, and 100% SOC, respectively. The influence of environmental pressure and SOC on the heat of combustion is basically the same as that of $LiFePO_4$ battery.

At present, the classification and safety control of lithium battery fire hazards are still not perfect. The current consensus is that it is necessary to reduce the SOC of the LIBs when storage and transportation to ensure that it releases less combustion heat, and protect the safety of life and property. However, there is no specific quantitative grading of SOC and fire risk. Research on the fire hazard and hierarchical control of LIBs is extremely scarce and cannot meet the fire safety management requirements. Combined with the results of experimental research, it is recommended to have the classified discussion by detail the cathode materials, SOC and environmental conditions of LIBs when analyzing the hazard of thermal runaway and fire. For example, the fire risk of the warehouse or plant that stores LIBs is safely classified according to the basic conditions of SOC and environment. Formulate standards and procedures for the comprehensive use of LIB cathode materials, SOC and environmental pressure conditions.

4. Conclusion

In this study, an experimental study of LIBs thermal runaway and fire behaviors at two environmental pressures was presented. The detailed analysis of the burning processes, TML, and THR provides a comprehensive understanding of the complex fire hazard.

The SOC has effects on the TML and THR results of LIBs fire, and the LIB with larger SOC has greater TML and THR. At the same time, the environmental pressure has little impact on the mass loss. The maximum TML difference between two pressures is 1.1 g for 100% SOC $LiFePO_4$ battery and 1.7 g for 100% SOC $LiCoO_2$ battery. The environmental pressure has a significant impact on the combustion heat. The THR values of LIBs at 100.8 kPa is significantly

higher than that at 64.3 kPa. The unit growth rate in combustion heat between the two pressures increases with the SOC. The batteries at high environmental pressure also have a greater unit growth rate of combustion heat for every 1% increase in SOC.

LIBs are in a low-pressure environment for a long time in air transportation, so it is necessary and urgent to study the thermal failure and combustion behaviors of LIBs in this environments. The experimental results can provide a reference for the safety issues of LIBs used in low environmental pressure. It can provide data theoretical support for the safety research of air cargo LIBs.

Acknowledgement

This research was supported by the Programs of Senior Talent Foundation of Jiangsu University (17JDG036).

References

Bjerre, M., Eriksen, J.G.I., Andreasen, A., Stegelmann, C., Mandø, M., 2017. Analysis of pressure safety valves for fire protection on offshore oil and gas installations. Process Saf. Environ. Prot. 105, 60–68.

Chen, M., Dongxu, O., Cao, S., Liu, J., Wang, Z., Wang, J., 2019. Effects of heat treatment and SOC on fire behaviors of lithium-ion batteries pack. J. Therm. Analysis Calorim. 136 (6), 2429–2437.

Chen, M., Yuen, R., Wang, J., 2017a. An experimental study about the effect of arrangement on the fire behaviors of lithium-ion batteries. J. Therm. Anal. Calor 129 (1), 181–188.

Chen, M., Liu, J., He, Y., Yuen, R., Wang, J., 2017b. Study of the fire hazards of lithium-ion batteries at different pressures. Appl. Therm. Eng. 125, 1061–1074.

Chow, W.K., Han, S.S., 2011. Heat release rate calculation in oxygen consumption calorimetry. Appl. Therm. Eng. 31 (2–3), 304–310.

Feng, X., Ouyang, M., Liu, X., Lu, L., Xia, Y., He, X., 2018. Thermal runaway mechanism of lithium ion battery for electric vehicles: A review. Energy Storage Mater. 10, 246–267.

Fu, Y., Lu, S., Li, K., Liu, C., Cheng, X., Zhang, H., 2015. An experimental study on burning behaviors of 18650 lithium ion batteries using a cone calorimeter. J. Power Sources 273, 216–222.

Fu, Y., Lu, S., Shi, L., Cheng, X., Zhang, H., 2018. Ignition and combustion characteristics of lithium ion batteries under low atmospheric pressure. Energy 161, 38–45.

Giurcan, V., Mitu, M., Razus, D., Oancea, D., 2017. Pressure and temperature influence on propagation indices of n-butane–air gaseous mixtures. Process Saf. Environ. Prot. 111, 94–101.

Guo, L.S., Wang, Z.R., Wang, J.H., Luo, Q.K., Liu, J.J., 2017. Effects of the environmental temperature and heat dissipation condition on the thermal runaway of lithium ion batteries during the charge-discharge process. J. Loss Prev. Process. Ind 49, 953–960.

Huang, P., Wang, Q., Li, K., Ping, P., Sun, J., 2015. The combustion behavior of large scale lithium titanate battery. Sci. Rep. 5, 7788.

Huang, P., Ping, P., Li, K., Chen, H., Wang, Q., Wen, J., Sun, J., 2016. Experimental and modeling analysis of thermal runaway propagation over the large format energy storage battery module with Li4Ti5O12 anode. Appl. Energy 183, 659–673.

Jiang, F., Liu, K., Wang, Z., Tong, X., Guo, L., 2018. Theoretical analysis of lithium-ion battery failure characteristics under different states of charge. Fire Mater. 42 (6), 680–686.

Larsson, F., Bertilsson, S., Furlani, M., Albinsson, I., Mellander, B.E., 2018. Gas explosions and thermal runaways during external heating abuse of commercial lithium-ion graphite-$LiCoO_2$ cells at different levels of ageing. J. Power Sources 373, 220–231.

Larsson, F., Andersson, P., Blomqvist, P., Lorén, A., Mellander, B.E., 2014. Characteristics of lithium-ion batteries during fire tests. J. Power Sources 271, 414–420.

Larsson, F., Andersson, P., Blomqvist, P., Mellander, B.E., 2017. Toxic fluoride gas emissions from lithium-ion battery fires. Sci. Rep. 7 (1), 10018.

Lecocq, A., Eshetu, G.G., Grugeon, S., Martin, N., Laruelle, S., Marlair, G., 2016. Scenario-based prediction of Li-ion batteries fire-induced toxicity. J. Power Sources 316, 197–206.

Lee, C., Said, A.O., Stoliarov, S.I., 2019. Impact of State of charge and cell arrangement on thermal Runaway propagation in lithium ion Battery cell arrays. Transportation Res. Rec., 0361198119845654.

Li, J., Zhang, B., Liu, W., Tan, Z., 2011. Research on OREMS-based large-scale emergency evacuation using vehicles. Process Saf. Environ. Prot. 89 (5), 300–309.

Li, Y., Jiang, J., Zhang, Q., Yu, Y., Wang, Z., Liu, H., Shu, C.-M., 2019a. Static and dynamic flame model effects on thermal buckling: fixed-roof tanks adjacent to an ethanol pool-fire. Process Saf. Environ. Prot. 127, 23–35.

Li, H., Duan, Q., Zhao, C., Huang, Z., Wang, Q., 2019b. Experimental investigation on the thermal runaway and its propagation in the large format battery module with $Li(Ni_{1/3}Co_{1/3}Mn_{1/3})O_2$ as cathode. J Hazard. Mater. 375 (5), 241–254.

Lisbona, D., Snee, T., 2011. A review of hazards associated with primary lithium and lithium-ion batteries. Process. Saf. Environ. Protect. 89 (6), 434–442.

Liu, X., Wu, Z., Stoliarov, S.I., Denlinger, M., Masias, A., Snyder, K., 2016a. Heat release during thermally-induced failure of a lithium ion battery: impact of cathode composition. Fire Saf. J 85, 10–22.

Liu, J., He, Y., Zhou, Z., Yuen, R., Wang, J., 2016b. Investigation of enclosure effect of pressure chamber on the burning behavior of a hydrocarbon fuel. Appl. Therm. Eng. 101, 202–216.

Lv, D., Tan, W., Zhu, G., Liu, L., 2019. Gasoline fire extinguishing by 0.7 MPa water mist with multicomponent additives driven by CO2. Process Saf. Environ. Prot. 129, 168–175.

MacNeil, D.D., Dahn, J.R., 2001. The reaction of charged cathodes with nonaqueous solvents and electrolytes: I. Li0. 5CoO2. J. Electrochem. Soc. 148 (11), A1205–A1210.

Mao, B., Chen, H., Cui, Z., Wu, T., Wang, Q., 2018. Failure mechanism of the lithium ion battery during nail penetration. Int. J. Heat Mass Transfer 122, 1103–1115.

Ouyang, D., He, Y., Weng, J., Liu, J., Chen, M., Wang, J., 2019. Influence of low temperature conditions on lithium-ion batteries and the application of an insulation material. RSC Adv. 9 (16), 9053–9066.

Ouyang, D., Liu, J., Chen, M., Weng, J., Wang, J., 2018a. An experimental study on the thermal failure propagation in lithium-ion Battery pack. J. Electrochem. Soc. 165 (10), A2184–A2193.

Ouyang, D., He, Y., Chen, M., Liu, J., Wang, J., 2018b. Experimental study on the thermal behaviors of lithium-ion batteries under discharge and overcharge conditions. J. Therm. Anal. Calor 132 (1), 65–75.

Panchal, S., Dincer, I., Agelin-Chaab, M., Fraser, R., Fowler, M., 2016. Experimental and theoretical investigations of heat generation rates for a water cooled LiFePO 4 battery. Int. J. Heat. Mass. Transf. 101, 1093–1102.

Ping, P., Peng, R., Kong, D., Chen, G., Wen, J., 2018. Investigation on thermal management performance of PCM-fin structure for Li-ion battery module in high-temperature environment. Energy Convers. Manage. 176, 131–146.

Said, A.O., Lee, C., Liu, X., Wu, Z., Stoliarov, S.I., 2019. Simultaneous measurement of multiple thermal hazards associated with a failure of prismatic lithium ion battery. Proceedings of the Combustion Institute, 4173–4180, 37(3).

Said, A.O., Lee, C., Stoliarov, S.I., Marshall, A.W., 2019b. Comprehensive analysis of dynamics and hazards associated with cascading failure in 18650 lithium ion cell arrays. Appl. Energy 248, 415–428.

Scarponi, G.E., Landucci, G., Heymes, F., Cozzani, V., 2018. Experimental and numerical study of the behavior of LPG tanks exposed to wildland fires. Process Saf. Environ. Prot. 114, 251–270.

Shah, K., Chalise, D., Jain, A., 2016. Experimental and theoretical analysis of a method to predict thermal runaway in Li-ion cells. J. Power Sources 330, 167–174.

Tang, Y., Si, S., Zhong, X., 2019. Experimental investigation of the performance of an effective self-suctioning water mist generator for controlling underground coal fires. Process Saf. Environ. Prot. 126, 98–105.

Tao, C., He, Y., Li, Y., Wang, X., 2013. Effects of oblique air flow on burning rates of square ethanol pool fires. J. Hazard. Mater. 260, 552–562.

Wang, Q., Ping, P., Zhao, X., Chu, G., Sun, J., Chen, C., 2012. Thermal runaway caused fire and explosion of lithium ion battery. J. Power Sources 208, 210–224.

Wang, Q., Jiang, L., Yu, Y., Sun, J., 2018. Progress of enhancing the safety of lithium ion battery from the electrolyte aspect. Nano Energy.

Wang, Q., Huang, P., Ping, P., Du, Y., Li, K., Sun, J., 2017. Combustion behavior of lithium iron phosphate battery induced by external heat radiation. J Loss Prev. Process. Ind 49, 961–969.

Wang, Z., Ning, X., Zhu, K., Hu, J., Yang, H., Wang, J., 2019a. Evaluating the thermal failure risk of large-format lithium-ion batteries using a cone calorimeter. J. Fire Sci. 37 (1), 81–95.

Wang, Z., Tong, X., Liu, K., Shu, C.M., Jiang, F., Luo, Q., Wang, H., 2019b. Calculation methods of heat produced by a lithium-ion battery under charging-discharging condition. Fire Mater. 43 (2), 219–226.

Wu, H., Wu, D., Zhao, J., 2019. An intelligent fire detection approach through cameras based on computer vision methods. Process Saf. Environ. Prot. 127, 245–256.

Ye, X., Zhao, Y., Quan, Z., 2018. Thermal management system of lithium-ion battery module based on micro heat pipe array. Int. J. Energy Res. 42 (2), 648–655.

Yuan, C., Wang, Q., Wang, Y., Zhao, Y., 2019. Inhibition effect of different interstitial materials on thermal runaway propagation in the cylindrical lithium-ion battery module. Appl. Therm. Eng. 153, 39–50.

Zhao, R., Gu, J., Liu, J., 2018. Performance assessment of a passive core cooling design for cylindrical lithium-ion batteries. Int. J. Energy Res. 42 (8), 2728–2740.

Zhou, Z., Wei, Y., Li, H., Yuen, R., Jian, W., 2014. Experimental analysis of low air pressure influences on fire plumes. Int. J. Heat Mass Transfer 70, 578–585.

TOWN OF FARMINGTON PLANNING BOARD RESOLUTION
2022 MAJOR THOROUGHFARE OVERLAY DISTRICT (MTOD) AND MAIN STREET OVERLAY DISTRICT (MSOD) SITE DESIGN GUIDELINES
ADOPTED MAY 18, 2022

SEE MRB GROUP PROJECT #0610.12001 SHT #1 OF 12 REV. #5 DATED 8-1-17

WHEREAS, the Town of Farmington Planning Board (hereinafter referred to as Planning Board), in accordance with the provisions of Chapter 165, Section 100. D. (3) of the Farmington Town Code, has reviewed the above reference Action at its meeting on Wednesday, May 18, 2022.

NOW, THEREFORE, BE IT RESOLVED that the Planning Board does hereby accept the above referenced Site Design Guidelines for the calendar year 2022, as further provided for in Local Law #6 of 2009 and as contained herein.

RECEIVED TOWN CLERK'S OFFICE TOWN OF FARMINGTON MAY 16 AM 8:41

1. Adoption by the Planning Board

The creation of these Site Design Criteria is an implementation action identified in the adopted *Town of Farmington Comprehensive Plan*. The following site design guidelines have been established by the Farmington Town Board as part of Chapter 165, Section 100, of the Farmington Town Code and the powers provided to the Planning Board as set forth in Article 16, Sections 271 and 274-b, of the New York State Town Law. These guidelines shall remain in effect each year subject to Planning Board review and adoption as part of their annual organizational meeting, or at other times subject to formal Planning Board action. Certified copies of these Guidelines are on file in the Town Development Office and may be purchased from the Town Clerk's Office during normal business hours. A copy of these MTOD and MSOD Site Design Guidelines is available for viewing online at the Town's website www.townoffarmingtonny.com.

2. Authority

These guidelines are provided for in Local Law Number 6 of 2009, adopted by the Town Board on December 22, 2009, and Local Law Number 6 of 2021, and as updated thereafter annually by Planning Board resolution. When adopted by the Planning Board they establish standards for Site Plan approvals as provided for under the established Major Thoroughfare Overlay District (MTOD) and the Main Street Overlay District (MSOD) provisions of the Farmington Town Code. These guidelines pertain to all applications subject first to Site Plan approval by the Planning Board as provided for in Chapter 165 of the Town Code. The Planning Board reserves the right to modify, waive or request additional requirements of any application depending upon the scope, location or nature of development. It is hereby declared the Planning Board's intent to be consistent in applying the standards of these guidelines throughout the two overlay zoning districts cited where site plan approval is required.

3. Overall Site Design Objectives

The purpose of these Site Design Guidelines is to communicate to applicants the expectations that the Planning Board has for enhancing the appearance of development within the mapped MTOD

Major Thoroughfare Overlay District and MSOD Main Street Overlay District, in the Town of Farmington, through its site plan approval process by:

a. fostering attractive building and site designs with enduring aesthetic appeal;

b. fostering attractive, inviting, pedestrian-friendly designs that are likely to evoke a strong "sense of place;"

c. fostering designs that have continuity with the best design traditions and values of the community;

d. fostering designs which are likely to evoke feelings of pride in one's community;

DIRECTLY ADJACENT TO A 64 UNIT RESIDENTIAL COMMUNITY?

e. fostering the preservation and enhancement of significant views and characteristics of the natural landscape including topographic and water course features;

f. enhancing the use and pedestrian appeal of spaces around and between buildings for the enjoyment of the public;

g. promoting and enhancing the interconnection of on-site pedestrian walkways with off-site pedestrian access ways;

h. encouraging opportunities to allow pedestrian accessibility to areas with strong natural features such as wooded areas, wetlands and water courses, by the attainment of public rights-of-access, and

i. promoting multi-modal travel between adjacent sites.

4. Relationship to Surrounding Neighborhoods and Land Use

The design of buildings and sites should be undertaken by design professionals who are sensitive to the surrounding landscape, views and character of the community. Site and building designs are expected to have cohesive, appealing stand-alone design qualities as well as to have design scale and design continuity that allows them to complement and enhance the best design traditions of the community.

5. Architectural Design Characteristics

The Planning Board expects that building and site design professionals will be sensitive to the character of residential areas adjacent to a non-residential site that is seeking Site Plan approval under these guidelines. In addition, the Planning Board expects that building and site design professionals will be sensitive to the site improvements which will also be attractive and appropriate to the character of adjacent sites.

6. **Design Treatments.** The Planning Board and its consultants will review the scale and design character of proposed building and site designs, and require design treatments that are appealing to, and in scale with, pedestrian neighborhoods whenever possible. Such design treatments may include, but are not limited to, the following:

a. *Façades, roof forms and exterior walls.* Façades, roof lines and exterior walls should have three dimensional variations to provide interest and variety. In large buildings, suggested techniques include: organizing large building masses into a series of smaller masses; providing offsets in exterior walls; providing an accent form or forms, and providing a variation in roof lines or heights that are compatible with the design theme. The areas and patterns of glazing used in facades should be interesting and compatible with the three-dimensional design of the building.

Exterior walls above grade that are attached to buildings should appear to be integral to the building, i.e., walls attached to brick building surfaces should be brick. Other above grade screening walls, such as dumpster enclosures or transformer screen walls, should match materials and colors used in the building façade.

b. *Building entrances.* Building entrances should be interesting, attractive, obvious, in scale with the building façade and have a weather cover that is a permanent component of the building extending outward from and above the entrance and providing shelter from the elements. In no instance will a canvas canopy suffice for adequate covering of a building entrance. In addition, depending upon the orientation of the entrance on the site, additional design considerations shall be required so as to adequately protect persons entering and exiting the building. Individual tenants should have separate entrances.

c. *Screening of equipment.* Rooftop screening equipment shall appear to be integral with the building design. That is, parapet walls or sloped roof forms integral to the design of the building are preferred. Other equipment located at grade such as compactors, dumpsters, HVAC equipment, electrical transformers and switchgear located on site shall be totally screened from public view in a manner approved by the Planning Board. Screening materials and design should be attractive and compatible with the building design and overall landscape design.

d. *Color and material of primary building components.* The Planning Board has a preference for the use of brick and clear glass as primary façade materials. Alternative materials may be chosen if they are more appropriate to adjacent residential communities. Where other materials are being proposed, the Planning Board may ask that brick be incorporated as a major component. The use of reflective glass, split face concrete masonry units or metal siding is discouraged. Façade material colors should be selected to avoid being dreary and also to avoid being excessively bold.

e. *Character of exterior space.* Exterior space design is an integral component of good site design. Special attention should be taken in the design and coordination of landscape treatments of exterior spaces around and between buildings to allow them to be inviting and attractive to pedestrian users. Well-designed exterior spaces will soften the impact of a building on a site and help it appear to belong there. There should be an exterior design concept on each project and it should complement the building design. Opportunities to embellish pedestrian gathering spaces with compatible landscape accessories are encouraged. Landscape planting, pedestrian paving treatments and landscape accessories will be requested between the parking lot or driveway curb lines and primary building façades. Larger areas of pedestrian walkway pavements should be subdivided by aesthetically arranged control and expansion joint patterns. The Planning Board encourages the use of colored unit pavers for incorporation into the overall hardscape design layout to provide pattern and color variation to other more standard paving materials and to accent the location of landscape accessories such as tree grates, tree guards, planters, plant beds, trash containers and bicycle stands. For additional information, see Section 9 of these Guidelines.

f. *Building canopies and canopy lighting.* The Planning Board may allow back lighted canopies up to eight (8) feet wide and eight (8) feet in height over the entire main entrance area to a building. Lighting fixtures, lamps or lenses may not project below canopy soffits. Back lighting larger canopies is not recommended. The underside of building canopy heights shall not exceed fourteen (14) feet above grade or pedestrian/vehicular pavement surface below. Canopy colors, excluding signage graphics, should not be bright attention-getting colors. In no event shall a canvas awning be accepted as a suitable canopy covering for a building entrance under these guidelines.

g. *Gasoline pump canopies.* Canopies covering gasoline pump islands, which are free-standing or attached to buildings, should not be back lighted, except for any approved signage or logo. Any lighting of the area underneath the canopy that covers the gasoline pump islands shall be down ward oriented and fully shielded to reduce glare. Canopies covering gasoline pump islands should not exceed fourteen (14) feet in height above grade or pavement surface below.

h. *Prototype building designs.* Prototype building designs will be considered if they are consistent in design, material, color and detail with the design intent of these Guidelines. The Planning Board reserves the right to require design alterations to standard building designs that the Planning Board deems to be inconsistent with the general intent of these Site Design Guidelines.

7. Architectural (Building, Site and Landscape) Regulations

a. All development within the MTOD Major Thoroughfare Overlay District and the MSOD Main Street Overlay District that is subject to site plan review and approval shall meet the requirements contained within this Section and those contained elsewhere within Chapter 165, Section 100 of the Farmington Town Code. A separate landscape plan shall be submitted and approved, approved with conditions or denied as part of this review procedure.

b. The landscape plan shall be prepared by a licensed landscape architect.

c. An amended site plan shall not diminish the landscaping of the site below the requirements in this section.

8. Landscape Standards and Criteria

a. Required landscaped areas shall be designed as an integral part of the site development and shall be dispersed throughout the site.

b. Landscaping shall provide screening for adjacent land uses in accordance with the provisions within Section 9 below, with visual, noise and air quality factors considered.

c. Vegetation shall be compatible with soil conditions on the development site and the regional climate.

d. Existing and natural features and vegetation shall be preserved and incorporated in the landscaped area wherever possible.

e. The primary emphasis of the landscape treatment shall be on trees. Shrubbery, hedges, grass and other vegetation may be used to complement the use of trees but shall not be the sole contribution to the landscape treatment.

f. Plastic or other types of artificial plantings or vegetation shall not be permitted.

g. All large and small deciduous trees planted shall have a minimum caliper of two and one-half inches, measured six inches above the ground. All large deciduous trees planted in multi-stem form shall have a minimum height of 12 feet above the finished grade. All small deciduous trees planted in multi-stem form shall have a minimum height of 10 feet above the finished grade. All coniferous trees planted shall have a minimum height of five feet above the finished grade. All ornamental trees planted shall have a minimum caliper of one and three-quarters inches measured six inches above the ground. All ornamental trees planted in multi-stem form shall have a minimum height of eight feet above the finished grade. All shrubs planted shall have a minimum height of 24 inches above the ground except when

being used as a ground cover. All evergreen shrubs used for screening shall have a minimum height of 48 inches (4 feet) above the finished grade.

9. Required Landscaped Area Adjacent to Buildings

A landscaped area with a minimum average width of three feet shall be provided between each and every side of the proposed principal use building and any off-street parking or internal access road with the exception of building entrances/exits, drive-throughs and covered pedestrian walkways. A minimum of 50 percent of this landscaped area shall be planted with small trees, shrubs, perennials or combinations thereof. The balance of the landscaped area not planted with trees, shrubs or perennials shall be lawn or groundcover (see subsection [5] below).

Where the side or rear façade of a principal building or accessory structure faces a public or private street/right-of-way, the entire area of the required yard (with the exception of building entrances/exits and loading areas) between the street/right-of-way and the building shall be landscaped with a combination of evergreen and deciduous trees, shrubs and perennial plants sufficient to mitigate the visual impact of the building on the adjacent street/right-of-way as determined by the Planning Board or Director of Planning and Development, as applicable.

10. Interior Landscaped Area

a. Minimum interior landscaped areas shall be provided in accordance with the following table:

Parking Area	Minimum Interior Landscaped Area (Percent of Parking Area)
0–2,999 square feet	0%
3,000–7,500 square feet	5%*
7,501–43,560 square feet	5%
More than 43,500 square feet (one acre	10%

**For parking areas of 7,500 square feet or less, where the configuration of the site permits, yard area at least five feet wide in excess of the minimum required yard in the district shall be credited to the interior landscaped area requirement.*

b. An interior landscaped island shall be provided for every 15 spaces. Each island shall have a minimum width of eight feet inside the curb and a minimum length of 16 feet for a single row and 32 feet for a double row. Interior islands may be con-

solidated or intervals may be expanded in order to preserve existing trees or facilitate snow plowing if approved by the Planning Board or the Director of Planning and Development, as applicable.

c. All rows of spaces shall terminate in a landscaped island. Each island shall conform to the specifications described in (b) above. Terminal island intervals may be modified in order to preserve existing trees or facilitate snow plowing if approved by the Planning Board or Planning Director, as applicable.

d. Divider medians may be substituted for landscaped islands described in (b) above. Divider medians are landscaped areas located between rows of parking spaces, between parking spaces and driveways or between areas of parking. Divider medians shall have a minimum width of six feet.

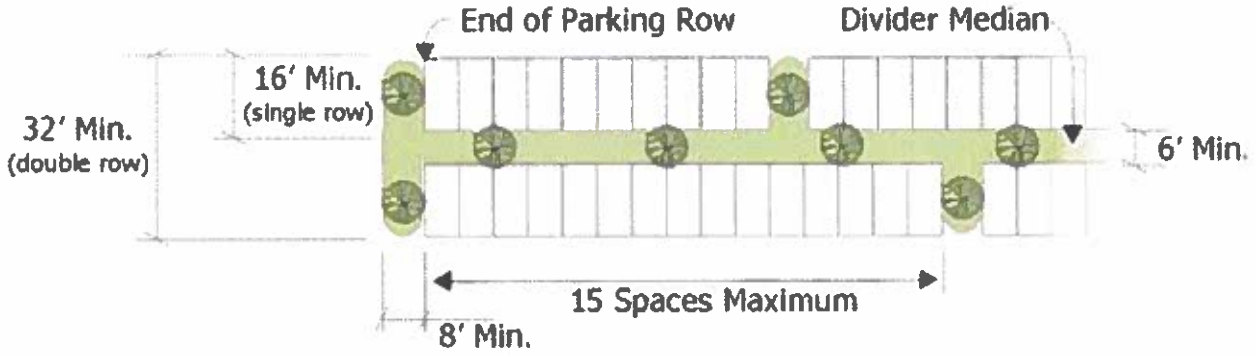

e. A minimum of one large deciduous tree shall be provided for each landscaped island that exceeds 128 square feet. One additional large deciduous shade tree shall be provided within landscaped islands for each 100 square feet in excess of 128 square feet. The Planning Board or Planning Director may, permit the substitution of smaller ornamental trees within landscaped islands. A minimum of 2 small ornamental trees shall be provided for each landscaped island that exceeds 128 square feet. One additional small ornamental tree shall be provided within landscaped islands for each 90 square feet in excess of 128 square feet.

f. A minimum of one large deciduous shade tree shall be planted for every 200 square feet of landscaped area within any divider median, planted individually or in groups separated by a maximum of 40 feet. The Planning Board or Planning Director may, permit the substitution of smaller ornamental trees within divider medians. A minimum of one small ornamental tree shall be provided for every 90 square feet of landscaped area within any divider median.

g. When divider medians and mid row islands have a width of 10 feet or greater, evergreen trees may be provided in addition to large deciduous trees. Evergreen trees should be spaced a maximum of 10 feet on center.

h. Parking Lot Pedestrian Medians required by the Planning Board shall have a minimum dimension of 16 feet and contain a concrete walkway with a minimum width of six feet. Planting areas with a minimum width of five feet shall be provided on both sides of the walkway. At each point the walkway crosses a parking lot or internal driveway, the walkway shall be clearly defined through a change in the texture, color or height of the paving materials.

i. In addition to trees, all landscaped islands and divider medians shall be landscaped with grass, groundcover, shrubs or other landscape material acceptable to the Planning Board or Director of Planning and Development.

j. All interior landscaped areas shall have a minimum planting soil depth of three feet and be free from all forms of construction debris and foreign material.

k. All islands and medians shall have six-inch-high concrete curbing as a minimum to protect plant materials from damage.

l. The dimensions of all islands and medians shall be measured from the landscaped side of the curb.

11. **Internal Site Landscaping Requirements—Off-Street Parking.** All site plans proposing off-street parking areas to be approved by the Planning Board, located upon properties within the mapped MTOD and MSOD zoning overlay districts, shall contain the following minimum landscaping requirements.

a. At least five percent (5%) of the off-street parking shall be devoted to internal landscaping.

b. The required internal landscaping shall be placed in appropriate planting areas within the delineated parking areas.

c. Any landscaped island in which trees are planted shall be at least six (6) feet in width.

d. All landscaped areas shall be protected from vehicular damage by the use of traditional curb, wheel stops, or other protective device approved by the Planning Board, which shall be placed to prevent any vehicle from protruding into the landscaped or lawn areas.

e. There shall be no more than 225 linear feet of parking between landscape islands.

f. Landscape Maintenance is required and shall be the responsibility of the property owner and or tenant(s), and all landscaping shall be maintained in a healthy condition. Plants damaged by insects, disease, vehicular traffic, acts of God, or vandalism shall be replaced within 30 days of being notified by the Code Enforcement Officer,

unless such notification is given between November 1st and April 1st. If the notification is given within this period, the material shall be replaced no later than May 31st of the following calendar year.

12. Preservation of Existing Trees

Efforts shall be made to preserve trees in a manner set forth below in this section.

a. An existing tree can qualify for credit in accordance with subsection c. of this section if it meets all the following criteria:

(i) The tree is healthy, free from disease, damage or active insect infestation which is potentially lethal to the tree; and

(ii) The tree is not a variety that has weak or brittle wood, or one which has excessive or noxious seed, pollen or fruit; and

(iii) The tree is expected to live for a minimum of ten (10) years; and

(iv) The tree is not seriously deformed or contorted; and

(v) The tree is preserved in accordance with subsection b. below.

b. A root protection zone shall be established around any tree which is identified on the landscape plan as a tree to be preserved. The root protection zone is identified by creating a circle around the tree, the size of which is determined by providing one foot of radius for every inch of diameter of the tree measured at breast height (DBH). The root protection zone shall be marked in the field with a physical barrier such as temporary fencing or other means which shall prevent construction activities from occurring within the tree root protection zone. Methods for preserving and protecting existing trees shall be included as part of the landscape plan.

c. Existing trees preserved in accordance with this Section will be credited towards the fulfillment of a portion of the requirements for tree planting contained in these regulations in accordance with the following schedule:

Size of Existing Tree that is Preserved

Deciduous Trees (DBH)	Evergreen Trees (height)	**Credits Toward Number** of Required New Trees
Less than 4 inches	Less than 5 feet	0.5
4 in. or more but less than 6 in.	5 ft. or more but less than 10 ft.	1
6 in. or more but less than 12 in.	10 ft. or more but less than 15 ft.	2
12 in. or more	15 ft. or more	3

d. The diameter of a single-stem tree that has a crotch between two feet and four and one-half feet above the ground shall be measured at the narrowest point between

the ground and the crotch. The size of multi-stem trees shall be determined by adding together the diameter of the three largest stems as measured four and one-half feet above ground level.

13. Buffers and Screening

a. The portion of the required front yard area which cannot be utilized for parking, loading, stacking or driveways shall be suitably landscaped and maintained by the owner in accordance with sub-section b. below.

b. Vehicle Use Areas (VUAs) located adjacent to a public street shall not be screened from the street with tree and shrub plantings, earthen berms, walls or a combination of these methods so as to establish an effective visual screen which is not less than 36 inches above the grade at the adjacent VUA within two years of installation. A minimum of one large deciduous tree, two small deciduous/ornamental trees or three evergreen trees or any combination of shall be planted within the required yard area for each 40 linear feet of lot frontage along a street.

c. Developments shall provide sufficient buffering and screening for the VUA. Buffering and screening may consist of trees and shrubs existing on the site prior to development. Supplemental plantings may be required in addition to the existing vegetation as determined by the Planning Board or the Director of Planning and Development in order to improve the screening of properties of the buffer. Buffering and screening may also consist of tree and shrub plantings, earthen berms, fences, walls or a combination of these methods so as to establish an effective visual screen. When fences or walls are utilized for screening, trees and other plant material (shrubs, vines, ground covers, perennials) shall also be used.

d. All fences provided or required shall have an attractive, finished appearance facing any public right-of-way or adjacent property.

e. Minimum impact of screening required. The following table and criteria shall be used to determine the level of screening between adjoining land uses. Single Family Residential Districts include RS-25, R-1-10, R-1-15, R-7.2, and R-2 Districts. Multifamily Residential Districts includes the RMF and IZ Districts.

Proposed Land Use	Existing Adjacent Zoning				
	SF Res	**MS Res**	**RB**	**NB/GB**	**LI/GI**
MF Res.	High	Medium	High	High	High
Office	High	High	Low*/ Medium^	Low*/ Medium^	Medium
Commercial	High	High	Medium	Low*/ Medium^	Low*/ Medium^
Industrial	High	High	Medium	Low*/ Medium^	Low*/ Medium^

Key: * = 0–3 acres. ^=3+ acres (proposed use)

f. High impact screening required. When the proposed development is considered to have a high impact on the existing zoning according to the table below, one of the following methods for buffering and screening shall be provided between the VUA and the nearest property line.

(i) Buffering and screening may consist of healthy trees and shrubs existing on the site prior to development providing that they form an immediately effective visual screen at least 36 inches above the grade at the adjacent VUA and that the existing trees and shrubs are thoroughly protect from damage during construction by establishing a work limit line on all site plan drawings. The work limit line shall be delineated in the field prior to site clearing in the vicinity of the required yard area. Supplemental plantings may be required in addition to the existing vegetation as determined by the Planning Board in order to improve the screening properties of the buffer.

(ii) Buffering and screening may consist of an earthen berm, masonry/stone wall or opaque wooden/vinyl fence with a minimum height of 36 inches above the grade at the adjacent VUA and one medium impact landscape screen evenly distributed within the required yard area.

g. Medium impact screening required. When the proposed development is considered to have a moderate impact upon the existing adjacent zoning one of the following methods for buffering and screening shall be provided between the VUA and the nearest property line.

(i) Buffering and screening may consist of healthy trees and shrubs existing on the site prior to development, providing that they form an immediately effective visual screen at least 36 inches above the grade at the adjacent VUA and that the existing trees and shrubs are thoroughly protected from damage during site construction by establishing a work limit line on all site plan drawings. The work limit line shall be delineated in the field prior to

site clearing in the vicinity of the required yard area. Supplemental plantings may be required in addition to the existing vegetation as determined by the Planning Board in order to improve the screening properties of the buffer.

(ii) Buffering and screening may consist of either: (1) one medium impact landscape screen evenly distributed throughout the required yard area; or (2) an earthen berm, masonry/stone wall or opaque wooden/vinyl fence with a minim height of 36 inches above the grade at the adjacent VUA and one low impact landscape screen evenly distributed throughout the required yard area (refer to Medium and Low Impact Screen Tables below).

Medium Impact Landscape Screen Options

Plant Type	Screen 1	Screen 2	Screen 3	Screen 4
Large Deciduous Trees	1/25 L.F.	1/40 L.F.	1/50 L.F.	1/50 L.F
Small Deciduous/ Ornamental Trees	0	0	1/60 L.F.	1/60 L.F
Evergreen (Coniferous)	0	1/40 L.F.	1/15 L.F.	1/20 L.F
Evergreen and Deciduous Shrubs	1/5 L.F.	1/5 L.F.	0	1/15 L.F

Screen One (1) shall be used only when yard area is less than 10 feet in width.

Trees and shrubs shall be provided based upon the number of linear feet per applicable site or rear yard.

Fractions of trees or shrubs shall be rounded to the nearest whole number.

h. Low impact screening required. When the proposed development is considered to have a low impact on the existing adjacent zoning one of the following methods for buffering and screening shall be provided within the required minimum rear and side yards for the VUA's (for yard dimensions, refer to the Dimensional Standards for each zoning district).

(i) Buffering and screening may consist of healthy trees and shrubs existing on the site prior to development, providing that they form an immediately effective visual screen at least 36 inches above the grade at the adjacent VUA and that the existing trees and shrubs are thoroughly protected from damage during construction by establishing a work limit line on all site plan drawings. The work limit line shall be delineated in the field prior to site clearing in the vicinity of the required yard area. Supplemental plantings may be required in addition to the existing vegetation as determined by the Planning Board in order to improve the screening properties of the buffer.

(ii) Buffering and screening may consist of one low impact landscape screen evenly distributed within the required yard are (refer to low impact screen tabled below).

Low Impact Landscape Screen Options

Plant Type	Screen 1	Screen 2	Screen 3	Screen 4
Large Deciduous Trees	1/40 L.F.	1/60 L.F.	1/80 L.F.	1/75 L.F
Small Deciduous/ Ornamental Trees	0	0	1/100 L.F.	1/75 L.F
Evergreen (Coniferous0 Trees	0	1/50 L.F.	1/25 L.F.	1/50 L.F
Evergreen and Deciduous Trees	1/10 L.F.	1/10 L.F.	0	1/20 L.F

Trees and shrubs shall be provided based upon the number of linear feet per applicable site or rear yard.

Fractions of trees or shrubs shall be rounded to the nearest whole number.

(iii) Screening adjacent to Residential Zoning requirements. When adjacent to the following districts: RS-25, R-1-10, R-1-15, R-7.2, RMF, IZ, RB, NB, GB, LI or GI and building or structure must provide the following landscape buffering and screening within the required side and/or rear yard(s):

(a) An earthen berm with a minimum height of three (3) feet (measured at the top of a 1:3 +/- grade) or an opaque wood or vinyl fence, stone or ornamental concrete masonry unit wall with a minimum height of 4 feet and the following plant materials: a minimum of one evergreen tree per each 10 linear feet of property line adjacent to one of the above listed residential districts, one small deciduous or ornamental tree per each 15 linear feet of property line adjacent to one of the above listed residential districts and one large deciduous tree per each 40 linear feet of property line adjacent to one of the above listed residential districts.

i. Screening of Mechanical Equipment required. Non-single-family residential properties which may be viewed from residential uses, public streets or public park areas shall screen all roof, ground and wall mounted mechanical equipment (utility structures, multiple meter boards, generators, air conditioning units, backflow preventer [RPZ], hot boxes, etc.) from view at ground level of the property line.

(a) All mechanical equipment shall be limited to that area shown on an approved site plan.

(b) Roof-mounted mechanical equipment shall be screened or arranged so as to not be visible from residential uses, public streets or park areas and be shielded from view on all four sides. Screening shall consist of materials consistent with the principal building materials, and may include metal screening or louvers which are painted to blend with the principal building.

(c) Wall or ground-mounted equipment screening shall be constructed of:

(i) Planting screens; or

(ii) Brick, stone, reinforced concrete, vinyl stockade or other similar material as approved by the Planning Board; or

(iii) Redwood, cedar, preservative pressure treated wood, or other similar materials; and

(iv) All fence posts shall be rust-protected metal, concrete-based masonry or concrete pillars, or an equivalent material as approved by the Planning Board.

(d) Mechanical equipment shall not be mounted on the roof or located in the front yard in a single-family residential district listed above herein.

14. Dumpsters and Other Refuse Containers. The following standards shall apply to dumpsters and other refuse collections areas in the RMF, RB, NB, GB, LI and GI Districts.

a. All dumpster areas shall be limited to that area shown on an approved site plan. Such area dumpsters and other refuse containers may be located between the front face of the building and the adjacent roadway only with the approval of the Planning Board.

b. Dumpster containers, other refuse containers, and all refuse shall be visually screened on all sides from adjacent properties and private or public rights of way with an opaque material, which may include shrubs, walls, fences or berms. Materials and dumpsters stored in said area shall not protrude above the screen.

c. Where vegetative material is used, said material shall form an opaque screen within two years from the time of first planting.

d. When dumpster enclosure gates are used to address (b) above, the gate shall consist of materials that visually conceal 100 percent of the contents of the enclosure. Gates shall remain in the closed position except when the dumpster is being loaded or unloaded or when access to the interior of the enclosure is needed for maintenance or other purposes.

e. The setbacks for dumpsters in nonresidential districts shall be five (5) feet from the property line of adjacent nonresidential districts and ten (10) feet from the property line of adjacent residential district.

15. **Parking Credits for Landscaping.** The Planning Board may reduce the minimum number of off-street parking spaces required in Chapter 165, Article V, Section 37 of the Farmington Town Code, by not more than 25 percent, provided that the land area so removed is not used to meet the landscape area required in this section and is used exclusively for landscaping in accordance with the standards and criteria of this section. If, at any time thereafter, the Zoning Enforcement Officer (ZEO) determines that the land area so removed is suitable for and is need to provide necessary off-street parking, the ZEO may order the installation of such parking. The issuance of any Certificate of Occupancy or Certificate of Compliance by the Town Code Enforcement Officer shall be deemed conditional upon the possible requirement for the future installation of the additional off-street parking, upon such order by the applicable site plan approval authority. Failure to comply with such order within the time fixed thereby shall constitute a violation of these regulations.

16. **Existing Development Parking Area.** Where an existing development, located within the MTOD or MSOD, that proposes an increase in the Parking Area of 3,000 or more square feet which requires site plan approval, the proposed site plan shall provide interior landscaped areas for the added Parking Area as required by the Planning Board. The proposed site plan shall also provide buffering and screening for the added Parking Area consistent with the standards contained herein.

17. **Building and Site Lighting.** Site and exterior building lighting should be similar in color of light. The Planning Board preference is for LED lamped site lighting (as opposed metal to halide or sodium vapor). Exterior building lighting should have a light color that is compatible with the LED light color. Pedestrian walkway lighting should be appropriate in style with the design character of the space and should not exceed fourteen (14) feet above surrounding grade. Parking lot light poles should not exceed thirty (30) feet mounted on a maximum three (3) foot base and should be located within landscaped islands or on lawn area wherever possible. All building mounted exterior light fixtures must be shown on building elevations and must be approved by the Planning Board for design location and fixture color. All building mounted lighting and site lighting shall be shielded from adjoining properties and public rights-of-way. Light cut-sheets and distribution patterns shall be submitted with all lighting plans.

Subtle landscape lighting shall not glare into vehicular or pedestrian circulation areas. Landscape lighting design components include, but are not limited to the following:

a. Exterior electrical outlets at building canopies and at tree bases that allow building managers to provide seasonal low wattage mini-lights is encouraged.

b. Subtle landscape lighting may include lighted bollards along walkways, surface-mounted exterior lighting to highlight or backlight plant materials and subsurface light fixtures that are recessed below finished grade. These should be located to highlight plants and portions of building walls.

c. Building façade lighting should be subtle in nature and could ideally be accomplished with upward directed landscape lighting that filters through, or backlights, landscape plantings onto building walls.

d. The use of bright colors, neon or similar materials, motion lighting, strobe lights and similar attention-getting lighting devices is strongly discouraged.

18. Site and Building Signage

Sign graphics and lighting should be designed to allow for clear communication but should otherwise not be over lighted. Signs with exterior illumination shall not glare into vehicular or pedestrian traffic areas. Internally illuminated signs should have the sign letters and logos highlighted with dimmer background lighting of the sign. This concept applies to all site and building signage, including traffic control signs. Sign site lighting should not glare to either on-site or off-site locations. The wattage of sign lighting should be submitted for Planning Board review as part of any Site Plan or Sign Site Plan application.

Larger signs that are allowed by Code which are attached directly to buildings should have separate letters with no box or cabinet background.

19. Site Design Characteristics

The natural characteristics (e.g., tree masses, streams, topography, etc.) of each site should be preserved and enhanced where possible.

The Planning Board encourages the incorporation of curved edges and surfaces where possible as accents in the layout of pedestrian walkways, planting beds, finish grade contours, ponds and drainage swales to achieve a more natural appearance. Drainage ponds and swales with straight edges should be avoided wherever possible.

Finish grading plans should incorporate soft, irregular, undulating, landscaped earth forms to enhance pavement and plant locations and to provide an appealing visual transition between parking areas and both streets and neighboring parcels.

Site amenities such as pedestrian walkways and landscape accessories should be included where space allows. This adds to the pedestrian friendly appeal of exterior spaces. See Section 10 for additional information.

The following is a checklist of landscape considerations and features that should be incorporated into the landscape designs for all site plans:

a. *Preservation of natural character.* Try to preserve all of the best natural resources of the site, such as trees, stream, rock out-cropping, natural topography, viewscapes and wetlands.

b. *Viewscapes.* Carefully study the site's good, as well as bad, views. Analyze preliminary site views for both positive and negative attributes.

1) Keep attractive views open and framed for greatest landscape value.

2) Screen out unattractive and objectionable views either by constructing structures or by an aesthetically unique landscape design.

3) The landscape design should have unity, harmony and fitness to use. There must be a harmonious landscape relationship with the vertical and horizontal lines of the buildings.

c. *Landscape lighting design standards.* The Planning Board recommends the use of landscape lighting to create soft night lighting of plants, where appropriate. Lighting designs should incorporate two or more of the following techniques based on available opportunities.

1) Down Lighting is the most natural and efficient form of lighting like sunlight or moonlight. The light sources are hidden and directed straight down through plant and tree material.

2) Up Lighting is achieved by placing the light fixture in the ground and directing it up through plant material. The internal structure of plants becomes dramatically lighted and large shadows can be produced.

3) Back Lighting is the soft wash lighting of a background such as a wall or a fence and is a very subtle form of lighting. The plant material is viewed in silhouette against the lighted backdrop.

4) Subminiature lamps on a flexible ribbon or tubular lighting may be appropriate for seasonal displays indoors or out.

5) Electrical outlets should be located at the base of designated trees and plants to allow the future use of seasonal lighting.

6) Bollards are available with internal illumination. The use of lighted bollards is optimal.

7) Flood Lighting on a residential or commercial level is soft, gentle flood lighting used as background lighting to create visual depth. Avoid using discharge mercury and sodium-vapor lighting used as security lighting. These lights should not cause glare.

8) Recreational Lighting for small court games (i.e., shuffle Planning Board, or putting greens, etc.) requires special study and selection. The light must be even and general, yet not in the eyes of the players. Large court games,

(i.e., volleyball, badminton, or tennis) may require specialized lighting design. These lights should not glare off site.

9) Landscape Lighting should be used as a feature of the landscape design to highlight designated design elements such as plants, walkways, walls, building façades or a combination thereof.

10) A combination of various lighting techniques such as down lighting, up lighting or back lighting to create a more interesting setting is suggested.

11) The source of light should be concealed to enhance the effect rather than the fixture itself.

12) Avoid over lighting that can produce glare and limit visibility.

13) Use LED lamps as a type of light source to avoid mixing light color on site.

14) Fixture colors should be coordinated with building colors. Typical colors available are solid brass, copper or bronze in color; black, white, natural non-corrosive plastic; redwood (clear, all heart, kiln dried); cast aluminum or satin aluminum and glass in combination with flexible ribbon lighting.

d. *Landscape plant forms.* Plants should be selected to be natural looking and graceful. Plants should be chosen to be as mature as possible to attain their desired shapes in relatively short periods of time. Each shape has its own place in landscape design. For example, deciduous shrubs are usually upright, round or spreading. Deciduous trees are round, weeping, oval, vaselike, erect or columnar, and pyramidal. Evergreens are columnar, narrow pyramidal, broad pyramidal, round, spreading or creeping. Different shapes provide variety and interest by accenting the major type with other forms. This is recommended to avoid monotonous repetition.

e. *Plant texture and color.* Color and texture are important qualities that should be considered along with the form of plants. The Planning Board expects that landscape architects will take special efforts to include the right balance of plant textures in the overall plant selection process. Texture is a plant feature that offers another chance to add variety and interest to a planting picture. Texture can be defined as the relation between foliage and twig size and the remainder of the plant. Close up, texture comes from the size, surface, and spacing of leaves and twigs at different seasons. At a distance, texture is the entire mass effect of plants and the quality of light and shadow. Patterns created by light and shade are an important part of texture. These patterns vary from season to season and even from hour to hour. The shadows cast by fine-textured plants are weak because of the spacing and size of the mass and because of light filtering through the foliage. The shadows cast by coarse-textured plants are strong because the foliage is large or dense and light is reflected from the surface. This play of light and shadows emphasizes the fineness

or coarseness of the texture of the plants. Landscape lighting is expected to highlight these features.

The Planning Board expects that the color of plants will be taken into account by the landscape architect to achieve the best overall design results.

The variety and location of landscaping should be appropriate for the environmental conditions, use, purpose and care that it will be subject to.

f. *Plant material and minimum sizes.* The following is a list of recommended plantings:

1) Evergreens (conifers and ornamentals)
Abies (fir)
Chamaecyparis (cypress)
Erica (health)
Juniperus (juniper)
Picea (spruce)
Pinus (pine)
Pseudotsuga (fir)
Taxus (yew)
Tsuga (hemlock)

2) Broadleaf Evergreens
Buxus (boxwood)
Calluna (heather)
Euonymus (euonymus ever)
Ilex (holly)
Pieris (andromeda)
Rhododendron (rhododendrun)
Rhododendrun (azalea)

3) Deciduous Trees (shade and ornamental flowering)
Acer (maple)
Amelanchier (shadbush-service berry)
Betula (birch)
Carpinus (hornbeam)
Cercis (redbud)
Cornus (dogwood)
Crataegus (hawthorn)
Fagus (beech)
Gleditisia (locust)
Magnolia (magnolia)
Malus (flowering crabapple)
Prunus (flowering–cherry)
Pyrus (flowering pear)

Tilis (linden)
Syringa (tree lilac)

4. Deciduous Shrubs
Aronia (choke cherry)
Clethra (summersweet)
Cornus (dogwood)
Cotoneaster (contoneaster)
Deutzia (deutzia)
Forsythia (forshythia)
Hamamelis (witch hazel)
Ilex (holly)
Philadelhpus (mock organe)
Spiraea (spirea)
Syringa (lilac)
Viburnum (viburnum)
Weigela (weigela)

5. Herbaceous Perennials including
Daylilies, Hostas, Sedum and Fern

6. Ornamental Grass, Sedges, Reeds
Calamagrostis (feather reed grass)
Festuca (dwarf clumping grass)
Miscanthus (large clumping grass)
Panicum (switch grass)
Pennisetum (fountain grass)

7. Ground Covers
Ajuga (Bugleweed)
Euonymus (wintercreeper)
Hedera (English ivy, Baltic ivy)
Lonicera (halls honeysuckle)
Pachysandra (pachysandra)
Vinca (myrtle)

The following is a list of minimum sizes for the recommended Plant groups at the time of planting:

Evergreen (conifer) 6' to 8'
Evergreen (ornamental) 24" to 48"
Broadleaf Evergreens 24" to 48"
Deciduous trees (shade) 3" caliper
Deciduous trees (ornamental flowering) 2" to 2½" caliper
Deciduous Schrubs 18" to 48" or 2–3 gal.
Herbaceous Perennials 1–3 gal.

Ornamental Grass 1–3 gal.
Ground Cover 2 year 2½" pot

All landscape plant material must meet the American Standard for Nursery Stock quality. All plant material must be No. 1 or heavy specimen quality grade.

All landscaping shall be installed and maintained to ensure growth. All landscaping materials shall be maintained free from disease, pests, weeds, and litter. The regular maintenance shall also include prompt replacement, where necessary, of any landscaping plantings that die, turn brown or defoliate. The replacement plantings shall be of the same size, species and quantity as shown on the approved plans. Substitutions shall be approved by the Town Planning Department and so noted on the approved drawings. A two-year maintenance bond or cash equivalent may be required to be posted with the Town if determined by the Code Enforcement Officer (CEO) to be appropriate.

The following trees/shrubs are considered undesirable in most applications. These plants have a tendency to become over-dominant, also are soft or brittle and tend to break during high winds or heavy snows.

Acer	Box Elder, Amur Maple, Silver Maple
Ailanthus	Tree of Heaven
Populus	White Poplar, Carolina Poplar, Lombardy Poplar
Salix	All willows
Prunus	Purple Leaf Plus
Elaeagnus	Russian Olive, Autumn Olive
Juniperus	Andorra Juniper, Hetzi Juniper
Thuya	All Arbor Vitaes
Juglans	All nut trees

Any changes to the approved landscape design, including variety and size of plants, must be made in writing to the Town CEO for change approval.

20. Applicant Submissions

Both conceptual site and conceptual building designs should be incorporated into the applicant's plans, beginning with the applicant's concept, or sketch plan, reviews submission. Subsequent submissions should include sufficient drawings, photos and text to clearly and thoroughly communicate the complete design intent of the project, to the satisfaction of the Planning Board. The applicant is encouraged to have a pre-planning submission conference with the CEO, the Director of Planning and Development and the landscape consultant. Submission information to the Planning Board shall include, but not be limited to the following:
Conceptual/sketch Plan:

a. All drawings should have a scale that is indicated on the drawing, along with the direction of north and each sheet should be numbered and dated.

b. The design character of the building(s) should be shown on the plan along with a three-dimensional concept sketch indicating anticipated size, shapes, materials and relationship to the site.

c. Generic landscape ideas and exterior space concepts should be included.

Preliminary Plan:

a. Provide building plans and elevation drawings to scale that are numbered and dated. Provide a first-floor plan.

b. All building elevations must be in color. All colors shown shall be the colors of the building to be constructed and identified by an objective manner, paint identification number or nomenclature, or similar material.

c. Three-dimensional representations of primary building façades should be included that include roof forms, method of screening visible building equipment, trash and loading areas. These drawings shall indicate color and material representations.

d. The Planning Board may request: a site profile incorporating a key building profile; an additional three-dimensional rendition or electronic 3-D walk-through; or even a mass model, if necessary to fully understand the three dimensional characteristics of proposed buildings.

Final Plan:

a. Provide final design drawings that include final design refinements that incorporate Planning Board comments from prior submissions. Provide colored elevations of all building elevations, screening, light fixtures, roof penetrations, HVAC grilles, building-mounted lights, signs and canopies. Clearly identify all materials and colors, including exterior soffit materials.

b. Provide colored exterior elevations of all sides of building and provide three-dimensional renditions, if requested by the Planning Board. Provide a first-floor plan and a roof plan. Provide elevations of exterior screen walls.

c. Provide a "hardscape" plan at least 1/8"–1' 0" in scale indicating: pedestrian paving materials; surface patterns; control and expansion joint locations; key dimensions and location of landscape accessories; and all site accessories. This plan shall include all dimensioning necessary for accurate layout of all paving including control and expansion joint locations.

d. Final grading plans and landscape planting plans shall be prepared and sealed by a Licensed Landscape Architect.

e. Provide a written list of all exterior building materials with samples of each material. A sample of glass will be required if anything other than clear glass is being proposed.

f. Provide catalog cuts with color selections of site lighting fixtures and landscape accessories including: fencing, tables, benches, trash containers, tree grates, tree guards, pedestrian walkway light fixtures, landscape lighting fixtures, bollards, fountains, clocks and bicycle racks, etc. Provide material and color samples of unit paving materials. Lighting fixture submittals shall indicate type of lamp and wattage per fixture.

g. Provide a signage package including drawings to scale of all site signage, including building-mounted signs, site signage including vehicular traffic control signs. This material shall clearly indicate the graphic layout, dimensions, colors, type of illumination, lamp wattage.

h. Provide finished grading plans and landscape plans. Finish grading and landscape plans shall be prepared and sealed by a NYS licensed landscape architect. Final landscape drawings shall include a plant schedule that clearly keys each plant type to the site. This schedule shall include the Latin name, common name, plant group, height, ball size, quantity and caliper required. See landscape section for additional requirements.

21. Terminology

For the purposes of these Guidelines, the following shall serve to clarify the meaning of special terminology included in this text:

a. *Earth Forms:* This term describes the three-dimensional character of subtle earth mounds or depressions which may be used to aesthetically enhance the locations of site plan features such as pedestrian walkways, pedestrian gathering areas, paved parking areas, locations of featured plant groupings, signage or landscape elements, among other things. Irregular earth forms are preferred. This term refers to visually soft, curvilinear earth shapes that undulate in both the vertical and horizontal planes. Earth forms where possible, should be interconnected into groups, the tops of which might vary from 12 inches to 30 inches and in special cases, higher or lower. The slope of grades used in defining earth forms could be gradual enough to allow for the mowing of sloped surfaces.

b. *Hardscape:* This term describes that portion of a finished landscape design which includes, but is not limited to, the dimensional layout of pedestrian

paving materials and patterns; the location of paving score lines and expansion joints; the location of landscape accessories including but not limited to bicycle racks, tables, benches, trash containers, tree grates, tree guards, bollards, trellises, gazebos and decorative walkway lighting; and the location of raised planters, curbed plant beds and decorative fountains. Hardscape elements are any of the above listed landscape accessories that are used to enhance the overall landscape design.

c. *Pedestrian Friendly:* This term describes the positive aesthetic character of exterior space design that is likely to be inviting, interesting and enjoyable to pedestrians. Design components that impact on the pedestrian friendly and pedestrian scale of spaces include: pedestrian paving materials and their colors, textures and patterns; plant material including seasonal variety and color; subtle earth forming; size and character of pedestrian signage; use of park-like landscape accessories such as plant beds, benches, tree grates, tree guards, bollards and decorative lighting, to mention a few. It is important to note that pedestrian scale spaces can and should be inviting to passing motorists as well.

d. *Sense of Place:* This term describes the ambiance of exterior spaces that are designed to have a personality that is inviting and attractive to pedestrians. Such spaces are best located between parking areas and building entrance façades, between buildings or between building wings.

BE IT FURTHER RESOLVED that the Planning Board does hereby adopt the above regulations as the official Site Design Guidelines for applications located within the mapped MTOD and MSOD zoning overlay districts, for the calendar year 2022.

BE IT FINALLY RESOLVED that a certified copy of these Guidelines is to be filed with the Town Clerk's Office, posted on the Town's website and distributed to members of the Planning Board, Town Development Staff, Town Engineer and made available to the general public upon request.

■ The above resolution was offered by MR. BELLIS and seconded by MR. DELUCIA at a meeting of the Town of Farmington Planning Board held on May 18, 2021. Following discussion thereon, the following vote was taken and recorded in the Official Minutes of the Planning Board.

Adrian Bellis	Aye
Timothy DeLucia	Aye
Edward Hemminger	Aye
Aaron Sweeney	Aye
Douglas Viets	Excused

Motion carried.

I, John M. Robortella, Clerk of the Planning Board, do hereby attest to the accuracy of the above resolution and to it being acted upon by the Planning Board at a meeting held on May 18, 2022.

_____ L.S.
John M. Robortella
Clerk of the Town of Farmington Planning Board

Chapter 165. Zoning

ZONE LI LIMITED INDUSTRIAL DISTRICT (SECT. 165-29)

Article VI. Special Permit Uses

PARAGRAPH "D" LINE 13 ALLOWS SOLAR SYSTEMS

§ 165-84.3.4. Criteria for accepting and approving application for site plan approval.

PARAGRAPH "E" LINE 1 "RB" ADDITIONAL PROVISIONS APPLY (LINE 5 - ALL UTILITIES SHALL BE PLACED UNDERGROUND.)

[Added 1-25-2022 by L.L. No. 2-2022]

No application for site plan approval for a large-scale ground-mounted solar photovoltaic (PV) system shall be deemed to be complete by the Planning Board until the following conditions are met:

A. Setbacks to nonresidential districts. Large-scale ground-mounted solar PV systems are subject to the minimum yard and setback requirements for the nonresidential zoning district (e.g., RB, NB, GB, LI and GI Districts) in which the system is located. No part of a large-scale ground-mounted solar PV system shall extend into the required yards and/or setbacks due to a tracking system or short-term or seasonal adjustment in the location, position or orientation of solar PV related equipment or parts.

~~40~~ B. Setback to residential districts. The location of large-scale ground-mounted solar PV collectors shall meet the setbacks specified below herein but shall not be less than 40 feet from any public highway right-of-way and/or utility easement; and said natural vegetation (e.g., landscaping) buffer shall be provided within this area in a manner to be effectively and exclusively used as a visual barrier between the solar system site and adjacent residential property(ies). The setbacks established herein are intended to provide space for planting a visual buffer of natural vegetation to be created between the large-scale ground-mounted PV solar site's security fence surrounding such a PV solar system and adjacent property lines where residential dwellings either exist or are permitted to exist. Plantings within this area are to be, at the time of installation, at a height to provide, as much as practicable, a visual screening of the large-scale ground-mounted PV system from adjacent residential properties. The species type, location, and planned height of such natural vegetation (landscaping) shall be subject to further approval by the Planning Board as part of the required site plan approval application. Such heights may be further subject to changing topography on the ground-mounted PV solar site from that of adjacent properties.

C. Large-scale ground-mounted solar PV systems located in a zoning district where residential dwellings are permitted. Such solar PV systems shall be set back an additional 120 feet from the minimum yard setback along all property lines that abut a lot or parcel of land located in the zoning district(s) permitting residential dwellings, unless said property contains soils classified as "prime" or "unique" (Soils Groups 1 through 4) and the land is being actively farmed or used for livestock. In this instance, the minimum setback shall be 40 feet from the property line. This additional setback dimension shall also apply to the front yard portion of the lot or parcel of land located on the opposite side of the street which is also located in a zoning district allowing residential dwellings.

ADDITIONAL 110'

D. Large-scale ground-mounted solar PV systems located in restricted business, commercial or industrial districts. Such solar PV systems shall be set back an additional 110 feet from the minimum yard setback along all property lines that abut a lot located in the A-80, RR-80 and other zoning districts permitting residential dwellings, or an IZ Incentive Zoning District. This additional setback dimension shall also apply to the front yard setback when the lot on the opposite side of the street is in a residential or an incentive zone district.

E. Large-scale ground-mounted solar PV systems located upon strategic farmland. Large-scale ground-mounted solar PV systems that are to be developed upon land identified on the Town of Farmington Active Farmland — Strategic Farmland Map, Map Number 8, of the adopted Town of Farmington Farmland Protection Plan shall be allowed on soils classified as Class 1 through 4, as documented upon the Soil Group Worksheets prepared by the Ontario County Soil and Water Conservation District and used by the Town of Farmington Assessor in calculation of the agricultural use exemption values, a part of the New York State Department of Agriculture and Markets Agricultural District Law, once it can be determined, by the Planning Board, that there is no feasible alternative location on the lot/parcel at issue to place the proposed solar system. Where there is no feasible alternative location on the lot/parcel at issue, then the solar system applicant shall provide an agricultural conservation easement (ACE) on another lot/parcel of land, containing Class 1 through 4 soils, which is shown on the above-referenced Map Number 8, and said acreage is to be in the total amount of acreage equal to the acreage of Class 1 through 4 soils that are proposed to be used as part of a proposed large-scale ground-mounted solar PV system. Said ACE shall be placed only upon land having Class 1 through 4 soils and fronting along a public highway and shall not be in some remote interior portion of a lot/parcel. Said ACE shall remain in effect for the same period associated with the time limit specified in the special use permit that is granted for a proposed large-scale ground-mounted solar PV system. Said ACE may be terminated once the subject solar PV system has been decommissioned, or upon a determination by the Town Board that said solar system is no longer operating under the terms of the original submission.

F. The following standards are to be implemented by the Planning Board as part of site plan approval for any large-scale ground-mounted solar PV system:

(1) Where large-scale ground-mounted solar PV systems are to be located on Class 1 through 4 soils, then the following shall apply to the construction, follow-up monitoring of a solar PV system during its useful life and restoration of these portions of the site in accordance with the latest Guidelines for Agricultural Mitigation for Solar Energy Projects promulgated by the New York State Department of Agriculture and Markets; and

(2) Requirement for an environmental monitor (EM). Depending upon the total acreage of the large-scale ground-mounted solar PV system, any system occupying 10 or more acres in total shall have an environmental monitor (EM) retained by the solar PV system operator(s) to oversee the construction, follow-up monitoring of the solar PV system, decommissioning of the system and restoration of the agricultural field(s) to their original state, to the extent practical. The EM is to be on site whenever construction, decommissioning or restoration work is occurring on the Class 1 through 4 soils; and his/her work is to be coordinated with staff at the Ontario County Soil and Water Conservation District, the New York State Department of Agriculture and Markets, and the Town Code Enforcement Officer and other Town officials. Said work is to be based upon a schedule for inspections during each of the above-referenced phases to assure the soils are being protected to the greatest extent possible.

(3) Solar PV system(s) located upon more than one lot. In the event a large-scale ground-mounted solar PV system is to be located upon more than one lot/parcel, then the total acreage involved as part of such system is to be based upon the overall acreage of the system and not its individual pieces of land.

(4) Requirement for an EM on more than one lot. Where a large-scale ground-mounted solar PV system is located upon more than one lot/parcel, then each lot/parcel may have its own EM. Where there is more than one EM associated with a large-scale ground-mounted solar PV system, then it shall be the responsibility of the system's operator to coordinate the duties and responsibilities of each EM with the state, county and Town officials referenced above in § **165-84.3.4F(2)**.

(5) Security fence. Each large-scale ground-mounted solar PV system site is to be completely enclosed by a security fence having a minimum number of gates and a height not to exceed eight feet above existing ground elevation. Said security fence shall also display the project's contact information sign and safety warning signs to be spaced around the perimeter of the site. Any security fence enclosure shall not unnecessarily interfere with or impede watering

systems associated with rotational grazing systems of an established agricultural operation. In addition, such security enclosure shall not create an excessive and unnecessary reduction in the amount of acreage remaining for farmland operations. Design details for the proposed fence are to be shown on the site plan drawings; and photographs showing the perimeter of the installed fence are to be filed in the Town Development Office. Public information signs and warning signs shall be provided on a security fence as further regulated in § **165-84.3.4l** below. The site plan drawings shall identify the locations, size and number(s) of such signage.

(6) Visual simulation site photos. Every application for a proposed large-scale ground-mounted solar PV system on the site shall include photo simulations of the proposed large-scale ground-mounted solar PV system with the site plan drawings.

(7) Visual simulation landscaping photos. Every application for a proposed large-scale ground-mounted solar PV system shall include a visual simulation of the proposed landscaping plantings, both at the time of installation and as expected to appear in year five of the system's operation. The landscaping area is to be shown surrounding the outside of the security fence for the proposed solar PV system and is to be included with the preliminary site plan drawings and shall be presented to the public early in the site plan application process. A detailed landscaping design and planting schedule are to be provided as part of any site plan application.

(8) Structures for overhead collection lines. Structures for overhead collection lines for a large-scale ground-mounted solar PV system are to be located upon the nonactive agricultural portions of the site and along field edges wherever possible.

(9) Access roads. There are hereby established three classes of access roads to be used for any large-scale ground-mounted solar project. They include the following: a) solar system site access road, which is the main point of access to the site extending from the pavement edge of the adjacent public highway. The solar system site access road is to be designed to the Town's industrial road specification and to have a minimum width of 24 feet and shall be paved for 100 feet from the edge of the travel lane of the adjacent public street; b) solar system's PV panel(s) access road(s), which are the access roads within the site that provide access to the solar panels for maintenance purposes. These are "hard surface" access roads and are to be located along the edge of agricultural fields and designed to meet the Town of Farmington's private drive specifications; c) solar system subsurface stabilized maintenance access roads, which involve the space between the solar panels and the perimeter of the solar site's security fence. This area is to be designed to meet the Town's subsurface stabilized maintenance access road specifications. These areas are mainly for emergency access purposes. To the extent practical, the solar system's PV panel(s) access roads and the solar system subsurface stabilized maintenance access roads are to be in areas next to hedgerows and on the nonagricultural portions of the solar PV system site.

(10) Access gates. There shall be a minimum of one access gate sized to accommodate maintenance equipment and/or emergency response equipment of local public safety agencies. Depending upon the length of each side of each of the sides of the security fence, the Town Fire Marshal shall have the authority to require more than one access gate to be provided for vehicles to and from the solar system's PV panel(s) where it is deemed to be in the interests of promoting public safety of first responders.

(11) Emergency personnel exit gates. One emergency personnel exit gate is to be provided along the security fence perimeter on all sides of the site to facilitate emergency egress from the enclosed area by system operators and first responders involved with extinguishing a solar panel fire or brush fire within the interior portion of a large-scale ground-mounted solar PV system site. Depending upon the length of each side of the security fence, the Town Fire Marshal shall have the authority to require more than one emergency access gate to be provided around the perimeter of the site where it is deemed to be in the interests of promoting public safety of first responders.

(12) Access road widths. The width of the large-scale ground-mounted solar system's PV panels access road is to be no wider than 20 feet to minimize the loss of agricultural lands and comply with the design standards of the State of New York Fire Access Code. The width of the solar system access road shall have a minimum width of 24 feet and shall be paved.

(13) Prohibition on cut and fill. There shall be no cut and fill of a large-scale ground-mounted solar PV system site for creating on-site access roads which would create on-site drainage problems. Any on-site access road, which is proposed to cross agricultural fields is instead to be located along ridge tops and follow existing field contours to the greatest extent possible. The locations of all on-site access roads are to be shown on the site plan drawings.

(14) Site drainage. All existing site drainage is to be maintained to the greatest extent practical. Any drainage structure(s) and/or erosion control measure(s) to be installed, such as diversions, ditches, and field drainage tile lines, shall take appropriate measures to maintain natural drainage flows and the effectiveness of such structures. Any existing drainage structure that is disturbed or damaged during site construction is to be repaired and the drainage structure is to be returned, as close as possible, to the original condition, unless such structures are to be eliminated based upon the site plan for the large-scale ground-mounted solar PV system.

(15) Access road profile. The profile of a large-scale ground-mounted solar PV system access road that is to be constructed through agricultural fields is to be level with the adjacent field surface wherever possible. The design for this site improvement is to be shown on the site plan drawings. No access road shall be permitted that alters existing drainage patterns on the site.

(16) Maintaining natural drainage patterns. Culverts and water bars are to be installed so as to maintain natural drainage patterns within the large-scale ground-mounted solar PV system area. The design for these site components is to be shown on the site plan drawings.

(17) Topsoil stripping and storage. All topsoil areas stripped for vehicle and equipment traffic, on-site parking and equipment laydown and storage areas are to remain on the site during the useful life of the large-scale ground-mounted solar PV system. The designated area(s) on the site to be used for topsoil stockpiling are to be shown on the site plan drawings. All topsoil stockpiles are to be stabilized and seeded in accordance with the Town's MS 4 Program requirements.

(18) Site excavation storage. All excavated materials (e.g., rock and/or subsoil) from on-site work areas (e.g., on-site parking area(s), electric cable trenches and site laydown areas, etc.) are to be stockpiled on site and separate from other excavated materials (e.g., topsoil). The design for these site components is to be shown on the site plan drawings.

(19) Maximum temporary workspace area width. A maximum width of 50 feet for any temporary workspace is to be provided along any open-cut electric cable trench for property topsoil segregation. All topsoil will be stockpiled immediately adjacent to the workspace area where stripped and shall be used for restoration on that portion of the solar PV system site as soon as practical after the installation of the electric cable.

(20) Electric interconnect cables and transmission lines. Electric interconnect cables and transmission lines are to be buried in agricultural fields wherever practical. All such buried lines are to be shown on the site plan drawings and the record drawings for said large-scale ground-mounted solar PV system.

(21) Electric interconnect cables and transmission lines. Electric interconnect cables and transmission lines that must be installed above ground shall be located outside agricultural field boundaries. When aboveground cables and transmission lines must cross agricultural fields, then taller support structures are to be used providing longer spanning distances and all such structures are to be located on the edges of the agricultural fields, to the greatest extent practical. Details for all such structures are to be shown on the site plan drawings.

(22) Buried electric cables and transmission lines. All buried electric cables and transmission lines buried in cropland, hay land and improved pasture shall have a minimum depth of 48 inches of

cover. At no time shall the depth of cover be less than 24 inches below the existing soil surface. The location(s) of all buried electric cables and transmission lines is to be shown on the site plan drawings.

(23) Intercept drain lines. The Ontario County Soil and Water Conservation District is to be consulted concerning the type of intercept drain lines whenever buried electric cable alters the natural stratification of soil horizons and natural soil drainage patterns. Their report shall be taken into consideration and design details shown on the site plan drawings.

(24) Pasturelands. Where a proposed large-scale ground-mounted solar PV system design affects existing and continued pasture areas, it is necessary to construct temporary or permanent fences around work areas to prevent livestock access which are to be based upon landowner written agreements. Said agreements are to be referenced on the site plan drawings and copies thereof filed with the Town's project file.

(25) Excess concrete. Excess concrete used in the construction of the large-scale ground-mounted solar PV system site shall not be buried or left on the surface in active agricultural areas of the project. Concrete trucks are to be washed, in documented washout areas, outside of active agricultural areas. A washout site is to be shown on the site plan drawings, along with notes that identify the reclamation of these areas.

(26) Materials disposal. All permits necessary for disposal of materials brought onto a large-scale ground-mounted solar PV system site, under local, state and/or federal laws and regulations, must be obtained by the contractor with the cooperation of the landowner. Copies of all such permits are to be noted on the site plan drawings and filed with the Town Development Office.

G. The following restoration requirements for all agricultural areas that are part of a large-scale ground-mounted solar PV system which are temporarily disturbed by construction or decommissioning shall:

(1) Be decompacted to a depth of 18 inches with a deep ripper or heavy-duty chisel plow. Soil compaction results should be no more than 250 pounds per square inch (PSI) as measured with a soil penetrometer. In areas where the topsoil was stripped, soil decompaction should be conducted prior to topsoil replacement. Following decompaction, remove all rocks that are four inches or greater in size from the surface of the subsoil prior to replacement of topsoil. Replace the topsoil to original depth and reestablish original contours where possible. Remove all rocks sized four inches and larger from the surface of the topsoil. Subsoil decompaction and topsoil replacement shall be avoided between October 1 of each year and May 1 of the following year.

(2) Regrade all access roads to allow for farm equipment crossing and farm animals and to restore original surface drainage patterns or other drainage pattern incorporated into the approved site design by the Planning Board.

(3) Seed all restored agricultural areas with the seed mix specified by the landowner to maintain consistency with the surrounding areas.

(4) All damaged subsurface or surface drainage structures are to be repaired to preconstruction conditions, unless said structures are to be removed as part of the site plan approval by the Planning Board. All surface or subsurface drainage problems resulting from construction of the solar energy project are to be corrected with the appropriate mitigation as determined by the EM, Soil and Water Conservation District and the landowner.

(5) Postpone any restoration practices until favorable (workable, relatively dry) topsoil/subsoil conditions exist. Restoration is not to be conducted while soils are in a wet or plastic state of consistency. Stockpiled topsoil shall not be regraded, and subsoil shall not be decompacted until plasticity, as determined by the Atterberg field test, is adequately reduced. No project restoration activities are to occur in agricultural fields between the months of October and the following May unless favorable soil moisture conditions exist.

(6) Following site restoration, remove all construction debris from the site.

(7) Following site restoration, at which point in time shall be agreed to by the landowner, the project sponsor is to provide a monitoring and remediation period of no less than two years from said agreed-to date to enable the revegetation of cover for the disturbed ground to make sure erosion is controlled. General conditions to be monitored include topsoil thickness, relative content of rock and large stones, trench settling, crop production, revegetation, drainage and repair of severed subsurface drain lines, fences, etc.

(8) Mitigate any topsoil deficiency and trench settling with imported topsoil that is consistent with the quality of topsoil on the affected site. All excess rocks and stones larger than four inches in diameter shall be removed from the site.

(9) All aboveground solar array structures are to be removed and all areas previously used for agricultural production are to be restored and accepted by the landowner, the Soil and Water Conservation District, and the State Department of Agriculture and Markets.

(10) All concrete piers, footers, or other supports are to be removed to a depth of 48 inches below the soil surface. Underground electric lines are to be abandoned in place. Access roads in agricultural areas are to be removed, unless otherwise specified by the landowner.

H. Utility connections. Utility lines and connections from a large-scale ground-mounted solar PV system shall be installed underground, unless otherwise determined by the Planning Board for reasons that may include poor soil conditions, topography of the site, and requirements of the utility provider. Electric inverters and transformers for utility interconnections may be above ground if required by the utility provider.

I. Fences. Notwithstanding the provisions found in § **165-61**, Fences, of this chapter, fences not exceeding eight feet in height, including open-weave chain-link fences and solid fences, shall be permitted for the purpose of screening or enclosing a large-scale ground-mounted solar PV system, regardless of the district in which the system is located, provided said system is classified as a principal use.

J. Barbed wire. Notwithstanding provisions for barbed wired found in § **165-61A** of this chapter, fences intended to enclose a large-scale ground-mounted solar PV system may contain barbed wire canted out.

K. Height. Large-scale ground-mounted solar PV systems may not exceed 12 feet in height, excepting weather monitoring equipment, which may extend to a height of 15 feet or such height as the Planning Board finds appropriate and not objectionable under the circumstances, and excepting utility poles and lines needed to transport solar energy to the utility grid and connection facilities of the local utility.

L. Minimum lot size. Large-scale ground-mounted solar PV systems shall adhere to the minimum lot size requirements for the zoning district in which the system is located, except that for residential districts the minimum lot size shall be one acre.

M. Lot coverage requirements. Large-scale ground-mounted solar PV systems shall adhere to the maximum lot coverage requirement for principal uses within the zoning district they are located. The lot coverage of a large-scale ground-mounted solar PV system shall be calculated based on the definition of "lot coverage" found in Article **II**, § 165- 10, of this chapter.

N. Signs. Large-scale ground-mounted solar PV systems classified as a principal use shall adhere to the sign requirements for the zoning district in which they are located. However, a project information sign and public warning signs shall be affixed to the project fence and the warning signs are to be spaced apart at intervals recommended by the Federal Energy Regulatory Commission (FERC) and shall be of the size recommended in said FERC regulations.

O. Location in front yard. Notwithstanding the requirements regulating location of accessory structures found elsewhere in this chapter, large-scale ground-mounted solar PV systems classified as an accessory use shall be prohibited in a front yard, including location in any front yard on a corner lot.

August 14, 2023

Fires at New York Battery Energy Storage System Facilities Ignite State Response

Farrell Fritz, P.C.

On July 28, 2023, in response to three separate fires at Battery Energy Storage System ("BESS") locations in New York, Governor Kathy Hochul announced the creation of an inter-agency fire safety working group.

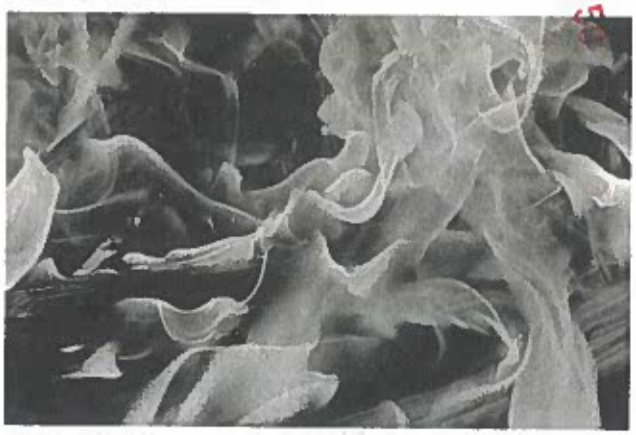

Max Kukurudziak, Unsplash

The Fire Safety Working Group, to be comprised of the Division of Homeland Security and Emergency Services Office of Fire Prevention and Control, New York State Energy Research and Development Authority (NYSERDA), New York State Department of Environmental Conservation, Department of Public Service, and the Department of State.

The Fire Safety Working Group will conduct a root cause and emergency response analysis to evaluate and identify the cause and effect of the battery storage fires. Beyond the cause of the fire, the focus will include evaluation of air monitoring results and other potential community impacts. In addition, on-site inspections of energy storage facilities will be organized to examine the condition of batteries and verify on-site fire suppression equipment and emergency-response plans at operational BESS facilities.

The recommendations developed by the Fire Safety Working Group will be shared with the New York City Fire Department, National Fire Protection Association, International Code Council, the New York State Fire Prevention and Building Code Council and Underwriters Laboratories.

The fires in question occurred between May 31st and July 27th in Suffolk, Orange and Jefferson counties and come at a time when battery storage siting and development is rapidly expanding on Long Island. Growth of these systems is attributable in part to energy storage being identified as a critical component in the 2019 Climate Leadership and Community Protection Act. The Act initially called for 3 GW of storage by 2030, a goal that ultimately increased to 6 GW of storage by 2030, enough to represent 20 percent of the peak electricity load of New York State. News of the fires triggered immediate scrutiny, including editorials calling for local boards to pause and revisit battery storage proposals and battery storage codes pending the results of the Fire Safety Working Group's investigation.

The model Battery Energy Storage System Law developed by NYSERDA, and adopted almost verbatim by several Towns, includes a number of fire-safety provisions, including development of fire safety compliance plans, emergency operations plans, compliance with fire-related building and electric codes, and specific access parameters for local fire departments. It will be interesting to follow the recommendations of the Fire Safety Working Group and how they impact local regulation of BESS facilities and the development of energy storage.

[View source.]

LATEST POSTS

- **My Relative Has Been Missing For Years. What Do I Need To Do To Have That Relative Declared Deceased?**
- **Termination, Adequate Alternative Remedies Sends Dissolution Proceeding Packing**
- **Stay in Your Lane! Delaware Court Invalidates Stockholder Agreement Provisions that Encroach on Board Authority**
- **Second Circuit Defines "Willfulness" Standard Under Anti-Kickback Statute**
- **AI Etiquette: A User's Manual Provided by the NYSBA**

See more »

WRITTEN BY:

Farrell Fritz, P.C.

Contact + Follow

PUBLISHED IN:

- Battery + Follow
- Energy Storage + Follow
- Fires + Follow
- Infrastructure + Follow
- New York + Follow
- Renewable Energy + Follow
- Safety Inspections + Follow
- Safety Standards + Follow
- State and Local Government + Follow
- Working Groups + Follow
- Energy & Utilities + Follow

FARRELL FRITZ, P.C. ON:

5. Once the Final Re-Subdivision Plat Map is signed the applicant has 62 days from the date of signing to file a mylar and two paper copies of the plat in the Office of the Ontario County Clerk.

6. Final Re-Subdivision Plat Approval is valid for a period of 180 days and shall automatically expire unless final signature has been affixed on the final plat.

BE IT FINALLY RESOLVED that the Planning Board directs the filing of a certified copy of this resolution with the project file and requests copies be provided to the Applicant and the Applicant's Surveyor.

The following vote on the above resolution was recorded in the meeting minutes:

Adrian Bellis	Aye
Timothy DeLucia	Aye
Edward Hemminger	Aye
Aaron Sweeney	Aye
Douglas Viets	Aye

Motion carried.

7. NEW SPECIAL USE PERMITS AND PRELIMINARY SITE PLANS

PB #0408-24 **New Preliminary Site Plan Application**

Name: Sky Solar Inc., 1129 Northern Boulevard, Suite 404, Manhasset, N.Y. 11030

Location: Northern Portion of Commercial Drive with the north end of the southern portion of Commercial Drive and located on Tax Map Accounts 029.07-1-057 and -058.

Zoning District: LI Limited Industrial

Request: An application for Preliminary Site Plan approval to allow for the construction of solar arrays and a transformer area on the eastern portion of the Sky Solar, Inc., Commercial Drive Solar Project; and the construction of a section of Town Road with sidewalks, crosswalks, streetlights, water line and fire hydrants completing the missing link between the south end and the northern portion of Commercial Drive with the north end of the southern portion of Commercial Drive and located on Tax Map Accounts 029.07-1-057 and -058 which contains a total of 7.75 acres of land.

• • •

PB #0409-24 **New Preliminary Site Plan Application**

Name: Sky Solar Inc., 1129 Northern Boulevard, Suite 404, Manhasset, N.Y. 11030

Location: Tax Map Account #29.00-1-84.112 with access from along East Corporate Drive and a future extension of Commercial Drive.

Zoning District: LI Limited Industrial

Request: An application for Preliminary Site Plan approval to allow for the construction of solar arrays, a transformer area and a stand-alone battery energy storage system to be located upon a portion of Tax Map Account #29.00-1-84.112 comprised of a total of 5.5 acres of land with access from along East Corporate Drive and a future extension of Commercial Drive.

• • •

PB #0406-24 **New Special Use Permit Application**

Name: Sky Solar Inc., 1129 Northern Boulevard, Suite 404, Manhasset, N.Y. 11030

Location: Tax Map Account #29.00-1-84.112 with access rom along East Corporate Drive and a future extension of commercial Drive.

Zoning District: LI Limited Industrial

Request: An application for a Special Use Permit to allow for the construction and operation of solar arrays, a transformer area and a stand-alone battery energy storage system upon a portion of Tax Map Account #29.00-1-84.112 comprised of a total of 5.5 acres of land with access from along East Corporate Drive and a future extension of Commercial Drive. This parcel is to be known as the western portion of the Sky Solar, Inc., Commercial Drive Solar Project and is located south of the American Lumber property which fronts along the south side of Collett Road and extends south to the north property line for Tax Map Account #29.00-1-84.113.

• • •

PB #0407-24 **New Special Use Permit Application**

Name: Sky Solar Inc., 1129 Northern Boulevard, Suite 404, Manhasset, N.Y. 11030

Location: Tax Map Account #29.00-1-84.112 with access from along East Corporate Drive and a future extension of Commercial Drive.

Zoning District: LI Limited Industrial

Request: An application for a Special Use Permit to allow for the construction and operation of solar arrays and a transformer area upon a portion of Tax Map Account #29.07-1-057. This parcel is known as the eastern portion of the Sky Solar, Inc., Commercial Drive Solar Project and is located south of A Safe Place Self-Storage property which fronts along the south side of Collett Road and extending south to the north property line for New Energy Works and the western properties of Tax Map Account #'s 29.07-4-055 through -070 and Account #'s 29.0-4-073 and -074 which are located along the west side of Redfield Drive.

The above four applications were reviewed by the Project Review Committee on September 7, 2023; November 2, 2023; December 7, 2023; January 4, 2024; February 1, 2024; and March 7, 2024.

On April 3, 2024, the Planning Board determined that the applications were complete, declared its intent to be designated as the Lead Agency for making the State Environmental Quality Review (SEQR) environmental declaration, and scheduled the Public Hearings to begin this evening (April 17, 2024).

The SEQR Involved Agencies are:

New York State Department of Environmental Conservation, Region 8
New York State Department of Health
Canandaigua–Farmington Water and Sewer District
Town of Farmington Highway Department

The SEQR Interested Agencies are:

Lance S. Brabant, CPESC, MRB Group, D.P.C., Town Engineers
Dan Delpriore, Farmington Code Enforcement Officer
Matthew Heilmann, Farmington Construction Inspector

Also on April 3, 2024, the Planning Board directed the Town staff to prepare the Project Notification Review Letter, related electronic documents and the SEQR Response Form for distribution to the Involved Agencies and the Interested Agencies. The SEQR Coordinated Review Period began on Wednesday, April 10, 2024, and will conclude at 12:00 p.m. on Friday, May 10, 2024.

Prior to the meeting, Ms. Lukasik provided the following information:

Dear Planning Board Members:

Sky Solar, LLC is proposing the construction of one (1) 0.5 MW-AC Community Solar Photovoltaic Array and an access road to be converted to Town of Farmington ownership after project completion on the lands of K&P Associates, Ltd. (tax parcels 29.07-1-57.00, and 29-07-1-58.000). Lands currently owned by K&P Associates, Ltd. to be purchased by Sky Solar, LLC upon successful completion of Town approval.

The project is located just south of the dead end of Denny Drive on the east side of the parcel. Per Town Code Chapter 165-65.3 Solar Photovoltaic (PV) Systems, Sky Solar, LLC is required to proceed through the site plan review and approval process along with receiving a Special Use Permit from the Town Board. We are requesting to appear before the Planning Board at the April 3, 2024, Town Planning Board meeting.

The subject properties are a combined 7.2 acres, currently zoned Limited Industrial (LI). Large-scale solar is a permitted use within the LI Zoning District. The project will utilize a leased area of approximately 4.29 acres within the subject property. The project is bordered by commercial and industrial properties to the north, south, and west and a housing development to the east.

The proposed solar array for the property includes the installation of approximately 57 racks of panels set on fixed tilt racking placed on the site to accommodate existing topography. Each rack will stand approximately ±16-feet 3-inches in height. The racking will be spaced at 27-foot 2.5-inch intervals on center, with a minimum width of 13-foot 7.25-inch aisles provided between rows. A 7-foot high chain link fence will surround the array for security purposes. The Commercial Drive Solar East Project meets all Town zoning code as it relates to large-scale solar energy systems.

The electricity produced by the array will be converted from DC power to AC power via central inverters located on equipment pads. The AC power will be collected and transformed to medium voltage power, which will then be sent out via grid distribution. The equipment pads will include switchboards, transformers, and DAS equipment.

Sky Solar, LLC is proposing that the array is utilized for Community Solar purposes. The Community Solar program will allow local residences and businesses to purchase power from the array at a discounted rate compared to the current electricity provider. Sky Solar, LLC is excited to pursue this project within the Town of Farmington and looks forward to providing an opportunity for clean, alternative energy to the Town and its residents.

We submit the following for your review and consideration:

0. Project Narrative (10 copies)
1. Preliminary Planning Board Application for Site Plan Approval (10 copies)
2. Preliminary Planning Board Application for Special Use Permit (10 copies)
3. Commercial Drive Solar Plan Set (10 24" x 36" copies)
4. Stormwater Pollution Prevention Plan (one (1) copy) ?
5. Full Environmental Assessment Form (10) copies)
6. Decommissioning Plan (10 copies)
7. Equipment Specification Sheets (10 copies)
8. Operations and Maintenance Manual (10 copies)
9. Construction Cost Estimate (10 copies)
10. Abstract of Title (10 copies)
11. RG&E Invoices (10 copies)
12. Copy of Application Fee Check (10 copies)

REVIEW ALL DOCUMENTS.

WHERE IS A LANDSCAPE PLAN? SEE MTOD GUIDELINES - PG. 5+23

—Emily Lukasik, EIT
Project Manager, LaBella Associates, Rochester, N.Y.

Mr. Hemminger opened the Public Hearings on these applications.

Mr. Ruffolo of Sky Solar Inc. of Manhasset, N.Y., and Ms. Lukasik of LaBella Associates of Rochester, N.Y., presented these applications.

The discussion on these applications was held concurrently.

Mr. Hemminger said that the board must first deal with the environmental record of these applications [as required by the State Environmental Quality Review Act] prior to considering the Preliminary Site Plan and Special Use Permit applications.

He requested that residents provide facts, figures and data as to how this project would affect the environmental record, the discussion of which will begin this evening.

Mr. Ruffolo and Ms. Lukasik presented a set of PowerPoint slides on the video screens in the meeting room and full-size drawings of the project area which included a brief history of the company and photographs of some of the company's other solar installations such as the Vermont Landfill Solar Project which is the largest landfill solar project in the State of Vermont. Mr. Ruffolo said that the company is working on eight solar projects which are now under construction in New York State.

Ms. Lukasik said that the Farmington project has been designed as one site, that it would be constructed on both sides of Commercial Drive, and that a new section of Town-dedicated roadway will be constructed to connect the current two dead-end sections of Commercial Drive. She said that the installation of utilities and the construction of a sidewalk to connect the neighborhood to Collett Road are all part of the project.

Ms. Lukasik said that each side of the site will provide ½ megawatt of electricity with a 5.0 megawatt battery storage facility on the west side.

Project data:

- Approximately 7.87 acres of development out of a total 13.2 acres.
- Approximately 1.15 acres of new impervious surfaces, connecting the two ends of Commercial Drive.
- Proposed as fixed tilt racking with racks spaced 13.61 feet apart.
- New section of Commercial Drive to be dedicated to the Town at completion of project.
- New Town water, overhead electric lines, fire hydrants, streetlights and sidewalk proposed along Commercial Drive.
- Two proposed equipment pads with inverters for solar.
- Two 20-foot-wide pervious access roads.
- One proposed equipment pad for battery storage.
- Majority of proposed stormwater treatment is through two bioretention basins and grass filter strips.
- Seven-foot-high chain link security fence.
- Nine new utility poles proposed within the parcel boundaries, and one off site.
- All underground wiring until the new utility poles.

With reference to the project drawing, Ms. Lukasik described the stormwater design. She said that the project will not increase any flows off the site and that stormwater treatment will be provided from two facilities on the property and by grass strips. Ms. Lukasik also said that the solar arrays would be located within a security fence.

Mr. Brand said that the State Environmental Quality Review (SEQR) coordinated review with the Involved and Interested Agencies began on April 10, 2024, and will end on May 10, 2024. He identified the Agencies by name (*see* the listing on p. 24, above). He said that the Planning Board is expected to be designated as the SEQR Lead Agency at the meeting on May 15, 2024, and subsequently will prepare Parts 2 and 3 of the Full Environmental Assessment Form, will review the environmental criteria in the SEQR regulations, will make findings, and ultimately will make the environmental determination of significance on this project.

Mr. Brand said the purpose of the meeting this evening this evening is to hear the residents' concerns about the project, and most importantly their environmental concerns associated with this.

Mr. Hemminger said that the environmental record is part of the New York State requirements and that we have to do it.

Mr. Delpriore said that the Town staff has spent time reviewing these applications and that the project is still under review. He said that the site has been challenging regarding stormwater and that the staff has worked with the applicant on the Municipal Separate Storm Sewer System (MS4) regulations. He said that this portion of the plan is still under engineering review as the applicant works to comply with the MS4 requirements.

Mr. Ford said that this project includes a road connection to join the northern and southern portions of Commercial Drive at the developer's expense. Mr. Hemminger said that the construction of the road is part of the applicant's plan for this project and is included in the Town's adopted *Comprehensive Plan* [*2021 Edition, Town of Farmington Comprehensive Plan*].

Mr. Brabant said that the Commercial Drive road connection also has been identified in the Town's Major Thoroughfare Overlay District (MTOD) and that any project which came before the Town in this location would have had this requirement to make the road connection between the north and south portions of Commercial Drive. He said that this requirement makes this project unique because most solar projects do not have to construct town roads and sidewalks.

Mr. Brabant also said that there is a fairly large substantial drainage plan which is being reviewed by the Town and by the New York State Department of Environmental Conservation (DEC). He said that this is also unique because most solar facilities would not have the substantial stormwater runoff as this project will have [because of the road and sidewalk construction]. Mr. Brabant said that the plans as received tend to meet the Town and DEC requirements but that he has not yet completed the engineering review and will provide comments upon the completion of the engineering review.

Mr. Brabant said that the applicant has submitted an Operations and Maintenance Plan which governs the operation of the site, such as day-to-day operations, and details such as when staff will visit the site, and how the site will be maintained, among other topics. He said that he is now reviewing the draft Operations and Maintenance Plan which the applicant has submitted for compliance with the Town standards.

He also said that a Decommissioning Plan is required for any solar project. Mr. Brabant said that this plan governs the removal of the solar equipment if the project falls through or if the site were to be abandoned and includes the steps and cost estimates for removal.

Mr. Hemminger said that the road will be curved so that stormwater will flow into the catch basins and into the internal drainage system to avoid having any runoff to the side land from the road itself. RUNOFF FROM THE ROADWAY EMBANKMENT DISCHARGES ONTO ADJOINING RESIDENTS LAND.

Mr. Hemminger said that a large solar facility is now operating on Yellow Mills Road. During that application, he said that the Planning Board and the Town staff went through all the issues including the Operations and Maintenance, and the Decommission plans. He said that the board and the staff are familiar with the process which is required for a solar project.

Mr. Hemminger also said that in his recent research on other solar projects he identified other documents such as a viewshed analysis and a glare analysis. He said that he requested that the applicant provide these types of documents for this project, and that the applicant has done so. ← WHERE ARE THESE? WHO REVIEWS?

Mr. Hemminger asked if anyone in the meeting room or on the remote video conference wished to comment or ask questions on this application.

Mr. Raymond (6010 Redfield Drive): Now we're very concerned about the woods that back up to the back of our lot, and we're about 180 yards down the road. [Are] there going to be any woods taken out of there? THERE WILL BE NO TREES REMAINING BEHIND RESIDENCES AT 6010 THROUGH 6028.

Mr. Hemminger: I believe the answer to that is very little, if any. Correct? No

Mr. Ruffolo: We have a plan—do we have it with us?—that shows some trees will be removed, but away from the residence, and there will be—is it a 75 feet—

ALL TREES REMOVED FOR A NEW RETENTION POND.

Mr. Hemminger: Very few trees, if any. And if you look at the viewshed documents they gave us, you can see that you won't be able to see through there.

Ms. Lukasik: The majority of the clearing—I don't know how familiar you guys are all with that site—there is an established woods and then there's more sort of like scrubby sort of marsh area—that's where the majority of the clearing is that's going to take place.

Mr. Raymond: Is that where the road is going to be?

Ms. Lukasik: Yes, the road runs through that section, as well.

Mr. Hemminger: But very little, if any, of the trees said that back to the houses will be removed, if any. ?

[Discussion about slides on the screen.]

Mr. Hemminger: You can see there how much is still going to remain.

Mr. Bellis: The tree line there—

Ms. Lukasik: Yes, that's just under a hundred feet.

Mr. Ruffolo and Ms. Lukasik then reviewed the locations of the woods, the proposed solar panels, their property line, and Redfield Drive on the drawing which was displayed on the video screen.

Mr. Raymond asked about the location of Redfield Drive on the drawing. Mr. Ruffolo and Ms. Lukasik said that the gray area on the drawing represents Redfield Drive.

A resident asked which way was north on the drawing. There was a brief discussion regarding the delineations on the drawing of the locations of the woods, homes, and proposed roads.

Ms. McConnell (6012 Redfield Drive): I don't know much about solar, I mean, as far as I've seen solar equipment out, things like that. Talk about transformers—is there noise? Is there like a generator—some people have generators and they spark up, you know, for five minutes—

Mr. Ruffolo: There is a transformer on site. It is not a generator so you will not hear an engine-type noise. You would hear a hum. It would be similar to any transformer that's already servicing commercial properties. From a residence, I don't believe you'll hear anything. It's a hum, it's a humming sound. It's not an engine. There's no—one of the beauties of solar—

Ms. McConnell: Do they run 24/7 or do they come on—

Mr. Hemminger: When the sun's out—

Ms. McConnell: When the sun's out. Okay.

Mr. Hemminger: Can't pick up solar at nighttime.

Ms. McConnell: Right, okay, so that's when you'll hear that humming?

Ms. Lukasik: You wouldn't hear it unless you were very close. This question's come up at a lot of my meetings lately so I did the deep dive—what decibels mean—and the sound

associated with the transformer equate—and this is if you're basically next to it—is roughly the same as a light rainstorm or a refrigerator sound. That's the sound that it makes.

Mr. Hemminger: So if you're walking down the street you might hear it a little, maybe, on a good day with the wind blowing the right way, but you're not going to hear it most of the time.

Ms. Lukasik: It's similar to the equipment you would see on a residential street—the type of equipment that's on poles. It's not substation type equipment.

Ms. McConnell: Okay.

Mr. Bellis: I think you're going to hear the Thruway more than this. You can hear the Thruway from my house.

Ms. McConnell: It's operated by something. I was just wondering—

Mr. Brabant: As part of the process one of the items to be requested is a noise study, which is typical to any application such as this, and that would have very similar data as to what you're hearing. He said that the applicant will be able to provide some documentation that justifies what you are hearing.

Ms. McConnell: The only other question I had—you mentioned something about water and drainage, or something. We do have water in our area over there. So, and some people have had issues with water.

Mr. Hemminger: This will not create any additional water issues and in fact it probably will help with any existing water issues

Ms. McConnell: Because of . . .

Mr. Hemminger: Because of the way it is going to be engineered.

Ms. McConnell: OK, so, do you built it, I mean, do you make it, where the water is, do you make it deeper so that it doesn't . . .

Mr. Hemminger: We will have this discussion when we get to the site plan, there's no doubt.

Mr. Hemminger then asked Mr. Brabant to comment on the stormwater plan.

Mr. Brabant: The applicant's engineering firm has designed the plan to put the water obviously in its lowest spot where natural flow is going to bring it on their site. As part of that, they are not allowed to discharge directly off site. Anything that they are constructing has to be retained on their site and then collected and treated before it runs off their site, and that has to be done in a manner that doesn't increase runoff from their site. It cannot

be greater or substantially changing from what currently exists today. So, the improvements that are there have a runoff but it has to be collected on their site, treated on their site, before it ultimately discharges from their site. He said that there are rules and regulations that they have to design to, and they have to meet.

Mr. Hemminger: So the end result should be the same or better water flow.

Mr. Weilert (6000 Redfield Drive): So that fence you're going to put in, around, tell me about the fence, made of what, how high?

Mr. Hemminger: Pretty early to discuss, but we will go ahead and let you guys do that. Again, we're talking about the environmental record here, but we'll go ahead and do a quick overview on the fence. Emily.

Ms. Lukasik: This will be a seven-foot-tall chain link fence for security and safety to keep people away from the panels.

Mr. Hemminger: It's a security fence, basically. Because there's so many trees there to block it, it's not for aesthetic reasons. It's for security reasons for their purpose.

Mr. Finn (6020 Redfield Drive): We actually live in the third building down coming from 96. It looks like the road is right close to our building. How far is that away and will those trees be removed?

Mr. Hemminger: Again, we're talking about site plan issues, but we'll go ahead, Emily, give him a quick overview. I'm not going to get too much into the weeds on this.

Ms. Lukasik: Part of the back and forth we've been doing with the Town to get everything situated—this is sort of set up like a flag lot, so there is a very narrow space through here [reference to the drawing] to get down to Commercial Drive, so this has to go right here, to get up here and go through the site, so the trees where the roads are will be removed. After our last discussion [with the Town], we're going to actually look and see to keep more than we're already planning on that side of the site, but where the road is going, we have to clear it to build the road.

Mr. Hemminger: That's the only spot they have on their property to build the road.

Mr. Finn: Unless you go in the other way.

Mr. Hemminger: Can't go in the other land. They don't own it.

Mr. Finn: Alright. And how far away would that be from our backyard, because . . .

Mr. Hemminger: It will be no closer than your back property line. I mean, it's going to be on their property. They're going to have all the proper distances and easements, and all the

other things so they can put water, sewer, or whatever down through there, but it's going to be on their property, not on yours.

Mr. Finn: I understand, but is there a buffer between my property . . .

Mr. Hemminger: Probably not. There won't be any buffer at all through there, I doubt.

Mr. Finn: So my house is going to have a road in the front of it, and in the back of it.

Mr. Hemminger: Correct. Same way, again, remember, this road has been planned for 20/30 years. The developer certainly knew about it and certainly any of you that wanted to look could have seen this exact situation happening because that road's been planned—I've been doing this for almost 30 years and it's been planned for as long as I can remember.

Mr. Finn: I know this is not part of the environmental [review]. Why is this road necessary now with the solar farm going in on that property?

Mr. Hemminger: This is to connect that road up. Commercial Drive has been planned that way—forever.

Mr. Finn: I understand that, but now that you know what's there, why is this road now necessary? Is it part of the master plan?

Mr. Hemminger: It's part of the Town's master plan to get traffic through there and get it over to the other side. I'm not going to debate that. It's part of the *Comprehensive Plan* and it's been discussed numerous times for the requirement to add it.

Mr. Finn: When does that come up in the process?

Mr. Hemminger: What does what? It's part of the site plan.

Mr. Finn: . . . to argue the road?

Mr. Hemminger: You can argue the road any time, but the road is going to be part of the discussion on the site plan, when we get to the site plan.

Mr. Finn: Okay, I understand, this is the environmental piece.

Mr. Hemminger: This is the environmental piece. The subdivision happens next. The preliminary site plan is open, so once we're done with the environmental record, we'll begin to discuss the site plan.

Mr. Finn: And is the last discussion on the road?

Mr. Brand: No.

Mr. Hemminger: No, it's never the last discussion of anything until we close the Public Hearing.

Mr. Finn: I'm trying to understand the process.

Mr. Hemminger: I understand. Until we close the Public Hearing it's never the last discussion on anything. You can talk about the road any time you want. Just understand that the road is in there as part of the *Comprehensive Plan* which has been approved by the Town Board, and as well as the MTOD [Major Throughfare Overlay District], which again has been approved by the Town Board.

Mr. Hemminger: The Town Board probably is more of a group to discuss the road with than the Planning Board because we know that it's what the Town Board and the residents want, is to put that in there. We just try to make the project as good as we can given what we have, and there's almost no property there to put that road on, other than what they have there. REALLY?

Ms. deForet (6028 Redfield Drive): So, my backyard is 46 feet, so the road is going to be, like, right there. My environmental questions—three—and thank you for covering the drainage. Number 1: Our houses built by New York standards are air tight. We've got one intake. Trucks going across that road are going to be emitting both organic compounds and particulates. How am I going to know that that's not coming into my house?

Mr. Delpriore: All those houses in that subdivision are built [with devices] with filters which clean those particulates as they come in.

Ms. deForet: The filters down by our heater, the filters I change out?

Mr. Delpriore: No. You should have a box in the basement that has a filter in it that actually takes in outdoor air . . .

Ms. deForet: That's the filter that I change . . .

Mr. Delpriore: Not the one on your furnace . . . [Several people speaking; inaudible.]

Ms. deForet: Okay, alright, but I would also want to know that the air I'm breathing is clean if I ever should choose to open my window or go in my backyard. I only own 46 feet of it, but I do own 46 feet of it, okay.

Ms. deForet: Here's another environmental question. When DC current is converted to AC current, a pitch results. It is not just a noise like a refrigerator. It is a pitch. Some people—and unfortunately I am one of them—have unusual hearing. I would like to know where I can go to hear [this sound], because whoever is doing the environmental study—99.999 percent of the chance is that their hearing is not as good as mine. Okay, so. I'm just saying you say it's that quiet, tell me where I can go?

Mr. Hemminger: Dan, can we get her to go out to our solar project, just built.

Mr. Hemminger (to Ms. deForet): If you work with staff to go out to the project we just built, and I assume they're similar transformers, I mean, a transformer's a transformer.

Ms. Lukasik: They didn't have a substation as part of that project, right?

Mr. Brand: No.

Ms. Lukasik: Then it would be similar equipment. I would also add just one thing. You [Ms. deForet] said that you're down at the south end. Right?

Ms. deForet: Right near the pond.

Ms. Lukasik: Okay, so, the equipment that would make any sound is all the way at the top. It's all up there.

Ms. deForet: Understood.

Ms. Lukasik: It's very far away from your house.

Ms. deForet: Understood. I can hear like a dog. Okay.

Ms. deForet: I have three. One more. The environmental assessment report—as someone who has quite a bit of a stake in this—do I get to see it?

Mr. Hemminger: Everything we do is public.

Ms. deForet: Okay. How do I get my hands on it?

Mr. Hemminger: Talk to staff. You'll be able to see it. Staff will have it. We'll publish the Part 3, when we get ready—we'll publish all the parts, when we do that. We publish it all. It's all on the website. It's all available. We're an open book.

Ms. deForet: Okay, sorry. And the trucks—the road is for trucks—right?

Mr. Hemminger: The road is for anybody who wants to drive it.

Ms. deForet: But the intent is for trucks.

Mr. Hemminger: Basically, I mean it's in an industrial area.

Ms. deForet: So, the sound is going to cover the rumbling ground?

Mr. Brand: Of what?

Mr. Hemminger: Part of the environment, I mean—

Mr. Brand: If you provide us with information that identifies what the level of what those decibels are from the rumbling trucks, and we'll look at it. WHY IS THIS THE RESIDENTS RESPONSIBILITY?

Ms. deForet: This is the first time I've seen the map of where my house is, and the road, so how am I supposed to provide that to you right now?

Mr. Hemminger: Well, let's not get into an argument about it. We're going to an environmental review. We'll do what we can. I mean honestly, there are many, many, many locations in this Town that are near someplace where a truck would drive. So, it is what it is. We'll go from there.

Mr. Delpriore: Just one quick correction on the record. That solar project [on Yellow Mills Road] is not a Town project. It is another applicant.

Mr. Hemminger: True. That is true. When I say "ours" I spent two years working on it. It feels like it's mine. But we'll work with the people that own it to try to do that.

John Grady (6018 Redfield Drive): I'm a retired land surveyor and I had several meetings with Dan [Mr. Delpriore] regarding the road, to get as much information as I could about the road. I'll just talk about the environmental conditions, and that deals with noise pollution. The road coming in from the south from Route 96, with that "S" turn in the road, the traffic which is going from the north to the south goes into a slope on the road—a design slope, according to the plan—of about five percent grade, that's uphill. You're going to get tractor trailers—and that is the primary amount of traffic, it's going to be tractor trailers—you're going to get tractor trailers shifting, making a lot of noise, going up that road. And that road is exactly that far from my property line. It comes right to the property line, according to your plan. There's no buffer, there's no provision for controlling the noise, and with the amount of truck traffic that goes there—it is going to be day and night, I'm assuming—that is something like that the environmental record should show and should be dealt with.

Mr. Hemminger: Appreciate the feedback. We'll take it under consideration.

Mr. Costanza (6022 Redfield Drive): When I moved here from Perinton, we know Farmington has a long-established history of creating green space and wanting green space. When I bought that property, I knew the Town owned that, but I always thought they would keep it green . . .

Mr. Hemminger: The Town owns it? The Town doesn't own it. No. He [referring to the applicant] bought it from somebody—either bought it or are buying it from another landowner.

Mr. Costanza: Well, as I'm looking at that road, I'm right on that "S" curve, I could shake hands with the person driving down the street pretty much. I do want that in my backyard. (DON'T)

I would rather have the green space that's there—it's beautiful in the fall and it's nice in the summertime. If you can swing that road around and keep that space there . . .

Mr. Hemminger: Swing it where?

Mr. Costanza: The other way.

Mr. Hemminger: They don't own that property.

Mr. Costanza: Well, there's something called eminent domain.

Mr. Hemminger: That's a Town Board issue, not a Planning Board issue.

Mr. Costanza: But—

Mr. Hemminger: There's nothing we can do about that.

Mr. Costanza: But—it's got to be brought up.

Mr. Hemminger: You've got to bring it up to the Town Board. You can't bring it up to us. We can't do that. We have nothing to do with eminent domain.

Mr. Costanza: Well, taking the suggestions here about the noise pollution and air pollution, I mean, I'm right there. I'm getting it all. And those fans that they were talking about they put on Redfield Drive above your furnace—they don't do anything. They do nothing. So I'm going to get all the particulates. I'm going to get the rumbling of the trucks. I mean, this piece of property is going to be worthless for any of the neighbors who bought in that area.

Ms. Finn (6020 Redfield Drive): I'm where I can roll out of bed onto the road, which is a problem that I have, too. But, being environmental, last summer there were three fires in battery storage facilities in New York State (Jefferson County, Orange County, Suffolk County). People had to remain in their homes or go somewhere, until they could figure out if the air was going to be okay. They still don't know about water. So that's a safety environmental concern, along with the road.

Mr. Hemminger: Well, certainly the water wouldn't be affected since we get our water from Canandaigua. It wouldn't be an issue unless they have one down there, and certainly it's tested. The rest of it—we will take and put on record and we will consider it during the environmental record.

Ms. Willard (6011 Redfield Drive): My concern is all of you. I guess I don't understand this process. You're telling us we can't do anything about the road because it was approved 20 or 30 years ago, so what is the point of having a Public Hearing?

Mr. Hemminger: To take your feedback and try to make this the best project we can, given what we have. It's what we do every day. It's what we're required to do. We have to stay within the property that this—that this person is going to have. We can't turn around and do eminent domain on someone—that's not our role. That's a Town Board issue if they want to do stuff like that. We're looking at the environmental record, and if the environment record for some reason comes out as a negative, then we'll have to deal with and come up with mitigations that will address any and all of the issues as it relates to the environmental record.

Mr. Hemminger: This is a very preliminary discussion. This is the first time we're having this discussion. We'll will take all the feedback we have. We hope to see you at as many meetings as we go on. Because this will go on for a while as we deal with the environmental record based on this project. I mean, if you're worried about us, we've been doing this for a long time. We do it in a very professional manner. This Town has a reputation to uphold and that has been upheld by the courts numerous times, that we do the things the right way, and will continue to do them the right way, as it relates to the requirements of New York State and the requirements of what this Town does.

Ms. Willard: What is our recourse? I mean, you're saying you're going to take it in consideration that we all have questions, problems, issues with this road. And the other man came out and said, well, it has been planned for 20 or 30 years. That's it.

Mr. Hemminger: I didn't say "that's it." We're trying to help you understand the history behind all of the different pieces here. If we decide that we shouldn't put the road in because it environmentally doesn't fit, then we will address that when that time comes. When it gets to the point where we [the Planning Board] approve the environmental record, if you don't think that the environmental record is correct, your recourse is to take the Town to court.

Ms. Willard: To file an injunction?

Mr. Hemminger: Well, no, that there is a process to go through. I'm not going to go through all the details. But, you know, I'm trying to help you understand the overall process, probably more than I should, actually. Somebody's going to shoot me in the foot if I say too much more, so I'll stop there.

Mr. Schell (5976 Redfield Drive): I'm concerned about two things in the environmental impact. We've had a neighborhood discussion with our building inspector about the retention pond at the top of the hill that has, on torrential downpours, zero runoff. We were told that the water is supposed to come from Route 96 into that, and then down to the lower retention at the bottom.

Mr. Hemminger: That's is an existing environmental problem. Let staff know about that, and you guys have looked at it?

Mr. Schell: We currently, in the lower one, we had to hire—or we have to hire—a re-engineering firm to re-evaluate whether the land developer did it properly because there is so much water in basements on both sides of Redfield Drive that the underground runoff is not satisfactorily dealing with the runoff. So where is the runoff from the solar farm? Is it going to go into the lower retention pond before it gets evacuated out?

Ms. Lukasik: No, we're not connecting to any of those retention areas that are in the neighborhood. We're completely separate from those.

Mr. Schell: I have inspected probably about 25 solar sites of 25 megawatts or larger, and every one that I have been on all have runoff.

Mr. Hemminger: This is a very small project.

Mr. Schell: 1.2 megawatts is not that small, and up to 25 megawatts. They all have runoff.

Mr. Hemminger: They all handle it onsite.

Mr. Schell: They usually come in and just scrape the ground so they get the topography that they want for the drainage, and then they start putting the pedestals in. So, we'll have a fence line that visually goes behind the Phase 2 portion of Redfield Drive. Most of the solar projects that I've seen—the towns have made them put the little diagonal green striping in the chain link fences and then line them with pine trees, so that they look pleasingly to someone, but there's an upper half of that, that is going to be bare to the eye.

Ms. Lukasik: Can I just add one, to help with that. We are not proposing any grading within the arrays. It's only for the road. There's no grading in the site. It will stay as is—the topography where the arrays are.

Ms. Spitzer (5999 Redfield Drive): I have a couple quick questions. You talk about the environmental record. I'm naïve. What is that, actually?

Mr. Hemminger: It's a process we have to go through, fill out a bunch of forms, answer a bunch of questions, address certain areas. State of New York has created a very—almost said complex, but I shouldn't say it that way—a very intense process for review of projects to make sure that all the issues that might affect a neighborhood are addressed from an environmental standpoint. It's called State Environmental Quality Review process. It's a process we go through, so we answer a bunch of questions, we go through a bunch of process, and make sure we've addressed everything. And anything that comes up that might be of an environmental sensitivity, we have to provide work-arounds for that. It's a process. It's a New York State process.

Ms. Spitzer: Thank you for the clarification.

Mr. Hemminger: No problem.

Ms. Spitzer: A couple times people objected to the road. You said they owned that property. Is this a triangular piece of property?

Mr. Hemminger: It's kind of like a flag lot.

Ms. Lukasik reviewed the property boundaries on the drawing on the video screen. She pointed out and described the property owned by the applicant and the property owned by others. There was a brief discussion.

Mr. Hemminger: It's a very thin piece of property.

Ms. Spitzer: I guess I go back to describing it as flag-shaped.

Mr. Hemminger: Yes, it's a flag lot.

Ms. Spitzer: It's very narrow at the bottom but clearly it opens up on the top.

Mr. Hemmering: Yes, that's why the road is moved over. As it gets up there, it gets moved over.

Mr. Ruffolo: As soon as we can turn, we turn onto our property.

Ms. Spitzer: That's what I'm seeing now.

Mr. Ruffolo: Unfortunately, there's only this strip—60 feet wide—it's the only access to the site on the southern part of it.

Ms. Spitzer: My last one: Are any electromagnetic fields created by this for those of us with pacemakers.

Mr. Ruffolo: The transformers and inverters will have, but there are very few components and they will be far enough away from [?]. As we mentioned, most of the electronic equipment is up in this corner [reference to the drawing] of the property.

Mr. Piccola (6026 Redfield Drive): You said this road has been in your *Comprehensive Plan* for 20 or 30 years.

Mr. Hemminger: Yes.

Mr. Piccola: Is this the original layout in your *Comprehensive Plan* for this road.

Mr. Hemminger: I'm pretty sure. If not, it may have gone further to the east maybe, but it has to connect up to the existing Commercial Drive. It has to start down here, so there may be have been a straighter line, but nothing that would bring it . . .

Mr. Piccola: But it would take it away from the residents if it went back to what you have stated.

Mr. Hemminger: No, it has to go there because that what we decided . . . it's on that one person's property, and then down.

[Unidentified] We're those one people.

Mr. Piccola: We're the building on the end.

Mr. Hemminger: I'm talking about the fact that . . . we never actually finalized the design, and it just was there.

Mr. Piccola: But you then have the final "say" of where this road for this developer goes.

Mr. Hemminger: Yeah, but they can't put it on somebody else's property.

Mr. Piccola: Would it be their responsibility to get an easement from the people who own the other property?

Mr. Hemminger: I don't believe so. Not at all.

Mr. Piccola: But it's your choice to allow the road to go where their putting it.

Mr. Hemminger: The Planning Board cannot deal with anybody else's property, other than the person that comes before us. Period.

Mr. Piccola: I understand that. But that you have the right to say if they can put the road where they're putting it.

Mr. Hemminger: Well, yeah, given their property, yes, we have to do that, yes.

Mr. Piccola: So, if you said they can't make that connection at this time, which road was never totally completed 30 years ago, when Commercial Drive was originally put in your *Comprehensive Plan*, they could enter their property from Collett and still dead-end it until that road was finished—correct?

Mr. Hemminger: The answer is I don't know. We'll take your comments under advisement, but it's not something that we have *ever* done before.

Mr. Piccola: There's always a first time.

Mr. Hemminger: I understand. I understand. We'll take your comments under advisement.

Ms. Whitford (5970 Redfield Drive): I don't know a whole lot about solar, but I did Google a lot of things . . .

Mr. Hemminger: Google.

Ms. Whitford: Yes, good old Google, and I asked—the question was—how close to a residential area is it safe to have a solar farm? And it came up with different things, but the least one was 528 feet and the other ones were between ½ and 1½ miles from a residential area. So I'm not sure why this would even be a consideration so close to a residential area.

Mr. Hemminger: Well, we certainly need more than just that comment. If you've got any data that would support that, you could certainly pass it to staff. We [would] certainly include that and look at as part of our environmental record.

Ms. Whitford: Is this something that you should have looked at already?

Mr. Hemminger: We just got the project. We're just in the process of looking at the environmental record. I mean, we have just received this project. This is the first presentation of this project. It certainly [is] part of it. We certainly have staff looking at and reviewing it. We certainly are going to look at everything we can, but if you—the residents—have data, facts, figures, for us that can help us in this process, you can either give it to us or we can try to find it. So, it's kind of up to you.

Mr. Brabant: I think it's important—it was mentioned earlier, so—as part of this environmental review process, what it is, is this application that is before the Planning Board, is the first meeting really that this board has had on this application . . .

Mr. Hemminger: The very first.

Mr. Brabant: And so what they're doing now for the environmental review is they're forwarding out this application and all the components to all these agencies that Ron Brand mentioned earlier to get their input on whether or not they feel—those agencies that govern those types of critical environmental areas like wetlands, roadways, environmentally endangered species—those type of things—we're forwarding out to all those agencies to get their input. That input then comes back to this board, and also they're soliciting comments from staff—all of our reviews of this application and all of the environmental reports and application reports the applicants provide, like the glare study, like a noise analysis, a Stormwater Pollution Prevention Plan, that tells us about the stormwater runoff from the site—all of these components are being reviewed now by all of the departments, all of these agencies. And then all of that information comes back to this board prior to them making a decision on the environmental.

Mr. Brabant: Today and probably at future meetings, the goal is to get additional input from the community on some of the things that you guys—being that you live there—have issues with, with it. The goal of that is to retain that information and utilize the reports that we receive to determine whether or not information you provided has been mitigated by the plan that is before us, or if there is an impact on the reports that we received, that has to be mitigated or requires a plan change. If there isn't anything that shows that a plan change needs to occur, then we move on to the next step. If there's changes that have to be

addressed, then the board will identify those—we call them impacts—and those impacts will have to be mitigated by the applicant. It's a very long process. This is Step One, but right now we're all kind of, for the first time, getting our feet wet with this application. I just wanted to point that out.

Ms. Dunford (6007 Redfield Drive): I just have a few thoughts. Some of them are environmental, one of which is, I find it strange to overlay a 30-year-old plan on an environment that has drastically changed. The creation of developments like Redfield Drive and the property taxes that are being generated by the reassessments on these townhouses are what is theoretically funding this road, which we can debate whether it's a thoroughfare that's a value to anyone else except the residents in that commercial area. So, I just want you to consider that "environment" is not just land, sky, earth water. It's the community of people who are being affected. I hope that that's not being taken off the table.

Mr. Hemminger: It's part of the process, and by the way, this road will be built by the applicant, and not by the taxpayers. WHY WOULD THE APPLICANT AGREE TO PAY FOR A ROAD THEY DON'T NEED?
Ms. Dunford: A second question: Would this project be permitted if they were not willing to build that connection piece.

Mr. Hemminger: Well, I guess we won't know, since they said they were going to do it. I don't know.

Ms. Dunford: I would be interested, personally, if the engineering company could generate more to the community information on how many megawatts are being generated, what the tax status of this development is, how many tax abatements they're getting from the State or from the Town—just information like that which I think is interesting for us to consume.

Ms. Dunford: Also Cornell [University] is putting in a 10-acre solar field right by the airport which is completely deforested, you know, no residential areas around it. It's generating 320—enough energy to power 320 homes for a year. This struck me as a lot. But I was also wondering if the Town is getting any kind of electricity or commitment.

Mr. Hemminger: It's a private development.

Mr. Clark (6025 Redfield Drive): Do you own this property right now?

Mr. Ruffolo: No.

Mr. Clark: Okay. They're planning on doing something on property which they do not even own yet. I like the point that she made, Ed, that this 20- or 30-year road that's there—at the time, was that zoned residential for the current Redfield Drive residents, because . . .

Mr. Hemminger: I don't know the answer, but probably so, yes. THE ANSWER IS NO.

[Unidentified] The answer is no.

Mr. Clark: I doubt that it would be zoned that way for residential on top of that road. Now, you approved the residential neighborhood but 30 years ago, when that road was there, I don't think it was approved to have residential there.

Mr. Hemminger: Was that Incentive Zoning?

Mr. Brand: Originally that area was zoned Restricted Business on one side and Light Industrial on the other, and over the years they tried to develop it with different proposals. At one point, there was even going to be that an indoor gun-shooting range.

> *Clerk's Note:* The Redfield Drive property was rezoned by the Town Board to Incentive Zoning on February 24, 2015:
>
> **Town Board Resolution #103-2015:**
>
> Resolution adopting Local Law #5 of 2015 directing the amendment of the Town Official Zoning Map affecting tax accounts #29.11-3-5.100, consisting of a total of 16.5 acres of land from RB Restricted Business and LI Limited Industrial to IZ Incentive Zoning; #29.00-2-3.800, consisting of a total of 5.6 acres of land from R-1-10 Residential Single Family to IZ Incentive Zoning; and #29.11-3-1.00, consisting of a total of 0.89 acres of land from GB General Business to IZ Incentive Zoning; and establishing the Incentive Zoning District site amenities and incentives controlling the development of this Redfield Grove Incentive Zoning Project.
>
> Carried.

Mr. Hemminger: So it went to Incentive Zoning. So the Town Board made the decision that that would go residential.

Mr. Brand: A portion of it.

Mr. Hemminger: A portion of it. The rest of it stayed as it was.

Mr. Brand: Commercial.

Mr. Hemminger: And the road was part of the part they left as Commercial.

Mr. Clark: Your Code Enforcement Officer over here—he made reference to these filters and I would like to get information from him and the knowledge he has about those filters.

Mr. Hemminger: Okay, you can certainly reach out to him . . .

Mr. Clark: Is that a requirement that's set out by the Code Enforcement or was that something that Pride Mark offered?

Mr. Delpriore: No, every new house has one of those.

Mr. Hemminger: State requirement.

Mr. Clark: Are they all the same units?

Mr. Delpriore: Similar units. They all do the same . . .

Mr. Clark: I would like to have data on that, please, on the similar units that do the same thing.

Mr. Delpriore: Sure you can request that . . .

Mr. Clark: Because those units do not do what [?] they are made to do.

Mr. Hemminger: Okay, we're getting down to . . .

Mr. Clark: I make a request to have him provide, if he could . . .

Mr. Hemminger: You can reach out to the Building Department any time and he will work with you on that.

Ms. McConnell (6012 Redfield Drive): Seeing that the property isn't purchased by you yet, you don't own the property, and still doing a lot of investigating, or whatever, what is the time plan, your time plan, for when you feel that you would be able to have this working and available, and doing what you purchased the property for? I mean, is this like five years from now?

Mr. Ruffolo: Our intention is to purchase the property shortly. We have been working on this with staff and that there is a separate process designed with the utility. The utility has a very long process. So before we even got to this stage, we had to apply and get approval from the utility that they can take the power from this site and safely integrate into their grid. So, we have that approval. There's a payment process in there, 25 percent, and actually this week making the 25 percent deposit of the cost to the utility to connect this project. So that's been done. The land purchase is in the next week. The project, depending upon how long we go through the [?] process, as I mentioned early on, the project would be a 2025 build, so probably next summer, and it would not take more than four months to build this project, so it probably would be in operation until the end of next year.

Ms. Karpinski (6008 Redfield Drive): I guess my concern are property values, and, you know, I don't think any of us moved into this neighborhood thinking that—especially the people that are up where this road is going to come in—that, you know, there was going to be this big giant commercial road put in. I just question why you would ever have approved

to have a residential area knowing that this was the potential for what you were going to do with this road and this property. I mean, I'm sure that you all own homes, and this is our property, this is our investment, these are not cheap townhouses, okay, these are expensive homes. And I feel really bad for the people that are going to be living near this road because what buffer are they going to get? Are you going to put in fences there so that there's some, you know, noise reduction, so they don't have to look at a road? I mean, seriously, I'm just saying for the people that live in this community. I mean, you have to put yourself in our shoes right now because these are our homes. We want to be able to have the value that we put into these homes. So, I just want you to be thinking about that. I hear that, you know, you had this road planned for 30 years and all this stuff, but you approved for us—for this development—to be put in. DID THE PLANNING BOARD REVIEW & APPROVE THE CHANGE TO INCENTIVE ZONING?
Mr. Hemminger: The Town did that.

Ms. Karpinski: You had to have known that this was maybe coming down the pike and I just hope that you would just think about us as residents and what you're going to do to make it so that we have the value of our homes.

Mr. Hemminger: We certainly will keep that mind. The Town Board is the one who did the Incentive Zoning. We deal with it after that happens.

John Grady (6018 Redfield Drive): Just one thing that I forgot to mention regarding the environmental record. The part the southern section of the road which is very close—adjoins the property line. The proposal that shows on the plot plan shows that the road will be approximately eight feet higher than the existing ground throughout that area, which means if you are standing in my backyard, you are looking at the side of a highway embankment, which is going to be above your head. If you are stand in my bedroom and look at it, you would still be looking into the side of a highway embankment. This road design is not a good solution. ~~MY FIRST COMMENTS ON THIS PROJECT WERE OMITTED FROM THESE MINUTES.~~

Mr. Raymond (6010 Redfield Drive): Ed, do you hear what's going on here? There's 40 people here or more, and none of us want this road in this position, or even close to our houses.

Mr. Hemminger: I do. I certainly do.

Mr. Raymond: Do you? It seems though we're all bringing up these problems that we have, and bringing them up to you, and what they are hearing back from you is put us off, go out and get some information and bring it into the Town, I go this, I go that, or that it was always planned that way, or that it is fine that it is straight up to the backyard of the house. It's fine if there are trucks, you know, going in and out, and everything. It isn't fine. There isn't anybody in here, and I hope that you all agree with me, this is not fine.

(Audience applause)

Mr. Hemminger: I certainly understand you, and I understand where you're coming from. And it certainly isn't my first rodeo here. I've been doing planning and zoning for some 20-some-odd years. On the other hand, our responsibility is pretty simple, by law, we take the project as it's presented and try to make it the best project possible. I don't have the ability, unless there's an environmental issue, that says there's an environmental issue that can't be mitigated to just say, "we're not going to do the project." Okay? This is zoned, available for this. This is the way the Town has made decisions to set things up. So we have to do the best job we can with what we have. WHAT YOU HAVE IS A RESIDENTIAL SUBDIVISION WHICH THE TOWN PERMITTED AND IS NOT NOW PROTECTING.

Mr. Hemminger: We're going to look at the road. Certainly, that's a big issue. We'll talk to the Town Board. They did the issue with the Incentive Zoning and see where they were coming from on the whole project. We'll look at some different pieces of this. I'm not saying—this is the very first time we've had a meeting on this. This is the first time we've heard from the applicant—the first time you've heard from the applicant. So, this is not a done deal. If I came off—I'm trying to help you understand the reality of the situation as opposed to—and that's why we have an environmental review and we have the whole process. I'm trying to help you understand some of the reality of the situation. That is zoned for this kind of thing in that position. That road has been set up to be there forever. I'm just saying that doesn't mean that it has to stay that way. It doesn't mean we can't change things, but this is the beginning of the process. Okay? THE TOWN CHANGED EVERYTHING WHEN IT APPROVED REDFIELD GROVE. THE TOWN NOW HAS THE RESPONSIBILITY TO PROTECT THE RESIDENTS OF REDFIELD GROVE FROM THE DAMAGE OF THIS ADJOINING PROPOSAL.

Mr. Schell (5976 Redfield Drive): Thank you, Ed, for listening to everbody here.

Mr. Hemminger: Thank you.

Mr. Schell: With the general complaint all about the same thing—What's the process for us to take this to the [Town] Board so that they will hear us and then maybe come back and bend your ear?

Mr. Hemminger: Well, first off, the Town Board doesn't bend our ear. We are independent of the Town Board. We are appointed to do our job as a Planning Board. The Town Board, by law, is not supposed to interfere with the Planning Board. Now, that being said, your development [Redfield Grove] was an Incentive Zoning project. The Town Board approved that, not us. We then took what they approved and made it the best we could and you have a very, very nice area over there, which is right across the street from me, by the way. I live over there on King Hill, across the street. So I know that area very well.

Mr. Hemminger: But if you want to talk to the Town Board, all you got to do is show up at a meeting or better yet, get a meeting, sit down, talk to the supervisor. Tell him what your concerns are with that road, yadda, yadda, yadda. I don't know what they can and can't do. That's not my area of responsibility. I'm not trying to shove it off. But that, we have our role here. They have their role there. And really, the two don't really connect. It sounds kind of funny that the Town Board can't and doesn't tell us what to do. They don't, they can't, by law.

Mr. Hemminger: You know what I always try to do, and maybe I shouldn't do it, and I tell you that the Supervisor probably tells that I shouldn't do it as much as I do, part of, I think my job is to try and help educate you on the process—educate you, the citizens, who don't do this stuff every day like we do, haven't done it for 25 years like I've done it, try to help you understand the process a little bit. And if it sounds a little cold, if it sounds a little rigid, it's government. It's the way things end up being as we do things. It doesn't mean we can't adjust and adapt, and do other things, but I try to help you understand the process. And if you don't like the process, I'm sorry, we didn't establish the process. It's established by the State of New York and the laws of the State of New York and that's what we're stuck with. It doesn't mean we don't care. It doesn't mean we don't sympathize with you. It doesn't mean we don't care about the value of your property. It doesn't mean we don't do any of that. At the same time we care about the developer, what they're doing and how they're doing it, and the other types of things. So, I hope you don't leave here angry at us, but hopefully you leave here with an understanding of the process and know that there will be many more meetings like this where we will discuss different things. And we will attempt to do the best we can.

Ms. deForet: I'm sorry sir, I wanted to ask you a clarifying question. You said that you all just started this. This gentleman said multiple times, and he stopped himself from saying how long he is doing this, and as soon as that sign went up by the pond I called and I met with Dan Delpriore, okay. And I looked at a map that had not just been written that day. So, I'm a little offended.

Mr. Hemminger: The staff has been looking at it. The Planning Board just received it. The staff has been looking at it, working with the applicant. I know numerous meetings. But, we, as the Planning Board, is what I meant. This is *our* first time seeing this and hearing this. I apologize if I didn't made that clear.

Ms. deForet: Okay, I just want to reiterate what other people have said. This is my only house. I worked my whole life to be able to live in this house. I don't know what I am going to do with the road being built closer to my backdoor than the road in the front, and people giving me smoke and mirrors that the fumes aren't coming into my house. I am feeling like . . . I just don't even know how to explain to you how angry I am with the way you keep saying, "We'll take that under advisement." I don't feel like you're understanding.

Mr. Hemminger: That's the process we're in. We're in the environmental review. That's what we do. We take your feedback. We get it on the record and we go through the process. What do you want me to say, right now? I have no process to go through except the State-mandated process. I understand how you feel, but I can't turn around and violate the laws of the State of New York because you feel the way you feel. I have to follow the law. I mean, I know it's cruel, but it is the process that we have to go through. I can't just turn around and go, "no, I looked at it, I don't like it. Cancel it." It doesn't work that way.

Ms. deForet: I still don't understand why you're even listening to us because what you say to me is that it doesn't matter what we say. [Another person speaking.] You're coming

across like it doesn't matter what we say, and then you're telling me I need to bring data. Dude, do you want me to [unintelligible]. I'm a chemist. I can collect data. Trust me.

Mr. Hemminger: I'm sorry. We still have to go through a process.

Mr. Cammarata (6009 Redfield Drive): Thank God, I'm on the other side of these townhomes that you're going to build this road by. The one thing that keeps going through my mind—this whole board seems to be infatuated with the idea that these people are going to pony up the money. That's the two ends of Commercial Drive.

[Brief applause]

Mr. Cammarata: This board seems to be—that's the greatest thing. Let's just shove this road through there. And it's going to be commercial vehicles, big heavy vehicles coming up and down this road, for what? So they can get from one end of Collett to 96? Is that worth all of this?

Mr. Hemminger: Appreciate your feedback and all we can do is put it on the record and consider it when we do the environmental record.

[Unidentified] Is there any thought to not doing that? To not putting that . . .

Mr. Hemminger: We have to go through the environmental review process.

[Several people speaking briefly at once.]

Mr. Costanza (6022 Redfield Drive): You were asking "what can I say?" Well, what you can say is, and what would give us a bit more confidence, is that even though this [road] was planned 30 years ago, needs of the community change in 30 years. What was there 30 years ago probably were vacant lots, and that was fine at that time. But you've got to consider that the needs of this community are changed. As they've said up here, we've got our investment here. Our investment is going to be zero with a road that's eight feet higher than we are, than our own homes. If something tips off that road, it's going to be right in our house.

Mr. Hemminger: I appreciate the . . . and again, we're going to look at everything.

Ms. Cammarata (6009 Redfield Drive): Why are they purchasing this property if this has not been approved?

Mr. Hemminger: It's their choice. It's a commercial venture.

Ms Cammarata: But why would I buy a property . . . I mean, they must be in this process.

Mr. Hemminger: It is what it is. They can decide what they purchase and when they purchase it.

Mr. Hemminger asked three times if anyone on the remote video conference wished to speak for or against this project. There were no requests to speak from anyone on the remote video conference.

Mr. Hemminger said that the board has four resolutions for consideration this evening for the continuation of the Public Hearings until May 15, 2024.

Mr. Hemminger then asked board members if they had comments.

Mr. Sweeney asked about the decommissioning of the site and if there is a procedure for restoring the land, especially that a portion of the property is now wooded. Mr. Ruffolo said that their general plan is to remove the equipment and reseed the property to return the land as a field.

Mr. Sweeney also asked about the revised surety for emergency decommissioning if the site is abandoned prior to the end of its functional life. Mr. Ruffolo said that a bond or a similar financial instrument would be put in place for the benefit of the Town if the company abandons the site.

Mr. Hemminger said that the solar company will create a bond if this company is not able to restore the property. He said that the Town will review the bond every five years to assure that the dollar amount remains adequate for the Town to perform the recovery.

Mr. Sweeney said that oils are not listed in the Table of Waste in the Decommissioning Plan. Mr. Ruffolo said that oils, if any would be contained within the transformer. He said that no oils or other liquids would be stored on the site, other than any in the transformer. Mr. Ruffolo also said that the Operations and Maintenance Plan includes procedures for emergency response. He said that his company will work with the appropriate department regarding the skills for handling emergencies.

Mr. Hemminger said that the Town has been through this on the larger solar project [on Yellow Mills Road] and that the Town has some good experience on the decommissioning plans if we get to that point. He said that the environmental review will cover everything that we need. He also highly encouraged everyone to review the environmental review documents when they come out. He said that feedback is important.

[Unidentified] A resident asked about the planting of grass and if the plan is to remove all the woods. Mr. Ruffolo said that there will be a buffer of woods which would remain, and that where the solar arrays will be located will be restored to grass. He said that the maximum height of the solar arrays is 9 to 10 feet high from the ground. Mr. Ruffolo said that the front end of the solar panels would be about three feet off the ground.

Ms. Grady (6018 Redfield Drive) asked why did the company agree to build the road. Mr. Brand said that the road connection has been part of the Town's ongoing *Comprehensive Plan*. Mr. Hemminger said that the company decided to develop this land and that part of the development of this site is the construction of the road connection. The resident asked

if the Town will have the road after the decommissioning of the site or regardless of the success [of the project] or not. Mr. Hemminger said that this correct.

There were no additional comments or questions on this application this evening.

■ A motion was made by MR. BELLIS, seconded by MR. VIETS, that the reading of the following resolutions be waived and that the resolutions be approved as submitted by the Town staff:

TOWN OF FARMINGTON PLANNING BOARD RESOLUTION
ADJOURNMENT AND CONTINUATION OF THE PUBLIC HEARING UPON THE PROPOSED SPECIAL USE PERMIT FOR THE PROPOSED EAST PORTION OF THE SKY SOLAR, INC. SOLAR PROJECT

PB #0406-24

APPLICANT: **Sky Solar, Inc., 1129 Northern Boulevard, Suite 404, Manhasset, N.Y. 11030**

ACTION: **Adjournment and Continuation of the Public Hearing on the application for a Special Use Permit to allow for the construction and operation of solar arrays, a transformer area and a stand-alone battery energy storage system upon a portion of Tax Map Account #29.00-1-84.112 comprised of a total of 5.5 acres of land with access from along East Corporate Drive and a future extension of Commercial Drive. This parcel is to be known as the western portion of the Sky Solar, Inc., Commercial Drive Solar Project and is located south of the American Lumber property which fronts along the south side of Collett Road and extends south to the north property line for Tax Map Account #29.00-1-84.113.**

WHEREAS, the Town of Farmington Planning Board (hereinafter referred to as the Planning Board) has tonight opened the Public Hearing on this application; and

WHEREAS, the Planning Board has tonight received testimony upon this application; and

WHEREAS, the Planning Board has on April 3, 2024, classified the proposed Action in accordance with the procedures contained within the State Environmental Quality Review Act (SEQRA) as being an Unlisted Action, determined a coordinated review necessary and on April 4, 2024, provided notification to the Involved and Interested Agencies, and declared the Planning Board's intent to be designated the Lead Agency at their scheduled meeting on Wednesday, May 15, 2024; and

WHEREAS, in accordance with the provisions contained in 6NYCRR Part 617 of article 8 of the New York State Environmental Conservation Law (ECL) no decision may be made

upon this Action under a Lead Agency has completed the environmental record and has made a determination of significance thereon.

NOW, THEREFORE, IT RESOLVED that the Planning Board does hereby adjourn this public hearing tonight and moves to continue it at the scheduled May 15, 2024, public meeting.

BE IT FINALLY RESOLVED that a certified copy of this resolution is to be provided to the Town Staff, the Applicant, the Applicant's Engineers, the Town Director of Planning and Development, the Town Code Enforcement Officer, and the Town Zoning Enforcement Officer.

TOWN OF FARMINGTON PLANNING BOARD RESOLUTION
ADJOURNMENT AND CONTINUATION OF THE PUBLIC HEARING UPON THE PROPOSED SPECIAL USE PERMIT FOR THE PROPOSED WEST PORTION OF THE SKY SOLAR, INC. SOLAR PROJECT

PB #0407-24

APPLICANT: **Sky Solar, Inc., 1129 Northern Boulevard, Suite 404, Manhasset, N.Y. 11030**

ACTION: **Adjournment and Continuation of the Public Hearing on the application for a Special Use Permit to allow for the construction and operation of solar arrays and a transformer area upon a portion of Tax Map Account #29.07-1-057. This parcel is known as the eastern portion of the Sky Solar, Inc., Commercial Drive Solar Project and is located south of A Safe Place Self-Storage property which fronts along the south side of Collett Road and extending south to the north property line for New Energy Works and the western properties of Tax Map Account #'s 29.07-4-055 through -070 and Account #'s 29.0-4-073 and -074 which are located along the west side of Redfield Drive.**

WHEREAS, the Town of Farmington Planning Board (hereinafter referred to as the Planning Board) has tonight opened the Public Hearing on this application; and

WHEREAS, the Planning Board has tonight received testimony upon this application; and

WHEREAS, the Planning Board has on April 3, 2024, classified the proposed Action in accordance with the procedures contained within the State Environmental Quality Review Act (SEQRA) as being an Unlisted Action, determined a coordinated review necessary and on April 4, 2024, provided notification to the Involved and Interested Agencies, and declared the Planning Board's intent to be designated the Lead Agency at their scheduled meeting on Wednesday, May 15, 2024; and

WHEREAS, in accordance with the provisions contained in 6NYCRR Part 617 of article 8 of the New York State Environmental Conservation Law (ECL) no decision may be made upon this Action under a Lead Agency has completed the environmental record and has made a determination of significance thereon.

NOW, THEREFORE, BE IT RESOLVED that the Planning Board does hereby adjourn this public hearing tonight and moves to continue it at the scheduled May 15, 2024, public meeting.

BE IT FINALLY RESOLVED that a certified copy of this resolution is to be provided to the Town Staff, the Applicant, the Applicant's Engineers, the Town Director of Planning and Development, the Town Code Enforcement Officer, and the Town Zoning Enforcement Officer.

TOWN OF FARMINGTON PLANNING BOARD RESOLUTION
ADJOURNMENT AND CONTINUATION OF THE PUBLIC HEARING UPON THE PROPOSED PRELIMINARY SITE PLAN FOR THE PROPOSED EAST PORTION OF THE SKY SOLAR, INC. SOLAR PROJECT

PB #0408-24

APPLICANT:	**Sky Solar, Inc., 1129 Northern Boulevard, Suite 404, Manhasset, N.Y. 11030**
ACTION:	**Adjournment and Continuation of the Public Hearing on the application for Preliminary Site Plan approval to allow for the construction of solar arrays and a transformer area on the eastern portion of the Sky Solar, Inc., Commercial Drive Solar Project; and the construction of a section of Town Road with sidewalks, crosswalks, streetlights, water line and fire hydrants completing the missing link between the south end and the northern portion of Commercial Drive with the north end of the southern portion of Commercial Drive and located on Tax Map Accounts 029.07-1-057 and -058 which contains a total of 7.75 acres of land.**

WHEREAS, the Town of Farmington Planning Board (hereinafter referred to as the Planning Board) has tonight opened the Public Hearing on this application; and

WHEREAS, the Planning Board has tonight received testimony upon this application; and

WHEREAS, the Planning Board has on April 3, 2024, classified the proposed Action in accordance with the procedures contained within the State Environmental Quality Review Act (SEQRA) as being an Unlisted Action, determined a coordinated review necessary and on April 4, 2024, provided notification to the Involved and Interested Agencies, and

declared the Planning Board's intent to be designated the Lead Agency at their scheduled meeting on Wednesday, May 15, 2024; and

WHEREAS, in accordance with the provisions contained in 6NYCRR Part 617 of Article 8 of the New York State Environmental Conservation Law (ECL) no decision may be made upon this Action under a Lead Agency has completed the environmental record and has made a determination of significance thereon.

NOW, THEREFORE, BE IT RESOLVED that the Planning Board does hereby adjourn this Public Hearing tonight and moves to continue it at the scheduled May 15, 2024, public meeting.

BE IT FINALLY RESOLVED that a certified copy of this resolution is to be provided to the Town Staff, the Applicant, the Applicant's Engineers, the Town Director of Planning and Development, the Town Code Enforcement Officer, and the Town Zoning Enforcement Officer.

TOWN OF FARMINGTON PLANNING BOARD RESOLUTION
ADJOURNMENT AND CONTINUATION OF THE PUBLIC HEARING UPON THE PROPOSED PRELIMINARY SITE PLAN FOR THE PROPOSED WEST PORTION OF THE SKY SOLAR, INC. SOLAR PROJECT

PB #0409-24

APPLICANT:	**Sky Solar, Inc., 1129 Northern Boulevard, Suite 404, Manhasset, N.Y. 11030**
ACTION:	**Adjournment and Continuation of the Public Hearing on the application for Preliminary Site Plan approval to allow for the construction of solar arrays, a transformer area and a stand-alone battery energy storage system to be located upon a portion of Tax Map Account #29.00-1-84.112 comprised of a total of 5.5 acres of land with access from along East Corporate Drive and a future extension of Commercial Drive.**

WHEREAS, the Town of Farmington Planning Board (hereinafter referred to as the Planning Board) has tonight opened the Public Hearing on this application; and

WHEREAS, the Planning Board has tonight received testimony upon this application; and

WHEREAS, the Planning Board has on April 3, 2024, classified the proposed Action in accordance with the procedures contained within the State Environmental Quality Review Act (SEQRA) as being an Unlisted Action, determined a coordinated review necessary and on April 4, 2024, provided notification to the Involved and Interested Agencies, and

declared the Planning Board's intent to be designated the Lead Agency at their scheduled meeting on Wednesday, May 15, 2024; and

WHEREAS, in accordance with the provisions contained in 6NYCRR Part 617 of Article 8 of the New York State Environmental Conservation Law (ECL) no decision may be made upon this Action under a Lead Agency has completed the environmental record and has made a determination of significance thereon.

NOW, THEREFORE, BE IT RESOLVED that the Planning Board does hereby adjourn this Public Hearing tonight and moves to continue it at the scheduled May 15, 2024, public meeting.

BE IT FINALLY RESOLVED that a certified copy of this resolution is to be provided to the Town Staff, the Applicant, the Applicant's Engineers, the Town Director of Planning and Development, the Town Code Enforcement Officer, and the Town Zoning Enforcement Officer.

The following vote on the above four resolutions was recorded in the meeting minutes:

Adrian Bellis	Aye
Timothy DeLucia	Aye
Edward Hemminger	Aye
Aaron Sweeney	Aye
Douglas Viets	Aye

Motion carried.

(The meeting was in recess from 8:54 p.m. to 9:00 p.m.)

8. OTHER BOARD ACTIONS

A. Review of Norbut Solar Farm Project (Town of Victor referral):

Pursuant to General Municipal Law Section 239-nn, the board received a referral on March 26, 2024, from the Victor Town Clerk regarding the Norbut Solar Farm, LLC, a project which is proposed for a parcel of land in Victor, N.Y., on the south side of County Road 41 adjacent to the Victor/Farmington town line.

Mr. Hemminger continued the discussion of this application which began at the Planning Board meeting on April 3, 2024.

(See Planning Board Minutes, April 3, 2024, for a summary of this application.)

An expert talks solar battery farms, how they work and the risks (https://www.northcountrypublic expert-talks-solar-battery-farms-how-they-work-and-the-risks)

BY CATHERINE WHEELER (ST. LAWRENCE VALLEY REPORTER)

(/NEWS/REPORTERS/276/CATHERINE-WHEELER)

(https://www.northcountrypublicradio.org/news/images/14492228979_c

Photovoltaic battery storage system. (Photo: U.S. Department of Energy)

Sep 11, 2023 —

A solar battery fire in Jefferson County this summer raised concerns (/news/story/48280/20230811/solar-battery-fire-in-jefferson-county-raises-concerns-for-the-future) about existing and potential solar projects across the North Country. There have been two other such fires around New York State.

Not all solar installations have batteries. Many in the North Country are just solar panels that feed straight into the grid. But batteries can increase solar's usefulness on the power grid by saving energy to release when the sun isn't shining.

We wanted to learn more about how solar batteries work and what communities need to know about the risks.

Catherine Wheeler reached out to an expert.

05:23

Catherine Wheeler
An expert talks solar battery farms, how they work and the risks

Catherine Wheeler: Battery storage helps address the challenges of solar generation. Cornell University mechanical engineering professor Max Zhang says while solar is renewable energy, what's generated can

vary over the course of a day, season and even year to year. He says that's called variance. On top of that, there's intermittence- the unpredictable stuff, like cloud cover.

Max Zhang: For power system operators, their role is to balance supply and demand. And if your supply, which means solar generation, is variable and the intermittence it becomes very difficult to dispatch that generation, right. And with the battery storage, you know, you can basically make more variable generation into more predictable generation by serving as a buffer.

Catherine Wheeler: Zhang says there are generally two types of places for these solar batteries to live. One is at a solar farm where the energy is produced. The other isn't found in New York State often: dedicated energy storage farms. He says there are three in the state, including one in Franklin County that recently started operating. It's New York's first-ever state-owned utility-scale energy storage facility.

Over the past couple of months, there have been a couple of incidents with battery storage across the state. How common are these accidents?

Max Zhang: First of all, I will say, it's a manageable risk, in general. So, the majority of the battery storage that we see is at least in lithium ion batteries, right? They are generally safe. They are generally safe until something happens, such as overheating, being damaged, or short-circuiting or just manufacturing defects, right. So, those do not happen

very often. But in rare occasions, it can cause fire and other damages. It's not common, right, but is definitely a risk. But I think it's a manageable risk.

Catherine Wheeler: What are the health and safety concerns when there is an incident like a fire at a lithium ion battery storage facility?

Max Zhang: I think it's very important for a community to decide when hosting a solar farm with a battery or with dedicated battery facilities, it's very important to bring the emergency response, the fire department, on board. Because, especially lithium ion batteries, once the accident happens, they don't behave like the typical fire we've seen. It can happen really quickly. And it's really hard to stop. It's just not like a normal fire. So that's why it's important to have the emergency responder on board and, you know, have, you know, provide them with sufficient training to prepare for the potential risk.

Catherine Wheeler: Zhang says when he's weighing the pros and cons of battery storage, he thinks about the widespread use of the batteries and that different states have much larger battery operations.

Max Zhang: In other parts of the country, they are actually much larger, much larger scale implantation of those batteries. For example, in California, currently, they already have five gigawatts of dedicated battery storage in the state. So, Texas has about 3 gigawatts. Right now, New York, as I mentioned here, I think they about have totally, roughly 60 megawatts, so much smaller than what California and Texas have. So I will say this is my personal view. Right. So, as more we use it, the more we learn.

Zhang says researchers are working on ways to make lithium ion batteries safer or find alternatives, like zinc-based batteries. He says lithium ion batteries are energy dense, which means they can store more energy at a smaller size. That's what makes them great for so many different applications, like cars and computers, which means more people want to make and sell them, and they get cheaper to produce.

Catherine Wheeler: So you think, especially when balancing like the state and the country's climate goals, you think that this is a good way to help achieve those goals?

Max Zhang: In short answer, yes. So the longer answer is that this year, we already see a variety of impacts from climate change, right. And accelerating renewable generation to mitigate greenhouse gas emissions, is really the option, I don't think we have any other option to take at this point. You know, we have to take action fast. And there are, you know, research and development efforts to make lithium ion batteries safer, right. And also, there are other alternatives that are safer than these batteries, right. So, I think the question is how, as a society, we can incentivize the production of those safer choices, right? So, I think that's back to an economic question.

Related Topics

solar power (/news/tags/solar-power) · solar battery (/news/tags/solar-battery) · environment (/news/pages/environmental-news) · renewable energy (/news/tags/renewable-energy) · economy (/news/pages/economic-and-business) · health (/news/pages/health)

NCPR is supported by:

Comments

Feel like talking about this? Join us on Facebook (https://www.facebook.com/NorthCountryPublicRadio).

More from NCPR

UTILITY DIVE

DIVE BRIEF

New York battery storage owners may face new safety rules after fires

The fires did not lead to any reported injuries, or release harmful levels of toxins, initial findings from an inter-agency fire safety working group organized by Gov. Kathy Hochul concluded.

Published Jan. 11, 2024

Kavya Balaraman
Freelance reporter

A working group of New York agencies is preparing to issue recommendations to bolster battery storage safety. Adeline Kon/Utility Dive

Dive Brief:

- Multiple fires that broke out at battery energy storage facilities in New York last year did not lead to any reported injuries, or release harmful levels of toxins, an analysis conducted by an inter-agency fire safety working group organized by Gov. Kathy Hochul, D, concluded in late December.
- The group is assessing battery system projects across the state, as well as fire codes, and intends to release draft recommendations to ensure building and fire codes are up to par in the first quarter of 2024.
- The American Clean Power Association commended the Hochul administration's "thoughtful and proactive approach in their

thorough investigation of how New York can best promote safety at electric grid infrastructure facilities," spokesperson Phil Sgro said in an email. "As national safety standards have developed and continually improved, the instances of energy storage fires have become increasingly rare. If they do happen, incidents are properly managed, and any impacts are contained within the facility's secure site," Sgro added.

Dive Insight:

Hochul announced the creation of the fire safety working group, tasked with overseeing energy storage systems in the state in August. The move came after multiple fires at battery storage facilities, including four battery storage trailers that caught fire at a Convergent Energy solar farm.

The group includes representatives from the Division of Homeland Security and Emergency Services, Office of Fire Prevention and Control, and New York State Energy Research and Development Authority, among others. Over the past several months, it has been working with project developers, equipment manufacturers and other stakeholders to gather data about the fires.

Initial findings from the group indicate no reported injuries or harmful levels of toxins attributable to the fires. Now, it is focused on inspecting all battery systems above 300 kW that are operating in the state, a process that is expected to finish in the second quarter of 2024. Based on these inspections, the group will update evaluation checklists and best practices to be used before energizing these battery systems, and during emergency response measures.

The group is also working with national laboratories and others on assessing existing fire codes, with proposed changes expected early

this year.

The measurements and data obtained from these incidents are a positive finding and consistent with air and ground monitoring done at other post-incident monitoring, Matthew Paiss, technical advisor at the Pacific Northwest National Laboratory, said in an email.

"The take-away can be that electrical devices can fail, and when they do, it is the safety certifications and testing that should offer protections to limit the incident," Paiss added.

The state should incorporate best practices and requirements outlined in the National Fire Protection Association's safety standard for energy storage — called NFPA 855 — which provides mandatory requirements for the design, installation, commissioning, operation, maintenance, and decommissioning of energy storage facilities, ACP's Sgro said.

"Uniformity in adopting this standard across states and jurisdictions will ensure that clear evidence-based rules guide future development and operation of energy storage facilities," he added.

More broadly, Sgro said the energy storage industry's leadership on safety is resulting in safety incidents becoming increasingly rare, even as it brings storage projects online at an exponential rate.

"The energy storage industry uses a suite of well-established codes and standards to ensure safety at facilities. Beyond seeking to meet and exceed safety best practices, the energy storage companies engage in extensive collaboration with fire departments and first responders to ensure that, if a rare safety incident does occur, a plan is in place to safely manage and resolve any incident," he said.

In terms of how the industry can deploy lithium-ion batteries while also keeping in mind safety concerns, designing energy storage systems to the best practices as opposed to the minimum local requirements is one way to ensure the safest system possible, Paiss said.

"Another is to consider appropriate siting with adequate separation that, should a failure occur, it remains within the unit of origin," he added.

U.S.

Solar farm fire in Upstate New York sends possible toxic smoke billowing into surrounding community

July 27, 2023 / 10:52 PM EDT / CBS News

New York Gov. Kathy Hochul issued an advisory Thursday night due to potentially toxic smoke billowing from a battery fire at a solar farm burning near the Canadian border.

…orts that the fire broke out at about 1 p.m. Eastern

time at a solar farm in the Jefferson County town of Lyme, located on Lake Ontario.

In a statement, Hochul said that the "large battery fire" had "caused significant damage and is emitting large amounts of smoke that may pose health

I

Read More

First published on July 27, 2023 / 10:52 PM EDT

ENERGY TRANSITION See all articles

New York Governor Kathy Hochul. Photo: Metropolitan Transportation Authority via Flickr

After three fires and a solar plant toxic fumes scare, New York launches safety probe into battery energy storage

State governor sets up Fire Safety Working Group after residents told to stay at home in third recent incident at solar farm

31 July 2023 11:34 GMT *UPDATED 31 July 2023 13:12 GMT*

By Cosmo Sanderson

New York governor Kathy Hochul launched a special taskforce to investigate the safety of battery energy storage facilities after a third blaze in the state this year left residents warned to stay indoors.

Hochul announced the creation of the Fire Safety Working Group and immediate inspections of storage sites in the state after a battery fire at a solar farm sent potentially toxic smoke billowing across the area late last week.

The stay-at-home order was lifted some hours later after local authorities and emergency services – including a hazmat team – had confirmed there was no indication of toxic chemicals either in the air or in groundwater.

Hochul on Friday was among those to urge local residents to "protect themselves and their families" from exposure to smoke or other toxins following the "large battery fire" in Jefferson County, which borders Canada.

Safety crackdown after string of fires hit wind and solar batteries

Read more

Hochul said the latest blaze followed others in Orange and Suffolk counties, prompting her to set up the taskforce "to mobilise the personnel and resources necessary to keep New Yorkers safe".

Video of the Jefferson County solar farm showed flames and smoke billowing from the facility, which reportedly has four lithium battery storage trailers.

"Mechanical equipment which supports the operation of the solar project malfunctioned, causing a fire," according to local officials.

The operator of the facility, Convergent Energy and Power, issued a statement quoted in local media apologising for the fire.

"When we install battery storage systems, we partner with reputable third-party manufacturers who provide the systems, including the batteries that are inside them," said Convergent. It continued that it was the manufacturers who "ensure that their products satisfy highest-level safety standards" set by an independent agency, "including fire containment and fire suppression capabilities".

Convergent has **previously partnered with GE Renewable Energy** to supply 100MWh of battery capacity in California to support renewable energy generation.

Why new long-duration energy storage technologies will soon replace lithium-ion on grid

Read more

Fires at lithium-ion battery facilities have long been a spectre that has haunted the renewables industry. Last year, a fire broke out at a Telsa battery unit in California. Another fire broke out at a 20MW battery facility operated by Danish renewables giant Orsted in Liverpool, UK, in 2019. That same year, four US firefighters were seriously injured by an explosion at a 2.16 MWh battery storage system in Arizona.

Battery fires are most commonly caused by thermal runaway, when a battery's temperature increases, leading to cell short-circuiting or disintegration. Thermal runaway can be caused by factors including mechanical damage, poor air conditioning and electrical issues such as overcharging.

A new generation of zinc-ion batteries has been **touted as a potential remedy** to the deficiencies of their lithium counterparts. Zinc batteries are fireproof as they do not require heating or cooling, while developers have also claimed they will be **cheaper and longer-lasting**. (Copyright)

Storage **Americas** **US** **solar** **New York**

[redacted]

(Spectrum News 1/Brian Dwyer)

ENVIRONMENT

Questions remain after Jefferson Co. solar farm battery fire

BY BRIAN DWYER | JEFFERSON COUNTY
PUBLISHED 1:27 PM ET AUG. 01, 2023

Susan Nichols lives one-tenth of a mile from a solar farm in the Jefferson

County town of Lyme that saw its battery storage area catch fire Thursday.

It's been five days of wondering what's in her air and in her water, and she's concerned.

"Basically [I fear] it's in our well. Once it's in our well, you're not going to get it out," Nichols said.

What You Need To Know

- Thursday, the battery storage area of a solar farm in Jefferson County caught fire
- Officials say there's a lot to learn about battery fires such as this and hope this is a chance for people to learn
- Gov. Kathy Hochul has called for a working group to be created specifically for this purpose

---

And while there were 24 hours or so of concern over air quality, officials are no longer asking people to stay inside, or even wearing protection at this point — however, they admit with air or especially, water, no one can say anything with 100% certainty.

"We have no way of digging into the ground and answering that question," Jefferson County Fire and Emergency Management Deputy Director Niel Rivenburgh said.

That answer, he says — like everything else involved with this fire — will come in time.

Spectrum News 1 is told the storage area is no longer burning, but it is far too hot at this point for anyone to approach the direct area or determine any cause.

"We have all kinds of state officials here. It will be investigated at the highest of levels," Town of Lyme Supervisor Terry Countryman said.

For now, crews will continue to watch the fire to ensure it doesn't reignite and secure the area, all while using the time to share information and help all the nearby departments better understand what they can do in a similar situation elsewhere.

"Not all of them have battery storage. Not all of them are built exactly alike,

but there's been an incredible opportunity to learn from this incident," Rivenburgh added, while saying split-second decisions need to be made in emergencies and the unknowns make that job incredibly difficult.

It's an opportunity New York State hopes will only grow as Gov. Kathy Hochul has ordered a special task force to be established to collaborate with first responders to better understand the safety aspects of these energy farms.

"And there needs to be strong education on lithium and how it is used in our communities across the board. It's in your back pocket. It's in your car. It is everywhere. We need to learn how to fight it best and how we're going to bring it in to our communities," Countryman said.

Countryman says while he expects the investigation and environmental testing to take time, he adds that Convergent, the company which operates the storage facility, will be — with the help & guidance of the DEC — taking care of all remediation.

Spectrum News 1 is told once the heat in the immediate battery storage area cools off, allowing investigators and testers to start working, fire departments will be able to get back to normal — with only a few people

stated the operator of the

ctric.

YOU MAY ALSO BE INTERESTED IN

PUBLIC SAFETY

Ex-Ivy Ridge employees placed on leave from state-run psychiatric center after Netflix doc sheds light on shuttered school

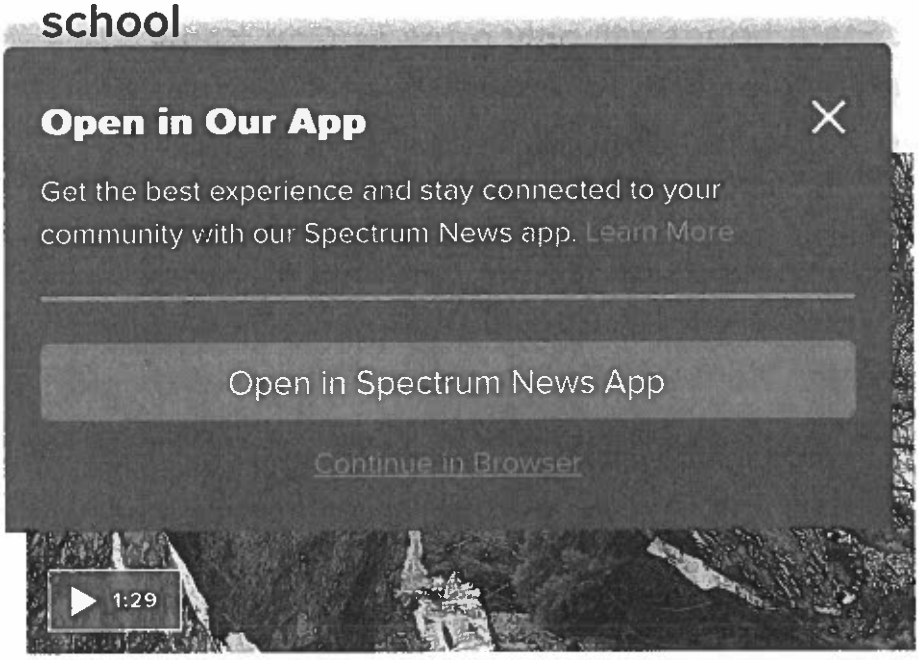

PUBLIC SAFETY

Heavy storm wreaks havoc on North Country

JEFFERSON COUNTY | 3 MONTHS AGO

PUBLIC SAFETY

Watertown water main break: Main pipe fixed

WATERTOWN | 5 MONTHS AGO

United States

U.S. solar expansion stalled by rural land-use protests

By **Nichola Groom**

April 7, 2022 7:45 AM EDT · Updated 2 years ago

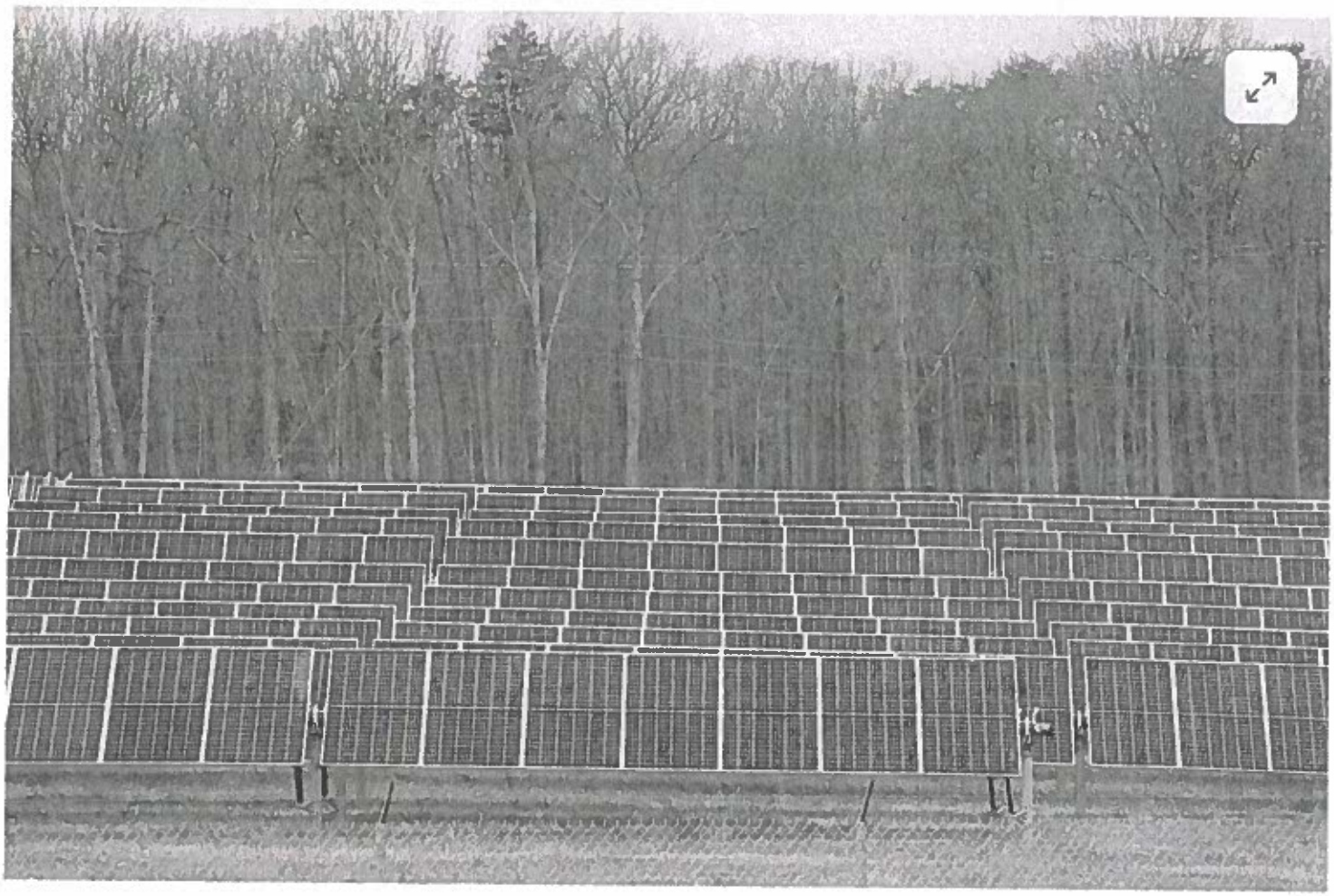

[1/32] Solar panels facing the sun are seen in the Spotsylvania Solar Energy Center, the largest solar project east of the Rockies, in Locust Grove, Virginia, U.S. April 4, 2022. REUTERS/Kevin Lamarque
Purchase Licensing Rights

Summary **Companies**

- **Utility-scale solar projects require far more land than comparable fossil-fuel plants**
- **Solar farms under attack as a blight on the small-town landscape**
- **Social media-fueled campaigns are blocking land-use permits**

April 7 (Reuters) - The Solar Star project in California is among the largest solar energy facilities in the world, boasting 1.7 million panels spread over 3,000 acres north of Los Angeles. Its gargantuan scale points to an uncomfortable fact for the industry: a natural gas power plant 100 miles south produces the same amount of energy on just 122 acres.

The dynamic encapsulates the industry's biggest obstacle to growth: Solar farms require huge amounts of land, and there's a fast-growing movement, fueled by politicized social-media campaigns, to prevent solar developers from permitting new sites in rural America.

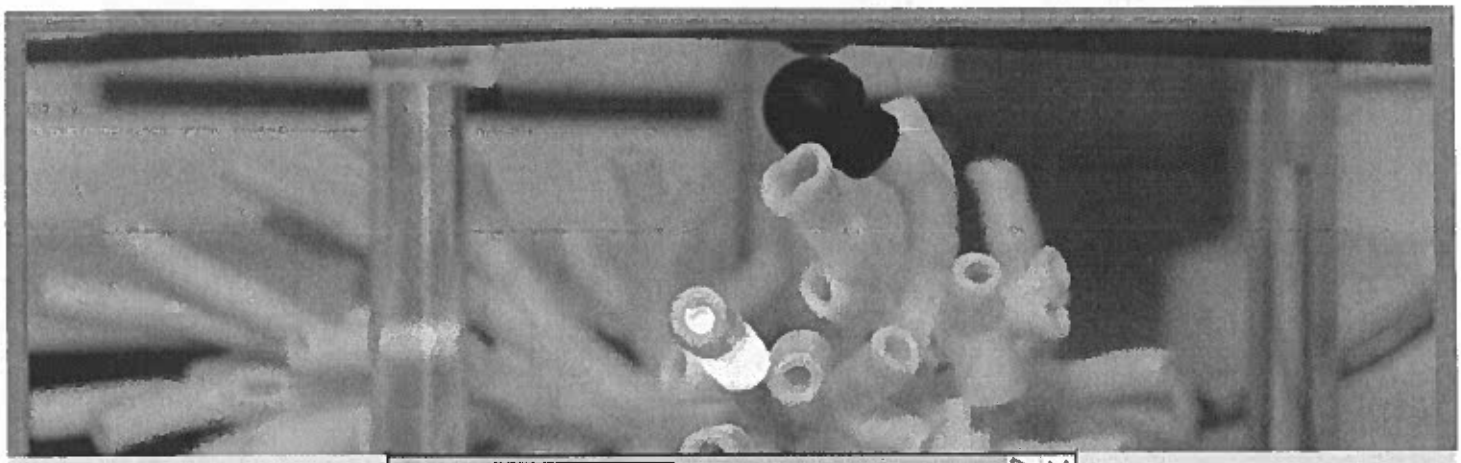

That's a major problem for the transition away from fossil fuels to combat climate change. Solar

currently makes up 3% of U.S. electricity supply and could reach 45% by 2050 to meet the Biden administration's goals to eliminate or offset emissions by 2050, according to the Department of Energy. To get there, the U.S. solar industry needs a land area twice the size of Massachusetts, according to DOE. And not any land will do, either. It needs to be flat, dry, sunny, and near transmission infrastructure that will transport its power to market.

As solar developers propose new, often sprawling projects in places like Kansas, Maine, Texas, Virginia and elsewhere, local governments and activist groups are seeking to block them and often succeeding. They cite reasons ranging from aesthetics that would harm property values to fears about health and safety, and loss of arable land, farm culture, or wildlife habitat.

"This is increasingly one of the top barriers that we're going to face," said Steve Kalland, executive director of the North Carolina Clean Energy Technology Center, a research center that supports clean energy development nationwide. "If we can't get projects sited and deployed, then we're going to have real problems on our hands."

WIN Learning Recognized in Three Categories in the 2024 EdTech Cool Tool Awards

BY WIN LEARNING

Officials at the White House and the Department of Energy, who are pushing for a rapid expansion of solar power, did not comment on the industry's land-acquisition problems.

In most cases, the opposition to these projects is being organized on Facebook, where the number of pages devoted to blocking solar development has exploded in recent years. The pages air a mix of legitimate concerns, such as the loss of scenic vistas, tree removal, and soil erosion, with misinformation about climate change and alleged health hazards from solar electricity. The false claims include arguments that climate change is a hoax to groundless assertions that solar farms leach the carcinogen cadmium into the soil and nearby waterways when it rains, or that they rarely produce electricity.

Reuters identified 45 groups or pages on Facebook dedicated to opposing large solar projects, with names such as "No Solar in Our Backyards!" and "Stop Solar Farms." Only nine existed prior to 2020, and nearly half were created in 2021. The groups together boast nearly 20,000 members.

"For every single large-scale solar project, you're seeing very well-organized opposition on social media," said Matthew Sahd, a solar market analyst for energy research firm Wood Mackenzie. "It's very impressive what these local communities are able to organize."

Beth Snider, of Virginia's Page County Citizens for Responsible Solar, said she believes solar developers are using the climate change issue to justify profit-making businesses that hurt the environment in other ways.

"The solar companies don't care about the environment - the farmland, and the rural communities they will destroy to get these projects," she said. "They are all about the money."

Construction of the first large solar projects, including Solar Star, completed in 2015, drew little opposition. They were sited mostly in remote areas such as the California desert. Now, tensions are rising as the sector plans bigger projects and reaches into more populated rural areas unfamiliar with solar.

The industry is expanding rapidly with government and corporate backing, and seeking permits or zoning revisions from county and town boards that oversee land use in residential neighborhoods and farmlands. Often, they are in politically conservative regions where citizens are less concerned about climate change and more supportive of fossil-fuel industries and jobs.

Their protests are persuasive. More than 1.7 gigawatts of proposed solar capacity was canceled during the permitting stage in 2021, according to an analysis by Wood Mackenzie conducted for Reuters. That's equivalent to a tenth of the 17 gigawatts of utility-scale solar capacity installed in the United States last year. Wood Mackenzie did not track the data on permitting prior to 2021.

Those figures do not account for the potential projects that have been preempted by locally imposed limitations or moratoria on solar applications. An analysis by Columbia Law School last year found 103 localities nationwide that have adopted policies to block or restrict renewable energy development – a list the report said is not exhaustive.

The American Clean Power Association, an industry trade group, said in a statement that the protests present a major challenge to the solar industry and threaten its role in addressing climate damage.

"Community concerns have made it harder for some developers to scale solar projects at the rate that science dictates that we need to," said David Murray, ACP's director of solar policy.

Site acquisition is at the top of the U.S. solar industry's list of threats to growth. In a poll of 44 developers last year by clean energy marketplace LevelTen Energy, 52% said permitting challenges were among the top three barriers to achieving the nation's solar energy goals and nearly 20% called out land availability. Other challenges included access to transmission lines and supply-chain disruptions.

"It's pretty obvious that, if there's a climate urgency, we're not behaving that way," said Armond Cohen, executive director of environmental group Clean Air Task Force. "There's this assumption that there's so much solar and wind available at such low cost, it's obviously going to get built... maybe it will, but something pretty serious is going to have to change."

ONLINE OFFENSE

Carrie Brandon's home sits near the proposed site for a 2,000-plus-acre solar farm that renewable-energy behemoth NextEra (NEE.N) hopes to build at the border of Kansas' Douglas and Johnson counties. When she heard about the planned 320-megawatt project, Brandon leapt into action to stop it. She hired a consultant, sent petitions to neighbors and produced a YouTube channel and Facebook site under the name Kansans for Responsible Solar.

"That's not what we signed up for," Brandon said, noting that she and her husband built their dream home on 40 acres in Douglas County in 2018.

Brandon says she does not oppose green energy but believes solar projects belong in places such as former industrial sites or on rooftops. She worries about her property value but said her primary concern is the health and safety of people residing nearby. She said she worries that herbicides on the site, used to prevent vegetation from growing on panels, could contaminate ponds and groundwater. She also said solar panels raise the risk of fires and health problems from exposure to electromagnetic fields.

"It's not about looking at it," she said. "It's about the health impacts."

Researchers have found no evidence to support increased fire risk or health concerns from solar panels.

Brandon found an ally in Kansas State Senator Mike Thompson, a Republican who has been criticized for spreading misinformation about the safety of COVID-19 vaccines and the science behind climate change.

"Why are we investing in all of these renewable sources of energy? A lot of people will say it's because we've got to combat climate change. And that is one of the biggest scams out there," Thompson, a former TV weatherman who chairs the Senate's utilities committee, said in a video on one of Brandon's sites.

Thompson did not respond to a request for comment.

Brandon says she considers some of the contributions on her group's Facebook page extreme but does not censor them. "I find opposing points of view to be stimulating conversation," she

said.

The impact of Brandon's group is being tested as Johnson County crafts zoning rules for large solar facilities that could determine the fate of the NextEra project. Planning officials initially drafted what would have been among the most restrictive rules for solar facilities in the nation - limiting leasing terms to a maximum 20 years and capping acreage at 1,000 acres - but were directed by a county board this week to reconsider their proposal next month.

NextEra's project is designed to last 30 years, and the company has already leased more than 2,000 acres of land.

A NextEra spokesperson did not comment on the opposition to its projects.

The Virginia solar protest group led by Beth Snider, in Page County, also uses Facebook to organize against solar development. Their focus is a 500-acre project in Virginia's Shenandoah Valley by Urban Grid, a unit of Canada's Brookfield Renewable (BEPC.N), one of the world's top renewable energy asset owners. Snider, who lives near the proposed site, worries it will mar the landscape.

Posts by her group's more than 500 members include wide-ranging criticisms of all kinds of renewable energy. One post included photos of solar panels in Arizona covered in snow and not producing electricity. Another cited a post from the climate change skeptic blog NoTricksZone saying that EV owners in Germany can barely afford to charge their vehicles because of surging electricity prices there.

The group brought an overflow crowd earlier this year to a planning meeting. After 33 people testified against the project - none in favor - the four-member panel voted unanimously to recommend rejection of the project by the county Board of Supervisors, which has a year to take up the application. Urban Grid would not comment on the project.

In central Texas, meanwhile, school district and county officials in at least four counties this year have dealt blows to solar development by refusing the requests of developers for tax breaks intended to ensure the projects are economical.

The projects would have generated millions in tax revenue over decades. Local officials, however, were convinced by arguments made by local residents on Facebook and in public meetings that the projects would undermine the region's rural culture and create few jobs.

"They call themselves solar 'farms,' which is irritating to me," Ron Pack, a landowner in Erath County, Texas, said in an interview. "They give the indication that it's all bunny rabbits and butterflies over there. And it's not. It's 2,400 acres of total destruction."

Pack, whose property is adjacent to where NextEra is planning a 225-megawatt solar plant, worries about soil erosion under the panels polluting the water of the nearby Bosque River.

Solar developers must often clear land of trees and other vegetation before they install their equipment to ensure the panels have unobstructed access to sunlight, which has in some cases led to erosion during heavy rains.

NextEra did not respond to requests for comment. On the project website, the company says: "No form of energy is free from environmental impact; however, solar energy has among the lowest impacts as it emits no air or water pollution."

NEW FRONT IN THE CULTURE WARS

The protests reflect declining support for renewables nationwide.

A Pew Research Center poll this year showed 69% of U.S. adults favored developing alternatives to fossil fuels, down from 79% two years ago. The drop came almost entirely from respondents on the political right, with just 43% of Republicans or those who lean Republican saying they support alternative energy development compared with 65% in 2020.

Joshua Fergen, a sociologist who has studied rural attitudes toward renewable energy development, said solar power has transformed into a subject of the U.S. culture war - a politically divisive issue along the lines of vaccine mandates, police reform or abortion.

"You can't divorce what you see on these anti-renewable Facebook groups from the larger political context," he said.

Residents of liberal-leaning areas, however, have also organized against large-scale solar installations.

Alameda County, a San Francisco Bay area Democratic stronghold, for example, is considering more restrictive solar policies after residents sued over the approval of a 100-megawatt project in a rural valley over concerns about the visual and environmental impact.

UTILITIES SQUEEZED

Local pushback could delay plans by utilities to retire aging coal plants and replace them with solar projects to appease climate-conscious investors and regulators.

The Northern Indiana Public Service Co (NIPSCO), for instance, plans to retire more than 2 gigawatts of coal and gas-fired generation by 2028, replacing it with wind and solar. But one of

the solar projects it had planned to start operating this year, a 200-megawatt facility in Boone County, was rejected last year by two separate local boards after residents organized against it, decrying the loss of farmland and rural culture, as well as the impact on views and local property values.

NIPSCO told Reuters that it continues trying to make the project work and remains confident about its broader clean-energy transition plan.

The difficulty finding workable solar project sites has led developers to pump up their bids for available land. Solar developers have been offering around $1,000 an acre for suitable land nationwide, far more than the $200 or so an acre landowners would get from a tenant farmer, according to Nathan Fabrick, executive vice president of solar for National Land Realty, a real estate brokerage that specializes in rural land.

"We get so many calls from landowners that are interested," he said.

It's a harder sell to communities as a whole, which often see little economic upside to offset the downsides of large installations, which often create only one or two full-time jobs.

The solar industry in some places has worked to make projects more palatable to the public. New Jersey, for instance, became a major market for solar despite the state's dense development, primarily by putting projects on landfills or other disturbed land. And Minnesota has voluntary standards that encourage establishing pollinator-friendly vegetation at solar sites to reduce environmental opposition. Such projects help dissuade local concerns about solar farms, according to the DOE.

The Land & Liberty Coalition - a pro-solar group backed by donors associated with the political left, such as the Rockefeller Brothers Fund and MacArthur Foundation - is also trying to improve the solar industry's chances by appealing to libertarian values. The coalition argues, for instance, that private landowners should be allowed to strike deals with developers without obstruction.

"Nobody ought to tell you, within reason of course, what you can and can't do with your land," said Tyler Duvelius, a spokesperson for the coalition.

The group has set up satellite offices in several states where battles over solar are raging, including Virginia, Indiana and Wisconsin, he said.

Landowners like Robert and Donna Knoche agree with the Land & Liberty Coalition's arguments. The couple has an agreement with NextEra for its Johnson County project in Kansas to lease hundreds of acres that have been in the family for generations, and they are hoping

their neighbors don't ruin their opportunity to make some money from it.

"Our six children, none of them are farmers," Robert Knoche, 94, said in an interview. "They'd probably get along better with NextEra than they would farming it."

> Get weekly news and analysis on the U.S. elections and how it matters to the world with the newsletter On the Campaign Trail. Sign up here.

Reporting by Nichola Groom; editing by Richard Valdmanis and Brian Thevenot

Our Standards: **The Thomson Reuters Trust Principles.**

Purchase Licensing Rights

Read Next

United States

Trump hush money trial: Tabloid publisher testifies he helped candidacy

5:19 PM EDT

Legal

US reaches $138.7 million civil settlement with victims of Larry Nassar

6:29 PM EDT

United States

US Supreme Court leans toward Starbucks in the case of pro-union workers

6:39 PM EDT

United States

US Congress poised to pass Ukraine aid, weapons coming soon

an hour ago

Citizens for Responsible Solar

10 reasons industrial-scale solar isn't right for agricultural-rural areas

1. Industrial-scale solar power plants should not be placed on land already zoned for A-1 (agricultural) and RA (rural area) use.

The local planning commission and boards of supervisors should vote to reject industrial-scale solar power plants based on this reason alone.

2. The land (forest, farmland, vegetation, soil) is forever destroyed.

Despite current discussions regarding decommissioning, the reality is that this rural land will be lost forever. Industrial-scale solar projects are typically for 30-40 years.

Construction of an industrial-scale solar power plant requires removal of trees, brush and root balls prior to installation of the arrays, creating an ecological wasteland. Grading, pile driving, blasting, electric cable trenching and road construction will compact the soil, likely delaying agricultural use for years after the project's end.

Stripping and compaction removes topsoil, destroys healthy soil organisms and allows for invasion of exotic plants that choke out native species.

3. Solar projects should not be placed near wetlands, rivers, streams, tributaries to avoid immediate damage to water quality,

and possible contamination-ecological disasters.

Uncontrolled runoff of water and topsoil is a well-documented byproduct of industrial-scale solar site development. This massive increase in watershed sedimentation impacts all downstream rivers and estuaries. Water contamination doesn't stop with the end of construction. Removal of all trees and deep-rooted plants, along with inadequate stormwater controls lead to long-term runoff and water contamination issues. Local municipalities usually do not have adequate resources to monitor construction and stormwater violations and, even when properly monitored, site developers have no problem paying fines, and there is no effective check on environmental damage.

4. Solar power plants destroy wildlife habitat.

Perimeter fencing, often 6-feet high and topped with barbed wire, will restrict movement of wildlife in the area. Removal of vegetation will impact bird population and other wildlife.

5. Solar power plants threaten preservation and should not destroy historic sites.

Many rural areas are the last undeveloped sites that contain prehistoric and historic archaeological deposits. Industrial development of these sites results in the irreversible loss of our history. In the Virginia Piedmont, this includes evidence of Native American settlements, early American settlement, Revolutionary and Civil War encampments and battlefields. Industrial development of these sites results in the irreversible loss of our history

6. A decline in eco and historical tourism.

Destruction of rural landscapes and areas of historic interest result in the decline in eco and historical-tourism (or may prevent the development

of these industries), reducing the prosperity of the local community.

7. Solar power generation is very inefficient when looking at the amount of land "consumed."

Solar power's inefficiency argues for proper siting on brownfields, industrial areas, and commercial and residential rooftops - not on open or forested, agricultural and rural land.

8. Undermining of local residents' property values.

Based on recent studies, the expected reduction in property value ranged from 5-25% depending on proximity.

9. The bill for decommissioning projects will likely be passed on to taxpayers.

Insufficient surety fund by the developer could result in county responsibility for decommissioning costs. Net Decommissioning costs can range from $43,584/MW to $101,915/MW. No plan and cost should ever be approved without a full understanding of the cost to return the land to its original condition, and the county should not be responsible for this cost.

10. When the local community has clearly expressed concern and opposition.

Local planning commissions and boards of supervisors should vote to reject industrial-scale solar power plants when people in the community oppose it. With time, greater awareness of solar issues and accountability will take place.

Citizens for Responsible Solar

PLEASE CONTACT US HERE TO JOIN OUR

EFFORT to protect agricultural-rural land from industrial-scale solar development.
We are a grassroots group of concerned citizens organized to promote responsible solar and other forms of renewable energy.
Destruction of habitat on an industrial scale is not green.

For our latest updates in your inbox fill in the below.

First Name *

Last Name *

Email *

☐ *I accept terms & conditions*

Submit

CONNECT & SUPPORT

Contact Us

Donate

CITIZENS FOR RESPONSIBLE SOLAR

Home

Video Hub

About Us

Culpeper's Story

Press Room

CITIZENS

Impacted Citizens

Page County

RESOURCES

Solar Toolkit for Citizens

Solar Ordinance

5 Things to Know About Solar

American Battlefield Report

Water- Ecological Concerns

Disclaimer: The information contained on the Citizens for Responsible Solar website is for general informational and educational purposes. The decision to use content on the Citizens for Responsible Solar website is the responsibility of the reader. While Citizens for Responsible Solar believes the information on its website is accurate, we encourage the reader to conduct their own research, as much information is subject to interpretation, and information may be updated, as new research, findings, materials, reports and studies become publicly available.

| Privacy Policy | Terms of Use |
Citizens for Responsible Solar is a 501(c)(4) Non-Profit Headquartered in Culpeper, Virginia

Air Cleaning Specialists, Inc.
11088 Gravois Industrial Court
St. Louis, MO 63128

Ph: (866) 210-8855 (tel:(866) 210-8855)
Email: info@fumeavent.com (mailto:info@fumeavent.com)

The Dangers of Vehicle Exhaust

To put it simply, Carbon monoxide Kills! Working near exhaust fumes exposes you to poisonous carbon monoxide (CO) gas, which is present in large amounts in vehicle exhaust fumes.

Overexposure to this odorless and colorless gas can cause death. Even mild exposure to CO can cause headaches, dizziness, nausea and fatigue.

Diesel exhaust, the ubiquitous black smoke that can be seen streaming out of large trucks, has recently been getting a lot of attention.

The Natural Resources Defense Council (NRDC) launched a Dump Dirty Diesels Campaign with the ad slogan in 1996: "Standing behind this bus could be more dangerous than standing in front of it." After eight years of research, the California air resources board (CARB) finally declared the soot, or particulate matter, from diesel exhaust to be a cancer causing pollutant.

CARB also identified forty chemicals found in diesel exhaust as toxic air pollutants. The U.S. Environmental Protection Agency (EPA) is currently conducting its own study of the health impacts of diesel exhaust.

They have already introduced new regulations reducing al[illegible]s and buses. The new standards, however, will not be applied u[illegible]el vehicles.

Diesel exhaust can cause a number of health impacts, which are listed in Table 1. The exhaust contains some known carcinogens and hazardous materials. Arsenic, benzene and nickel, are known carcinogens among many other suspected carcinogenic components of diesel exhaust.

The exhaust contains 38 other components that are hazardous pollutants listed by the EPA. (compared to the 40 recently identified by the CARB) including suspected carcinogens benzo[a]pyrene, 1,3-butadiene, and formaldehyde.

The exhaust itself is listed as a probable carcinogen by the EPA, NIOSH (National Institute for Occupational Safety & Health), and IARC (International Agency for Research on Cancer).

Vehicle Exhaust Removal Systems

(/exhaust-hose/crushproof/FLT400.html)

Crushproof (/exhaust-hose/crushproof/FLT400.html)

(/overhead-systems/rope-and-pulley/SDP-4C-0415-C.html)

Overhead (/overhead-systems/rope-and-pulley/SDP-4C-0415-C.html)

(/exhaust-hose-reels/spring-operated/HRS-3-0420.html)

Hose Reels (/exhaust-hose-reels/spring-operated/HRS-3-0420.html)

There is plenty of evidence from studies with rats and mice that diesel exhaust is carcinogenic. However, it is listed only as a "probable carcinogen" because the ubiquitous nature of diesel exhaust makes human carcinogenicity extremely difficult to prove. Diesel exhaust is very strongly linked with lung cancer, especially

for people who are occupationally exposed. Higher incidences of bladder cancer from occupational exposure to diesel exhaust have also been suggested but are still not proven. In addition to concerns over cancer, diesel exhaust has also been identified as a mutagen. Biochemical changes are induced or intensified in cells by mutagens, radiation being a famous example.

Table 1: Possible Health Effects of Diesel Exhaust

Type	Effects
Non-cancerous	Respiratory ailments, Asthma, Headache, Runny eyes & nose, and Nausea
Carcinogenic	Increased risk of lung cancer
Mutagenic	Increased rate of mutations

The EPA and Harvard School of Public Health as well as other experts in public health estimate that particulates in the air are responsible for at least 60,000 premature deaths in the U.S. each year [1].

Researchers believe majority of the health risk from diesel exhaust is caused by PM, which can carry many harmful organics and metals.

The PM averages 0.1 to 0.25 microns (1 x 10 -6 meters), with 75 percent of particles less than 1 micron. This is a size range easily inhaled, resulting in possible lung cancer or non-cancerous lung damage.

The particulate matter also, like other forms of air pollution, has the greatest impact on children, asthmatics, and the elderly.

Non-cancer toxicity from chronic exposure to diesel exhaust causes such respiratory ailments as airway restrictions, reduced pulmonary function, and immunological and allergenic reactions. This is much like the effect of smoking cigarettes, however, the inhalation of diesel exhaust is involuntary.

Acute exposure can cause tissue irritation and permanent respiratory damage. Exposure and sickness from diesel exhaust is usually hard to pinpoint, since affected people can exhibit cold-like symptoms of headache, runny eyes and nose, nausea, and asthma-like responses.

Exposure usually occurs directly through breathing exhaust, though particles can deposit on skin as well. Once inside the body, the pollutants are absorbed through tissue to the bloodstream and eventually are excreted as other toxins in the body are.

In addition to the health effects discussed above, most of the pollutants from diesel exhaust are regulated by federal air standards called NAAQS (National Ambient Air Quality Standards).

The standards were set up by the 1970 Clean Air Act to protect public health and welfare. Today, NAAQS put limits on the concentration in the air of CO, NO2, SO2, PM, Hydrocarbons excluding methane, Ozone, and lead.

When areas, such as Houston-Galveston for example, exceed these concentrations of air pollutants, they are said to be non-attainment areas and the state must create a plan (SIP -state implementation plan) to reduce pollutant concentrations below the NAAQS.

Air emissions of diesel exhaust are more than just another air pollution issue. Diesel exhaust can deposit onto water, soil, and vegetation, contaminating anything it comes into contact with. It contributes to global warming because it contains the greenhouse gases methane and carbon dioxide and fine carbonaceous PM.

Diesel exhaust also contributes to acid deposition because it contains nitric and sulfuric acids and other substances which can be transformed to acidic PM in the atmosphere.

The NOx portion of diesel emissions also contributes to ozone (O3) formation and eutrophication of coastal waters (spurring algae to bloom to such an extent that the algae blocks sunlight from aquatic life beneath the surface).

The contribution of NOx to the formation of ozone is significant in the Houston-Galveston area because it is a non-attainment area for ozone air pollution standards.

Ozone in the troposphere (caused by pollution), as opposed to stratospheric ozone (the good ozone) has been known to exacerbate asthmatics and increase hospital admissions on high ozone concentration days.

Exhaust emissions come from mobile sources, stationary area sources (oil & gas production and industrial), and stationary point sources including industrial, electric utilities, and commercial-institutional sources.

From mobile sources, heavy duty engines emit 60 percent of NOx, 17 percent of hydrocarbons, and close to 90 percent of total particulate emissions [3].

The following Figures 1 -3 show the sources of NOx, VOCs, and CO in the Houston-Galveston area in 1993. From these figures, it is apparent that mobiles sources in this area contribute to a significant amount of the total NOx and CO pollution, 31 and 57 percent respectively.

Though diesel emissions in Texas have not been studied extensively, California has analyzed its own diesel exhaust problem extensively.

In 1990, approximately 3.3 billion gallons of diesel fuel were burned in internal combustion engines in California, producing almost 58,000 tons of highly respirable diesel exhaust.

Motor vehicles emit ~ 70% of diesel exhaust particular matter (PM) in California in 1990. A study in Vienna, Austria showed that diesel exhaust comprised 12 - 33 % of total PM in the air.

Knowing this, one can easily ponder whether it's safer to stand in front of a truck or behind it. Diesel exhaust is a serious threat to public health.

[1] NRDC's Dump Dirty Diesels Campaign: The Facts on Fumes in New York City, 5/96.
[2] Williams, Paul T., G. E.. Andrews, and Keith D. Bartle, 1987, The Role of Lubricating Oil in Diesel Particulate and Particulate PAH Emissions, Society of Automotive Engineers, Inc.
[3] Regulators, Engine Makers Agree on Plan to Begin Reducing Diesel Emissions in 2004, Environment Reporter, 1995, p. 565.
[4] Volkswagen, 1989, Unregulated Motor Vehicle Exhaust Gas components, Volkswagen AG, Research and Development (Physico-Chemical Metrology), Project Coordinator: Dr. K.-H. Lies, 3180 Wolfsburg 1, F. R. Germany.

Components of diesel exhaust.

Also known as diesel fumes, diesel exhaust is a complex mixture of gases and diesel particulate matter (DPM). Components include

- carbon monoxide
- carbon dioxide
- sulphur dioxide
- nitrogen oxides
- aldehydes including benzene and formaldehyde
- hydrocarbons
- polycyclic aromatic hydrocarbons (PAHs)

- soot (carbon)

The major component of diesel exhaust is soot (60%-80%). This is what you see coming out of the exhaust pipe.

Most of the DPM, also known as fine particulate matter, consists of particles so tiny they are easily inhaled and deposited in the lower lungs where they cause various health effects.

Effects of Diesel Exhaust.

The small particles in diesel exhaust are readily inhaled and deposited deep into the lung tissue. These particles may cause damage to lung tissue. Pre-existing diseases, such as emphysema, asthma, or heart disease, can be aggravated by diesel exhaust.

Some short-term (or acute) health effects are:

- Irritation of the eyes, nose, & throat
- Vomiting
- Light-headedness
- Headache
- Heartburn
- Numbness
- Tightness in the chest
- Tingling in the extremities
- Wheezing

In addition to these immediate problems, diesel exhaust can cause chronic health problems. The National Institute for Occupational Safety and Health (NIOSH) considers diesel exhaust a potential human carcinogen (cancer-causing substance). It may take many years after the first exposure for diesel-related cancer and other health impacts to develop.

NIOSH Fire Fighter Fatality Project

In fiscal year 1998, President Clinton and Congress recognized the need to address the continuing national problem of fire fighter fatalities, and funded NIOSH to undertake National Fire Fighter Fatality Investigation Project.

Briefly, the overall goal of this program is to better define the magnitude and characteristics of work-related deaths and severe injuries among fire fighters, to develop recommendations for the prevention of these injuries and deaths, and to implement and disseminate prevention efforts. A five-part integrated plan, centered on the field investigation of fire fighter fatalities, is outlined below.

Cardiovascular Disease Fatality Investigations

Cardiovascular disease (CVD) has been a significant cause of work-related death among fire fighters for many years. This NIOSH activity includes a multi-factorial assessment of personal, physiological, psychological and organizational factors associated with CVD deaths among fire fighters while on duty. Other factors are considered such as measurement of carbon monoxide and assessment of other exposures and body burdens

at various types of fires. http://www.cdc.gov/niosh/fire/

1. NFPA 1500 states "the carcinogenic effect of diesel exhaust is present even if the particulates (soot) are filtered out of the exhaust (www.nfpa.org)
2. Even low doses of carbon monoxide contained in diesel exhaust will double the risk of heart attacks in humans of a given age category (Windsor Occupational and Health Council)
3. When nitrogen dioxide attaches itself to carbon particles of diesel exhaust, it is able to travel deep into the lung, where they collect along the bronchial-alveolar network and thereby damage the lungs defense mechanisms. This is particularly serious for a fire fighter who may already have some respiratory illness. (Windsor Occupational and Health Council PDF)
4. An International Personnel Protection, Inc. study concludes: "diesel exhaust can penetrate into and absorb onto clothing, furniture, and other items which fire fighters routinely get in contact with, where it can later absorb into a fire fighters skin" (International personnel Protection, Inc report PDF)

A. Source Capture - Capture at the source is the only feasible method to eliminate all diesel exhaust from the firehouse or garage. (www.NFPA.org)

- The capture 'at source' of airborne particles before they can spread throughout the local environment is the most efficient method of achieving a safe and healthy working environment.
- By minimizing air removal and movement there is a reduction in investment in air handling equipment and immediate savings can be made in energy consumption – reducing costs – increasing profits.

B. Ventilation

If an alternative energy source is not feasible, there are still ways to reduce worker exposure. Diesel exhaust in enclosed areas (such as idling, fueling, maintenance and cleaning areas) can be controlled using both local exhaust ventilation and general ventilation.
Local exhaust ventilation is the most effective ventilation system. It removes diesel exhaust before it gets into the air workers breathe. Tailpipe or stack exhaust hoses should be attached to a vehicle running indoors and exhausted to a place, such as the roof, where it will not re-enter the facility.
General ventilation involves using roof vents, opening doors and windows, roof fans, floor fans, or other mechanical systems to move air through the work area. General ventilation is not as effective as local exhaust ventilation.

C. Isolate the Worker from the Exhaust

As many workers as possible should be relocated away from areas containing diesel exhaust. This will prevent needless exposure for workers not directly involved in operating or maintaining diesel-powered vehicles.
Operator exposure to diesel exhaust should be controlled by closing the cab windows when vehicles are running. Air conditioned cabs are critical to providing this safeguard year round.
While diesel gases can seep into vehicle cabs when the windows are closed, this will limit contact with the particulate matter found in diesel exhaust.

Vehicle Exhaust Solutions

SOME ILLUMINATION —

Do solar farms lower property values? A new study has some answers

Researchers looked at sale prices of 1.8 million homes near utility-scale solar plants.

DAN GEARINO, INSIDE CLIMATE NEWS - 3/15/2023, 12:02 PM

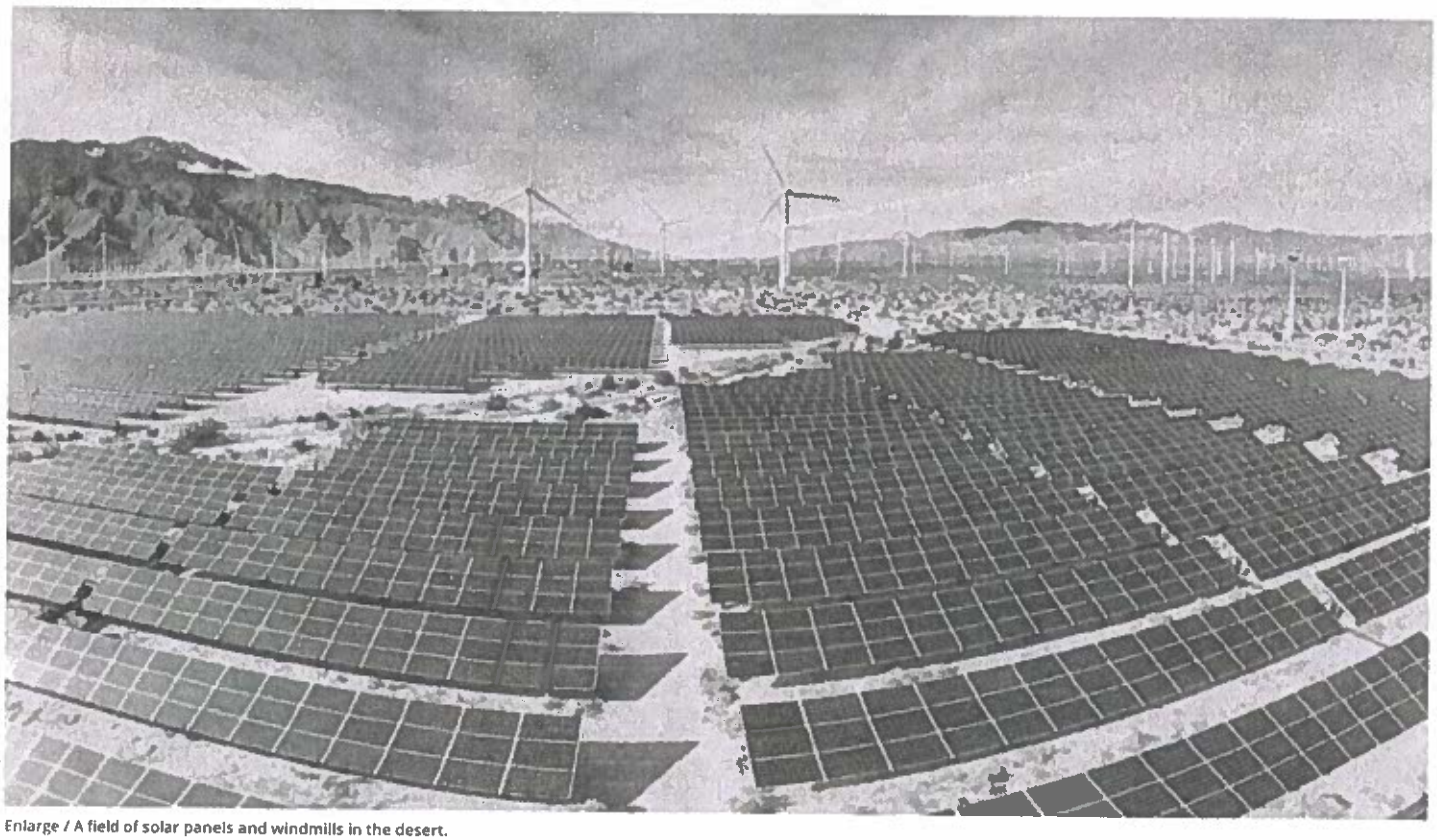

Getty

Enlarge / A field of solar panels and windmills in the desert.

A new study finds that houses within a half-mile of a utility-scale solar farm have resale prices that are, on average, 1.5 percent less than houses that are just a little farther away.

The research from Lawrence Berkeley National Laboratory helps to refute some of the assertions of solar opponents who stoke resistance to projects with talk of huge drops in property values. But it also drives a hole through the argument made by people in the solar industry who say there is no clear connection between solar and a drop in values.

The authors analyzed 1.8 million home sales near solar farms in six states and found diminished property values in Minnesota (4 percent), North Carolina (5.8 percent), and New Jersey (5.6 percent). The three other states—California, Connecticut, and Massachusetts—had price changes that were within their margins of error, which means the price effects were too close to zero to be meaningful. The paper was published in the journal Energy Policy.

The authors accounted for differences in property features, inflation, and other factors in order to isolate the effect of proximity to solar.

Ben Hoen, a co-author and research scientist at the Lawrence Berkeley lab, said the numbers are clear but additional research is needed to understand what's happening on the local level to lead to these price effects.

"We have a sense of the 'what,' but we don't know the 'why,'" he said.

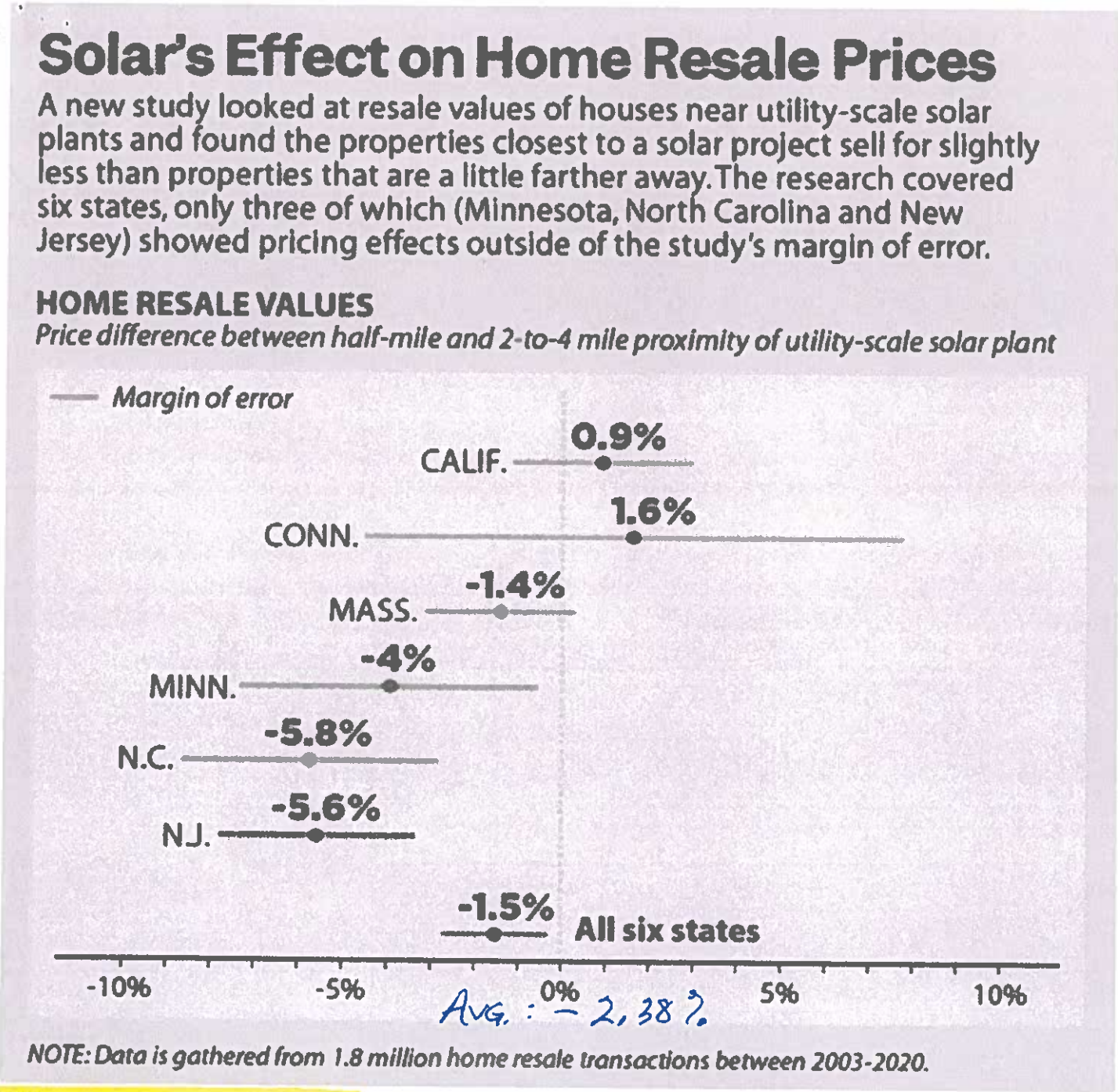

Enlarge / Data from Lawrence Berkeley National Laboratory.

For example, he doesn't have a thorough explanation for why the price differences are higher in some states than others.

The researchers chose this group of states because they were, except for Connecticut, the top five in the country for the number of solar installations of at least 1 megawatt as of 2019. They included Connecticut because it is an example of a state with a high population density near solar projects.

Hoen emphasized that the results show a period in time, with transactions that occurred from 2003 to 2020, and may not reflect prices right now.

Also, he noted that the paper's analysis doesn't take into account any of the financial benefits of solar for landowners and communities, which may include payments from the developer and a decrease in local taxes.

The study is being released at a time of rapid expansion in the number and size of solar projects, which is a key part of the country's push to reduce the emissions that contribute to climate change.

The scale of growth in solar development has been met with an intensifying resistance in local communities where some people argue that the projects are ugly and pose a threat to property values and human health. Solar opponents amplify these concerns on social media.

Of all the arguments against solar, the idea that it will hurt property values has been among the most potent, based on prior reporting by Inside Climate News about the local debates. At public hearings and in comments filed with regulators, some residents talk about how they fear reductions of 40 percent or more.

This story originally appeared on Inside Climate News.

READER COMMENTS 215

Biomarkers, from diagnosis to treatment

Scott Manley Reacts To His Top 1000 YouTube Comments

Teach the Controversy: Dowsing

WATCH
Biomarkers, from diagnosis to treatment

Biomarkers, from diagnosis to treatment

To find cancer before it strikes, look for the molecular clues

More videos

← PREVIOUS STORY

NEXT STORY →

Related Stories

Today on Ars

Chapter 165. Zoning

Article IV. District Regulations

§ 165-15. Application.

The regulations set by this chapter within each district shall be minimum regulations and shall apply uniformly to each class or kind of structure or land, and particularly, except as hereinafter provided:

A. No building, structure or land shall hereafter be used or occupied and no building or structure or part thereof shall hereafter be erected, constructed, reconstructed, moved or structurally altered except in conformity with all the regulations herein specified for the district in which it is located.

B. No building or other structure shall hereafter be erected or altered to exceed the height, to accommodate or house a greater number of families, to occupy a greater percentage of lot area or to have narrower or smaller yards or other open spaces than herein required or in any other manner contrary to the provisions of this chapter.

C. No part of a yard or other open space or off-street parking or loading space required about or in connection with any building for the purpose of complying with this chapter shall be included as part of a yard, open space or off-street parking or loading space similarly required for any other building, except as provided in § **165-37**.

D. No yard or lot existing at the time of enactment of this chapter shall be reduced in dimension or area below the minimum requirements set forth herein. Yards or lots created after the effective date of this chapter shall meet at least the minimum requirements established by this chapter.

§ 165-16. Multiple principal uses.

[Added 12-12-2000 by L.L. No. 1-2000]
Multiple principal uses shall be permitted in one or more buildings located on any approved lot in the NB, GB, LI and GI Districts.

§ 165-17. District regulations.

District regulations shall be as in §§ **165-18** through **165-34**.

§ 165-18. A-80 Agriculture District (80,000 square feet lot size).

[Amended 7-27-1981 by L.L. No. 4-1981; 7-28-1992 by L.L. No. 4-1992; 5-25-1993 by L.L. No. 2-1993]

A. Intent. The intent in creating Agricultural Districts is to protect predominantly agricultural areas from suburban and urban development, encourage the continuation of agriculture, reduce land use conflicts and preserve open space and natural resources.

A. Intent. The intent in creating Residential Two-Family Districts is to provide for a variety in dwelling unit and structure types to accommodate the needs of Town residents.

B. Permitted principal uses:

(1) Two-family detached dwellings.

(2) Principal uses permitted in the R-1-15 District.

C. Permitted accessory uses:

(1) Accessory uses permitted in the R-1-15 District.

(2) Public donation bins, subject to the provisions of § **165-65.2B** of this chapter.
[Added 12-22-2009 by L.L. No. 6-2009]

D. Special permit uses:
[Added 5-25-2010 by L.L. No. 4-2010]

(1) Special permit uses allowed in the RS-25 District, except for on-site-use wind energy systems which shall not be a specially permitted use in this district.

(2) Rooming and lodging houses.

§ 165-25. RMF Residential Multiple-Family District.

A. Intent. The intent in creating Residential Multiple-Family Districts is the same as that specified for R-2 Districts in § **165-24** of this chapter.

B. Permitted principal uses:

(1) Multiple-family dwellings, subject to provisions contained in § **165-79** of this chapter.

(2) Two-family detached dwellings.

(3) Principal uses permitted in the R-1-15 District.

C. Permitted accessory uses:

(1) Accessory uses permitted in the R-1-15 District.

(2) Public donation bins, subject to the provisions of § **165-65.2B** of this chapter.
[Added 12-22-2009 by L.L. No. 6-2009]

D. Special permit uses:

(1) Major home occupations.
[Amended 12-22-2009 by L.L. No. 6-2009]

(2) Public buildings.

(3) Essential services and structures, excluding power plants, maintenance yards, storage yards and personal wireless telecommunications facilities.
[Amended 4-22-1997 by L.L. No. 3-1997]

(4) Cemeteries.

(5) Rooming and lodging houses.

(6) Mobile home parks.

§ 165-26. RB Restricted Business District.

A. Intent. The intent in creating Restricted Business Districts is to provide areas for the location of professional and administrative offices, service uses and related activities in a setting which is attractive and convenient for public use while establishing employment opportunities and broadening the tax base. This district is intended to act as a buffer between residential areas and more intensively used business and industrial districts.

B. Permitted principal uses.
[Amended 3-24-1987 by L.L. No. 1-1987; 8-9-1988 by L.L. No. 8-1988]

(1) Business, professional and executive offices, including but not limited to offices for attorneys, architects, engineers, surveyors and accountants, real estate and insurance agents and salespersons, but not including retail sales, manufacturing or servicing of merchandise of any kind on the premises.

(2) Uses for the treatment and care of human beings, including but not limited to medical and dental offices and clinics for physicians, osteopaths, dentists, chiropractors, chiropodists, podiatrists, opticians, optometrists and ophthalmologists, all excluding any overnight occupancy or overnight care.

(3) Banks and lending institutions.

(4) Employment agencies.

(5) Artists of performing arts studio, photography studio, excluding the sale or rental of photographic supplies or equipment.

(6) Public or private membership clubs, lodges or fraternal organizations, neighborhood or community centers, YMCA or YWCA.

(7) Barbershops, beauty shops, hair salons and other personal service shops or uses.

(8) Public buildings and grounds.

(9) Similar uses to those listed above, which do not involve retail sales or services, may be permitted subject to special use permit approval by the Town Planning Board and a finding by the Board that such use is of the same general character as those permitted in this district and that such use, if permitted, will not cause adverse impacts or be detrimental to other uses within the district or to adjoining land uses.

C. Permitted accessory uses:

(1) Banks are permitted to have drive-in tellers if at least 10 reservoir spaces are provided for each drive-in teller's window.

(2) A restaurant, newsstand, pharmacy or accessory storage area incidental to a permitted principal use, but only when conducted and entered from within the building, and provided that no exterior display or advertising, other than permitted signage, is made of such use.
[Amended 3-24-1987 by L.L. No. 1-1987; 8-9-1988 by L.L. No. 8-1988]

(3) Off-street parking and loading areas, subject to the provisions of § **165-37** of this chapter.

(4) Signs, subject to the provisions of § **165-38** of this chapter.

(5) Residential uses within a structure in combination with other permitted uses, provided that such residential uses are accessory to the business conducted and are located elsewhere than on the street frontage of the ground floor and have a minimum area as required under § **165-79F**.

(6) Fences, subject to the provisions of § **165-61** of this chapter.

(7) Swimming pools, subject further to the provisions of § **165-62** of this chapter.
[Added 12-12-2000 by L.L. No. 1-2000]

(12) Fast-food and drive-in restaurants.
[Amended 3-24-1987 by L.L. No. 1-1987; 8-9-1988 by L.L. No. 1-1988]

(13) Commercial greenhouse or plant nursery or similar commercial agricultural uses.
[Added 3-24-1987 by L.L. No. 1-1987; amended 8-9-1988 by L.L. No. 8-1988]

(14) Rentals of automobiles, trucks, trailers or other vehicles.
[Added 3-24-1987 by L.L. No. 1-1987; amended 8-9-1988 by L.L. No. 8-1988]

(15) Mini-warehouse structures, subject further to the provisions of § **165-84.1** of this chapter.
[Added 3-24-1987 by L.L. No. 1-1987; amended 8-9-1988 by L.L. No. 8-1988; 12-20-2005 by L.L. No. 4-2005]

(16) Shopping plazas and shopping malls.
[Added 3-24-1987 by L.L. No. 1-1987; amended 8-9-1988 by L.L. No. 8-1988]

(17) Essential services and structures, excluding power plants, maintenance yards, storage yards and including personal wireless telecommunications facilities.
[Added 4-22-1997 by L.L. No. 3-1997]

(18) On-site-use wind energy systems.
[Added 5-25-2010 by L.L. No. 4-2010]

(19) Large-scale ground-mounted solar PV systems.
[Added 1-25-2022 by L.L. No. 2-2022]

E. Additional provisions and requirements. The additional provisions and requirements applicable in RB Restricted Business Districts, § **165-26E**, shall apply in GB General Business Districts.
[Amended 3-24-1987 by L.L. No. 1-1987; 8-9-1988 by L.L. No. 8-1988; 8-11-1998 by L.L. No. 4-1998]

§ 165-29. LI Limited Industrial District.

A. Intent. The intent in creating Limited Industrial Districts is to provide areas where light industrial uses may locate, said areas being suited for this purpose due to location, availability of utilities, proximity to transportation facilities and relationship to other land uses, as well as to provide job opportunities and expand the local tax base. This district specifically excludes residences other than a residence of a caretaker of a horse stable for not less than 10 horses to be kept on the premises, on the theory that the mixture of other residential uses and public services and facilities for residences with those for industry is contrary to the purposes of this chapter.
[Amended 6-10-1986 by L.L. No. 4-1986]

B. Permitted principal uses:

(1) Warehouses for enclosed storage of goods and materials, distribution centers, wholesale businesses, excluding the bulk storage of fuel and other flammable liquids or gases.

(2) Research and development laboratories.

(3) Administrative, banking, professional or executive offices.

(4) Essential services, excluding power plants.

(5) Agricultural operations.

(6) Stables.

(7) Health care facility.
[Added 2-26-2013 by L.L. No. 2-2013]

C. Permitted accessory uses:

(1) Banks are permitted to have drive-in tellers if at least 10 reservoir spaces are provided for each drive-in teller's window.

(2) A restaurant, newsstand, barbershop, hairdresser or other incidental personal service in connection with a permitted use, but only when conducted and entered from within the building, provided that no exterior display or advertising shall be made of such use.

(3) Off-street parking and loading areas, subject to the provisions of § **165-37** of this chapter.

(4) Signs, subject to the provisions of § **165-38** of this chapter.

(5) Fences, subject to the provisions of § **165-61** of this chapter.

(6) Public donation bins, subject to the provisions of § **165-65.2B** of this chapter.
[Added 12-22-2009 by L.L. No. 6-2009]

D. Special permit uses:

(1) Restaurants, including fast-food and drive-in.

(2) Airports.

(3) Hotels and motels.

(4) Motor vehicle service stations.

(5) Public buildings and grounds.[1]

[1] *Editor's Note: Former Subsection D(6), Truck terminals, which followed this subsection, was repealed 2-26-2013 by L.L. No. 2-2013, which local law also renumbered former Subsections D(7) through D(13) as D(6) through D(12).*

(6) Assembly and fabrication operations, provided that such uses are conducted entirely in an enclosed building and will not produce smoke, noise, vibration, glare, dust or any other similar emission which may be detectable beyond the property limits of such operations.
[Amended 6-10-1986 by L.L. No. 4-1986]

(7) A residence for a caretaker of a horse stable for not fewer than 10 horses to be kept on the premises.
[Added 6-10-1986 by L.L. No. 4-1986]

(8) Essential services and structures, excluding power plants, maintenance yards, storage yards and including personal wireless telecommunications facilities.
[Added 4-22-1997 by L.L. No. 3-1997]

(9) Outdoor storage of materials used in conjunction with a permitted use occurring on the premises as further regulated under § **165-83** of this chapter.
[Added 12-12-2000 by L.L. No. 1-2000]

(10) Excavation operations as further regulated under § **165-71** of this chapter.
[Added 12-12-2000 by L.L. No. 1-2000]

(11) Mini-warehouse structures, subject further to the provisions of § **165-84.1** of this chapter.
[Added 12-20-2005 by L.L. No. 4-2005]

(12) On-site-use wind energy systems.
[Added 5-25-2010 by L.L. No. 4-2010]

(13) Large-scale ground-mounted solar PV systems.
[Added 1-25-2022 by L.L. No. 2-2022]

(14) Agricultural/construction equipment repairs and painting operations.
[Added 3-22-2022 by L.L. No. 3-2022]

E. Additional provisions and requirements.
[Amended 12-12-2000 by L.L. No. 1-2000]

(1) Additional provisions and requirements applicable in RB Districts shall apply in LI Districts.

(2) No industrial structure shall be permitted within 100 feet of the nearest boundary line of any residential district.

(3) All utilities serving industries in this district shall be placed underground.

(4) Residential uses are prohibited.

(5) All processes shall take place within an enclosed building. Incidental storage out-of-doors shall be shielded from view from public streets and adjacent off-street parking areas by fencing, landscaping or other appropriate measures.

(6) Any vibration, odor, glare, heat or noises resulting from operations shall not be evident beyond the property line.

(7) Operations shall not result in the dissemination of smoke, dust, chemicals or odors into the air to such a degree as to be detrimental to the health, welfare and safety of the residents of the surrounding areas.

§ 165-30. GI General Industrial District.

A. Intent. The intent in creating General Industrial Districts is to provide areas for industrial uses which will provide employment opportunities and expand the local tax base. Said areas are considered suitable for this purpose because of their location, availability of utilities, proximity to transportation facilities and relationship to other land uses.

B. Permitted principal uses:

(1) Principal uses permitted in the LI District.

(2) Production and assembly operations, provided that such uses are conducted entirely within an enclosed building and will not produce smoke, noise, vibration, glare, dust or any other similar emission which may be detectable beyond the property limits of such operation.

(3) Agricultural operations.

(4) Stables.

(5) Contractors' storage yards.

C. Permitted accessory uses:

(1) Accessory uses permitted in the LI District are permitted accessory uses in the GI District.

(2) Public donation bins, subject to the provisions of § **165-65.2B** of this chapter.
[Added 12-22-2009 by L.L. No. 6-2009]

D. Special permit uses:

(1) Restaurants, including drive-in and fast-food.

(2) Airports.

(3) Hotels and motels.

(4) Motor vehicle repair stations and/or motor vehicle service stations.
[Amended 12-12-2000 by L.L. No. 1-2000]

Safety of Grid Scale Lithium-ion Battery Energy Storage Systems

EurIng Dr Edmund Fordham MA PhD CPhys CEng FInstP
Fellow of the Institute of Physics

Dr Wade Allison MA DPhil
Professor of Physics, Fellow of Keble College, Oxford University

Professor Sir David Melville CBE FInstP
Professor of Physics, former Vice-Chancellor, University of Kent

Sources of wind and solar electrical power need large energy storage, most often provided by Lithium-Ion batteries of unprecedented capacity.

Incidents of serious fire and explosion suggest that the danger of these to the public, and emergency services, should be properly examined.

5 June 2021

Executive Summary

1. Li-ion batteries are dominant in large, grid-scale, Battery Energy Storage Systems (BESS) of several MWh and upwards in capacity. Several proposals for large-scale solar photovoltaic (PV) "energy farms" are current, incorporating very large capacity BESS. These "mega-scale" BESS have capacities many times the Hornsdale Power Reserve in S. Australia (193 MWh), which was the largest BESS in the world at its installation in 2017.
2. Despite storing electrochemical energy of many hundreds of tons of TNT equivalent, and several times the energy released in the August 2020 Beirut explosion, these BESS are regarded as "articles" by the Health and Safety Executive (HSE), in defiance of the Control of Major Accident Hazards Regulations (COMAH) 2015, intended to safeguard public health, property and the environment. The HSE currently makes no representations on BESS to Planning Examinations.
3. Li-ion batteries can fail by "thermal runaway" where overheating in a single faulty cell can propagate to neighbours with energy releases popularly known as "battery fires". These are not strictly "fires" at all, requiring no oxygen to propagate. They are uncontrollable except by extravagant water cooling. They evolve toxic gases such as Hydrogen Fluoride (HF) and highly inflammable gases including Hydrogen (H_2), Methane (CH_4), Ethylene (C_2H_4) and Carbon Monoxide (CO). These in turn may cause further explosions or fires upon ignition. The chemical energy then released can be up to 20 times the stored electrochemical energy. Acute Toxic gases and Inflammable Gases are "dangerous substances" controlled by COMAH 2015. Quantities present "*if control of the process is lost*" determine the applicability of COMAH.
4. We believe that the approach of the HSE is scientifically mistaken and legally incorrect.
5. "Battery fires" in grid scale BESS have occurred in South Korea, Belgium (2017), Arizona (2019) and in urban Liverpool (Sept 2020). The reports into the Arizona explosion [8, 9] are revelatory, and essential reading for accident planning. A report into the Liverpool "fire" though promised for New Year 2021, has not yet been released by Merseyside Fire and Rescue Service or the operator Ørsted; it is vital for public safety that it be published very soon.
6. No existing engineering standards address thermal runaway adequately, or require measures (such as those already used in EV batteries) to pre-empt propagation of runaway events.
7. Lacking oversight by the HSE, the entire responsibility for major accident planning currently lies with local Fire and Rescue Services. Current plans may be inadequate in respect of water supplies, or for protection of the local public against toxic plumes.
8. The scale of Li-ion BESS energy storage envisioned at "mega scale" energy farms is unprecedented and requires urgent review. The explosion potential and the lack of engineering standards to prevent thermal runaway may put control of "battery fires" beyond the knowledge, experience and capabilities of local Fire and Rescue Services. BESS present special hazards to fire-fighters; four sustained life-limiting injuries in the Arizona incident.
9. We identify the well-established hazards of large-scale Li-ion BESS and review authoritative accounts and analyses of BESS incidents. An internet video [10] is essential initial instruction.
10. We review engineering standards relating to Li-ion BESS and concur with other authorities that these are inadequate to prevent the known hazard of "thermal runaway". We conclude that large-scale BESS should be COMAH establishments and regulated appropriately. We respectfully request evidence from the HSE that "mega-scale" BESS are *not* within the scope of COMAH.
11. We seek the considered response of relevant Government Departments as well as senior fire safety professionals to these concerns.

Contents

1. Introduction

Lithium-ion (Li-ion) batteries are currently the battery of choice in the 'electrification' of our transport, energy storage, mobile telephones, mobility scooters etc. Working as designed, their operation is uneventful, but there are growing concerns about the use of Lithium-ion batteries in large scale applications, especially as Battery Energy Storage Systems (BESS) linked to renewable energy projects and grid energy storage. These concerns arise from the simple consideration that large quantities of energy are being stored, which if released uncontrollably in fault situations could cause major damage to health, life, property and the environment.

Table 1. Comparison of some recent "battery fires" since 2014.
Note: this is not a comprehensive list of all Li-ion BESS battery "fires."

Location	Size	"Battery fire" cause	Time to bring under control	Water needed for cooling	Comments
Houston, Texas, April 2021	0.1 MWh	Driverless vehicle crash	4 hours	30,000 (US) gallons	Tesla Model S
South Korea	Various; 21 fires during 2018-19	Not known to Korean Ministry of Trade Industry and Energy	various	Not known	522 out of 1490 ESS facilities in Korea suspended (Korea Times 2 May 2019)
Drogenbos, Belgium. 2017	1 MWh	Not known.	"rapidly extinguished"	Not known	Occurred during commissioning of system by ENGIE
McMicken Facility Arizona, USA. 2019	2 MWh	Thermal runaway in a single rack out of 27 that were in the cabin – hence 74 kWh electrochemical energy released – less than the Tesla Model S crash.	2 hours from first report to "deflagration"		Explosion as H_2 and CO mixed with air and ignited. Critically injured 4 fire-fighters. Extensive forensic report.
Carnegie Rd, Liverpool, UK, 2020	20 MWh	Not known	11 hours		Full report [1] delayed 4 months; still unpublished.

Even battery electric vehicle (BEV) batteries store energy sufficient for "fires" that have taken hours to control. A Tesla Model S crashed In Texas on the weekend of 17-18 April 2021 igniting a BEV battery fire that took 4 hours to control with water quantities variously reported [2] as 23,000 (US) gallons or 30,000 gallons (87 -115 m^3). Yet the energy storage capacity in even the latest Tesla Model S vehicles is only 100 kWh. This is 1/20 the size of the BESS in Arizona [3] which failed in 2019, and 1/200 the size of the BESS in Liverpool [4] which caught fire [5] in September 2020, and 1/7000 the capacity of the Cleve Hill Solar Farm and Battery Store [6] approved in May 2020.

The past decade has seen a number of serious incidents in grid-scale BESS, which are summarised in Table 1. Despite these incidents, and our growing understanding of these, these large scale Li-ion BESS are not currently regarded by HSE as regulated under the COMAH

Regulations 2015. The legal basis for this attitude is unclear – simple calculations summarised in this paper argue that they should be – and the issue may yet be challenged in judicial review.

The reason the COMAH regulations should apply is the scale of evolution of toxic or inflammable gases that will arise in BESS "fires". In the Drogenbos incident (2017, Table 1), the inhabitants of Drogenbos and surrounding towns were asked to keep all windows and doors shut; 50 emergency calls were made from people with irritation of the throat and airways[1]. A chemical cloud which "initially had been enormous", was charted by helicopter. The Belgian Fire Services could not control what was described as "the chemical reaction" and filled the cabin with water. Fears of an explosion with 20 metre flames kept people confined for an hour. Although the initial visible flames were controlled quickly, cooling continued over the next 36 hours.

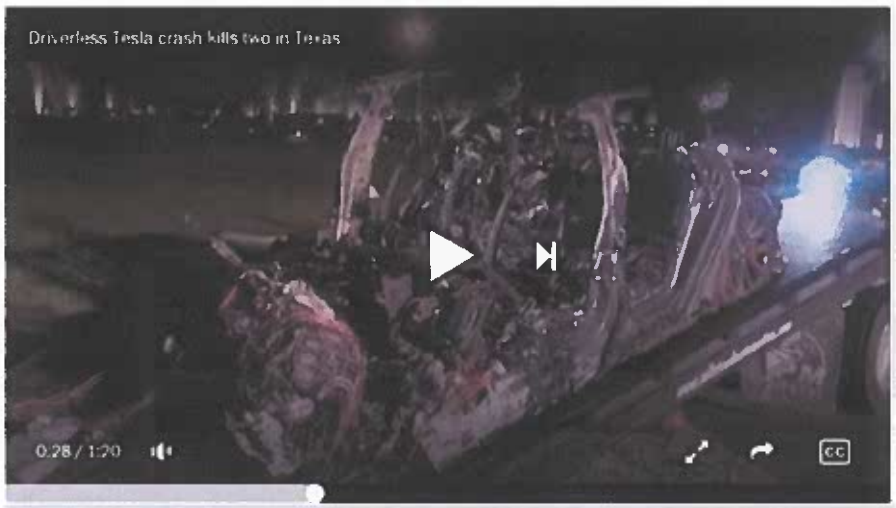

Two men died after a Tesla vehicle, which authorities said was operating without a driver, crashed into a tree in a Houston suburb on April 17. (Reuters)

Figure 1: Remains of the Tesla Model S crash and fire, 17 Apr 2021, after 4 hours and 30,000 gallons. Battery capacity 100 kWh.

Figure 2: Remains of a Korean BESS destroyed by a "battery fire". An energy storage system was destroyed at the Asia Cement plant in Jecheon, North Chungcheong Province, on Dec. 17. Courtesy of North Chungcheong Province Fire Service Headquarters (Korea Times 2 May 2019)

[1] Tom Vierendeels (2017) "Explosiegevaar by brand in Drogenbos geweken : 50-tal oproepen van mensen die zich onwel voelen door rook." *Het Laatste Nieuws,* 11 November 2017

Figure 3: "Battery Fire" at Drogenbos, Belgium 11 Nov 2017. Taken at the start of the incident and 15 minutes later (eye-witness footage). 1 MWh facility; fire occurred during commissioning.

Figure 4: The 2 MWh McMicken (Arizona) BESS after the explosion on 19 April 2019

Figure 5: The 20 MWh BESS at Carnegie Rd, Liverpool. Courtesy Ørsted.

Figure 6: The fire at Carnegie Road, 15 Sep 2020. Liverpool Echo report, which took 11 hours to control.

The incidents recorded in Table 1 are all in relatively small BESS or a single BEV. Yet "mega-scale" BESS are now planned on a very large scale in many current proposals in the UK, listed in Table 2 and illustrated in the subsequent Figures.

And no engineering standards are currently applied to pre-empt future accidents in grid-scale BESS, the most critical of which would be design features aimed at preventing the phenomenon of "thermal runaway", the process whereby failure in single cell causes over-heating and then propagates to neighbouring cells so long as a temperature (which can be as low as 150 °C) is maintained.

BEV batteries do now include thermal barriers or liquid cooling channels between all cells to safeguard against this phenomenon, but no such engineering standards exist for grid-scale BESS. A large BESS can pass all existing engineering design and fire safety test codes and still fail in thermal runaway – by now a well-known failure mode. This must be urgently addressed.

The consequences of major BESS accidents could be significant and emergency services need adequate plans in place to handle any such incident.

Table 2. "Mega" scale solar plant and/or Li-ion BESS in Australia and the UK*

Project	Location	Status	Solar PV Scheme Size	Battery Stores	Battery type	Battery capacity
Hornsdale Power Reserve	S. Australia	Operational	Not directly associated	Single site	Li-ion	193 MWh
Cleve Hill Solar + Battery Store	Kent	Permission granted (2020)	350 MW; land coverage 890 acres	Single site	Li-ion	700 MWh
Sunnica Solar + Battery Store(2)	Cambridgeshire/ Suffolk	Pending submission	500 MW; land coverage approx. 2792 acres	31.5 ha of land over 3 compounds [7] of 5.2, 10.7 and 15.6 ha	Li-ion	Undeclared. Estimate 1500 – 3000 MWh
Longfield Solar + Battery Store	Essex	Pending statutory consultation	500 MW; land coverage approx. 1400 acres	Stated as 3.7 acres: number of sites TBD	Li-ion	Undeclared. Estimate: 150 MWh

* Li-ion technology has been assumed in all these proposals as Li-ion battery electrochemistry is dominant in grid-scale BESS applications (deployment at this scale is unlikely to involve technologies with lesser experience). Estimated values for Battery Capacity for the Sunnica are calculated based on the McMicken facility in Arizona (Appendix 1) and the Cleve Hill DCO. For the Longfield site it is estimated from Energy Institute guidance on energy density [25] at about 100 MWh ha^{-1}. The exact specification for the battery units has not been disclosed by the developers at this present time.

Figure 7: The Hornsdale Power Reserve (South Australia) in the process of expansion from 100 MW/129 MWh to 150 MW/193.5 MWh, as of November 2017.

Figure 8: a "typical" BESS compound (abstracted from Sunnica PEIR, Ch 3)

Plate 3-10. Typical battery storage compound configuration (*Image reproduced courtesy of Fluence Energy*).

Figure 9: Artists impression of Tesla 250 MWh "Megapack".
Sunnica may have 3 ×this capacity in just one of its three BESS compounds.

2. Leading Concerns

The main concerns regarding large scale Li-ion BESS are:

1) The potential for failure in a single cell (out of many thousands) to propagate to neighbouring cells by the process known as "thermal runaway". Believed to be initiated by lithium metal dendrites growing internally to the cell, a cell may simply discharge internally releasing its stored energy as heat. Even sound Li-ion cells will spontaneously discharge internally if heated to temperatures which can be as low as 150 °C, releasing their stored electrical energy, thus overheating neighbouring cells and so on. Temperatures sufficient to melt aluminium (660 °C) at least have been inferred from analyses of such thermal runaway accidents. Eye-witness reports consistently speak of repeated "re-ignition" which is inevitable, even in the complete absence of oxygen, so long as the temperature anywhere exceeds the thermal runaway initiation threshold.
2) The emission of highly toxic gases – principally Hydrogen Fluoride – for prolonged periods, in the event of thermal runaway or other battery fires. At a minimum, respirators and complete skin protection would be required by any fire-fighters. Measures to protect the public from toxic plumes would also be necessary.
3) The emission of large quantities of highly inflammable gases such as Hydrogen, Methane, Ethylene and Carbon Monoxide even if a fire suppression system is deployed. These gases will be evolved from a thermal runaway accident regardless of such measures, with explosion potential as soon as they are mixed with air and in contact with hot surfaces. Such an explosion was the cause of the "deflagration event" at McMicken, Arizona in 2019 in a 2 MWh BESS, which critically injured four fire-fighters and was triggered simply by opening the cabin door.
4) The absence of any adequate engineering and regulatory standards to prevent or mitigate the consequences of "thermal runaway" accidents in Li-ion BESS.
5) The potential for thermal runaway in one cabin propagating to a neighbouring cabin. In Arizona [3] there were reports of *"fires with 10-15 feet flame lengths that grew into 50 - 75 feet flame lengths appearing to be fed by flammable liquids coming from the cabinets"*.
6) The significant volumes of water required to thoroughly cool the system in the event of a "fire", and how this water will be contained and disposed of (since this will be contaminated with highly corrosive hydrofluoric acid and, therefore, must not be allowed to drain into the surrounding environment).

Such incidents are routinely and repeatedly described in the Press as "battery fires" though they are not "fires" at all in the usual sense of the word; oxygen is completely uninvolved. They represent an electrochemical discharge between chemical components that are self-reactive. They do not require air or oxygen at all to proceed.

Hence the traditional "fire triangle" of "Heat, Oxygen, Fuel" simply does not apply, and conventional fire-fighting strategies are likely to fail (Figure 10, over).

Thermal runaway events are uncontrollable except by *cooling* all parts of the structure affected – even the deepest internal parts – below 150 °C. This basically requires water, in large volumes.

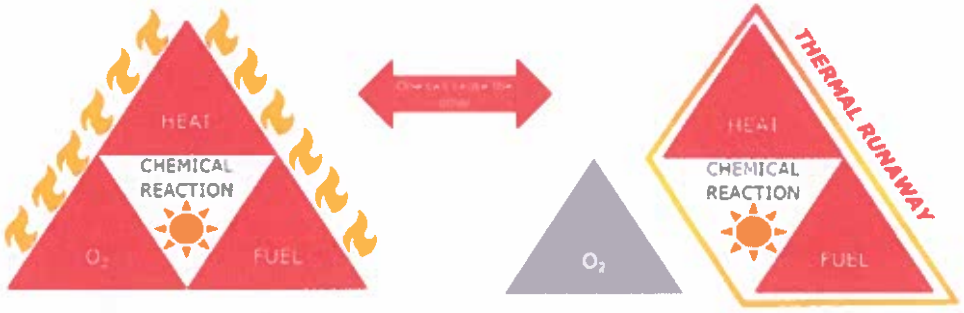

Figure 11 The fire triangle and its relationship to thermal runaway

Figure 10: The traditional "fire triangle" does not apply to "thermal runaway".

3. Thermal Runaway (Battery "fires")

Li-ion batteries are sensitive to mechanical damage and electrical surges, both in over-charging and discharging. Most of this can however be safeguarded by an appropriate Battery Management System (BMS) and mechanical damage (unless deliberate and malicious) should not be a hazard. Internal cell failures can arise from manufacturing defects or natural changes in electrodes over time; these must be regarded as unavoidable in principle. Subsequent escalation into major incidents can propagate from such apparently trivial initiation.

In July 2020 a thorough failure analysis by Dr Davion Hill of DNV GL [8] was prepared for the Arizona Public Service (APS), following the April 2019 thermal runaway and explosion incident in the 2 MWh Li-ion BESS facility at McMicken, Arizona. This report is revelatory and more detailed than any other failure analysis known to us. It is essential reading for any professional involved in fire safety planning for major BESS. (Figures 11 to 13).

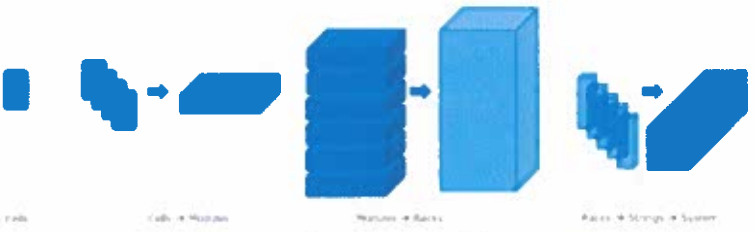

Figure 11: Cells stack into Modules; Modules into Racks; Racks into Strings; Strings into Systems.

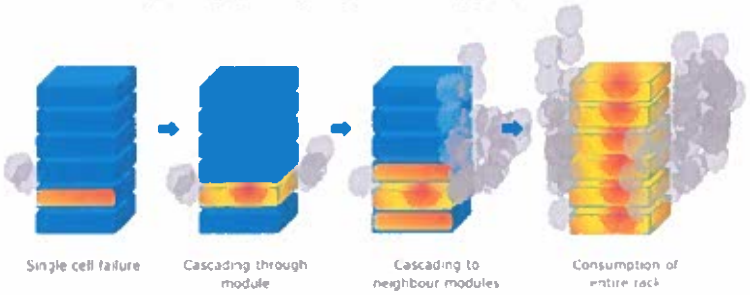

Figure 25 A single cell failure propagated through Module 2, then consumed the whole rack, releasing a large plume of explosive gases. This process could have occurred without visible flame, which would explain why the gases were not burned as they were emitted.

Figure12: Propagation of single Cell failure through Module; cascade to entire Rack.

A report by Underwriters Laboratories (UL) on the same incident [9] is less technical on the physics and engineering of the underlying causes and failure modes, but more comprehensive in terms of practical situations and consequences found, and suffered, by the "first-responders". Two fire-fighters suffered life-limiting brain injuries, one suffered spinal damage and fourth facial lacerations. This report is similarly essential reading for any fire and emergency response planning.

Figure 13: Destruction of Rack at McMicken.

Detail: molten aluminium pools (exceeded 660 °C)

Figure A.1 Photograph taken during decommissioning of the ESS shows a pool of solidified aluminum on the floor in front of Rack 15 [11].

Forensic analysis [8] of the 2019 Arizona "fire" identified a failure mode different from mechanical abuse or electrical mis-management. The initiating failure was localised to a single cell at a known position in the rack. Although the cell itself was of course destroyed during the incident, the failure mode is believed to have been lithium metal deposition and abnormal growth of lithium metal dendrites. These phenomena were also found in randomly selected *undamaged* cells from the same BESS and also from a different BESS of the same manufacture elsewhere. These phenomena must be regarded as common, and inherent to the cells themselves.

The lithium metal deposits will react with air moisture, causing overheating and smoke. Battery swelling, electrolyte degradation, and internal short circuits are all possible modes of failure with internal discharge and generation of locally intense heat.

Because of the known thermal breakdown of even non-faulty cells, above a threshold temperature (which can be as low as 150 °C), the loss of even a single individual cell can rapidly cascade to surrounding cells, resulting in a larger scale "fire." This is "thermal runaway" in which failures propagate from cell to cell within "modules" and from module to module within a "rack".

This is what happened at McMicken [8], with temperatures sufficient to melt Aluminium (660 °C) being reached. Such "fires" can be extremely dangerous to fire fighters and other first responders because, in addition to the immediate fire and explosion risks, they would have to deal with toxic gases (principally hydrogen fluoride HF, also hydrogen cyanide HCN and other fluorine compounds such as phosphoryl fluoride POF_3) and exposure to other hazardous materials.

Rack to rack propagation fortunately did not happen at McMicken, though an explosion did [8]. A local conventional fire involving the plastics materials or gases evolved from them could have

initiated rack-to-rack propagation; the only essential factor would have been sufficient heat to trigger thermal breakdown in just one cell in a neighbouring rack. Li-ion cells have been observed to eject molten metal during thermal runaway, another possible mode of propagation over distance. Propagation through a subsequent rack would then occur by exactly the same thermal runaway mechanisms, and potentially beyond between neighbouring cabins in large-scale BESS.

Thermal runaway is illustrated in dramatic fashion with tiny commercial Li-ion cells in a useful internet video [10] (Figure 14). The commercial cells involved in this demonstration have tiny capacities: a mere 2.6 Ah or about 10 Wh for typical terminal voltages.

A Tesla Model S would have the capacity of about ***10,000*** such cells.
A 20 MWh BESS has the capacity of about ***2 million*** such cells.

In the video, the cell is deliberately over-heated on a small electric stove. The fully charged cell goes into thermal breakdown, eventually rupturing the can. The cell flies off as a rocket and seconds later is discharged but red hot and will burn anything combustible. Although not illustrated, it is evidently hot enough to produce the same thermal breakdown in an adjacent cell within a battery.

This illustrates the damage done to a non-faulty cell, simply by overheating externally.

Figure 14: (a) A charged 2.6 Ah cell being deliberately overheated. (b) at the point of rupture (c) the cell takes off as a rocket (d) seconds later the discharge is complete, and the cell is red hot.

4. Toxic and flammable gas emissions

During a Li-ion "battery fire," multiple toxic gases including Hydrogen Fluoride (HF) [11], Hydrogen Cyanide (HCN) [13] and Phosphoryl Fluoride (POF_3) [11] may be evolved. The most important is Hydrogen Fluoride (HF), which may be evolved in quantities [11] up to 200 mg per Wh of energy storage capacity.

HF is toxic in ppm quantities and forms a notoriously corrosive acid (Hydrofluoric Acid) in contact with water. It is toxic or lethal by inhalation, ingestion and by skin contact. The ERPG-2 concentration (1 hour exposure causing irreversible health effects) given by Public Health England is just 20 ppm; the workplace STEL (15 minute Short-Term Exposure Limit) is just 3 ppm [12]. Major emissions of HF would form highly toxic plumes that could easily threaten nearby population centres, workplaces and schools.

Appendix 3 contains calculations of projected toxic gas quantities for 3 grid-scale battery stores that have been approved or are pending review by the Planning Inspectorate (Table 2).

The calculated capacities at the "mega-scale" sites listed in Table 2 are tens, or even hundreds, of times larger than the facilities in Table 1, which experienced significant fires or explosions.

In addition to evolution of toxic gases, even in an inert atmosphere (without Oxygen), multiple flammable gases (such as Hydrogen H_2, Carbon Monoxide CO, Methane CH_4, and Ethylene C_2H_4) would be evolved during thermal runaway. These are "typical of plastics fires" [8] and have been measured in sealed vessel tests [13]. As noted by Hill/DNV [8] and others [13], the proportions of H_2, CO, CH_4 and C_2H_4 do not in fact vary greatly between different cell technologies, simply because the chemical nature of the envelope polymers, separators, electrolyte solvents and electrolytes themselves do not differ greatly. The variations between Li-ion technologies are in the electrode systems, which are typically not polymeric.

Such inflammables can clearly create (ordinary, air-fuel) fires or explosions once mixed with air/oxygen. It is important to note that the Heats of Combustion of the inflammables may be up to 15 – 20 × the rated electrical energy storage capacity of the BESS. This has been demonstrated by the same tests which determined the quantities of HF evolved [11]. These were fire tests, not sealed vessel tests [13]. The stored electrical energy is therefore by no means a conservative estimate of the total energy release which could be released in a major (air-fuel) fire in a BESS, irrespective of whether the initiating cause was a conventional fire or Li-ion cell thermal runaway.

Appendix 2 estimates the inflammables potentially evolved from the BESS given in Table 2.

5. Total Energy Release Potential

Any large energy storage system has the risk that energy released in malfunction will be uncontrollable in ways that will do major damage. BESS can release electrochemical energy in the form of thermal runaway or "battery fires". In addition they can release chemical energy in the form of explosions or conventional fires of inflammable gases, or of polymer components. Many thermal runaway "fires" have now happened, as has explosion of evolved inflammable gases.

An important indicator of the foreseeable scale of a "worst credible hazard" is provided by the total stored energy in the system. For BESS, this comprises two components:

(i) The stored electrical energy which might be released in the event of thermal runaway incidents, a self-reactive electrochemical energy release not requiring oxygen at all, and

(ii) Stored chemical (fuel) energy which might be released in complete combustion of the inflammable gases which might be released by (i).

Electrochemical energy release is uncontrollable once started, by any measure except cooling – of all cells and cell parts – below about 150°C. Water is the only fire-fighting substance with the necessary heat capacity. Concurrent conventional fire would first heat cells above the thermal runaway temperature, causing more thermal runaway. Chemical energy release from inflammable gases is also uncontrollable once those gases are mixed with air and ignited: explosions result.

What might be the scale of such energy releases? The Sunnica proposal is estimated to have a stored energy between 1.5 – 3.0 GWh in total, spread across 3 separate sites called Sunnica East A, Sunnica East B and Sunnica West A (see calculations in Appendix 1). It is between 2 – 4 times the capacity projected for Cleve Hill (700 MWh). It is 8 – 15 times the capacity (193 MWh) of the "Hornsdale Power Reserve" in Australia, at installation (2017) the world's largest.

Compared to other energy storage technologies, the Dinorwig Pumped Storage Scheme in Snowdonia stores about 9 GWh [14]; the Sunnica BESS corresponds to 17 – 33 % of Dinorwig.

Compared to major explosions, the energy released in the Beirut warehouse explosion of August 2020 has been estimated [15] by Sheffield University at about 0.5 kilotons of TNT (best estimate) with a credible upper limit of 1.12 kilotons. A totally independent estimate [16] (based on seismic propagation instead of eye-witness footage) gives the same range, without specifying a "best" estimate. The popular measure of major explosions in "kilotons of TNT" has an agreed definition[2] of 1.162 GWh of released energy; in this paper we shall take "one Beirut" to be an explosive energy of 0.5 kilotons of TNT or about 580 MWh of released energy.

The projected BESS storage at Sunnica corresponds to 1.4 – 2.7 kilotons of TNT in total, across all three sites. In the "low" case, this would be "0.92 Beiruts" at the Sunnica West A site alone, or "2.7 Beiruts" over the whole scheme. In the "high" case "2.7 Beiruts" could be stored in the Sunnica East B site alone. Note that these are stored electrochemical energy only; the potential for conventional fire or explosion of evolved inflammables could be **up to 20 × larger** [11]. See Table 3, Appendix 1.

This is plainly a quantity of stored energy which, if released uncontrollably, could do major damage. Explosions and fires at individual BESS are matters of record. They can propagate from failure in a single cell out of many thousands. Cell-to-cell and module-to-module propagation occurred at McMicken. Rack-to-rack propagation was avoided, but could readily occur if continuous

[2] See e.g. Wikipedia.

fires start. Cabin-to-cabin propagation of a major BESS "battery fire" would be the critical link that would escalate major but manageable fires into catastrophes.

Yet this propagation route remains unanalysed. Significantly, Commissioner Sandra D Kennedy of the Arizona State Commission [3] reviewed reports on the 2019 McMicken battery fire and also a 2012 battery fire at the APS Eldon substation facility in Flagstaff, AZ. She quotes the Flagstaff fire department report on the latter incident as referencing :

"Fires with 10-15 feet flame lengths that grew into 50 - 75 feet flame lengths appearing to be fed by flammable liquids coming from the cabinets".

Finally, in the context of BESS, "Stranded Energy" will remain a hazard at any affected BESS cabins even assuming an initial incident is controlled. The accident investigation at McMicken required nearly 3 months, simply to discharge "stranded energy" safely [8].

'"Mega-scale" Li-ion BESS should, in all prudence, require the highest level of regulation. The COMAH regulations are designed for this, including establishments where dangerous substances may be generated "if control of the process is lost" [17] in a thermal runaway accident.

6. Applicability of the COMAH (Control of Major Accident Hazard) Regulations 2015

The governing criteria for application of the COMAH Regulations [17] are:

1. The presence of hazardous materials, or their generation, "if control of the process is lost."
2. The quantity of such hazardous materials present or that could be potentially generated.

There is no doubt that hazardous substances such Hydrogen Fluoride (an Acute Toxic controlled by COMAH) would be generated in a BESS accident (i.e., in "battery fires"). Similarly highly Inflammable Gases (also controlled by COMAH) would be evolved even if the atmosphere remained oxygen-free. Depending on the size of the "establishment" these could be produced in sufficient quantities to be in the scope of COMAH. In Appendix 2 we estimate quantities guided by the literature, where fire tests have directly measured evolution of the hazardous gases.

For small capacity BESS installations, under 25 MWh capacity, the quantities ("inventory") of the evolved hazardous substances might be outside COMAH. This paper however addresses the recent trend towards "mega-scale" Li-ion BESS (Table 2) with very large quantities of stored energy, where the inventory should be large enough to bring the installation within scope.

Broadly speaking, the threshold for applicability of COMAH will be dependent on the precise BESS technology chosen, but likely to be for BESS in the region of 20 – 50 MWh. See Appendix 2.

A letter to the HSE regarding applicability of COMAH to large-scale BESS (dated 25 Nov 2020 [18]) received no reply until follow-up letters were sent addressed personally to the Chief Executive on 7 February 2021, with the intervention of Mrs Lucy Frazer MP. The reply from the Chief Executive [19] dated 22 February 2021 stated that "*Li-ion batteries are considered articles and are not in scope of COMAH*".

We believe the current attitude of the HSE – that even large-scale Li-ion BESS are "articles" best regulated by operators – is not consistent with the law.

Unless tested in the Courts however, this throws the entire responsibility for ensuring the safety of major BESS "battery fires" onto the Fire and Rescue Services. Currently the HSE makes no representation to the Planning Inspectorate in respect of BESS hazards.

7. Engineering standards for BESS

As with any hazard, the basic principles of Prevention and Mitigation must be applied to minimise the risk to life, property and the environment. A major contribution of the Hill/DNV report [8] is a review of current engineering and fire protection standards. This did not concern planning, siting and electrical standards, but simply addresses the question: which standards, if any, offer Prevention or Mitigation of the phenomenon of thermal runaway? The answer appears to be none.

"Thermal runaway" is an electrochemical reaction, well-known in Li-ion BESS, that is largely uncontrollable once started. Since failures in single cells (among many thousands) can be sufficient to initiate thermal runaway, the only known Prevention measure is that adopted by the BEV industry, viz. thermal isolation of neighbouring cells, so that if failure occurs in any one cell, insulation or water cooling prevents easy thermal spread to neighbouring cells. Various design strategies have been adopted in BEV Li-ion batteries, usually involving some form of thermal barrier.

However these are not widely used in grid-scale Li-ion BESS. Current practice is the assembly of stacks of cells, typically "pouch" cells which are externally flat polymer bags, that are stacked side by side in low profile modules with no thermal isolation. This is not the construction adopted in current generation BEV batteries; BEV practice *(with* thermal isolation) extended to grid-scale BESS would obviously increase costs and complexity considerably.

The engineering standards reviewed by Hill/DNV [8] included NFPA 855, UL 1973 and UL 9540/9540A. UL 9540A is a US standard that is widely used in grid-scale BESS engineering, is routinely recommended by insurance and risk consultants [20] and was appealed to by the developer of the Cleve Hill solar farm (Table 2). The problem is that UL9540A is fundamentally a test procedure. It mandates no design features. It requires absolutely nothing that would prevent thermal runaway in any BESS design. This means that an operator can say truthfully that a given BESS is "fully compliant" with UL9540A, yet this would provide no assurances at all regarding thermal runaway prevention. It is therefore wholly insufficient as a safeguard to either the operator, the public, or to emergency services.

NFPA 855 [21], uniquely, requires evaluation of thermal runaway in a single module, array or unit and recognises the need for thermal runaway protection. However, it assigns that role, with complete futility, to the Battery Management System (BMS). Thermal runaway is an electrochemical reaction which once started cannot be stopped electrically. It is uncontrollable by electronics or switchgear. A BMS can locate faults, report and trigger alarms, but it cannot stop thermal runaway.

The Hill/DNV report [8] highlights the many shortcomings of existing standards, see Appendix 4. The basic issue is simple:

(1) Thermal Runaway has very few means of Mitigation once started.

(2) It is therefore essential to address Prevention as a priority.

(3) ***No current engineering or industry standards require the Prevention of thermal runaway events by thermal isolation barriers.***

Nothing in existing standards prevents runaway incidents happening again, requiring for initiation only single-cell failures from known common defects in cell manufacture.

8. Fire Safety Planning for BESS "fires"

Taking the recent Sunnica BESS proposal as an example, a joint statutory consultation response has been submitted by the four Local Authorities concerned. The Local Authorities in this case are Cambridgeshire and Suffolk County Councils, and West Suffolk and East Cambridgeshire District Councils. This joint consultation response [22] included a section on Battery Safety (pp 74-75) and states as follows:

***Suffolk Fire and Rescue Service (SFRS)** will work and engage with the developer as this project develops to ensure it complies with the statutory responsibilities that we enforce.*

Sunnica should produce a risk reduction strategy as the responsible person for the scheme as stated in the Regulatory Reform (Fire Safety) Order 2005. It is expected that safety measures and risk mitigation is developed in collaboration with services across both counties.

The response also later states: *As with all new and emerging practices within UK industry, the **SFRS would like to work with the developers** to better understand any risks that may be posed and develop strategies and procedures to mitigate these risks.*

It is clear that local Fire and Rescue Services have been given the lead responsibility for independent emergency planning, in concert with the developers. Because of the attitude of the HSE refusing to exercise regulatory control over BESS safety, local Fire and Rescue Services become the sole independent public body able to influence BESS safety issues at the planning stage.

Many detailed recommendations have been made by the Local Authorities in the case of Sunnica. It is unclear how much opportunity or input Suffolk FRS has had in these. However the recommendations offered betray some serious misunderstandings and a complete lack of awareness of the lessons and recommendations made in publicly available documents such as the Hill/DNV report [8] into the McMicken explosion.

These are taken point by point in Appendix 4 but some general points are made here.

1. Thermal runaway cannot be controlled like a regular (air-fuel) fire. The only way to mitigate "re-ignition" (a regular report of eye-witnesses) is by thorough cooling. Water is the only fire-fighting material with the necessary thermal capacity. Sprinkler systems, though with good records in conventional building fires, are likely to be completely inadequate. The purpose of the water is absorbing a colossal release of energy. The Hill/DNV report [8] called for so-called "dry pipe" systems allowing first responders to connect very large water sources to the interior without having to access the interior.

It is critical to appreciate that all parts of the battery system must be cooled down. Playing water on a battery "fire" may cool the surface, but so long as Li-ion cells deep inside the battery remain above about 150°C, "re-ignition" events will continue. It is not sufficient to estimate water requirements on the basis of calculations assuming water reaches everywhere, uniformly.

For example, in the recent Tesla car fire [2] the BEV battery kept re-igniting, took 4 hours to bring under control and used 30,000 (US) gallons of water (115 m^3). This was for a 100 kWh BEV battery, designed with inter-cell thermal isolation barriers.

In the case of Sunnica, the Local Authorities have suggested that water supplies of 1900 litres per minute for 2 hours (228 m^3) will be needed [22]. But this is grossly inadequate. Using the above Tesla BEV fire experience, this amount of water would suffice for just ***two*** Tesla Model S car fires. Scaling this up to even the smallest 2 MWh BESS (such as that in McMicken [8]), which contains

stored energy equivalent to ***twenty*** Tesla Model S cars, it is clear to see that a much greater amount of water would be needed.

The actual amount of water required will depend on the energy storage capacity per cabin which, in the case of Sunnica, is still unstated. Some simple estimates are, however, made below. **The requirements suggested to date by the Local Authorities for the Sunnica installation are completely inadequate and, if not addressed, would leave Suffolk FRS without the means to control a major BESS "fire".**

Taking a storage capacity of 10 MWh in just one of the Sunnica cabins (see Appendix 1), a complete thermal runaway accident in such a BESS would release that stored electrochemical energy, plus an indeterminate quantity of heat from combustion of hydrocarbon polymer materials or inflammable gases evolved from them. Such Total Heat Release may be up to twenty times the amount of the stored electrochemical energy in the BESS [11].

The thermal capacity of water is 4.2 kJ kg^{-1} K^{-1} or in kWh terms, about 1.17 kWh m^{-3} K^{-1}. If heated from 25 °C to boiling point about 87.8 kWh m^{-3} of thermal energy is required.

Hence the water volume required to absorb 10 MWh of released energy without boiling is about 114 m^3 or 30,000 US gallons, the same amount as required in practice to control a fire in a single Tesla Model S car with a mere 100 kWh battery, 100 times smaller than a 10 MWh BESS.

The quantity suggested by the Local Authorities' joint response is 228 m^3 (1900 L min^{-1} for 2 hours), twice the above estimate, which would naively be sufficient for a 20 MWh BESS fire. **However, from the experience of recent BEV fires, it could be insufficient by a factor of 100.**

No such calculations were presented in the Examination of the 700MWh Cleve Hill BESS [6].

2. "Clean agent" fire suppression systems are a common fire suppression system in BESS, but are ***totally ineffective*** to stop "thermal runaway" accidents. The McMicken explosion was an object lesson in this: the installed "clean agent" system operated correctly, as designed, on detection of a hot fault in the cabin [8]. There was no malfunction in the fire suppression system. But it was completely useless because the problem was not a conventional fuel-air fire, it was a thermal runaway event. Only water will serve in thermal runaway.

Indeed in the McMicken explosion the "Novec 1230" clean agent arguably contributed to the explosion by creating a stratified atmosphere with an air/Novec 1230 mixture at the bottom and inflammable gases accumulating at the cabin top.

The most probable cause of the explosion was mixing caused by the opening of the door by first responders. The explosive mixture contacted hot surfaces and ignited [8].

3. A further recommendation of the Hill/DNV report [8] into the McMicken explosion is for a means of ***controlled venting*** of inflammable gases ***before*** first responders attempt access. In the Local Authority response to the Sunnica consultation, ventilation is listed as a BESS requirement [22] but the reason given, bizarrely, is "to control the temperature" – at which ventilation or air-conditioning (also listed) would be totally ineffective, lacking any significant thermal capacity.

The critical reason for controlled ventilation is the removal of inflammable gases ***before*** an explosive mixture forms. Deflagration panels (to decrease the pressure of explosions that do occur) are also recommended.

It should be noted that although controlled venting provisions would mitigate the consequence of inflammable gas evolution, they would also require simultaneous venting of Hydrogen Fluroide that would be evolved concomitantly.

Toxic gas hazard would continue to present a risk to the community and the environment for the duration of the incident. Fire-water will be contaminated with, *inter alia*, highly corrosive Hydrofluoric Acid. Contamination of water supplies and waterways ***must*** be prevented.

It is strongly recommended that Fire Services study the Hill/DNV report [8], and the related Underwriters Labs report [9], act upon their recommendations, and make realistic, physics-based, calculations of the water quantities required to be available at every single BESS cabin. There could be as many as 150 BESS cabins at the Sunnica East B site alone – see Appendix 1; each of these would need a sufficient water supply.

References

[1] Major Emergency Report MER 49652 (Liverpool City Council, Environmental Health Dept) Report from Merseyside Fire and Rescue Services and operator Ørsted into the battery fire at Carnegie Rd, Liverpool, 14-15 September 2020.
Promised January 2021 but still not released as of May 2021.
MER 49652 is a Liverpool City Council file code.

[2] Washington Post 19 April 2021
https://www.washingtonpost.com/nation/2021/04/19/tesla-texas-driverless-crash/

[3] Letter 2 August, 2019 from Commissioner Sandra Kennedy, of the Arizona Public Service Commission. Docket E-01345A-19-0076, State of Arizona Public Service Commission.

[4] Energy Storage News.
https://www.energy-storage.news/news/fire-at-20mw-uk-battery-storage-plant-in-liverpool

[5] Liverpool echo, 15 September 2020.
https://www.liverpoolecho.co.uk/news/liverpool-news/live-updates-fire-rips-through-18934842

[6] Cleve Hill Development Consent Order.
https://infrastructure.planninginspectorate.gov.uk/wp-content/ipc/uploads/projects/EN010085/EN010085-001957-200528%20EN010085%20CHSP%20Development%20Consent%20Order.pdf

[7] Sunnica Preliminary Environmental Information Report, Ch 3: Scheme Description

[8] D. Hill (2020). McMicken BESS event: Technical Analysis and Recommendations, Arizona Public Service. Technical support for APS related to McMicken thermal runaway and explosion."
Report by DNV-GL to Arizona Public Service, 18 July 2020. Document 10209302-HOU-R-01

[9] McKinnon, M B, DeCrane S, Kerber S (2020).
"Four fire-fighters injured in Lithium-ion Battery Energy Storage System explosion – Arizona".
Underwriters Laboratories report July 28, 2020.
UL Firefighter Safety Research Institute, Columbia, MD 20145

[10] Li-ion batteries video.
https://www.youtube.com/watch?v=CUgbmCSmSNY

[11] Larsson F, Andersson P, Blomqvist P, Mellander BE (2017).
Toxic fluoride gas emissions from lithium-ion battery fires.
Scientific Reports **7**, 10018 doi: 10.1038/s41598-017-09784-z

[12] Public Health England (2017).
Hydrogen Fluoride and Hydrofluoric acid – Incident Management, PHE gateway number 2014790

[13] Golubkov A W, Fuchs D, Wagner J *et al.* (2014).
Thermal runaway experiments on consumer Li-ion batteries with metal-oxide and olivin-type cathodes.
RSC Advances **4**, 3633-3642 doi: 10.1039/c3ra45748f

[14] D J C MacKay (2009) "Sustainable Energy – Without the Hot Air" UIT Cambridge Ltd p329

[15] Rigby S E, Lodge T J, Alotaibi S *et al.*
Preliminary yield estimation of the 2020 Beirut explosion using video footage from social media. *Shock Waves*. doi:10.1007/s00193-020-00970-z

[16] Pilger, C, Hupe P, Gaebler P, Kalia A, Schneider F, Steinberg A , Henriette S & Ceranna L (2020). Yield estimation of the 2020 Beirut explosion using open access waveform and remote sensing data. Bundesanstalt für Geowissenschaften und Rohstoffe - submitted https://doi.org/10.31223/X5W027

[17] Understanding COMAH – a Guide for new entrants
https://www.hse.gov.uk/comah/guidance/understanding-comah-new-entrants.pdf
Appendix 1 Figure 1 flowchart.

[18] Letter from Dr E J Fordham to HSE, 25 November 2020.
Addressed impersonally but sent Recorded Delivery and receipted.

[19] Letter from Ms Sarah Albon, Chief Executive of HSE, to Dr E J Fordham, 22 February 2021.

[20] Allianz Risk Consulting (2019) Battery Energy Storage Systems (BSS) using Li-ion batteries, Technical Note Vol 26.

[21] National Fire Protection Association (2020)
Standard for the Installation of Stationary Energy Storage Systems Standard 855, Table 9.2

[22] Response of affected Local Authorities
(Cambridgeshire and Suffolk County Councils, West Suffolk and East Cambridgeshire District Councils) to Sunnica Consultation.
https://democracy.westsuffolk.gov.uk/documents/s39360/Sunnica%20Statutory%20Consultation%20Response.pdf

[23] Note (2/11/20) from Councillor Andrew Douch, Freckenham Parish Council, meeting 30 October 2020

[24] *Power Engineering,* 4/18/2017, "What you need to know about energy storage".

[25] Energy Institute (2019) Battery Storage Guidance Note 1: Battery Storage Planning, Sec 4.2 page 16

[26] A guide to the COMAH regulations (2015): https://www.hse.gov.uk/pubns/books/l111.htm

[27] A guide to the COMAH regulations (2015): https://www.hse.gov.uk/pubns/books/l111.htm
Schedule 1,Part 1, Col 2.

Appendix 1: Battery Capacity Calculations for the Grid-scale BESS proposed at the "Sunnica" site.

The Sunnica scheme will be taken as an example of a "mega-scale" solar plant with BESS. If approved, it would cover approximately 2800 acres and will include BESS on 3 separate sites.

The proposed BESS capacity in the Sunnica scheme has not been specified. Estimates of storage capacity can be made on the basis of the land areas allocated to the BESS compounds, assuming full use (per meeting with Parish Councillors, 30 October 2020 [23]). Li-ion battery technology has also been assumed because it is the most widely used in the industry today. Li-ion batteries have a high energy density, and the costs of these have fallen significantly over the past few years [24] .

Land areas and cabin size are quoted in the Sunnica Scheme Description as:
Sunnica East A: 5.23 ha
Sunnica East B: 15.6 ha
Sunnica West A: 10.65 ha
Total: 31.48 hectares.

One storage cabin size is 15 m length × 5 m width × 6 m height. This height is *double* that of a so-called "hi-cube" shipping container and has a larger footprint (75 m^2 *vs* 30 m^2 for a standard 40-foot shipping container).

Storage capacity can be estimated based on other BESS and storage cabin volumes:

Single cabin energy storage capacity:

The McMicken, Arizona, Li-ion BESS was a single cabin, footprint of 60 m^2 and 'shipping container' height. The Sunnica BESS cabins are 75 m^2, with 'double shipping container' height (6 m).
Energy storage at McMicken was 2 MWh.

Scaling by footprint and height yields a *single cabin* energy storage capacity estimate of 5 MWh for each of the "Sunnica" BESS cabins.

The Arizona cabin had empty space for expansion racks, so a larger single cabin energy storage capacity, up to say 10 MWh, is entirely conceivable.

Density of BESS cabins on allocated land:

This is unstated by Sunnica. We assume that 7.5% of the allocated land area will be occupied by the BESS cabins themselves (this allows for safety separations, fire access routes, Battery Management Systems (BMS) and other electrical plant, bunding for firewater in the event of incidents). This implies a total of 315 BESS cabins allocated over the three sites.

Total scheme storage capacity:

5 MWh (single cabin capacity) x 315 cabins yields a total energy storage capacity of **1575 MWh** (or 1.574 GWh), distributed over 3 separate battery compounds of unequal size (31.48 ha total). If the single cabin capacity were 10 MWh, the total doubles to **3150 MWh.**

A storage capacity between 1500 – 3000 MWh is therefore credible for the Sunnica proposal, depending on single cabin storage and the density of cabins on the land.

The area density of storage at this cabin density would be 50 MWh ha^{-1} for a single-cabin storage of 5 MWh. This figure of 50 MWh ha^{-1} is independent of the total area allocated; it depends only on the assumed fraction (7.5%) occupied.

For comparison, the corresponding density at Cleve Hill [3] is a very similar 69.2 MWh ha^{-1}.

The Energy Institute [25] gives 100 MWh ha^{-1} as 'typical' for Li-ion BESS planning. This density would be reached in our assumptions if the single cabin capacity were 10 MWh. The latter figure is entirely conceivable because the "base estimate" derives from an incompletely populated cabin. It is also readily achievable if the spacing of cabins is closer than implied by the assumption of 7.5% land occupancy.

The "base case" estimate of 315 cabins and 1574 MWh is an overestimate *only if* the project does *not* fully occupy the allocated land (i.e. BESS cabin density is less than the 7.5% assumed), but this would be contrary to advice from the developer in meetings with local Councillors.

It is also an overestimate if the single cabin storage capacity is less than 5 MWh. This is unlikely because it is estimated from a BESS cabin still incompletely populated.

These estimates are summarised in the following Table.

Table 3. Estimates of electrical stored energy under various assumptions at Sunnica.
Note: "1 kiloton TNT" is equivalent to 1.163 GWh. "One Beirut" is equivalent to 580 MWh.

Compound	Area	No. of cabins at area density of 7.5%	Energy storage capacity		Comments
(Single cabin) (per cabin land)	75 m^2 1000 m^2	1	5 MWh	10 MWh	Per cabin assumptions
Sunnica East A	5. 23 ha	52	260 MWh	520 MWh	Per compound estimates of stored energy
Sunnica East B	15.6 ha	156	780 MWh	1560 MWh	
Sunnica West A	10.7 ha	107	535 MWh	1070 MWh	
Whole Scheme	31.5 ha	315	1575 MWh	3150 MWh	Stored electrochemical energy only.
			1.575 GWh	3.150 MWh	
			1.36 kilotons	2.71 kilotons	
			2.72 "Beiruts"	5.44 "Beiruts"	Does not include chemical energy from inflammables.

Appendix 2: Applicability of the COMAH Regulations to large-scale BESS

The COMAH regulations (2015): COMAH regulates establishments with quantities of dangerous substances (categorised as toxic, flammable or environmentally damaging) that are present above defined thresholds. The substances do not need to be present in normal operation. If dangerous substances could be generated "if control of the process is lost", the likely quantity generated thereby must be considered. If the mass of dangerous substances that could be generated in loss of control exceeds the COMAH thresholds, the Regulations apply.

There are two "tiers" to COMAH, the "upper tier" imposing more stringent controls. Thresholds of hazardous substances are listed with thresholds for both tiers.

The regulations specify aggregation rules when more than one substance in a hazard category (e.g. flammables) may be present; even if all such substance are below the COMAH thresholds, others in the same hazard category must be quantified and the proportions of the threshold aggregated. If the total exceeds one, the establishment is subject to COMAH. It is also clear that the inventories of all "installations" – including pipework – must be considered as a whole.

Extracts from COMAH Regulations [26] ***2(1) (definitions):***

"establishment" means the whole location under the control of an operator where a dangerous substance is present in one or more installations, including common or related infrastructures or activities, in a quantity equal to or in excess of the quantity listed in the entry for that substance in column 2 of Part 1 or in column 2 of Part 2 of Schedule 1, where applicable using the rule laid down in note 4 in Part 3 of that Schedule;

"presence of a dangerous substance" means the actual or anticipated presence of a dangerous substance in an establishment, or of a dangerous substance which it is reasonable to foresee may be generated during loss of control of the processes, including storage activities, in any installation within the establishment, in a quantity equal to or in excess of the qualifying quantity listed in the entry for that substance in column 2 of Part 1 or in column 2 of Part 2 of Schedule 1, and "where a dangerous substance is present" is to be construed accordingly;

Application to grid-scale BESS: The Regulations refer to "*a dangerous substance which it is reasonable to foresee may be generated during loss of control of the processes*". Both Flammable Gases (P2) and Acute Toxics (H1 and H2) are certainly "*reasonable to foresee*" in thermal runaway incidents which are now well-documented. The evolution of regulated, named and categorised hazardous substances from Li-ion battery cells in thermal runaway is also well-documented. A "worst credible accident" would have to consider that the entire inventory of Li-ion cells would be destroyed in a single BESS cabin at least. Cabin-to-cabin propagation should also be considered.

The Regulations apply to the entire "establishment", controlled by a single operator. Whilst the individual BESS compounds at Sunnica might be regarded as separate establishments, it is less reasonable that individual BESS cabins should be regarded as separate "establishments". They are separate "installations" but "establishment" means the entire area under control of an "operator".

Only if the most stringent safeguards were in place to ensure that the disastrous consequences of cabin-to-cabin propagation of "battery fires" could not conceivably occur, could it be argued that dangerous substances, exceeding the COMAH thresholds in quantity, were not "*reasonable to foresee* [being] *generated during loss of control of the process*".

We believe the COMAH regulations apply to BESS and that the approach of HSE is wrong in law.

Dangerous substances "reasonable to foresee ... generated during loss of control of the processes": The literature and known experience of BESS accidents is clear that dangerous

substances in the hazard categories H1 and H2 (Acute Toxic) and P2 (Flammable Gases) are foreseeable in the event of thermal runaway accidents. One of the Flammable Gases is Hydrogen, which is a "Named Dangerous Substance" in Part 2 of Schedule 1 of the COMAH Regulations 2015. Lower thresholds are specified for Hydrogen than for other P2 Inflammable Gases.

It remains therefore to consider the quantities of dangerous substances which could be generated if "control of the process is lost" in a thermal runaway incident. Published literature sources quantify evolution of flammable gases from tests of various Li-ion cells in sealed vessels. Open "fire tests" quantify the evolution of toxic gases particularly Hydrogen Fluoride. Many other test results exist in the records of specialist test laboratories, but here we rely upon two primary published sources.

Golubkov *et al.* (2014) [13] report quantities of evolved inflammables from Li-ion cells of three different electrode chemistries in thermal runaway situations. The proportion of Hydrogen (H_2), Methane (CH_4), Ethylene (C_2H_4) and Carbon Monoxide (CO) does not in fact vary greatly between different types of Li-ion cell, reflecting an underlying inventory of hydro-carbon material (plastics, electrolyte solvents etc) that remain similar in all Li-ion technologies. This is consistent with DNV/GL test data cited in the Hill/DNV report [8]. The quantitative estimates here are taken from results derived from cells with Nickel-Manganese-Cobalt (NMC) electrodes, as used in the McMicken BESS. It was not possible in the apparatus of Golubkov *et al.* to determine the concentrations of HF evolved.

Larsson *et al.* [11] report evolved quantities of Hydrogen Fluoride (HF) from Li-ion cells in open "fire tests", and also the Total Heat Released (THR) from combustion of the inflammables. Again these vary between cell technologies and "form factors", especially whether the cells have an outer metal cannister or are in the "pouch" format. Quantities between 20 – 200 mg / Wh are reported. The worst case figure is used in the following estimates; the lowest evolution reported for "pouch" cells was 43 mg/Wh.

Both sources report evolved gas quantities on a per Wh basis. We scale these to a Li-ion BESS cell size on the basis of stored energy since this will be roughly proportional to the electrolyte solvents and other polymer materials in the cell. Scaling on a per mass basis would be preferable, but this would require further information on the exact composition of the cells in the literature tests, and indeed those for the BESS in question. During the McMicken investigation, the cell manufacturers refused to release such data.

H1 and H2 Acute Toxics. The applicability of COMAH is easiest to determine in respect of Hydrogen Fluoride (HF). This has a dual hazard classification [12] as H1 Acute Toxic (skin exposure) and H2 Acute Toxic (inhalation) and both exposure routes would apply to the general public nearby. The lower tier COMAH threshold for H1 Acute Toxics is 5 tonnes [27]; using the upper estimate of 200 mg/Wh from Larsson, the BESS capacity at which a BESS enters the scope of COMAH (lower tier) is 25 MWh.

This is far below the projected storage capacities given in Table 3 (Appendix 1). With high storage capacity cabins (of e.g. 12.5 MWh), it would require propagation of a fire from just one cabin to a second, to generate HF above the COMAH threshold. It is not necessary to foresee a major conflagration involving multiple cabin-to-cabin propagation to bring the establishment within scope of COMAH; just two cabins would suffice. If 25 MWh were stored in a single large cabin, the question of cabin-to-cabin propagation is irrelevant.

The upper tier for "H1 Acute Toxics" is entered at four times higher capacity (100 MWh), which is well below the estimated capacity of Cleve Hill, and is also below *each* of the three Sunnica BESS compounds individually.

Even on the lowest evolution figure of 43 mg/Wh reported by Larsson *et al.* for "pouch" cells, the lower tier of COMAH is entered at a storage capacity of 120 MWh, again well within the "low case" capacity of each of the Sunnica BESS compounds, and Cleve Hill.

There is little doubt that either the lower or upper tier of COMAH is applicable to Cleve Hill and all three of the Sunnica BESS compounds, on the basis of "H1 Acute Toxics" (HF, skin route) alone.

Carbon Monoxide (CO) is categorised as an H2 Acute Toxic as well as a P2 Inflammable Gas, and will also be evolved, but in application of the aggregation rule its presence does not materially alter these conclusions. It is sufficient to consider HF alone.

P2 Inflammable Gases. Assessing applicability of COMAH on the basis of inflammable gases is more complicated because of the evolution of Hydrogen (H_2), Methane (CH_4), Ethylene (C_2H_4) and Carbon Monoxide (CO) in significant quantities, and because Hydrogen is a "named dangerous substance" for which different COMAH thresholds apply. These must be taken into account when applying the Aggregation Rule. Although proportions are generally similar, quantities do depend on the different electrode chemistries in the different Li-ion cell types.

Taking the largest evolutions reported by Golubkov *et al.* [13] for the LCO/NMC electrode type tested by them these are equivalent to 335 mg/Wh of P2 inflammables. For the NMC cells tested (the McMicken cells were NMC) the evolution was 214 mg/Wh. Taking the higher figure and applying the aggregation rule, grid-scale BESS enter the lower tier of COMAH at about 30 MWh capacity. Taking the lower figure, they enter the lower tier at 45 MWh capacity.

Hence there is little doubt that grid-scale BESS are lower tier COMAH establishments on the basis of "P2 Inflammable Gases" at storage capacities between 30 – 45 MWh.

Because of the variability between cell types, and the difficulty of scaling laboratory tests to actual BESS cells without detailed composition data, there is room for adjustment. However the calculated estimates of the thresholds for applicability of COMAH are so far below the projected capacities that it is inconceivable that the Cleve Hill and Sunnica BESS compounds would *not* be COMAH establishments, in lower tier at the very least, and probably the upper tier also.

Conclusion: Grid-scale Li-ion BESS should be considered COMAH establishments in the lower tier on the basis of "H1 Acute Toxics" (HF) alone, at energy storage capacities in the region of **25 MWh**. Upper tier would apply at about **100 MWh**. They should be lower-tier COMAH establishments on the basis of "P2 inflammable gases" alone, at storage capacities between **30 – 45 MWh**. Again larger establishments could become upper tier COMAH. Laboratory closed vessel and fire tests on actual Li-ion BESS cells proposed to be deployed would be required to refine these estimates definitively.

It is difficult to see how these conclusions could be avoided if tested in litigation.

Appendix 3: Shortcomings of Existing Engineering Standards for Li-ion BESS

The July 2020 report for the Arizona Public Service by Dr D Hill [8] provides a comprehensive discussion of existing engineering standards relating to BESS, and how they are *inadequate* to address the known hazards of "thermal runaway" incidents in Li-ion BESS. This was the failure mode leading to the explosion at McMicken, Arizona.

Unfortunately, when the UK's first "mega-scale" solar plant and battery storage site was granted approval in May 2020, this paper had not been published. The Cleve Hill solar developers cited one standard, UL 9540A [3]. This is also cited by some insurance and risk consultants [20].

It is important to be clear that nothing in UL 9540A addresses thermal runaway, and as a test method standard, it can provide no "safety certification" for Li-ion BESS.

Specific criticisms made in the Hill/DNV report include the following:

1. UL 1973 allows for the complete destruction of a BESS and the creation of an explosive atmosphere so long as no explosion or external flame is observed. An installation can do all these things but still "pass" UL 1973. At McMicken one rack was completely destroyed and an explosive atmosphere created but no flame or explosion occurred until first-responders opened the cabin door.
2. UL 9540A is merely a test method for generating data. It does not define any "pass/fail" criteria for interpreting results. Specifically, it does not address cell-to-cell cascading in thermal runaway, nor the evolution of a potentially explosive atmosphere. It does not even prescribe that the cell-to-cell cascading rate be measured.
   It allows that thermal runaway may proceed to an entire rack (as at McMicken) and offers testing of fire suppression systems (which operated correctly at McMicken but cannot prevent thermal runaway, and did not prevent an explosion).
   Presentation of data generated under UL 9540A to an "AHJ" (Authority Having Jurisdiction) does not translate to a succinct understanding of potential risks.
3. NFPA 855 [21] does require evaluation of thermal runaway in a single module, array or unit and does acknowledge the need for thermal runaway protection. However, it assigns that role to the Battery Management System (BMS). Yet thermal runaway is an electrochemical reaction that once started cannot be stopped electrically. It is uncontrollable by electronics or switchgear, only by water cooling.

The evolution of engineering and safety standards has not yet incorporated the lessons of experience arising from the McMicken explosion [8] or explosion incidents in the UK like the Liverpool explosion and fire of 15 September 2020 [1]. Compliance with existing standards does not prevent such incidents happening again.

Articles in the industry press[3] do now recognise and discuss the problem of thermal runaway but make proposals such as: "*If off-gases can be detected and batteries shut down before thermal runaway can begin, it is possible that fire danger can be averted*".

Such statements betray a dangerous misunderstanding. Batteries cannot be "shut down", except by complete discharge, which cannot be done quickly. Taking cells "out of circuit" is useless; thermal breakdown and runaway will still occur.

[3] https://www.energy-storage.news/blogs/preventing-thermal-runaway-in-lithium-ion-energy-storage-systems

Appendix 4 – Fire Safety Planning requirements in the Local Authorities' Joint Response to the Sunnica statutory consultation

This Appendix deals point by point with the BESS requirements in the Local Authority response (text in blue) pp 74 – 75.

Sunnica should produce a risk reduction strategy as the responsible person for the scheme as stated in the Regulatory Reform (Fire Safety) Order 2005. It is expected that safety measures and risk mitigation is developed in collaboration with services across both counties.

The Local Authorities require that the Fire Services work with Sunnica to prepare fire safety and risk mitigation measures. The Cambridgeshire and Suffolk Fire Services are therefore the only public bodies with independent oversight of BESS safety.

The use of batteries (including lithium-ion) as Energy Storage Systems (ESS) is a relatively new practice in the global renewable energy sector. As with all new and emerging practices within UK industry, the SFRS would like to work with the developers to better understand any risks that may be posed and develop strategies and procedures to mitigate these risks.

This paper is provided as input to this process, which appears to be insufficiently understood.

The promoter must ensure the risk of fire is minimised by:

- Procuring components and using construction techniques which comply with all relevant legislation.

This overlooks the points made in this paper that (i) existing legislation is being ignored by the statutory regulatory body, the HSE (ii) no adequate engineering standards exist to exercise Prevention measures over what is by now a very well-known hazard, viz. thermal runaway. Public Health and Safety cannot be assured whilst either of these situations continues.

- Developing an emergency response plan with both counties fire services to minimise the impact of an incident during construction, operation and decommissioning of the facility.
- Ensuring the BESS is located away from residential areas. Prevailing wind directions should be factored into the location of the BESS to minimise the impact of a fire involving lithium-ion batteries due to the toxic fumes produced.

This is impossible to satisfy. All the BESS compounds in the Sunnica proposal are sufficiently close to residential areas to present a major danger of toxic fumes in the event of an accident. Plume dispersal modelling should be performed to ensure that concentrations of HF cannot exceed dangerous thresholds in the event of the worst credible accident in a BESS compound.

- The emergency response plan should include details of the hazards associated with lithium-ion batteries, isolation of electrical sources to enable firefighting activities, measures to extinguish or cool batteries involved in fire, management of toxic or flammable gases, minimise the environmental impact of an incident, containment of fire water run-off, handling and responsibility for disposal of damaged batteries, establishment of regular onsite training exercises.

This requirement is very broad but insufficiently detailed. Means of cooling would require water volumes many times in excess of those requested. Management of inflammable gases is best addressed by venting, but that exacerbates the hazard of toxic gas plumes. Large water volumes may lead to unrealistic or impossible requirements for the containment, and subsequent disposal, of the contaminated water resulting from the fire-fighting activity. Other sections of this paper address these points.

- The emergency response plan should be maintained and regularly reviewed by Sunnica and any material changes notified to SFRS and CFRS.

- Environmental impact should include the prevention of ground contamination, water course pollution, and the release of toxic gases.

Preventing the release of toxic gases is all but impossible. A thermal runaway event WILL release toxic gases. If inflammables are vented to avoid /mitigate explosion risk, toxic gases WILL be vented. Ground contamination and water course pollution is almost certain to occur if sufficient water to control a major thermal runaway event is deployed. It will pose a significant challenge to contain, and safely dispose of, such large volumes of contaminated fire water.

The BESS facilities should be designed to provide:

- Automatic fire detection and suppression systems. Various types of suppression systems are available, but the Service's preferred system would be a water drenching system as fires involving Lithium-ion batteries have the potential for thermal runaway.

This is a correct precaution, but no specification is made of likely water volume requirements, nor for a "dry pipe" system allowing water to be deployed without cabin entry. We provide some water estimates elsewhere in this paper.

Other systems, such as inert gas, would be less effective in preventing reignition.

This is also a correct insight. The so-called "clean-agent" fire suppression system at McMicken was triggered correctly, but was useless to control thermal runaway. Moreover the stratified atmosphere created allowed the build-up of inflammables to a dangerous level, before the explosion occurred.

- Redundancy in the design to provide multiple layers of protection.
- Design measures to contain and restrict the spread of fire through the use of fire-resistant materials, and adequate separation between elements of the BESS.

This comment only vaguely considers the true essentials. The "elements of the BESS" could be: cells, modules, racks, strings, and the entire system. As discussed in the Hill/DNV report what is required is for the industry as a whole to accept that thermal runaway in an unacceptable hazard, and demand engineering standards that Prevent thermal runaway by design, or if it occurs, Prevent its cascade or escalation to larger system elements. This requires

a. Thermal barriers (i.e. Low thermal conductivity barriers, not merely refractory barriers, ideally with water cooling, between all cells, so that propagation from cell to cell cannot occur. This is precisely the requirement the industry has so far ***NOT*** made in the development of its engineering standards.
b. Separation of modules by similar barriers to Prevent module-to-module cascade.
c. Separation of Racks to prevent rack-to-rack cascade, even with ejection of molten metals.
d. Spacing of BESS cabins such that even with "75 foot flame lengths" cabin to cabin escalation is impossible. This is probably the most critical of all, since cabin-to-cabin escalation could turn a major fire incident into an unprecedented catastrophe, on the scale of the Beirut explosion or a small nuclear weapon.

- Provide adequate thermal barriers between switch gear and batteries,
- Install adequate ventilation or an air conditioning system to control the temperature. Ventilation is important since batteries will continue to generate flammable gas as long as they are hot. Also, carbon monoxide will be generated until the batteries are completely cooled through to their core.

This comment is very strange. There is no possibility whatsoever that air conditioning could be adequate "to control the temperature". The importance of ventilation is however recognised, as is

the generation of carbon monoxide (toxic as well as inflammable). However the generation of Hydrogen Fluoride will also continue until the batteries are "completely cooled" and HF (H1 Acute Toxic by skin exposure) is much more toxic than CO (H2 Acute Toxic).

- Install a very early warning fire detection system, such as aspirating smoke detection.

The "very early warning" fire detection system required should be thermocouples to report continuously on the local temperature at every cell in the entire system. A single cell overheating can escalate via thermal runaway. By the time smoke is generated, this will be a "very late", rather than "very early" detection system. Just as thermal runaway events do not necessarily generate flame, neither do they necessarily generate smoke, until nearby combustibles are ignited.

- Install carbon monoxide (CO) detection within the BESS containers.

This is a good straightforward measure, but detectors for other gases expected (HF, H_2, CH_4) could equally well serve and multiple gas detection would provides additional security.

- Install sprinkler protection within BESS containers. The sprinkler system should be designed to adequately contain and extinguish a fire.

The excellent record of sprinkler systems in ordinary building fires shows they would help contain fire in regular combustible parts of the structure. However as discussed earlier in this paper, a mere sprinkler system would be useless to contain thermal runaway. Much larger water quantities would be needed.

- Ensure that sufficient water is available for manual firefighting. An external fire hydrant should be located in close proximity of the BESS containers. The water supply should be able to provide a minimum of 1,900 l/min for at least 2 hours. Further hydrants should be strategically located across the development. These should be tested and regularly serviced by the operator.

As discussed elsewhere, we believe these water requirements to be **under-specified by a factor of 100**, based on real experience with BEV fires. "Strategic location" is inadequate. Every single BESS cabin (potentially up to 150 of these at Sunnica East B alone) should have such a hydrant.

We remark elsewhere on the recommendation made by Hill/DNV for a "dry pipe" system to deploy water drenching inside via external connections, without cabin entry being needed.

- A safe access route for fire appliances to manoeuvre within the site (including turning circles). An alternative access point and approach route should be provided and maintained to enable appliances to approach from an up wind direction. Please note that SFRS requires a minimum carrying capacity for hardstanding for pumping/high reach appliances of 15/26 tonnes, not 12.5 tonnes as detailed in the Building Regulations 2000 Approved Document B, 2006 Edition, due to the specification of our appliances.

The requirement for safe access routes and space for appliances to manoeuvre could usefully be expanded into requirements for safe spacing of BESS cabins and thermal or flame barriers between cabins, to Prevent the "disaster scenario" of cabin-to-cabin propagation.

Final Comment: (over)

Final Comment:

The fundamental failure mode of Li-ion batteries presenting major hazard is thermal runaway. This paper is far from the first to identify the risk which is now well-known.

However the BESS industry as a whole has still not agreed or implemented adequate engineering standards to address basic Prevention measures to pre-empt thermal runaway accidents.

Until it does, Mitigation of major accidents by the Fire Services will remain the sole recourse for public protection and safety.

Journal of Hazardous Materials 381 (2020) 120916

Contents lists available at ScienceDirect

Journal of Hazardous Materials

journal homepage: www.elsevier.com/locate/jhazmat

A comprehensive investigation on the thermal and toxic hazards of large format lithium-ion batteries with $LiFePO_4$ cathode

Yang Peng, Lizhong Yang*, Xiaoyu Ju, Baisheng Liao, Kai Ye, Lun Li, Bei Cao, Yong Ni

State Key Laboratory of Fire Science, University of Science and Technology of China, Hefei, Anhui 230026, China

ARTICLE INFO

Editor: Dr. Deyi Hou

Keywords:
Lithium-ion battery
toxicity evaluation
thermal hazards
heat release rate
quantitative assessment

ABSTRACT

Toxic gases released from lithium-ion battery (LIB) fires pose a very large threat to human health, yet they are poorly studied, and the knowledge of LIB fire toxicity is limited. In this paper, the thermal and toxic hazards resulting from the thermally-induced failure of a 68 Ah pouch LIB are systematically investigated by means of the Fourier transform infrared spectroscopy (FTIR) and 1/2 ISO full scale test room. The LIBs with higher state of charge (SOC) are found to have greater fire risks in terms of their burning behavior, normalized heat release rate, and fire radiation, as well as the concentration of toxic gases. Specifically, the thermal hazards are evaluated by combining the effects of convective and radiative heat. The major toxic gases detected from the online analysis are CO, HF, SO_2, NO_2, NO and HCl. Furthermore, Fractional Effective Dose (FED) and Fractional Effective Concentration (FEC) models are used to quantitatively assess the overall gas toxicity. Results show that the effects of irritant gases are much more significant than those of asphyxiant gases. HF and SO_2 have much greater toxicity than the other fire gases. The maximum FEC value is approaching the critical threshold in such fire scenarios.

1. Introduction

Lithium-ion batteries (LIBs) are widely used in various applications today and are seen as the promising power source for electric vehicles (EVs), due to their high energy density and long cycle life (Wu et al., 2018; Wang et al., 2012). However, thermal runaway may occur, when the batteries are misused or encounter abnormal environmental conditions, which is generally accompanied by heat release, gas emissions, fire and possible explosions. Fire accidents caused by LIBs have been reported continually (Abada et al., 2016) and the safety problems have become a major obstacle that hinders the further development of EVs.

Considerable research has been carried out to investigate the thermal runaway features of LIBs. Experimental techniques such as differential scanning calorimetry (Zhang et al., 2019) (DSC), extended volume accelerating rate calorimetry (EV-ARC) (Feng et al., 2014a, b), vent sizing package 2 (VSP2) (Jhu et al., 2011, 2012; Chen et al., 2016), cone calorimeter (Fu et al., 2015; Zhong et al., 2018), Copper Slug Battery Calorimetry (CSBC) (Said et al., 2018; Liu et al., 2015, 2016) and even ISO 9705 room test apparatus (Ping et al., 2015) have been utilized to analyze the thermal hazards of single and multiple LIBs. For example, Said (Said et al., 2018) measured the energetics of thermally induced LIB failure by means of CSBC and cone calorimeter. The results showed that the heat released through flaming combustion of ejected battery materials was about three times as much as that generated inside the battery. Li et al. (2019) investigated the thermal runaway propagation mechanism of large format LIB with $Li(Ni_{1/3}Co_{1/3}Mn_{1/3})O_2$ cathode based on the results from the EV-ARC tests. The propagation time between adjacent LIBs was significantly delayed in 50% SOC module compared with 100% SOC module. Chen et al. (2017) conducted experiments in Hefei (100.8 kPa) and Lhasa (64.3 kPa) to investigate the fire behaviors of LIBs at different atmospheric pressures. It was determined that the low atmospheric pressure can largely weaken the combustion intensity of the LIBs. However, in some circumstances, the risks of fire effluents can be more serious than the fire itself, and the intense heat generated by LIB fires especially in enclosed environments. Deaths and injuries are mainly due to the inhalation of smoke and toxic gases in most fire accidents (Stec, 2017). To reduce the possibilities of safety problems, LIBs have to pass various abuse tests (overcharging, short circuit, crushing, penetration and overheating, etc.) before sales, yet there is no requirement to assess the toxicity of burning LIBs.

Until now, few studies have been done on evaluating the fire effluents of LIB and the knowledge of their toxicity is very limited. Fredrik (Larsson et al. (2014); Larsson et al., 2017, 2018; Andersson et al., 2016) conducted fire tests on various types of LIBs, which mainly focused on the quantitative analysis of toxic fluoride gases. It was observed that lower SOC batteries produced higher amounts of HF and the

* Corresponding author.
E-mail address: yanglz@ustc.edu.cn (L. Yang).

https://doi.org/10.1016/j.jhazmat.2019.120916
Received 4 April 2019; Received in revised form 27 June 2019; Accepted 21 July 2019
Available online 24 July 2019
0304-3894/

Nomenclatures

LIB	lithium-ion battery
EV	electric vehicle
SOC	state of charge
SEI	solid electrolyte interphase
$\dot{q}(t)$	heat release rate, kW
$\Delta h_c/r_0$	heat release per mass of oxygen, which was taken as 13.1 MJ/kg
C	orifice flow meter calibration constant,$m^{1/2}\cdot g^{1/2}\cdot K^{1/2}$
Δp	pressure differential, Pa
T_e	the absolute temperature of the gas, K
$X_{O_2}^0$	the initial value of oxygen analyzer reading
X_{O_2}	Oxygen analyzer reading
FED/FEC	fractional effective dose / fractional effective concentration
FED_{therm}	fractional effective dose due to thermal effects
V_{CO_2}	frequency factor
φ_i	the concentration of each gas, expressed in $\mu l\cdot l^{-1}$
F_i	the critical concentration of each irritant gas that is expected to seriously compromise occupants' tenability, expressed in $\mu l\cdot l^{-1}$
t_{Irad}	time to experience pain due to radiant heat
t_{Iconv}	time to experience pain due to convective heat

added water mist increased the peak production rate of the HF, but there was no significant change in the total amount of HF released. Ribiére et al. (Ribière et al., 2012) utilized a Fire Propagation Apparatus (FPA) to investigate the combustion characteristics of the materials ejected from a 2.9 Ah pouch cell. Significant concentrations of toxic gases including HF, CO, NO, SO_2 and HCl were identified, and HF was considered to be the most critical gas emitted from F-containing batteries. Fabian Diaz et al. (2019) calculated the theoretical contaminated volume to evaluate the hazards of gas emissions produced in mechanical and thermal treatment of spent lithium-ion batteries. It was found that the battery with $LiFePO_4$ cathode produced the most amount of toxic gases, with an environmental contaminated volume of 379 m^3 during pyrolysis in nitrogen atmosphere. Sun et al. (2016) investigated the combustion products of two types of commercial LIBs with electrochemical sensors, and more than 100 volatile organic compounds were identified. They showed that the types of combustion products were related to SOC, and the fully charged batteries had the most serious toxicity. Lecocq et al. (2016) performed fire tests on 1.3 Ah lithium iron phosphate batteries using FPA, and the gas emission data of HF and SO_2 were used to predict the toxicity of the whole Lithium-ion module. The nature of the salt was found to significantly affect the critical thresholds. However, large scale tests and more comprehensive gas species are needed to better extrapolate the measured toxicity to real fire conditions. The existed research has confirmed the types of emission gases and stressed the fact that they are toxic and can cause environmental issues, however, at present, the combined toxic effects of these gas products on human health have not been fully evaluated.

In this work, both the thermal and toxic hazards, resulting from thermal runaway of large format LIBs, are investigated using the FTIR and 1/2 ISO full scale test room. The gas toxicity and thermal hazard are quantitatively evaluated. Some important parameters such as heat release rate (HRR), time to ignition and fire radiation, as well as multiple gases emissions, are measured and analyzed in detail to present a comprehensive characterization of LIB fire hazards.

2. Materials and Methods

2.1. LIB samples

The PL15181210 LIBs employed in this work are manufactured by Beijing National Battery Technology, with $LiFePO_4$/graphite as their electrodes, and they are widely used in electric buses. The LIB has a nominal capacity of 68 Ah and a nominal voltage of 3.22 V. The initial mass is 1250 ± 3 g and its physical dimensions are shown in Fig. 1. A battery testing system of NEWARE CT-4004-10V100A-NFA controlled by a computer was employed to prepare LIBs to the expected SOC using the constant current/constant voltage method. The selected SOCs were 100%, 75%, 50% and 0%, with each SOC being repeated three times.

2.2. Experimental setup

The experimental setup is illustrated in Fig. 2. This apparatus comprises two main subsystems. The left part is the combustion chamber with dimensions of 150 × 150 × 180 cm, which is approximately half that of the ISO 9705 test room. The right part is the gas collection and analysis system.

(i) Details of left part. The fire tests were conducted in the chamber under well ventilated conditions. The LIB was placed upon a supporting mesh with the hole-size of 5 × 5 cm. A 3 kW electric heater was set under the battery at a vertical distance of 10 cm to simulate a radiative heat condition. An electric spark igniter was placed between the two lugs at the same height as the bottom of the battery. Four R-type thermocouples were placed at a horizontal distance of 20 cm away from the battery to measure the flame temperature, and the spacing distance was 10 cm as shown in Fig. 2. Two Hukseflux SGB01 heat flux sensors with a 50 kW/m^2 measurement range, and four K-type thermocouples were located 30 cm away from the side of the battery to quantify the convective and radiant heat. The schematic diagram of the thermocouples and heat flux sensors setup is shown in Fig. 3. A Sony FDR-AX40 camera with 25 fps was used to record the burning process.

(ii) Details of right part. The fire emissions from the LIB were collected entirely and mixed with ambient air. The pressure differential (Δp), and temperature (T_e) were measured by a pitot tube and a thermocouple in the exhaust duct. A Servomex 4100 gas analyzer was used

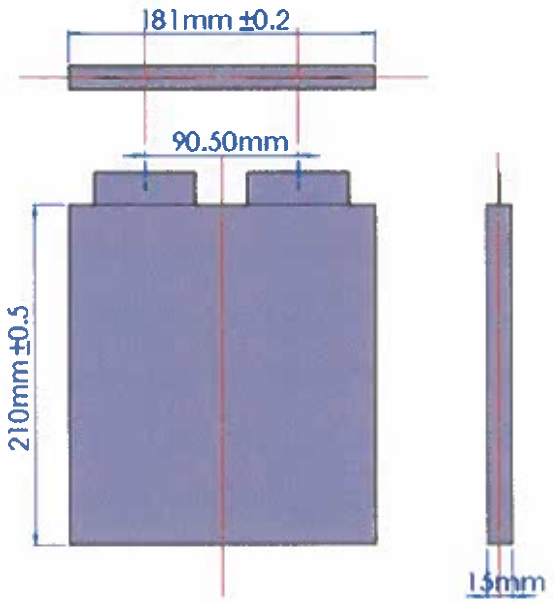

Fig. 1. The dimensions of the 68 Ah $LiFePO_4$ battery.

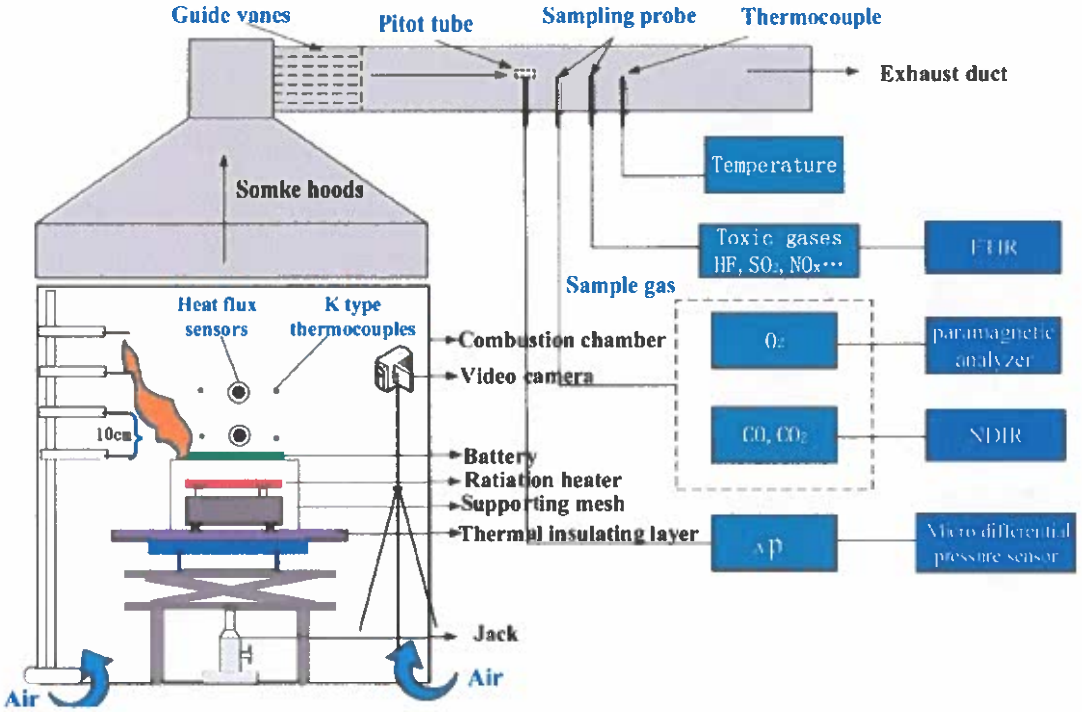

Fig. 2. Schematic of the experimental setup.

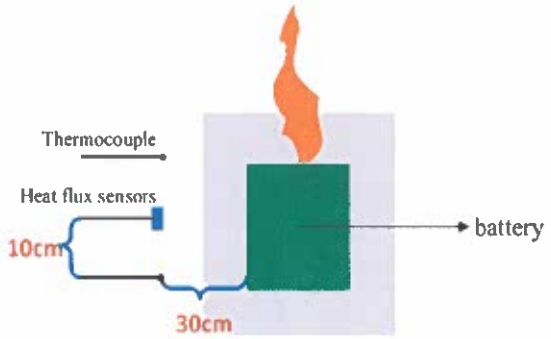

Fig. 3. Schematic of the thermocouples and heat flux sensors.

to measure the concentration of O_2 by a paramagnetic analyzer, and CO and CO_2 were determined by a non-dispersive infrared (NDIR) sensor. Based on the oxygen consumption principle (ISO 5660-1, 2015), the HRR of combustion can be calculated by:

$$\dot{q}(t) = (\Delta h_c/r_0)(1.10)C\sqrt{\frac{\Delta p}{T_e}}\cdot\frac{X_{O_2}^0 - X_{O_2}}{1.105 - 1.5X_{O_2}} \quad (1)$$

Meanwhile, online FTIR measurements of the toxic gases were performed using a portable Protea atmosFIRt, and the heart of which is a high-resolution FTIR spectrometer. The sample gas was extracted from the exhaust stream, with a flow rate of 2.5 L/min, and then passed through a primary filter before the heated PTFE hose. Thereafter the extracted gas was treated with a secondary filter before the analysis starting in the FTIR gas cell.

3. Fire Hazards Evaluation Method

3.1. Assessment of Fire Gas Toxicity

The concentration limits considered by the National Institute for Occupational Safety and Health (NIOSH) of USA to be Immediately Dangerous to Life or Health (IDLH) (The National Institute for Occupational Safety and Health (NIOSH), 2014), are taken into account to conduct a preliminary assessment. Moreover, toxic-gas models described in ISO 13571 (1357) are introduced in this study to evaluate the combined toxic effects. This method is a good way to quantitatively assess the overall gas toxicity, and has been widely used to evaluate the fire toxicity of building materials (Stec and Hull, 2011), upholstery materials (McKenna et al., 2018) and even vehicles (Truchot et al., 2018). Irritant and asphyxiant are distinguished in this methodology. Asphyxiating effects are evaluated by determining fractional effective dose (FED) as shown in Equation (2). These effects not only depend on the gas concentration, but also have a close relation with the exposure time. CO and HCN are generally considered as the only two significant asphyxiant gases in ISO 13571. Their harmful effects will be increased due to the inhalation of CO_2

$$FED = \sum_{t_1}^{t_2}\frac{\varphi_{CO}V_{CO_2}}{35000}\Delta t + \sum_{t_1}^{t_2}\frac{(\varphi_{HCN}V_{CO_2})^{2.36}}{1.2\times 10^6}\Delta t$$

$$V_{CO_2} = e^{(CO_2)/5} \quad (2)$$

Irritating effects are evaluated by calculating the Fractional Effective Concentration (FEC) as described in Equation (3). The toxicity of these irritant gases is instantaneous and directly determined by the concentration. F is the critical concentration that is expected to cause incapacitation. In this method, FED and/or FEC values of 1 means that 50% of the population would be expected to experience compromised tenability (ISO 13571, 2012).

$$FEC = \frac{\varphi_{HCl}}{F_{HCl}} + \frac{\varphi_{HBr}}{F_{HBr}} + \frac{\varphi_{HF}}{F_{HF}} + \frac{\varphi_{SO_2}}{F_{SO_2}} + \frac{\varphi_{NO_2}}{F_{NO_2}} + \frac{\varphi_{acrolein}}{F_{acrolein}} + \frac{\varphi_{formaldehyde}}{F_{formaldehyde}} + \sum\frac{\varphi_{irritant}}{F_{Cl}} \quad (3)$$

3.2. Assessment of thermal hazards

Thermal effects result from the convective and radiant heat which are determined by the exposure temperature of fire environment, and radiation received by skin, respectively. The time to experience pain due to radiant and convective heat can be calculated by Equations (4) and (5). These two effects are also related to the exposure dose. The corresponding evaluation method is similar to that used with toxic gases. The thermal hazards are calculated by combining the convective and radiative effect using Equation (6). The evaluation model is consistent with the studies of Purser (2002) and (Wieczorek and Dembsey, 2001).

$$t_{lrad} = 4.2q^{-1.9} \tag{4}$$

$$t_{lconv} = (5 \times 10^7)T^{-3.4} \tag{5}$$

$$FED_{therm} = \sum_{t_1}^{t_2} \left(\frac{1}{t_{lrad} + t_{lconv}}\right)\Delta t \tag{6}$$

where the term $1/t_{lrad}$ is set at zero if the radiant flux is under 2.5 kW/m^2.

4. Results and Discussion

4.1. Burning behaviors

Fig. 4 shows the typical burning behaviors of the 68 Ah batteries with 0%, 50%, 75% and 100% SOC. It can be observed that the LIBs, with different SOCs, all undergo several burning stages: (I) heating and expansion, (II) stable combustion with small flame, (III) jet fire, (IV) second stable combustion and (V) abatement and extinguishment. The LIBs show similar behaviors at stages I, II and V while significant differences can be seen at stages III and IV.

At stage I, the LIBs are continuously heated by the external heating source. Then the surface shows slow expansion due to the increase of inner pressure, which is caused by the gas products generated during thermal decomposition reactions inside the battery. Some flammable gases are released and ignited immediately by the electric spark igniter, marking the onset of stage II. The time interval from the exposure of radiation to the appearance of a continuous flame is defined as the ignition time (Torero and Handbook, 2004). As shown in Table 1, the ignition time is decreasing with SOC. The flame is small and stable during this stage. After a period of stable combustion, the separator loses its whole integrity, negative and positive electrode reactions occur that leads to thermal runaway. A great deal of gases and aerosols are

Table 1
Ignition time and heat release results of LIBs with different SOCs.

SOC	Ignition time/s	Peak HRR/kW	Total release heat/kJ
0%	825 ± 58	3.7 ± 0.5	4165 ± 356
50%	775 ± 68	25.8 ± 1.6	5644 ± 317
75%	759 ± 65	70.2 ± 7.2	6388 ± 431
100%	738 ± 7	80 ± 2.6	6660 ± 419

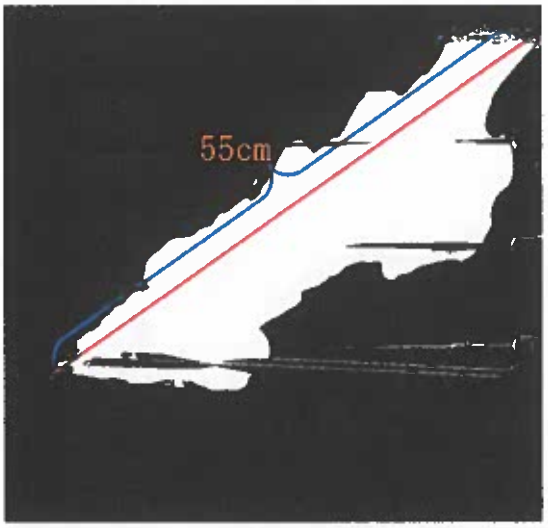

Fig. 5. The binary image of jet flame for battery with 100% SOC.

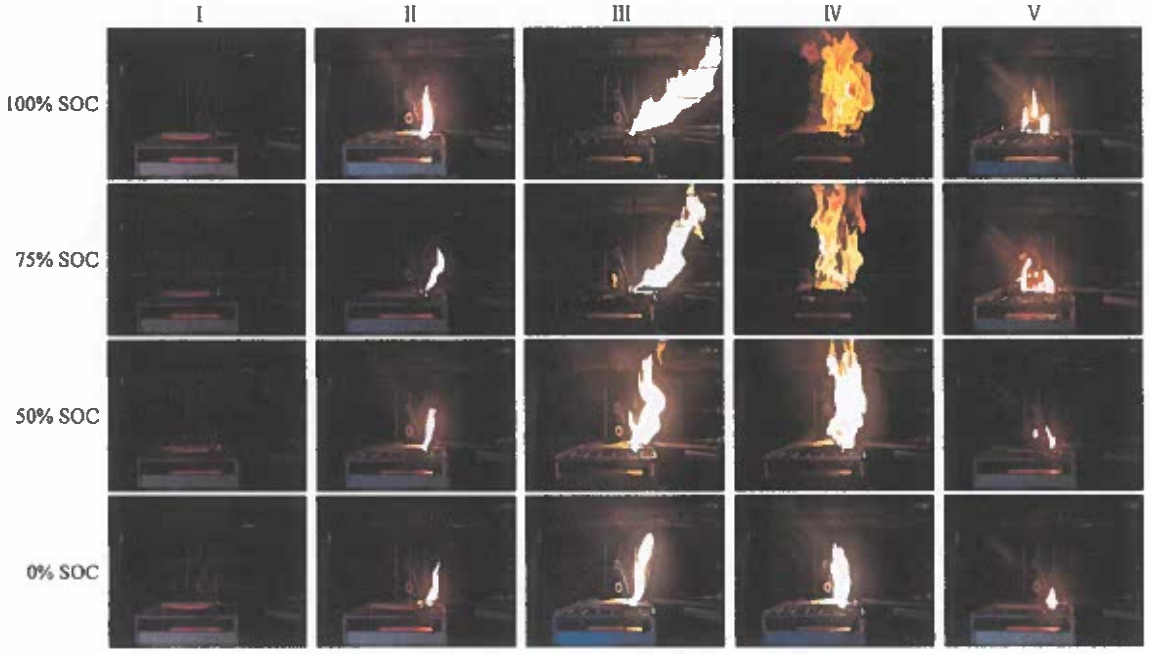

Fig. 4. Burning behaviors of the LIBs at different states of charge.

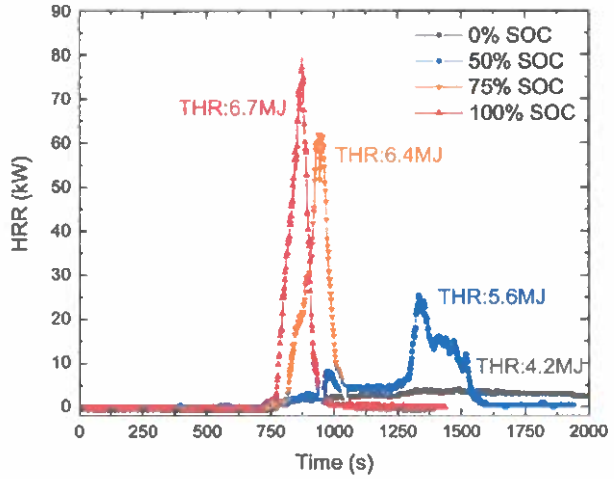

Fig. 6. The HRR curves of LIBs with 100%, 75%, 50% and 0% SOC.

released from the battery, forming a high-speed jet flame during stage III. The average length of jet flame is calculated by MATLAB software based on OTSU method (Otsu, 1979) and the flame reaches a length of more than 55 cm for the fully charged battery as shown in Fig. 5. Then the combustion becomes stable again and the flame is in the direction of vertical buoyancy at stage IV followed by a decay (stage V) until the fire is extinguished. Comparing the burning behaviors of LIBs with four different SOCs, it can be seen that the one with higher SOC shows a longer combustion flame and stronger ejection at stage III and also presents a larger scale of fire at stage IV. This is because both the amount of available O_2 released from cathode decomposing, and the intercalated Li in the anode increase with SOC. This contributes to the significant exothermic reactions such as the combustion of carbonous material and Li oxidation during thermal runaway (Golubkov et al., 2015). Therefore, the battery with higher SOC, has greater electrochemical potential energy that leads to a higher heat release and gas generation rate. It can be seen that SOC is one of the most important factors that affect the burning behavior of LIBs.

4.2. Thermal hazards

4.2.1. Heat release rate

Heat release rate (HRR) is one of the key parameters for characterizing the energy-releasing process (Chen et al., 2017). The HRR curves of LIBs with different SOCs are shown in Fig. 6. The peak HRR values are 80, 70.2, 25.8 and 4.2 kW for 100%, 75%, 50% and 0% SOC, respectively, as presented in Table 1. The results show that the peak HRR value increases with SOC. The normalized HRR value (kW/m^2) can be obtained by dividing the peak HRR values by surface area of the battery. The results are compared with those of common fuels and polymers, the data for which are taken from the SFPE Handbook. As shown in Fig. 7, the normalized HRR value of the fully charged LIB is very close to that of gasoline. The normalized HRR value of the 75% SOC LIB is higher than that of fuel oil. For the 50% SOC LIB, this is equal to that of PMMA and the 0% SOC LIB has the lowest value.

The total heat release (THR) is calculated by integrating the HRR profiles and the results are also presented in Table 1. It can be seen that the THR values increase with SOC. Moreover, when thermal runaway happens, the combustion heat is suddenly released within a very short time and the HRR increases more sharply for batteries with higher SOC. This occurs because more lithium ions embed into the negative electrodes at higher SOC and increase the instability of the intercalated carbon. Therefore, the activation energy is lower, and the reaction rate inside the battery is higher during the exothermic reactions.

4.2.2. Flame temperature

Fig. 8 shows the flame temperature curves of LIBs with 100%, 75%, 50% and 0% SOC. The temperatures measured by the four thermocouples increase sharply at the onset of thermal runaway for batteries with 50%, 75% and 100% SOC. The Thermocouple 3 always detects a higher temperature of flame than other thermocouples and the highest flame temperature is 798 °C, 807 °C and 863 °C for batteries with 50%, 75% and 100% SOC, respectively. The failure of a single LIB can easily trigger thermal runaway in neighboring batteries at such a high temperature and cause cascading failure due to the impact of flaming combustion. It also should be noted that more temperature peaks are observed for the batteries with higher SOC due to multiple jets of flame.

4.2.3. Thermal effects due to convective and radiant heat

The effects of convective and radiant heat are crucial in the assessment of fire hazards. The thermal effects are calculated by the average values of heat flux and temperature, which are obtained from different measuring points, located 30 cm away from the side of the batteries. Fig. 9 and Fig. 10 show the average heat flux and temperature curves. The heat flux is determined by the combustion intensity and has similar trends with HRR. This can be confirmed by the general observations on fire behavior as described in Section 4.1. The peak heat flux values are 23.9, 14.2, 2.5 and 1 kW/m^2 for batteries with 100%, 75%, 50% and 0% SOC, respectively. Skin temperature depends on the balance between the rate of heat absorption and heat dissipation. The tenability limit for exposure of skin to radiant heat is approximately 2.5 kW/m^2, below which exposure can be tolerated for at least several minutes (ISO 13571, 2012). The radiant heat, of the 100% and 75% SOC batteries, is above this threshold and would cause pain and skin burns within a few seconds. It can be observed in Fig. 10 that the average temperature significantly increases with SOC, and the peak temperature of 100% SOC can be as high as 172 °C, which exceeds the

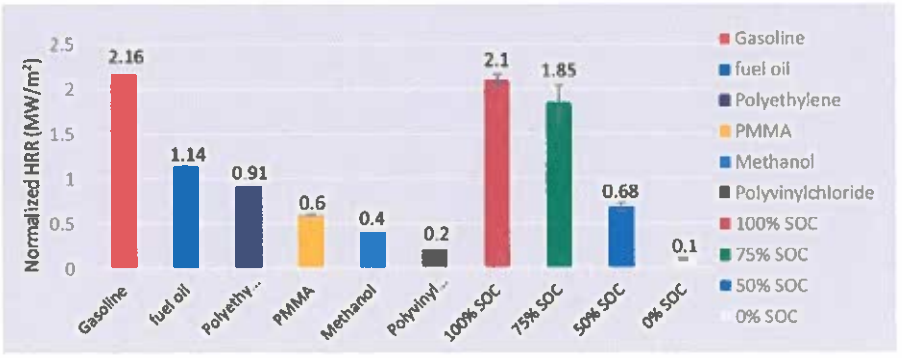

Fig. 7. The normalized HRR of LIB with 100%, 75%, 50% and 0% SOC in comparison with that of the common combustibles.

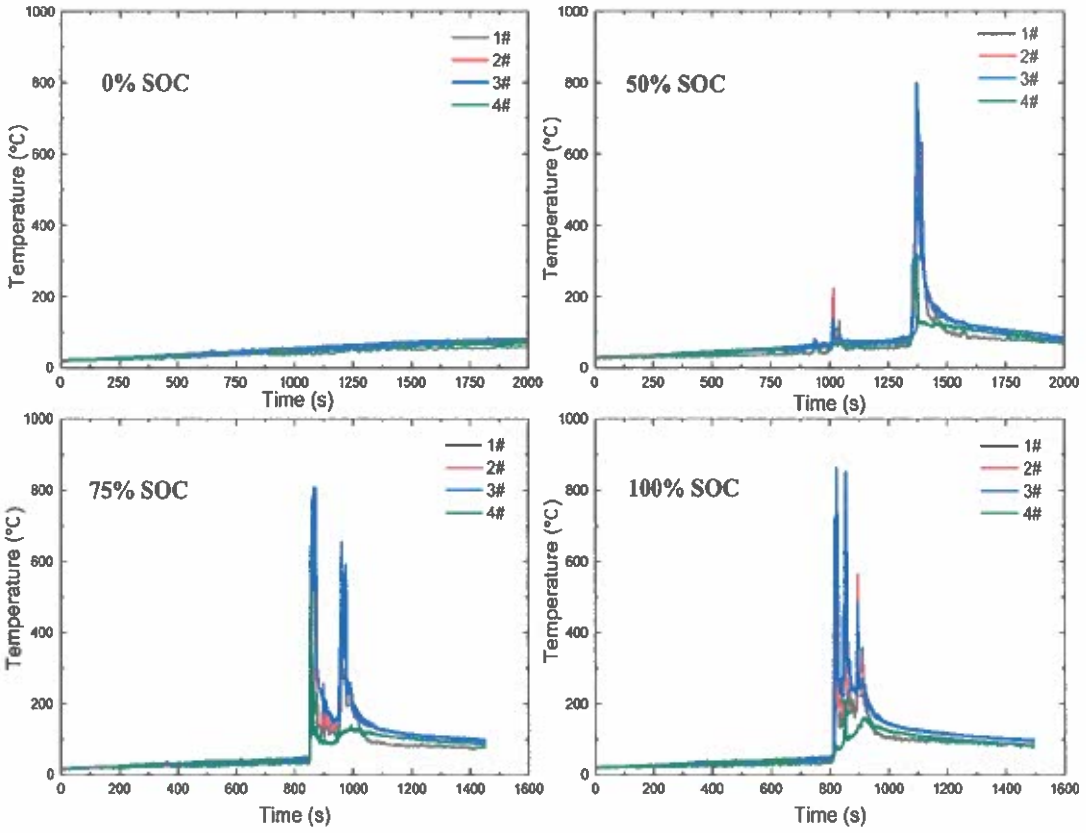

Fig. 8. Flame temperature curves of LIBs with 100%, 75%, 50% and 0% SOC.

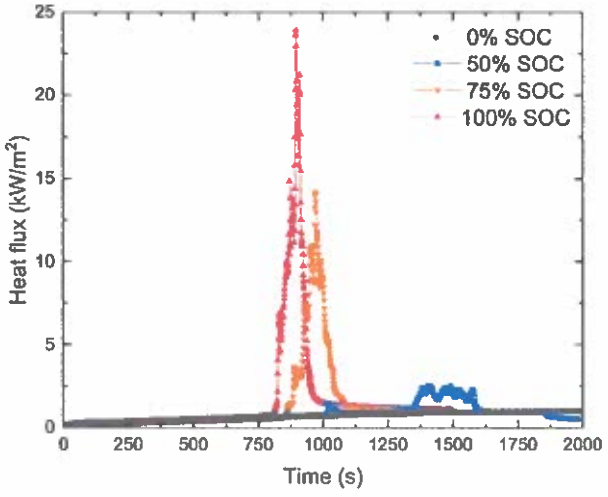

Fig. 9. Average heat flux curves of LIBs with 100%, 75%, 50% and 0% SOC.

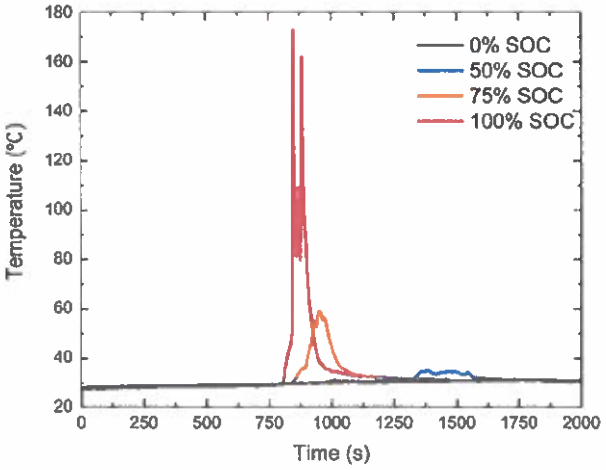

Fig. 10. Average temperature curves of LIBs with 100%, 75%, 50% and 0% SOC.

limit of 120 °C suggested by thermal tolerance data for unprotected skin of humans and would cause considerable pain within a few minutes (Purser, 2000).

Fig. 11 shows the results of FED calculated from thermal effects in such fire scenarios. A higher FED value represents more serious thermal hazards. The FED_{therm} curves of charged LIBs rise very steeply after the occurrence of thermal runaway which is accompanied by violent ejection. For batteries with 100% and 75% SOC, the FED_{therm} is higher than five within one minute after the onset of thermal runaway, indicating significant thermal effects from radiant and convective heat. Any people exposed to this fire scenario would suffer serious skin pain and burns. For the 50% SOC battery, the thermal effects are approaching the tenability threshold (FED of 1) after 24 min. It is considered that approximately 50% of people exposed to such fire scenarios would fail to escape due to the thermal hazards. The effects of 0% SOC battery can be negligible in comparison with those of batteries with higher SOC.

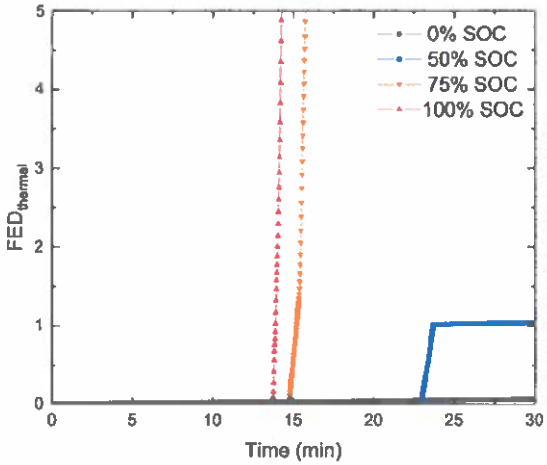

Fig. 11. Evolution of FED due to thermal effects of LIBs with 100%, 75%, 50% and 0% SOC.

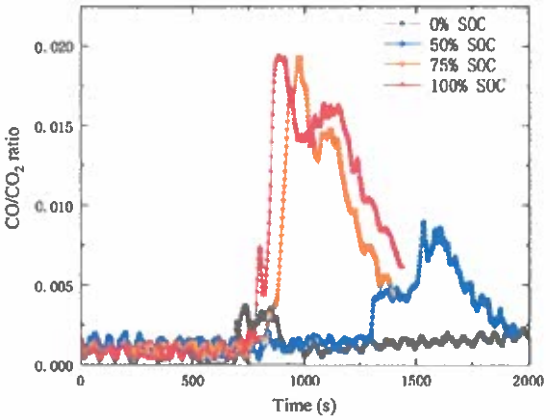

Fig. 13. The ratio of CO/CO_2 of LIBs with different SOCs.

4.3. Toxic threat

4.3.1. Asphyxiant gases

Carbon monoxide (CO) is generally considered to be one of the most poisonous components in fire gases (Kuligowski, 2009). The presence of CO_2 can increase the rate of asphyxiant uptake and hence increase the toxic effects. The CO and CO_2 concentration curves of LIBs with different SOC are shown in Fig. 12. The maximum CO concentration is 258 ppm, but the duration is very short. The maximum exposure allowed by occupational safety and health administration (OSHA) in the workplace over an eight-hour period is 50 ppm of CO. Individuals will experience slight headache and even loss of judgment within two to three hours of exposure to 200 ppm (Betterman and Patel, 2014). The maximum CO_2 concentration of batteries, with any SOC, is far from the threshold of 10% which may cause convulsions, coma and death (Permentier et al., 2017).

The CO/CO_2 ratio can reflect the fire hazards from another point of view as demonstrated in Fig. 13. For batteries with 100% and 75% SOC, the CO/CO_2 ratios are comparable and significantly higher than those of 50% and 0% SOC batteries, indicating a lower combustion efficiency for a higher SOC battery. This is in accordance with the observations in Section 4.1 in that the higher SOC battery has a more violent ejection during thermal runaway, which leads to incomplete combustion. That generally produces more toxic products including CO, HCN and other irritant gases, instead of the relatively harmless CO_2 and water.

4.3.2. Irritant gases

The major irritant gases analyzed by FTIR are HF, SO_2, NO_2, NO and HCl. Fig. 14 shows the concentration curves of these irritant gases. The production of these gases shows a significant increase when thermal runaway reactions take place, and then decreases quickly as the fire abates. HF primarily originates from the battery electrolyte ($LiPF_6$) and electrode binder (PVdF), but emissions can also come from coating materials such as AlF_3. The formation of HF can be described according to the following reactions (Yang et al., 2006; Kawamura et al., 2006):

$$LiPF_6 \rightarrow LiF + PF_5 \quad (7)$$

$$PF_5 + H_2O \rightarrow POF_3 + 2HF \quad (8)$$

$$LiPF_6 + H_2O \rightarrow LiF + POF_3 + 2HF \quad (9)$$

The toxicity of HF is well known and Table. 2 shows the IDLH limits and the maximum concentration values obtained in the tests. The maximum HF concentration is 165 mg/m^3 as shown in Table 2, which exceeds the IDLH value by one order of magnitude. This fire atmosphere poses an immediate threat to life and will cause irreversible health effects.

Fig. 14 (b) presents the sulfur dioxide production. SO_2 is generated

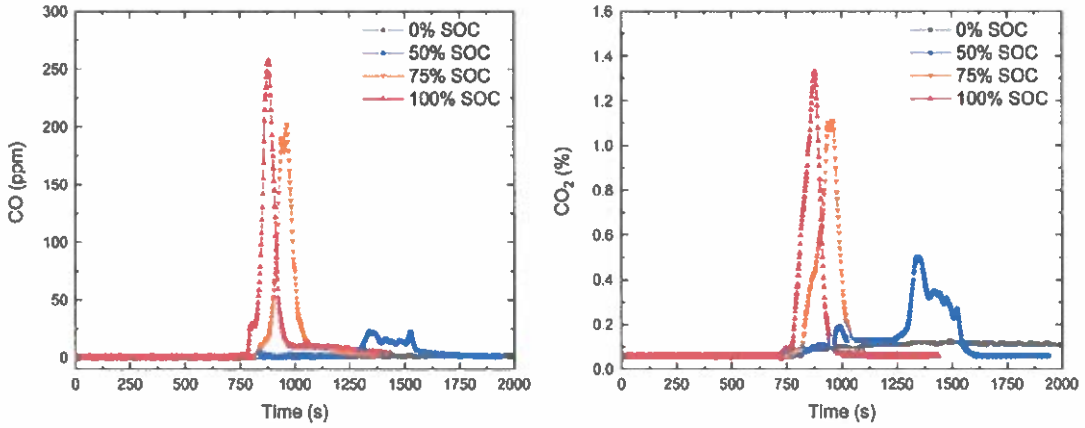

(a) (b)

Fig. 12. Concentration of CO and CO_2 as a function of time of LIBs with different SOCs.

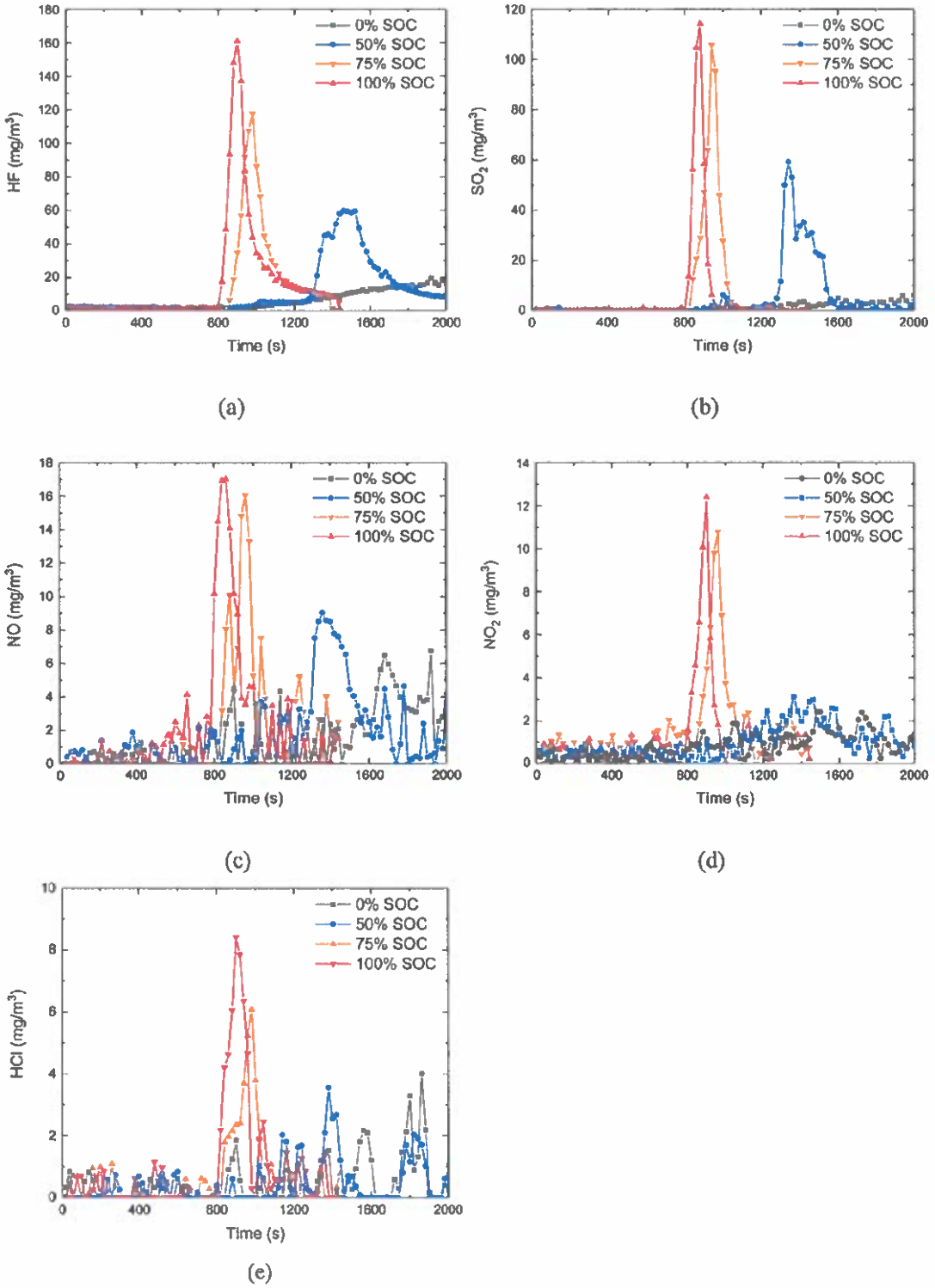

Fig. 14. Concentration of irritant gases as a function of time of LIBs with different SOCs.

from sulfur-based compounds which are used as reduction-type additives (Zhang, 2006) to assist solid electrolyte interphase (SEI) formation. The concentration of SO_2 depends on SOC, but it can also be detected at low SOCs. Previous published work (Ribière et al., 2012), conducted with 2.9 Ah pouch $LiMn_2O_4$/graphite batteries, showed a different result that only the fully charged battery released SO_2 in the test. This is attributed to the fact that the battery materials are different from those used in this work. In addition, large format LIBs with 75% and 50% SOC, still can release enough heat to support the formation of SO_2 during the exothermic reactions. Exposures of 10 to 20 ppm (US

Table 2
The maximum concentrations of irritant gases and IDLH values.

Substance	IDLH Value (mg/m^3)	Maximum value (mg/m^3)
Hydrogen fluoride (HF)	24.6	165 ± 10
Sulfur dioxide (SO_2)	262	115 ± 12
Nitric oxide (NO)	123	16 ± 2
Nitrogen dioxide (NO_2)	37.6	11 ± 1
Hydrogen chloride (HCl)	74.5	10 ± 2

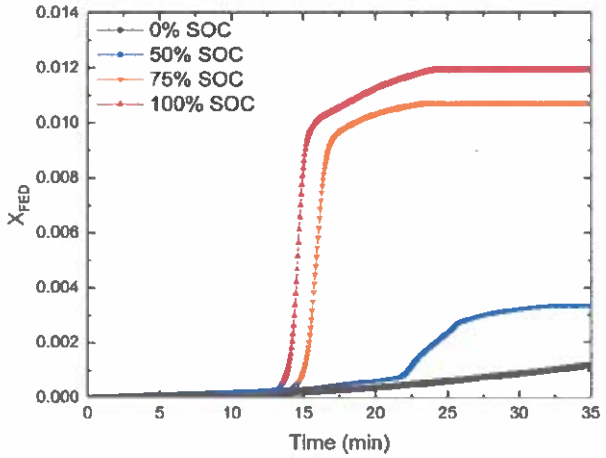

Fig. 15. Evolution of FED of asphyxiant gases (CO and CO_2).

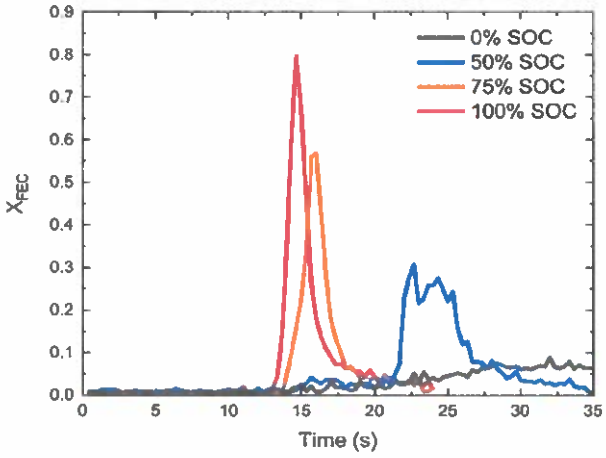

Fig. 16. Evolution of FEC of irritant gases (SO_2, HCl, NO_2, NO and HF).

Department of Health Human Services, 1998), namely 26.2 to 52.4 mg/m^3, can cause irritation to mucous membranes. Exposure to 262 mg/m^3 sulfur dioxide is considered immediately dangerous to life and health. The maximum concentration of SO_2 is 115 mg/m^3, at which sensible effects can be observed in the studied fire scenario.

Compared with HF and SO_2, the concentrations of nitrogen oxides are relatively low as shown in Fig. 14 (c) and (d). The nitrogen oxides are considered to be reaction products during high temperature combustion. The maximum concentrations of NO and NO_2 are 16 and 11 mg/m^3, which are far from IDLH limits.

HCl is also detected in the fire effluents as shown in Fig. 14 (e). Chlorine can be found as inorganic electrolyte in the form of e.g. $LiClO_4$ or in the plastic packaging as a flame-retardant additive (Diaz et al., 2019). A previous study (Kuligowski, 2009) found that greater than and equal to 5 ppm of HCl is immediately irritating, and 10 ppm to 50 ppm is the maximum concentration tolerable for one hour. The maximum concentration of HCl is 10 mg/m^3, or approximately 6.8 ppm, which will produce little effect.

The production of all the five irritant gases increases with SOC. As an irritant gas, HF has the greatest effect by comparing the maximum concentration with the toxicity thresholds available in the literature (Kuligowski, 2009; US Department of Health Human Services, 1998; Pohanish, 2008) or international safety standard (The National Institute for Occupational Safety and Health (NIOSH), 2014). The maximum values of other gases are lower than the IDLH limits. However, it should be highlighted that the battery system of a typical electric bus (i.e. ANKAI EV bus) consists of 6-8 modules and each module has 72 cells. Besides, the tests are conducted in well-ventilated conditions and the fire toxicity will be more serious in an enclosed environment. Therefore, the identification and quantification of fire gases are helpful for the design of new materials, risk assessment and management.

4.3.3. Toxicity evaluation

The combined toxic effects of various gas emissions are extremely required to be evaluated in a real, or near-real fire scenario after identifying their compositions. The toxic gas models described in ISO 13571 are used to estimate the expected toxicity based on the experimental data. Fig. 15 and Fig. 16 show the FED and FEC evolution during combustion of batteries with different SOCs. The curves clearly reflect a cumulative, and immediate effect for asphyxiant and irritant gases, respectively. Both the FED and FEC values increase with SOC. Effects of asphyxiant and irritant gases start to be visible after 800 s of the experiment. Values of FED remain very low, compared with those of FEC, and the difference is more than one order of magnitude, indicating that the effect of CO and CO_2 is limited. This also reveals the fact that the tests are conducted under well-ventilated condition. The effects of irritant gases are predominant. The maximum FEC values are 0.8, 0.56, 0.31 and 0.08 of LIB with 100%, 75%, 50% and 0% SOC, respectively. The higher the FED/FEC, the greater the toxicity of the effluent and FEC of 1 corresponds to loss of evacuation capability for half of the exposed people. Therefore, the results indicate that a critical situation might occur if the toxic gases are released in an electric vehicle in the case of a thermal event caused by LIBs.

The consequences are increased due to the fact that the maximum of emissions occur, for all irritant gases, almost at the same time, as shown in Fig. 14. Fig. 17 shows the peak FEC values contributed from each kind of irritant gas to illustrate the relative importance of the individual toxicants. The sum of contributions from HF and SO_2 accounts for 90%, 85%, 88% and 91% of all irritant gases released from 100%, 75%, 50% and 0% SOC. The data clearly show that HF and SO_2 are more important than the other gases. Thus, $LiPF_6$ needs to be replaced with a safer, and more environment-friendly salt in the future and the use of additives may lower the overall safety level after taking the smoke toxicity into consideration.

5. Conclusions

This paper presents a comprehensive study on the thermal and toxic hazards of 68 Ah pouch lithium iron phosphate batteries conducted in 1/2 ISO full scale test room under well-defined conditions.

It is observed that the batteries experience a peaceful burning stage with a small flame before the onset of thermal runaway, which is beneficial for possible early warning and emergency management. The jet flame reaches a length of 55 cm for the fully charged battery, which is more than 2.5 times that of the length itself. The normalized HRR value of the fully charged LIB is almost equivalent to that of gasoline. The thermal hazards have been quantitatively evaluated by combining the effects of convective and radiative heat and the batteries with higher SOCs are found to have greater thermal risks.

The major toxic gases analyzed in the experiments are CO, HF, SO_2, NO_2, NO and HCl. The production of all these gases increases with SOC.

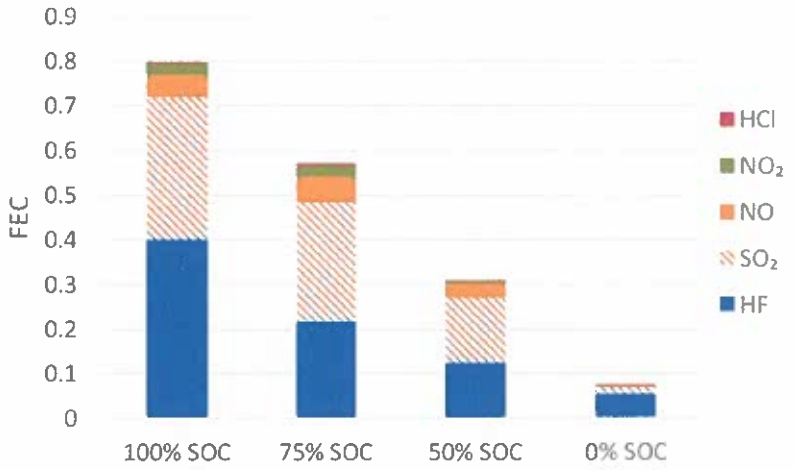

Fig. 17. The peak FEC values contributed from each irritant gas of LIBs with different SOCs.

FED and FEC models are used to perform a quantitative evaluation of the combined effects of toxic gases released from a LIB fire. According to the results, the effects of irritant gases are much more significant than those of asphyxiant gases with the difference being more than one order of magnitude. The maximum FEC value is 0.8, which means that nearly half of the exposed people will lose the evacuation capability in such a fire scenario. Besides, HF and SO_2 have much greater effects than the other toxic gases.

Acknowledgments

This work was supported by National Science Foundation of China (No.51636008), Key Research Program of Frontier Sciences, CAS [No. QYZDB-SSW-JSC029] and the Fundamental Research Funds for the Central Universities (No. WK2320000040).

References

Abada, S., Marlair, G., Lecocq, A., Petit, M., Sauvant-Moynot, V., Huet, F., 2016. Safety focused modeling of lithium-ion batteries: A review. J. Power Sources 306, 178–192. https://doi.org/10.1016/j.jpowsour.2015.11.100.

Andersson, P., Blomqvist, P., Lorén, A., Larsson, F., 2016. Using Fourier transform infrared spectroscopy to determine toxic gases in fires with lithium-ion batteries. Fire Mater. 40, 999–1015. https://doi.org/10.1002/fam.2359.

Betterman, K., Patel, S., 2014. Neurologic complications of carbon monoxide intoxication. Handbook of clinical neurology. Elsevier, pp. 971–979.

Chen, W.-C., Wang, Y.-W., Shu, C.-M., 2016. Adiabatic calorimetry test of the reaction kinetics and self-heating model for 18650 Li-ion cells in various states of charge. J. Power Sources 318, 200–209. https://doi.org/10.1016/j.jpowsour.2016.04.001.

Chen, M., Liu, J., He, Y., Yuen, R., Wang, J., 2017. Study of the fire hazards of lithium-ion batteries at different pressures. Appl. Therm. Eng. 125, 1061–1074. https://doi.org/10.1016/j.applthermaleng.2017.06.131.

Diaz, F., Wang, Y., Weyhe, R., Friedrich, B., 2019. Gas generation measurement and evaluation during mechanical processing and thermal treatment of spent Li-ion batteries. Waste Manage. 84, 102–111. https://doi.org/10.1016/j.wasman.2018.11.029.

Feng, X., Fang, M., He, X., Ouyang, M., Lu, L., Wang, H., Zhang, M., 2014a. Thermal runaway features of large format prismatic lithium ion battery using extended volume accelerating rate calorimetry. J. Power Sources 255, 294–301. https://doi.org/10.1016/j.jpowsour.2014.01.005.

Feng, X., Sun, J., Ouyang, M., He, X., Lu, L., Han, X., Fang, M., Peng, H., 2014b. Characterization of large format lithium ion battery exposed to extremely high temperature. J. Power Sources 272, 457–467. https://doi.org/10.1016/j.jpowsour.2014.08.094.

Fu, Y., Lu, S., Li, K., Liu, C., Cheng, X., Zhang, H., 2015. An experimental study on burning behaviors of 18650 lithium ion batteries using a cone calorimeter. J. Power Sources 273, 216–222. https://doi.org/10.1016/j.jpowsour.2014.09.039.

Golubkov, A.W., Scheikl, S., Planteu, R., Voitic, G., Wiltsche, H., Stangl, C., Fauler, G., Thaler, A., Hacker, V., 2015. Thermal runaway of commercial 18650 Li-ion batteries with LFP and NCA cathodes – impact of state of charge and overcharge. RSC Adv. 5, 57171–57186. https://doi.org/10.1039/c5ra05897j.

ISO 13571, 2012. Life-threatening components of fire- Guidelines for the estimation of time to compromised tenability in fires.

ISO 5660-1, 2015. Reaction to Fire Tests - Heat Release Smoke Production and Mass Loss Rate Part1 Heat Release Rate (cone calorimeter method) and smoke production rate (dynamic measurement).

Jhu, C.Y., Wang, Y.W., Shu, C.M., Chang, J.C., Wu, H.C., 2011. Thermal explosion hazards on 18650 lithium ion batteries with a VSP2 adiabatic calorimeter. J. Hazard. Mater. 192, 99–107. https://doi.org/10.1016/j.jhazmat.2011.04.097.

Jhu, C.-Y., Wang, Y.-W., Wen, C.-Y., Shu, C.-M., 2012. Thermal runaway potential of $LiCoO_2$ and $Li(Ni_{1/3}Co_{1/3}Mn_{1/3})O_2$ batteries determined with adiabatic calorimetry methodology. Appl. Energy 100, 127–131. https://doi.org/10.1016/j.apenergy.2012.05.064.

Kawamura, T., Okada, S., Yamaki, J.-I., 2006. Decomposition reaction of $LiPF_6$-based electrolytes for lithium ion cells. J. Power Sources 156, 547–554. https://doi.org/10.1016/j.jpowsour.2005.05.084.

Kuligowski, E.D., 2009. Compilation of data on the sublethal effects of fire effluent. NIST Technical Note 1644, 18.

Larsson, F., Andersson, P., Blomqvist, P., Lorén, A., Mellander, B.-E., 2014. Characteristics of lithium-ion batteries during fire tests. J. Power Sources 271, 414–420. https://doi.org/10.1016/j.jpowsour.2014.08.027.

Larsson, F., Andersson, P., Blomqvist, P., Mellander, B.E., 2017. Toxic fluoride gas emissions from lithium-ion battery fires. Sci. Rep. 7, 10018. https://doi.org/10.1038/s41598-017-09784-z.

Larsson, F., Bertilsson, S., Furlani, M., Albinsson, I., Mellander, B.-E., 2018. Gas explosions and thermal runaways during external heating abuse of commercial lithium-ion graphite-$LiCoO_2$ cells at different levels of ageing. J. Power Sources 373, 220–231. https://doi.org/10.1016/j.jpowsour.2017.10.085.

Lecocq, A., Eshetu, G.G., Grugeon, S., Martin, N., Laruelle, S., Marlair, G., 2016. Scenario-based prediction of Li-ion batteries fire-induced toxicity. J. Power Sources 316, 197–206. https://doi.org/10.1016/j.jpowsour.2016.02.090.

Li, H., Duan, Q., Zhao, C., Huang, Z., Wang, Q., 2019. Experimental investigation on the thermal runaway and its propagation in the large format battery module with $Li(Ni_{1/3}Co_{1/3}Mn_{1/3})O_2$ as cathode. J. Hazard. Mater. 375, 241–254. https://doi.org/10.1016/j.jhazmat.2019.03.116.

Liu, X., Stoliarov, S.I., Denlinger, M., Masias, A., Snyder, K., 2015. Comprehensive calorimetry of the thermally-induced failure of a lithium ion battery. J. Power Sources 280, 516–525. https://doi.org/10.1016/j.jpowsour.2015.01.125.

Liu, X., Wu, Z., Stoliarov, S.I., Denlinger, M., Masias, A., Snyder, K., 2016. Heat release during thermally-induced failure of a lithium ion battery: Impact of cathode composition. Fire Saf. J. 85, 10–22. https://doi.org/10.1016/j.firesaf.2016.08.001.

McKenna, S.T., Birtles, R., Dickens, K., Walker, R.G., Spearpoint, M.J., Stec, A.A., Hull, T.R., 2018. Flame retardants in UK furniture increase smoke toxicity more than they reduce fire growth rate. Chemosphere 196, 429–439. https://doi.org/10.1016/j.chemosphere.2017.12.017.

Otsu, N., 1979. A threshold selection method from gray-level histograms. IEEE Transactions on Systems, Man, and Cybernetics 9, 62–66. https://doi.org/10.1109/TSMC.1979.4310076.

Permentier, K., Vercammen, S., Soetaert, S., Schellemans, C., 2017. Carbon dioxide poisoning: a literature review of an often forgotten cause of intoxication in the emergency department. Int J Emerg Med 10, 14. https://doi.org/10.1186/s12245-017-0142-y.

Ping, P., Wang, Q., Huang, P., Li, K., Sun, J., Kong, D., Chen, C., 2015. Study of the fire behavior of high energy lithium-ion batteries with full-scale burning test. J. Power Sources 285, 80–89. https://doi.org/10.1016/j.jpowsour.2015.03.035.

Pohanish, R.P., 2008. Sittig's Handbook of Toxic and Hazardous Chemicals and Carcinogens. William Andrew.

Purser, D.A., 2002. Toxicity assessment of combustion products. The SFPE handbook of fire protection engineering 2, 83–171.

Purser, D.A., 2000. Toxic product yields and hazard assessment for fully enclosed design fires. Polym. Int. 49, 1232–1255. https://doi.org/10.1002/1097-0126(200010)49:10<1232::AID-PI543>3.0.CO;2-T.

Ribière, P., Grugeon, S., Morcrette, M., Boyanov, S., Laruelle, S., Marlair, G., 2012.

investigation on the fire-induced hazards of Li-ion battery cells by fire calorimetry. Energy Environ. Sci. 5, 5271–5280. https://doi.org/10.1039/c1ee02218k.
Said, A.O., Lee, C., Liu, X., Wu, Z., Stoliarov, S.I., 2018. Simultaneous measurement of multiple thermal hazards associated with a failure of prismatic lithium ion battery. Proc. Combust. Inst. https://doi.org/10.1016/j.proci.2018.05.066.
Stec, A.A., 2017. Fire toxicity–The elephant in the room? Fire Saf. J. 91, 79–90. https://doi.org/10.1016/j.firesaf.2017.05.003.
Stec, A.A., Hull, T.R., 2011. Assessment of the fire toxicity of building insulation materials. Energy and Buildings 43, 498–506. https://doi.org/10.1016/j.enbuild.2010.10.015.
Sun, J., Li, J., Zhou, T., Yang, K., Wei, S., Tang, N., Dang, N., Li, H., Qiu, X., Chen, L., 2016. Toxicity, a serious concern of thermal runaway from commercial Li-ion battery. Nano Energy 27, 313–319. https://doi.org/10.1016/j.nanoen.2016.06.031.
The National Institute for Occupational Safety and Health (NIOSH), 2014. Immediately Dangerous To Life or Health (IDLH) Values. in,. (accessed 20 June 2019. https://www.cdc.gov/niosh/idlh/.
Torero, J.L., Handbook, Ignition, 2004. Principles and Applications to Fire Safety Engineering, Fire Investigation, Risk Management and Forensic Science by Vytenis Babrauskas, PhD. J. Fire. Prot. Eng. 14, 229–232. https://doi.org/10.1177/1042391504042549.
Truchot, B., Fouillen, F., Collet, S., 2018. An experimental evaluation of toxic gas emissions from vehicle fires. Fire Saf. J. 97, 111–118. https://doi.org/10.1016/j.firesaf.2017.12.002.
US Department of Health Human Services, 1998. Toxicological profile for sulfur dioxide. Public Health Service, Agency for Toxic Substances and Disease Registry.
Wang, Q.S., Ping, P., Zhao, X.J., Chu, G.Q., Sun, J.H., Chen, C.H., 2012. Thermal runaway caused fire and explosion of lithium ion battery. J. Power Sources 208, 210–224. https://doi.org/10.1016/j.jpowsour.2012.02.038.
Wieczorek, C.J., Dembsey, N.A., 2001. Human variability correction factors for use with simplified engineering tools for predicting pain and second degree skin burns, J. Fire. Prot. Eng. 11, 88–111. https://doi.org/10.1106/0D9U-KLP9-TG1P-XJ1B.
Wu, T., Chen, H., Wang, Q., Sun, J., 2018. Comparison analysis on the thermal runaway of lithium-ion battery under two heating modes. J. Hazard. Mater. 344, 733–741. https://doi.org/10.1016/j.jhazmat.2017.11.022.
Yang, H., Zhuang, G.V., Ross Jr, P.N., 2006. Thermal stability of $LiPF_6$ salt and Li-ion battery electrolytes containing $LiPF_6$. J. Power Sources 161, 573–579. https://doi.org/10.1016/j.jpowsour.2006.03.058.
Zhang, S.S., 2006. A review on electrolyte additives for lithium-ion batteries. J. Power Sources 162, 1379–1394. https://doi.org/10.1016/j.jpowsour.2006.07.074.
Zhang, R., Fu, Y., Yang, X., 2019. Electrochemical and thermal characterization of $Li_4Ti_5O_{12}$|| $Li_3V_2(PO_4)_3$ lithium ion battery. Solid State Ionics 331, 43–48. https://doi.org/10.1016/j.ssi.2018.12.018.
Zhong, G., Mao, B., Wang, C., Jiang, L., Xu, K., Sun, J., Wang, Q., 2018. Thermal runaway and fire behavior investigation of lithium ion batteries using modified cone calorimeter. J. Therm. Anal. Calorim. https://doi.org/10.1007/s10973-018-7599-7.

Journal of Loss Prevention in the Process Industries 80 (2022) 104851

Contents lists available at ScienceDirect

Journal of Loss Prevention in the Process Industries

journal homepage: www.elsevier.com/locate/jlp

Assessment of the explosion risk during lithium-ion battery fires

Sin Woo Kim, Soo Gyeong Park, Eui Ju Lee *

Department of Safety Engineering, Pukyong National University, 45, Yongso-ro, Nam-Gu, Busan, South Korea

ARTICLE INFO

Keywords:
Lithium-ion battery
Battery fire
Heat release rate
Cone calorimeter
Explosiveness

ABSTRACT

Lithium-ion batteries are widely used for renewable energy storage and to deliver mobile power because of their high energy densities and electromotive forces. However, such batteries can catch fire and explode, potentially causing casualties and property damage. Here, we used a cone calorimeter to investigate the fire risk and assess the associated heat release rate (HRR). Standard cylindrical battery fires feature two combustion stages, the first of which is characterized by diffusion-like flames and the second by partially premixed flames with a higher peak HRR and a violent explosion. The overall combustion properties depend principally on the state of charge (SOC). A higher SOC battery is associated with a higher maximum HRR, a shorter HRR peak-to-peak time, larger CO and CO_2 emissions, and a greater instantaneous mass loss. The average rate of heat emission based on the measured combustion properties is introduced and its maximum value is expected to predict reactivity and explosiveness comprehensively in the event of fire.

1. Introduction

Fossil fuel has been restricted in the use of energy source because it causes various environmental problems such as air pollution and global warming, and hence many efforts are being made to replace it with renewable energy. Since the new energy is produced on small scale and intermittently, it is necessary to introduce an energy storage systems (ESSs). Rechargeable batteries are a key component of ESS and the battery use is rapidly increasing for home and electric vehicles (Poizon and Dolhem, 2011). In particular, lithium-ion batteries among secondary batteries are most commercialized because of the advantages of heavy metal free, no memory effect, and high energy density. Because the electrolyte is a combustible organic solvent, and the anode, cathode, and separator are also made of a combustible material containing unstable lithium, a fire or explosion caused by thermal runaway after physical, electrical, or thermal failure is possible (Zalosh et al., 2021) and this safety problem must be solved for more wide use (Tarascon and Armand, 2001).

The combustion properties associated with battery fires and explosions include the heat release rate (HRR), toxic gas concentration, and smoke yield. The most representative physical property is the HRR; this predicts other important physical quantities and also fire and explosion severity. The HRRs of rechargeable battery fires have been extensively studied (Ouyang et al., 2017; Larsson et al., 2014a; Larsson et al., 2014b; Tarascon and Armand, 2001; Chen et al. 2016, 2017a, 2017b; Henriksen et al., 2019; Andersson et al., 2016; Ribiere et al., 2012; Walters and Lyon, 2016; Chena et al., 2020b; Liu et al., 2015, 2016). The HRRs of lithium-ion batteries are measured using principally conventional cone calorimeters; oxygen consumption rates are assessed. The maximum HRR of a standard cylindrical battery increases as the state of charge (SOC) increases. Also, the greater the heat flux of the radiant heater that irradiates the specimen, the higher the maximum HRR; the experimental conditions thus affect the HRRs (Fu et al., 2015; Poizot and Dolhem, 2011; Ouyang et al., 2017). Practical studies on real-world battery cells, have examined the effects of battery arrangement and type on fires. The relevant parameters include the mass reduction rate, the ignition time, the HRR, the total heat release (THR), and fire behavior. Some studies used Fourier transform infrared spectroscopy (FTIR) to evaluate overall toxicity; gas concentrations were measured during combustion. Other HRR assessments employed copper slug battery calorimetry (CSBC) based on the heat transfer laws, and bomb calorimeters that measured the calorific values of chemical reactants (Andersson et al., 2016; Liu et al., 2015, 2016; Walters and Lyon, 2016). When an explosion occurs during a fire, the risk is increased and damage may spread. Most experimental studies measured pressure changes when explosions occurred in constant-volume chambers (Chena et al., 2020a; Henriksen et al., 2019); few works sought to predict and evaluate the explosive properties of battery fires.

Even though there are a lot of studies on a lithium ion-battery fires, there was a few study that classified a battery fire by the expected

* Corresponding author.
E-mail address: ejlee@pknu.ac.kr (E.J. Lee).

https://doi.org/10.1016/j.jlp.2022.104851
Received 24 February 2022; Received in revised form 23 June 2022; Accepted 21 July 2022
Available online 19 August 2022
0950-4230/

participating components (Fu et al., 2015; Chen et al., 2017b) and no studies have been conducted to classify it based on the combustion characteristics. Also, a new parameter to indicate combustion degree including explosiveness and define fire hazard is needed for a battery fire. We explored lithium-ion battery fires in terms of their characteristics and explosion risks. We used a cone calorimeter to measure combustion characteristics including the HRR, CO and CO_2 concentrations, particle density, and mass loss as revealed by the SOC. Through the experimental results, we classified the fire stages based on the combustion characteristics, and introduced a parameter that assesses battery fire explosiveness and verified that it could be used to evaluate the overall safety of a lithium ion-battery.

2. Experiments

Several combustion properties of a lithium-ion battery were measured using a cone calorimeter. A standard Samsung cylindrical battery (INR, 18650-35E) equipped with a protection circuit was used in all experiments; the diameter and length were 18.55 mm and 69 mm respectively. The battery capacity was 3500 mAh; lithium-Nickel-Cobalt-Manganese (NCM) served as the cathode material; the anode was graphite. When charging the battery to 100, 50, and 0%, we assumed that the charged energy was proportional to the power $P = V^2/R$; we read the battery voltages between the fully charged state (100% SOC) and full discharge (0% SOC).

The cone calorimeter HRR test followed the procedure of the ISO 5660-1 standard (ISO 5660-1, 2018); a schematic is shown in Fig. 1. The battery was fixed to a stainless steel specimen holder of 54 mm in height, with an aperture of 94 × 94 mm. As the battery may swell or deform when heated, it was fixed in the center of the frame using 0.8 mm thick metal wire at a spacing of 20 mm. Downstream of the duct connected to the hood, a sampling tube was installed to measure the concentrations of gases emitted; the mass flow rate was calculated using the dynamic pressure obtained by the pitot tube and the temperature of the K-type thermocouple. Mass change over time was recorded using a load cell and the particle density measured by a laser detector system based on light extinction; the soot extinction coefficient was set to 10.3.

The lithium-ion battery in the holder was ignited from above by a radiant cone heater. The heating power was 30 kW and all experiments commenced after the heater attained that power. The volume flow rate discharged to the duct through the hood was set to 24 l/min, and the delay times for all measurements during sampling of O_2, CO, and CO_2 were corrected and synchronized over time. The HRR was based on the oxygen consumption rate, assuming that the heat of combustion was 13.1 MJ/(O_2)kg. As combustion is always incomplete, the CO concentration was measured and used for correction of the HRR assessments (ISO 5660-1, 2018).

3. Results and discussion

Fig. 2 shows photographs taken as the battery went on fire at 50% SOC. Smoke resembling flammable vapor emitted from the heated battery was ignited at 295 s and the flame persisted for about 30 s. Strong combustion accompanied by an explosion was observed at 361 s. This affected the entire test area; combustible vapor that leaked between the first and second combustion filled the space. The fire then rapidly declined and was completely out by 421 s. The second stage combustion was similar to that of a partial premixed flame, with an explosion. At 100% SOC, the first and second combustion stages were observed at 245 and 275 s respectively. The overall pattern was similar to that at 50% SOC, but ignition was earlier for both stages and the explosion stronger as revealed by flame luminosity. At 0% SOC, the first combustion was observed at 280 s, followed by the second combustion at 520 s as the smoke ignited. Compared to the 100% SOC and 50% SOC fires, the second combustion differed greatly, being both delayed and lacking an explosion.

Fig. 3 shows the concentrations of O_2, CO, and CO_2 during the 50% SOC fire. As all oxidization was attributable to oxygen in the surrounding air, the oxygen concentration of the post-flame region approximately indicates the extent of oxidation. However, lithium-ion battery fuel includes not only the various electrolytes but also oxygen added via combustion of lithium oxide; this can create errors when evaluating the HRR based on the oxygen consumption rate. Two large reductions in oxygen concentration were observed at the times of both combustions as shown in Fig. 3. The time at which the oxygen concentration first decreased was also the ignition time; the ignitions of the first

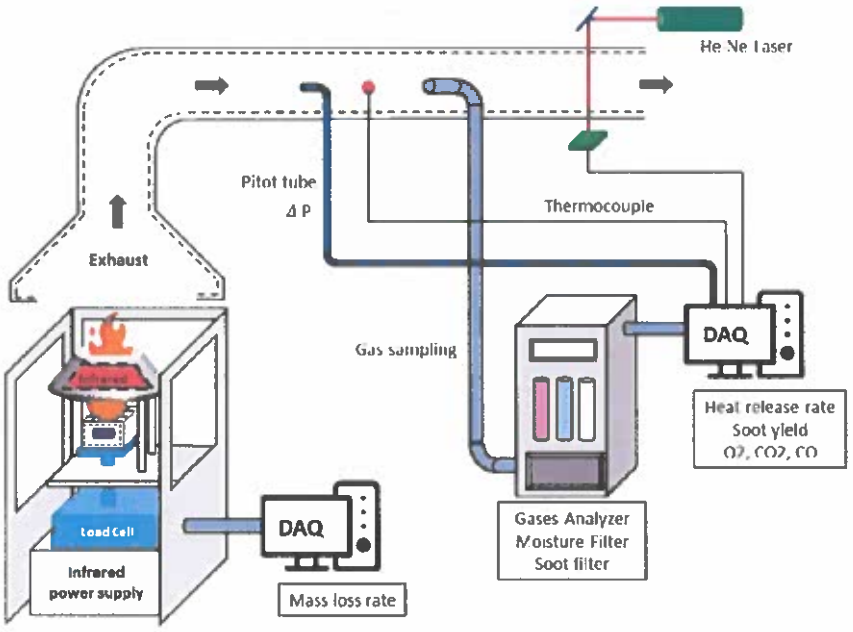

Fig. 1. Schematics of the lab-scale cone calorimeter and the experimental equipment.

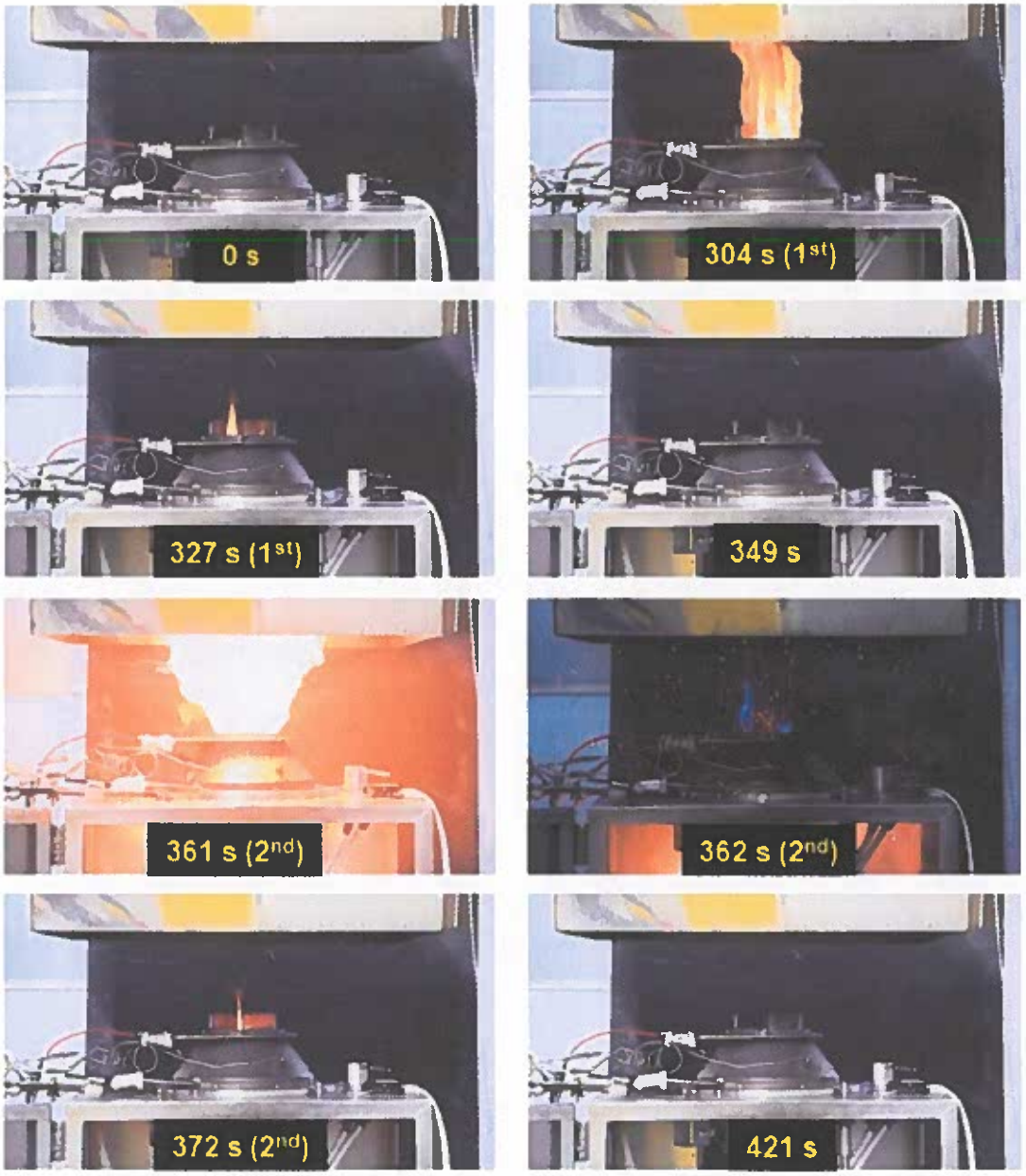

Fig. 2. Screenshots taken at various times during the fire test at 50% SOC.

and second combustion stages occurred at 290 s and 57 s later. Although the CO_2 and CO concentration peaks were delayed by several seconds compared to those of O_2, the peak CO and CO_2 times were the same, confirming that the overall oxidation involved the organic solvents (carbonates) of the electrolyte. In addition, the CO/CO_2 ratio as well as the concentrations were larger in the second than the first peak. A cone calorimeter test has been performed in over-ventilation condition in which sufficient oxidizing agent is present by the ambient air. The reason why a lot of CO generated in the combustion process is not converted to CO_2 is considered to be due to insufficient residence time, which indicates that the flow time (or mixing time) is smaller than the chemical time for CO to be converted into CO_2. Comparing the concentrations of CO and CO_2 at the two HRR peaks in Fig. 3, the CO/CO_2 ratio in the 2nd combustion stage is higher than in the 1st combustion stage. Considering that the 1st combustion stage is characterized by a diffusion flame and the 2nd combustion stage is by a partially premixed flame, it can be confirmed that the relatively high concentration of CO is due to the small flow time (or mixing time) in the process of conversion to CO_2. As the ratio reflects the extent of incomplete combustion, the first combustion occurred in an over-ventilated condition; the battery oxidizing agents affected the stoichiometry. The overall concentrations of CO and CO_2 at 100% and 0% SOC were similar to those at 50% SOC.

Fig. 4 shows the mass change of the 50% SOC battery measured by the load cell. The mass decreased at all times except initially regardless of flame presence or absence; the mass loss rate was greatly dependent on combustion. As heating commenced, mass reduction was gradual, but became larger after 300 s and very rapid with an overshoot caused by pressure generated by the instantaneous explosion at 350 s. When the mass loss during fire was compared with the oxygen consumption in Fig. 3, the mass reduction that occurs very slowly in the beginning is not

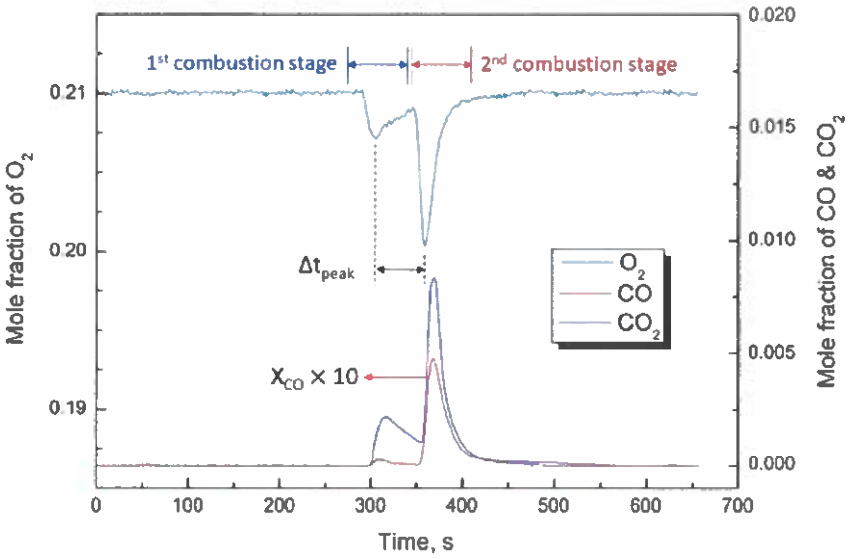

Fig. 3. Mole fractions of O_2, CO, and CO_2 as a function of time during the 50% SOC battery fire.

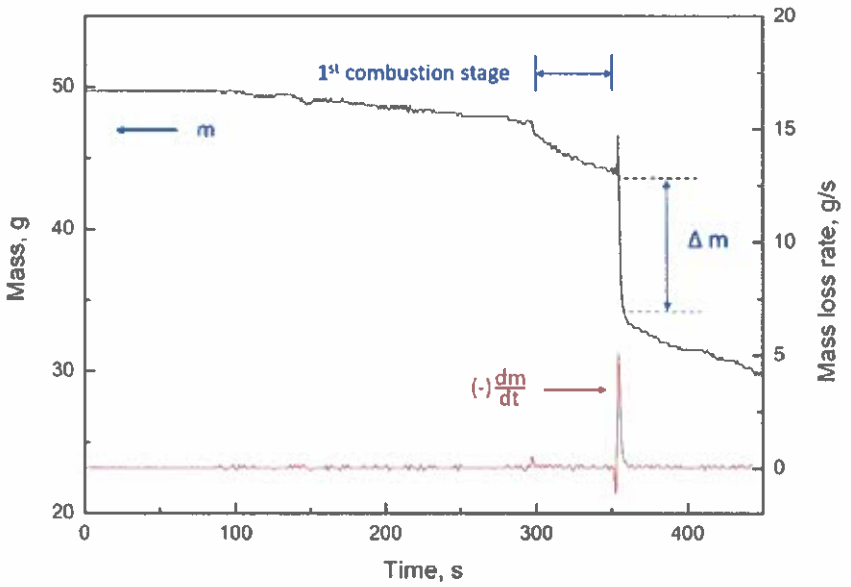

Fig. 4. Mass change and mass loss rate during the 50% SOC battery fire.

sufficient to produce a flammable concentration, and then when it is ejected with a larger mass rate, it is ignited and appears in the form of a flame within the first combustion stage. A large amount of combustible material had leaked in the flames at the end of the first combustion stage, became mixed with air inside the test section, and ignited instantaneously at 350 s. This large amount of combustible gas and the adequate mixing time produced an explosive flame and a larger HRR. The mass change during the 100% SOC fire was similar to that of the 50% SOC fire but began earlier and was more rapid during second-stage combustion. At 0% SOC, no rapid mass reduction was observed during fire.

Fig. 5 shows the HRRs calculated using the oxygen consumption rates but then corrected for incomplete combustion by reference to the CO levels. As the overall HRR profile of the 50% SOC battery is near-identical to the oxygen consumption rate of Fig. 3, any effect of incomplete combustion on the HRR was significant. The maximum HRRs were 5.04, 4.26, and 2.31 kW at 100, 50, and 0% SOC respectively; the maximum HRR increased significantly as SOC increased, and was larger than those of previous studies (Fu et al., 2015; Ribiere et al., 2012; Ouyang et al., 2017), perhaps because the materials used and the heating conditions varied. The various battery manufacturers employ different electrolytes and electrodes, and the heat fluxes of radiant heaters of the same power vary by heater location and angle. The effect of the SOC on the HRR is clearly reflected in the time between the two peaks and the maximum value. A shorter peak-to-peak time was obtained at a higher SOC; that time was very long at 0% SOC and the fire was not associated with an explosion. However, the ignition delay time at which leaked combustible gas began to react was independent of the

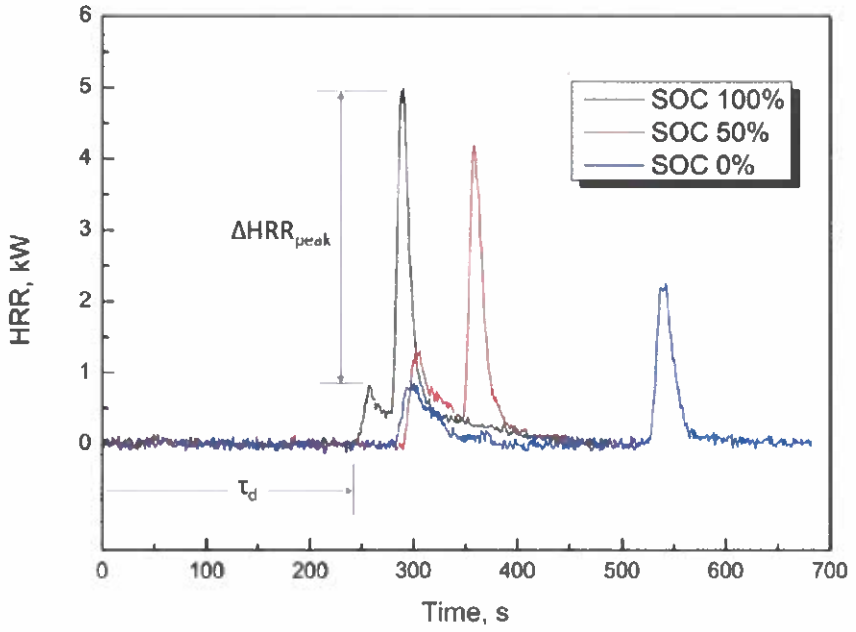

Fig. 5. HRRs of the Li-ion battery at different charge states during a fire.

SOC.

The energy release rate can also be estimated using the average energy per unit mass of all battery components and the mass loss rate during fire.

$$\dot{q} = \chi \dot{m}_{fuel} \Delta H_c$$

where $\dot{m}_{fuel}$ the mass loss rate of the sample, ΔH_c the heat of combustion, and χ is the combustion efficiency which assume that all released mass is not being converted to energy. As the bulk heat of battery combustion was 6.2 MJ/kg and the combustion efficiency 0.78 (Eshetu et al., 2013), the overall HRR curve is similar to the mass loss rate of Fig. 4, which is characterized by a rather short reaction time and a large maximum HRR. At 50% SOC, the maximum HRR based on the mass loss rate is about 25 kW, thus much larger than that yielded by the oxygen consumption rate (4.1 kW). The overestimation of peak HRR calculated by mass loss rate mainly suggests the assumption of all the potential combustion energy being released is far from being correct even though the effect can be included as the combustion efficiency. In addition, the reacting time varies greatly depending on HRR estimating method, which results from whether the time for mixing and reaction with the surrounding oxidizer is taken into account.

Particle density was measured using a laser extinction method in the

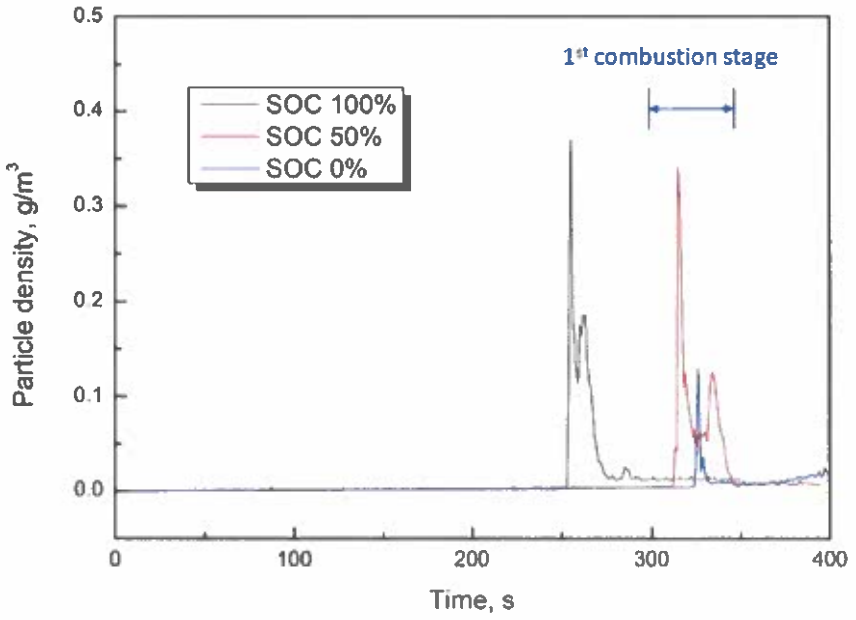

Fig. 6. Particle densities of the Li-ion battery fires at different SOCs. The 1st combustion stage is indicated for 50% SOC battery.

duct of the cone calorimeter and the results depict in Fig. 6. Among the various particles emitted during a battery fire, the possible substances to be detected by light extinction method may include the condensed gases including hydrocarbons, the metal oxides such as lithium, and soot particles. Although it is difficult to know exactly the fraction between the expected substances because the component analysis of the product particles was not performed in this study, soot might be the most significant particle considering the off-gases and the extinction coefficient of each material in the previous study. As shown in Fig. 6, two peaks are continuously found in the particle concentration similar to HRR, but it can be confirmed that all of them occur in the 1st combustion stage. That is, considering that the 1st combustion stage can be characterized as a diffusion flame, it can be inferred that soot is the main particle and some oxides or condensed particles are sequentially emitted without combustion. Also, it is found that the particle density is hardly detected at 100% and 50% SOC in the 2nd combustion stage, confirming that it is a characteristic of a partially premixed flame.

Fire hazard and risk have been evaluated by instantaneous HRR or total heat release in general fire, but a lithium-ion battery is composed of various heterogeneous combustible materials and is greatly affected by the thermal environment in case of fire (Fu et al., 2015). The results of this study show that various physical quantities such as two HRR peaks, the peak to peak time and whether explosion occurs according to the SOC were different from general fires. Therefore, the more comprehensive parameter is required to indicate combustion degree including explosiveness and define fire hazard for battery fires, in which the effect of SOC should be implicitly included in the parameter. When lithium-ion batteries catch fire, it is known that a larger SOC induces greater explosiveness as qualitatively confirmed by flame luminosity and mass loss overshoot. This can be quantified using various empirical properties. The shorter the HRR peak-to-peak time, the faster the battery mass decreases; the shorter the ignition delay time, the greater the explosiveness. The average rate of heat emission (ARHE) defined as the cumulative heat emission divided by time considers these data. The peak value (Maximum average rate of heat emission, MARHE) can be considered a good measure of the propensity for fire development generally; MARHE usefully represents explosiveness in this study. The ARHE is:

$$ARHE(t_n) = \left[\sum_{2}^{n} (t_n - t_{n-1}) \times \frac{q_n + q_{n-1}}{2} \right] \Big/ (t_n - t_0)$$

where t_n and q_n are the time and heat release rate of the n^{th} datum respectively. Fig. 7 illustrates the ARHEs and MARHEs derived from the HRRs of the three battery fires and Table 1 summarizes the combustion properties measured in the cone calorimeter (including the MARHE. The ARHE of Fig. 7 increases rapidly during the two combustion stages and then decays; the MARHE appears after the second HRR peak because of the time integral characteristic of the ARHE. As the SOC increases, so does the MARHE, because the ARHE is related to the overall HRR, the difference in the HRR peak-to-peak time, and the ignition delay time. Therefore, the MARHE might be very effective to predict the combustion degree and define hazard in the lithium-ion battery fires, and can be used a parameter to evaluate the explosiveness of clustered- and single-celled batteries. However, MARHE cannot be used directly for all battery fires, and hence more general parameter should be suggested through investigating the capacity and geometrical effects of batteries in the future.

4. Conclusion

We performed cone calorimeter experiments to investigate the fire characteristics of a lithium-ion battery including the HRR. A standard cylindrical battery equipped with a protection circuit was used in all experiments, and the concentrations of O_2, CO, and CO_2, the mass loss; and particle density were measured. The results may be summarized as follows.

1. The fire characteristics for 100, 50% and 0% SOC batteries

Table 1
Combustion properties yielded by battery fire tests at 100, 50, and 0% SOC.

SOC (%)	$\triangle t_{peak}$ (s)	$\triangle m$ (g)	t_d (s)	$\triangle HRR_{peak}$ (kW)	MARHE (kW)	t_{MARHE} (s)
100	33	17.0	249	4.13	0.32	353
50	52	10.3	291	2.89	0.28	388
0	242	N/A	285	1.32	0.12	571

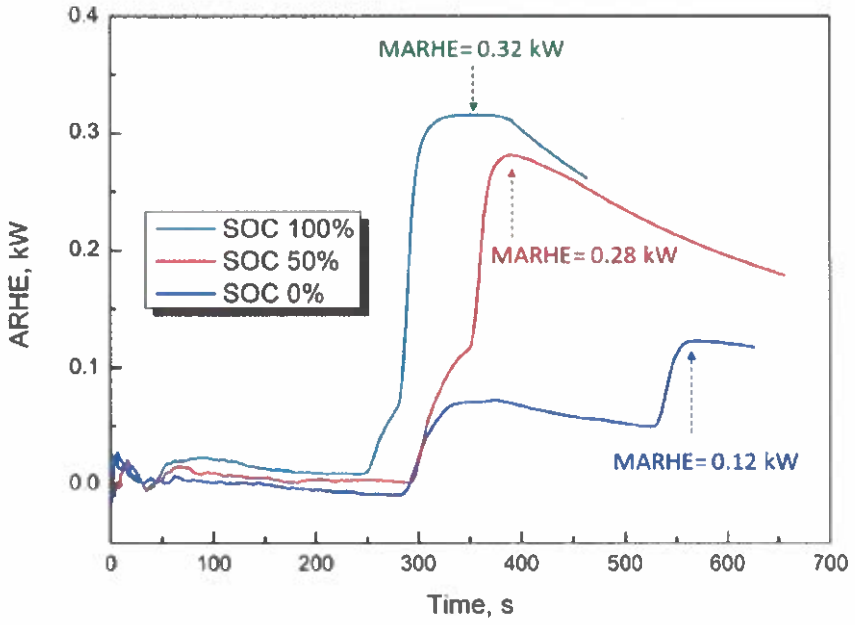

Fig. 7. The average rates of heat emission (ARHEs) and the maxima at different SOCs during fire.

featured two combustion stages. 1st and 2nd combustion stages were characterized by a diffusion flame and a partially premixed flame respectively based on combustion characteristics, which can be supported by various experimental results. An explosion occurred at the 2nd combustion stage for 50% and 100% SOCs batteries but no explosion for 0% SOC. Such an occasional explosion means that 2nd combustion stages is controlled by a partial premixed condition and whether explosion occurs or not is determined by premixedness. Also, comparing the concentrations of CO and CO_2 at the two HRR peaks, the CO/CO_2 ratio in the 2nd combustion stage is higher than in the 1st combustion stage. Considering that the 1st combustion stage is characterized by a diffusion flame and the 2nd combustion stage is by a partially premixed flame, it can be confirmed that the relatively high concentration of CO is due to the small flow time (or mixing time) in the process of conversion to CO_2. Lastly, particle concentration, unlike HRR or other gases, was detected only in the 1st combustion stage. Considering soot is the main particle emitted from a battery fire, it implies that 1st combustion stage can be characterized as a diffusion flame.

2. The HRR based on the oxygen consumption rates featured two peaks and clearly depended on the SOC; a high SOC was associated with a shorter peak-to-peak time, a higher peak HRR and a strong explosiveness. Considering these different features of lithium ion battery, a comprehensive parameter other than HRR and total heat release was required to indicate combustion degree including explosiveness and define fire hazard. As the MARHE considers the instantaneous maximum HRR, the peak-to-peak HRR time difference, and the ignition delay time implicitly, it can be used as an important parameter to evaluate the comprehensive risk such as explosion of a lithium-ion battery in the event of fire.

Author contribution statement

Sin Woo Kim: Methodology, Software, Validation, Formal analysis, Investigation, Data curation, Writing – original draft, Writing – review & editing, Visualization. Soo Gyeong Park: Methodology, Software, Validation, Formal analysis, Investigation, Data curation, Writing – original draft, Writing – review & editing, Visualization. Eui ju Lee: Conceptualization, Methodology, Validation, Formal analysis, Investigation, Resources, Data curation, Writing – original draft, Writing – review & editing, Supervision, Project administration, Funding acquisition.

Declaration of competing interest

The authors declare the following financial interests/personal relationships which may be considered as potential competing interests: EUIJU LEE reports financial support was provided by Pukyong National University.

Data availability

Data will be made available on request.

Acknowledgement

This research was supported by a Basic Science Research Program through the National Research Foundation of Korea (NRF) funded by the Ministry of Education (2020R1I1A3075066).

References

Andersson, P., Blomqvist, P., Lorén, A., Larsson, F., 2016. Using Fourier transform infrared spectroscopy to determine toxic gases in fires with lithium ion batteries. Fire Mater. 40, 999–1015. https://doi.org/10.1002/fam.2359.

Chena, S., Wang, Z., Yan, W., Liu, J., 2020a. Investigation of impact pressure during thermal runaway of lithium ion battery in a semi-closed space. Appl. Therm. Eng. 175, 115429 https://doi.org/10.1016/j.applthermaleng.2020.115429.

Chena, S., Wang, Z., Wang, J., Tong, X., Yan, W., 2020b. Lower explosion limit of the vented gases from Li-ion batteries thermal runaway in high temperature condition. J. Loss Prevent. Process Indus. 63, 103992 https://doi.org/10.1016/j.jlp.2019.103992.

Chen, M., Liu, J., He, Y., Yuen, R., Wang, J., 2017a. Study of the fire hazards of lithium-ion batteries at different pressures. Appl. Therm. Eng. 125, 1061–1074. https://doi.org/10.1016/j.applthermaleng.2017.06.131.

Chen, M., Yuen, R., Wang, J., 2017b. An experimental study about the effect of arrangement on the fire behaviors of lithium-ion batteries. J. Therm. Anal. Calorim. 129, 181–188. https://doi.org/10.1007/s10973-017-6158-y.

Chen, M., He, Y., De Zhou, C., Richard, Y., Wang, J., 2016. Experimental study on the combustion characteristics of primary lithium batteries fire. Fire Technol. 52, 365–385. https://doi.org/10.1007/s10694-014-0450-1.

Eshetu, G.G., Grugeon, S., Laruelle, S., Boyanov, S., Ledodq, A., Betrand, J.P., Marlair, G., 2013. In-depth safety-focused analysis of solvents used in electrolytes for large scale lithium ion batteries. Phys. Chem. Chem. Phys. 15, 9145–9155. https://doi.org/10.1039/C3CP51315G.

Fu, Y., Lu, S., Li, K., Liu, C., Cheng, X., Zhang, H., 2015. An experimental study on burning behaviors of 18650 lithium ion batteries using a cone calorimeter. J. Power Sources 273, 216–222. https://doi.org/10.1016/j.jpowsour.2014.09.039.

Henriksen, M., Vaagsaether, K., Lundberg, J., Forseth, S., Bjerketvedt, D., 2019. Explosion characteristics for Li ion battery electrolytes at elevated temperatures. J. Hazard Mater. 371, 1–7. https://doi.org/10.1016/j.jhazmat.2019.02.108.

ISO 5660-1, 2018. Reaction to Fire Tests – Heat Release, Smoke Production and Mass Loss Rate – Part 1: Heat Release Rate (Cone Calorimeter Method) and Smoke Production Rate (Dynamic Measurement).

Liu, X., Stoliarov, S.I., Denlinger, M., Masias, A., Snyder, K., 2015. Comprehensive calorimetry of the thermally-induced failure of a lithium ion battery. J. Power Sources 280, 516–525. https://doi.org/10.1016/j.jpowsour.2015.01.125.

Liu, X., Wu, Z., Stoliarov, S.I., Denlinger, M., Masias, A., Snyder, K., 2016. Heat release during thermally-induced failure of a lithium ion battery: impact of cathode composition. Fire Saf. J. 85, 10–22. https://doi.org/10.1016/j.firesaf.2016.08.001.

Larsson, F., Andersson, P., Mellander, B.E., 2014a. Battery aspects on fires in electrified vehicles. In: Proceedings of Third International Conference on Fire in Vehicles, pp. 209–220.

Larsson, F., Andersson, P., Blomqvist, P., Loren, A., Mellander, B.E., 2014b. Characteristics of lithium-ion batteries during fire tests. J. Power Sources 271, 414–420. https://doi.org/10.1016/j.jpowsour.2014.08.027.

Ouyang, D., Liu, J., Chen, M., Wang, J., 2017. Investigation into the fire hazards of lithium-ion batteries under overcharging. Appl. Sci. 7 (12), 1314. https://doi.org/10.3390/app7121314.

Poizot, P., Dolhem, F., 2011. Clean energy new deal for a sustainable world: from non-CO_2 generating energy sources to greener electrochemical storage devices. Energy Environ. Sci. 4, 2003–2019. https://doi.org/10.1039/C0EE00731E.

Ribiere, P., Grugeon, S., Morcrette, M., Boyanov, S., Laruelle, S., Marlair, G., 2012. Investigation on the fire-induced hazards of Li-ion battery cells by fire calorimetry. Energy Environ. Sci. 5, 5271–5280. https://doi.org/10.1039/C1EE02218K.

Tarascon, J.M., Armand, M., 2001. Issues and challenges facing rechargeable lithium batteries. Nature 414, 359–367. https://doi.org/10.1142/9789814317665_0024.

Walters, R.N., Lyon, R.E., 2016. Measuring energy release of lithium ion battery failure using a bomb calorimeter. Final Report DOT/FAA/TC-15/40. Federal Aviation Administration.

Zalosh, R., Gandhi, P., Barowy, A., 2021. Lithium-ion energy storage battery explosion incidents. J. Loss Prevent. Process Indus. 72, 104560 https://doi.org/10.1016/j.jlp.2021.104560.

Health Effects of Diesel Exhaust

A fact sheet by
Cal/EPA's Office of Environmental Health Hazard Assessment and
The American Lung Association of California.

AMERICAN LUNG ASSOCIATION. of California

Diesel fuel is widely used throughout our society. It powers trucks that deliver products to our communities, buses that carry us to school and work, agricultural equipment that plants and harvests our food, and backup generators that can provide electricity during emergencies. It is also used for many other applications. Diesel engines have historically been more versatile and cheaper to run than gasoline engines or other sources of power. Unfortunately, the exhaust from these engines contains substances that can pose a risk to human health.

In 1998, the California Environmental Protection Agency's Office of Environmental Health Hazard Assessment (OEHHA) completed a comprehensive health assessment of diesel exhaust. This assessment formed the basis for a decision by the California Air Resources Board (ARB) to formally identify particles in diesel exhaust as a toxic air contaminant that may pose a threat to human health. The American Lung Association of California (ALAC) and its 15 local associations work to prevent lung disease and promote lung health. Since 1904, the American Lung Association has been fighting lung disease through education, community service, advocacy and research.

This fact sheet by OEHHA and ALAC provides information on health hazards associated with diesel exhaust.

Diesel exhaust contains more than 40 toxic air contaminants

What is diesel exhaust?

Diesel exhaust is produced when an engine burns diesel fuel. It is a complex mixture of thousands of gases and fine particles (commonly known as soot) that contains more than 40 toxic air contaminants. These include many known or suspected cancer-causing substances, such as benzene, arsenic and formaldehyde. It also contains other harmful pollutants, including nitrogen oxides (a component of urban smog).

How are people exposed to diesel exhaust?

Diesel exhaust particles and gases are suspended in the air, so exposure to this pollutant occurs whenever a person breathes air that contains these substances. The prevalence of diesel-powered engines makes it almost impossible to avoid exposure to diesel exhaust or its byproducts, regardless of whether you live in a rural or urban setting. However, people living and working in urban and industrial areas are more likely to be exposed to this pollutant. Those spending time on or near roads and freeways, truck loading and unloading operations, operating diesel-powered machinery or

working near diesel equipment face exposure to higher levels of diesel exhaust and face higher health risks.

What are the health effects of diesel exhaust?

As we breathe, the toxic gases and small particles of diesel exhaust are drawn into the lungs. The microscopic particles in diesel exhaust are less than one-fifth the thickness of a human hair and are small enough to penetrate deep into the lungs, where they contribute to a range of health problems.

Diesel exhaust and many individual substances contained in it (including arsenic, benzene, formaldehyde and nickel) have the potential to contribute to mutations in cells that can lead to cancer. In fact, long-term exposure to diesel exhaust particles poses the highest cancer risk of any toxic air contaminant evaluated by OEHHA. ARB estimates that about 70 percent of the cancer risk that the average Californian faces from breathing toxic air pollutants stems from diesel exhaust particles.

Diesel exhaust increases the risk of cancer…

In its comprehensive assessment of diesel exhaust, OEHHA analyzed more than 30 studies of people who worked around diesel equipment, including truck drivers, railroad workers and equipment operators. The studies showed these workers were more likely to develop lung cancer than workers who were not exposed to diesel emissions. These studies provide strong evidence that long-term occupational exposure to diesel exhaust increases the risk of lung cancer. Using information from OEHHA's assessment, ARB estimates that diesel-particle levels measured in California's air in 2000 could cause 540 "excess" cancers (beyond what would occur if there were no diesel particles in the air) in a population of 1 million people over a 70-year lifetime. Other researchers and scientific organizations, including the National Institute for Occupational Safety and Health, have calculated cancer risks from diesel exhaust that are similar to those developed by OEHHA and ARB.

Exposure to diesel exhaust can have immediate health effects. Diesel exhaust can irritate the eyes, nose, throat and lungs, and it can cause coughs, headaches, light-headedness and nausea. In studies with human volunteers, diesel exhaust particles made people with allergies more susceptible to the materials to which they are allergic, such as dust and pollen. Exposure to diesel exhaust also causes inflammation in the lungs, which may aggravate chronic respiratory symptoms and increase the frequency or intensity of asthma attacks.

… And it can cause coughs and aggravate asthma

Diesel engines are a major source of fine-particle pollution. The elderly and people with emphysema, asthma, and chronic heart and lung disease are especially sensitive to fine-particle pollution. Numerous studies have linked elevated particle levels in the air to increased hospital admissions, emergency room visits, asthma attacks and premature deaths among those suffering from respiratory problems. Because children's lungs and respiratory systems are still developing, they are also more susceptible than healthy adults to fine particles. Exposure to fine particles is associated with increased frequency of childhood illnesses and can also reduce lung function in children.

Like all fuel-burning equipment, diesel engines produce nitrogen oxides, a common air pollutant in California. Nitrogen oxides can damage lung tissue, lower the body's resistance to respiratory infection and worsen chronic lung diseases, such as asthma. They also react with other pollutants in the atmosphere to form ozone, a major component of smog.

What is being done to reduce the health risks from diesel exhaust?

Improvements to diesel fuel and diesel engines have already reduced emissions of some of the pollutants associated with diesel exhaust. However, diesel exhaust is still one of the most widespread and toxic substances in California's air.

ARB's Diesel Risk Reduction Plan, when fully implemented, will result in a 75 percent reduction in particle emissions from diesel equipment by 2010 (compared to 2000 levels), and an 85 percent reduction by 2020. The plan calls for the use of cleaner-burning diesel fuel, retrofitting of existing engines with particle-trapping filters, and the use in new diesel engines of advanced technologies that produce nearly 90 percent fewer particle emissions, as well as the use of alternative fuels.

Diesel exhaust contributes to smog and fine-particle pollution

The use of other fuels, such as natural gas, propane and electricity offer alternatives to diesel fuel. All of them produce fewer polluting emissions than current formulations of diesel fuel. As a result of ARB and local air-quality regulations, public transit agencies throughout California are using increasing numbers of passenger buses that operate with alternative fuels or retrofitted equipment.

For further information

Office of Environmental Health Hazard Assessment

1001 I Street, P.O. Box 4010, Sacramento, CA 95812-4010
(916) 324-7572
www.oehha.ca.gov

Air Resources Board

1001 I Street, Sacramento, CA 95814
(800) 363-7664
www.arb.ca.gov

American Lung Association of California

921 11th Street, Suite 700, Sacramento, CA 95814
(916) 442-4446
For your local office, call (800) LUNG-USA
www.californialung.org

The energy challenge facing California is real. Every Californian needs to take immediate action to reduce energy consumption. For a list of simple ways you can reduce demand and cut your energy costs, see OEHHA's web site at www.oehha.ca.gov